Synthesis of Planar Chiral Rhodium(II) Paddlewheel Catalysts

A thesis presented in partial fulfillment of the requirements for the degree of

Master of Science

in Chemistry

at Massey University, Manawatū,

New Zealand.

Samantha Staniforth

Supervised by Dr Gareth J. Rowlands and Professor Shane G. Telfer

2024

For Jenni V.

Abstract

Catalysts are the most efficient tools for the construction of large complex molecules. They offer an unparalleled way to solve problems and new ways to build molecules. Site-selective catalysts control the site of reaction in molecules that contain multiple sites with similar reactivity. C-H groups are the most abundant sites in all organic molecules but are very unreactive and difficult to functionalise. C-H functionalisation catalysis aims to install functionality at these sites by replacing the C-H bond with a C-C, C-O, C-N or C-X bond. Controlling the selectivity of these reactions is extremely difficult but highly rewarding, as it allows complex molecules to be made from very simple starting materials. Rh(II) paddlewheels are a class of selective C-H functionalisation catalysts that are capable of highly site-selective and enantioselective transformations. The organic ligands of the complex create different shapes around the catalyst active site that force a single C-H site to be targeted.

This project aimed to synthesise a new class of Rh(II) paddlewheel catalysts that possess a planar chiral ligand and to investigate their activity and selectivity in C-H insertion reactions.

In this work a novel resolution route for dibromide [2.2]paracyclophane carboxylic acids was developed. The carboxylic acids ligands were then used to synthesise three Rh(II) catalysts. Two of these paddlewheels were used to develop a late-stage catalyst functionalisation method through Suzuki-Miyaura coupling. In total, five Rh(II) catalysts were synthesised, of which four were assessed in both intermolecular and intramolecular nitrene insertion reactions.

Acknowledgements

My first enormous thank you is to my supervisor, Dr Gareth J. Rowlands. Thank you for letting me loose in the Rowlands' group research lab as an undergrad, this truly captured my passion for organic chemistry. I am indebted to the dedication, knowledge, and encouragement you have provided to both me and all your students over the years, we have all been lucky to have you. Any written form of 'thanks' I could put here would honestly be an understatement of how much of an impact you have truly made through your teaching and supervision.

To Professor Shane Telfer, thank you for your supervision over the latter part of my MSc.

Suraj/lil' d_z^2… Thank you for dealing with me from being an annoying undergrad to a *really* annoying MSc student. Thank you for sharing your knowledge on everything health and safety and synthesis. Thank you for growing and collecting my crystal structures and interpreting the data. Thank you for looking after our little group. Thank you for everything else unmentioned. I never said ya don't do anything for me.

Thank you to all past and present chemistry staff members I've encountered who've made chemistry fun. Thank you especially to Dr Pat Edwards for NMR support accompanied with a good yarn. Graham Freeman for synthetic and instrument guidance. Dave Lun for technical support with HPLC and running HRMS samples.

Thank you to all past and present members of the Rowlands group. A notable thanks to Clayr Asia for sharing common precursors. To the wider chemistry postgraduate groups, thank you to the Filichev, Telfer, Waterland and Whitby groups for their kindness and support.

My thanks must also be extended outside of the lab. To Ma and Soph, thank you for being an ever-present help and calmness in my life in difficult times. To Lud, for the shared frustrations, suggestions, coffee breaks and distractions, thank you for keeping me afloat. To Blair, my right arm and left leg, I would not have started this degree if you hadn't encouraged me. Thank you.

Table of Contents

List of Abbreviations

[2.2]PC	[2.2]Paracyclophane	**NSFI**	*N*-Fluorobenzene sulfonimide
Ac	Acetyl	**NPEA**	4-Nitrophenyl ethylamine
Bz	Benzoyl	**NTTL**	Naphthoyl-*tert*-leucinate
CIP	Cahn-Ingold-Prelog	**Pfbs**	Pentafluorobenzyl sulfamate
d	Doublet	**ppm**	Parts per million
DCE	1,2-Dichloroethane	**PTAD**	Phthalimido adamantane
ddd	Doublet of doublet of doublets	$\boldsymbol{R_f}$	Retention factor
DG	Directing group	**s**	Singlet
DMF	*N*,*N*'-Dimethylformamide	**t**	Triplet
dppf	Diphenylphosphino ferrocene	**TBDPS**	*tert*-Butyl diphenylsilyl
dt	Doublet of triplets	**TCPTAD**	Tetrachloropthalimido adamantane
ee	Enantiomeric excess	**TFPTAD**	Tetrafluoropthalimido adamantane
eq	Equivalents	**THF**	Tetrahydrofuran
Fmoc	Fluorenyl methoxycarbonyl	**TLC**	Thin layer chromatography
HOMO	Highest occupied molecular orbital	**TPA**	Triphenylacetate
HPLC	High-performance liquid chromatography	**TPCP**	Triphenylcyclopropane
Hz	Hertz	**Tp^x**	Hydrotrispyrazolylborate
IR	Infrared	**Troc**	Trichloroethoxycarbonyl
LUMO	Lowest unoccupied molecular orbital	**UV**	Ultraviolet

Chapter 1

Introduction

1.1 Site-selectivity

When predicting the outcome of a reaction, chemists often look to the functional groups of molecules that determine where and how they will react. Chemoselective transformations are the easiest to control as they take advantage of the inherent differences in reactivity between different functional groups (Figure 1a).[1] Site-selective transformations are much more difficult to control as they must distinguish between multiple groups that have similar reactivity, and only differ by their placement in the molecule (Figure 1b).[1,2,3]

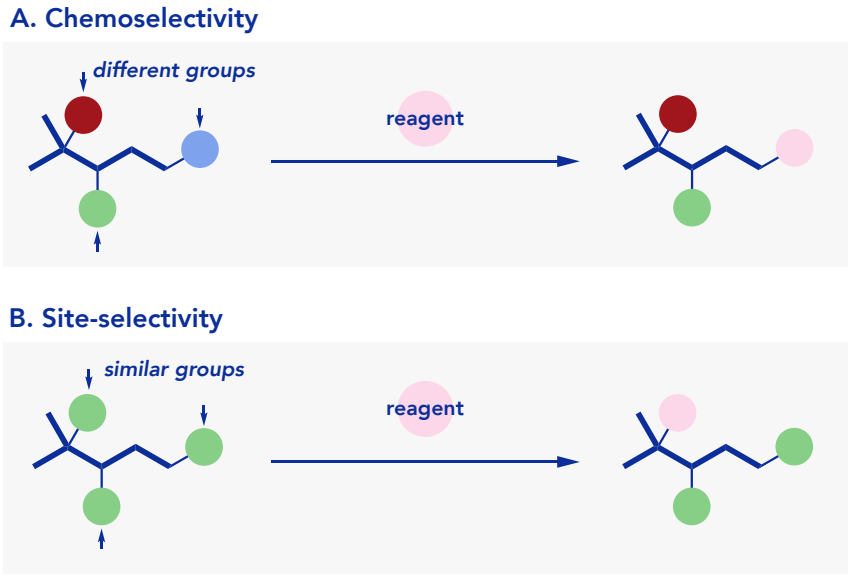

Figure 1: a) Simplified representation of a chemoselective transformation. b) Simplified representation of a site-selective transformation.

Generally, if a reaction is not inherently site-selective, a complicated mixture of products will be formed. This mixture arises from the similarity in energy barriers that must be overcome to obtain each product (Figure 2a).[4] Although the different sites in the molecule are not completely identical, the difference between the energy barrier for each product is extremely small.[5] This is best demonstrated by the halogenation of a branched alkane such as 2-methylpentane, that possesses primary, secondary, and tertiary C-H positions (Figure 2b). Light catalysed chlorination of 2-methylpentane delivers five different mono-chlorinated products.[1] Each C-H position has an almost identical chemical environment to

its counterparts, leading to no obvious preference of reaction site and no distinct product. If this reaction was site-selective, only one C-H site would be targeted for halogenation.

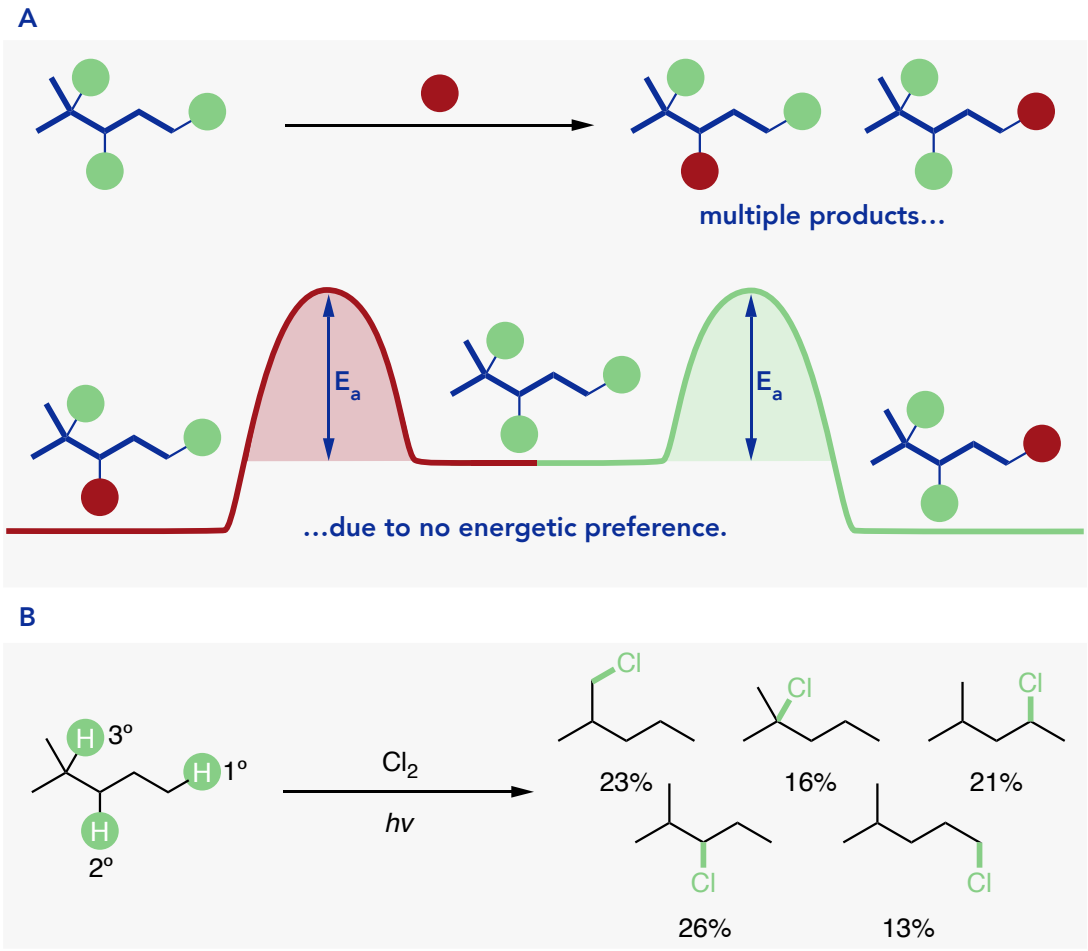

Figure 2: a) Similarity in energy barriers that arise from the chemical similarity of sites in a molecule. b) Lack of site-selectivity in C-H bonds of 2-methylpentane leads to multiple products from light-catalysed chlorination.

1.2 Site-selectivity of C-H functionalisation

C-H sites are the most abundant sites present in all organic molecules that are notoriously unreactive and very difficult to functionalise.[6] C-H functionalisation chemistry deals with installing functionality at these unreactive positions by replacing the C-H bond with a C-C, C-O, C-N or C-X bond.[7] These reactions often require a catalyst; commonly based on transition metals such as palladium, rhodium, ruthenium, iridium or cobalt. Transition metals traditionally facilitate the difficult C-H activation step, which is the insertion of the transition metal into the C-H bond.[7] The transition metal then facilitates the formation of a bond between carbon and the desired group, before departing (Figure 3).

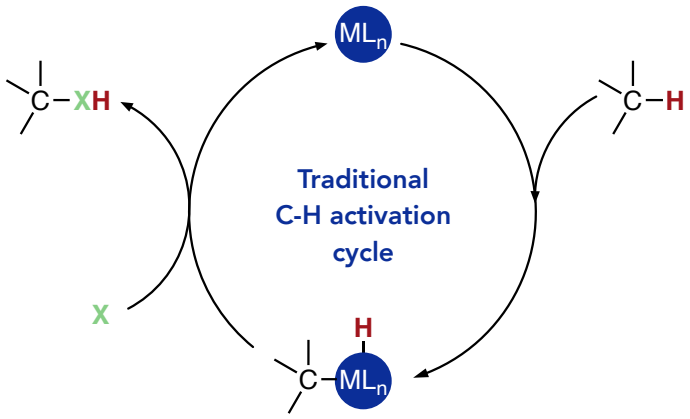

Figure 3: General C-H functionalisation mechanism involves direct insertion of the metal complex into the C-H bond.

Due to their abundance and lack of reactivity, site-selectivity of C-H functionalisation is extremely hard to achieve. Controlling the site-selectivity of these reactions would allow the synthesis of complex molecules from simple starting materials.[6] Approaches such as using modified substrate molecules, selective reagents, enzymes, molecular containers and catalysts have all been used.[8,9,10] However, only the major approaches in the field will be discussed below.

1.2.1 Substrate-directed C-H functionalisation

Substrate directed selectivity occurs when a group within the substrate internally directs the reaction. These directing groups act as an internal ligand for coordination with the metal catalyst, placing it within proximity of a specific C-H site (Figure 4).

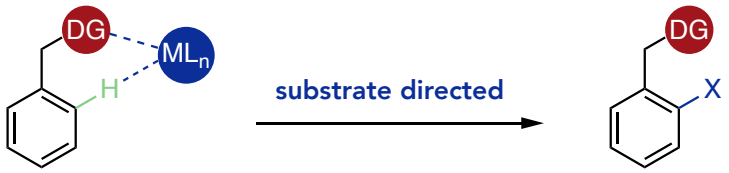

Figure 4: Substrate directed C-H functionalisation. DG = directing group.

If no directing groups are present, the substrate may be chemically modified with them.[11] Nitrogen containing groups have been used for the selective *ortho* alkylation of biaryl systems. Ru(II) catalyst **1** coordinates to a pyridine group in the biaryl substrate and forces metal insertion and alkylation to occur at the *ortho* C-H position. This method provides reliable *ortho* alkylation using a range of alkyl halides in contrast to previous Ru(II) catalysed alkylations, where selectivity was often *meta* selective (Scheme 1).[12]

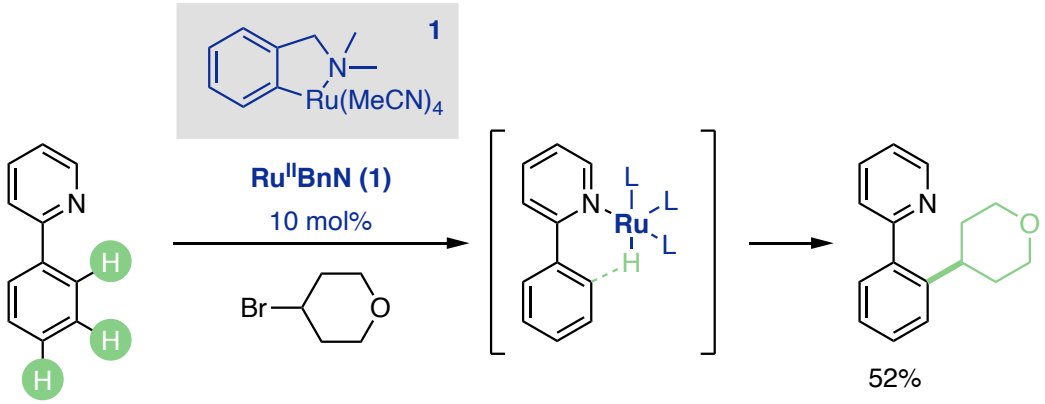

Scheme 1: Directed C-H alkylation of aryl systems under Ru(II) catalysis, where selectivity arises from the pyridine directing group forcing oxidative insertion at the *ortho* position.

1.2.2 Reagent-directed C-H functionalisation

Substrate modification is not always possible and using directing groups requires more synthetic steps to add and remove them.[11] To avoid this situation, reagent control can be used, where a stoichiometric reagent elicits the desired selectivity. Selective C-H halogenation of alkyl chains was achieved by modifying an *N*-chloroamide halogen transfer reagent **2** (Scheme 2).[13] The positioning of electron withdrawing CF_3 groups on the aryl ring

of the reagent leads to a change in selectivity. Placement *meta* to the amide provides little bias between C-H bonds, whereas CF_3 in the *ortho* position shows selectivity for less sterically hindered C-H bonds. The selectivity arises from the *ortho* CF_3 groups congesting the *N*-centered radical, leading to the abstraction of the most accessible hydrogen.

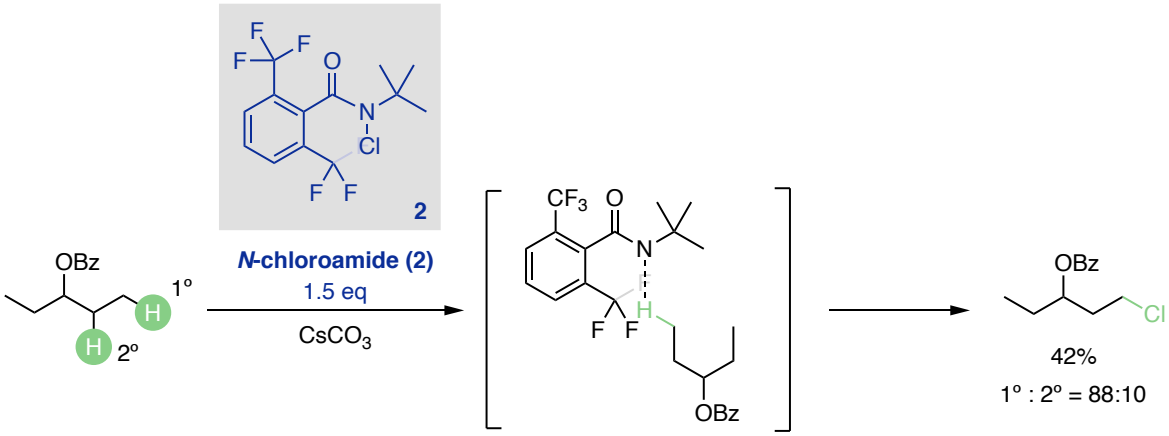

Scheme 2: C-H halogenation of 1° C-H bonds with an *N*-chloroamide halogen transfer reagent.

1.2.3 Catalyst-directed C-H functionalisation

Reagent modification can be performed with a catalyst rather than a stoichiometric reagent to obtain the desired selectivity.[11] Selectivity of these reactions is completely controlled by the catalyst. In contrast to substrate-directed selectivity, the metal does not interact with groups on the substrate and selectivity is entirely transferred through the shape of the catalyst. Catalyst shape is controlled by modifying the organic ligands of the complex, which are arranged in a fashion that creates a highly specific environment around the metal active site. This environment confines the reaction to a single C-H site, delivering a specific product.

Catalyst-directed carbene and nitrene insertion into C-H bonds

Many different metal approaches for catalyst-directed C-H functionalisation exist. However, one of the more promising segments of this field focusses on the use of metal carbenoids and nitrenoids to functionalise unactivated C-H bonds. Rather than the 'traditional' C-H activation approach, where the metal inserts itself into the C-H bond, a metal complex coordinated to a divalent carbon (carbene) or monovalent nitrogen (nitrene) is inserted into the C-H bond (Figure 5).[14] Carbene and nitrene transfer is energetically easier, as the metal itself never interacts with the C-H bond, avoiding oxidative insertion altogether. Traditional C-H activation can also suffer from the inability to regenerate the metal catalyst, rendering

the process non-catalytic. Whereas, the metal complex is easily and rapidly regenerated after carbene or nitrene insertion.[14,15]

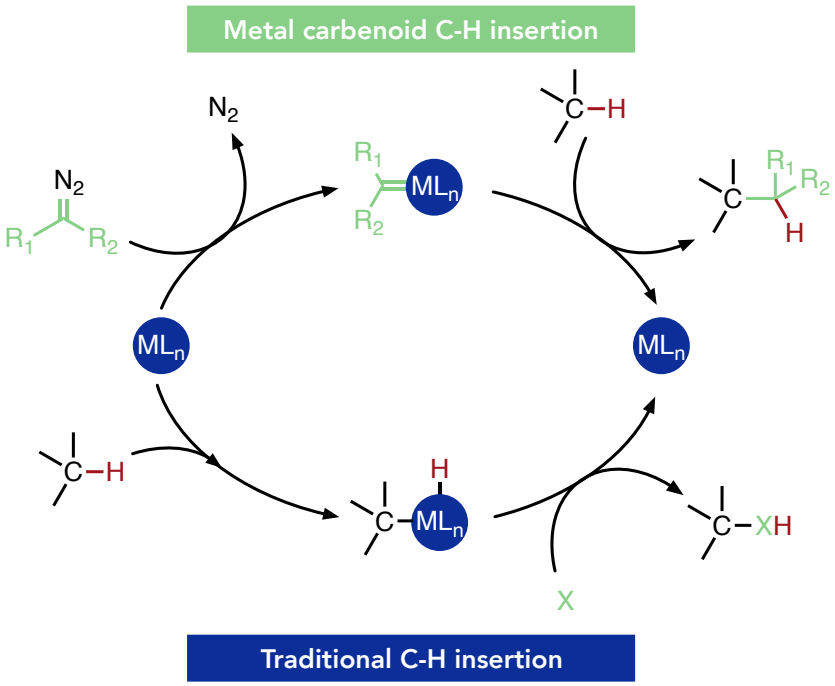

Figure 5: Traditional C-H insertion mechanism, that involves metal insertion into the C-H bond, compared with metal carbenoid mediated C-H insertion, that avoids C-H metal insertion.

Chiral transition metal catalysts can introduce selectivity by overcrowding the active site.[16] Iridium(III)-salen complexes are one class of catalysts capable of both site-selective and enantioselective carbene and nitrene insertion at activated C-H sites. Salen **3** is known for providing reliable benzylic C-H selectivity amongst an array of aromatic substrates (Scheme 3).[17] Ir(III)-salens generally prefer C-H sites next to oxygen, however **3** prefers benzylic C-H sites over oxygen adjacent sites.[18] A different salen variant **4** is also capable of intramolecular C-H bond amination using sulfonyl azides (Scheme 3).[19] The reaction is highly stereoselective, however amination to form either a five membered or six membered ring is highly dependent on the nature of the substrate. The capability of Ir(III) salens currently remains limited to activated C-H sites, preventing their use for functionalising more challenging unactivated substrates.

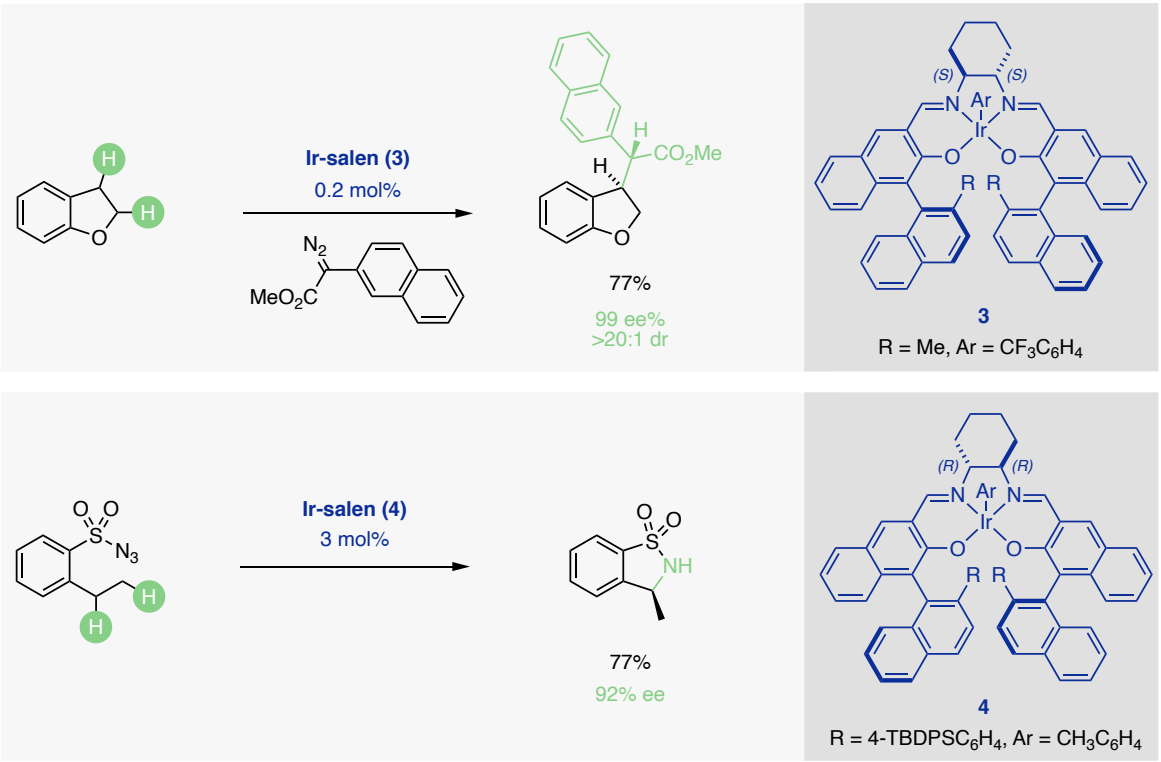

Scheme 3: Chiral iridium(III)-salen complexes for asymmetric carbene and nitrene insertion.

If functionalisation of unactivated C-H bonds is desired, hydrotrispyrazolylborate (Tp^x)-based silver catalysts provide the extra reactivity required for these difficult substrates. Recent development has shown a bulkier Tp^x ligand such as **5**, enforces alkylation to occur at the most terminal secondary C-H site in linear chain alkanes (Scheme 4).[20] This selectivity trend is also applicable for intermolecular nitrene insertion, where Tp^{Br3} ligands **6** target the same secondary C-H site (Scheme 4).[21] $AgTp^x$ catalysts are a more reactive class of catalysts for unactivated sites, this consequently makes their site-selectivity and stereoselectivity much harder to control.[22]

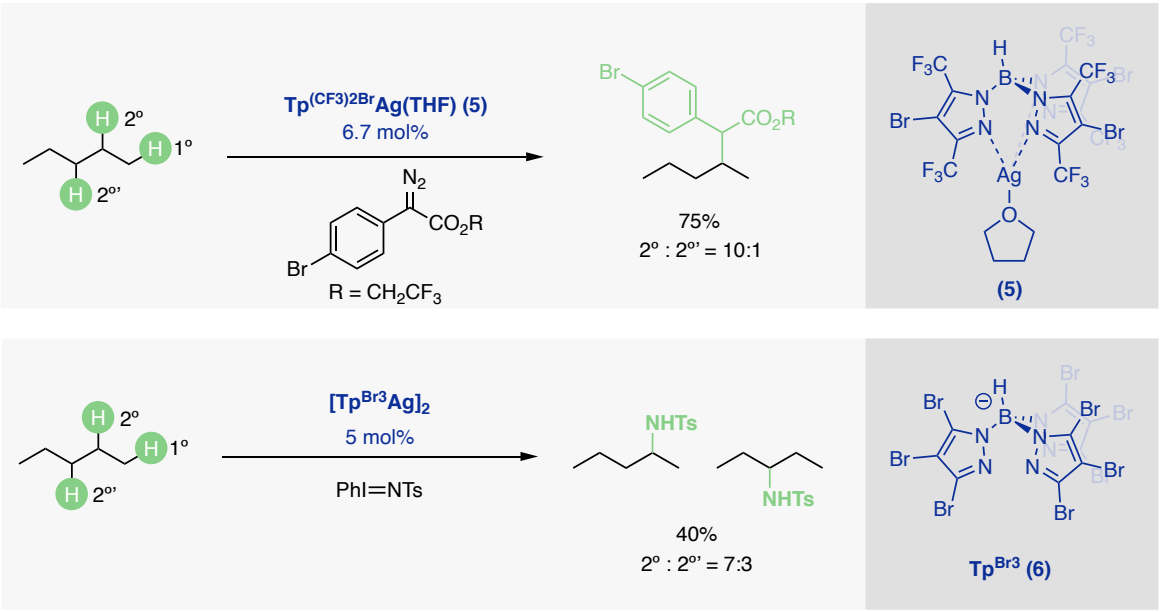

Scheme 4: Silver Tp^{x} catalyst systems for carbene and nitrene insertion into linear chain alkanes.

Ir(III) catalysts are highly selective C-H functionalisation catalysts but lack reactivity to functionalise unactivated sites. Tp^{x}Ag catalysts have the reactivity to functionalise unactivated sites but not in a selective manner. Rh(II) paddlewheel catalysts are another class of C-H insertion catalysts that are both highly reactive and highly selective. Their utility is best demonstrated by the stereoselective and site-selective intermolecular C-H alkylation of linear alkanes.[22] Rh(II) carbene and nitrene insertion chemistry is an extremely diverse field, as these complexes and their reactions constitute the main subject of this thesis an in-depth discussion will be continued in the next section.

1.3 Rhodium(II) paddlewheel catalysts

1.3.1 Structure, properties, and preparation

Rhodium(II) paddlewheels are highly symmetrical complexes based on a dirhodium centre where both Rh atoms are in the +2 oxidation state (Figure 6a).[23] Four bidentate ligands coordinate in the equatorial positions that bridge across each Rh atom and create its 'paddlewheel' shape.[23] Common equatorial ligands are carboxylate based, however carboxamide, phosphinate and amidate examples also exist. Along the axis of the Rh-Rh bond are two labile coordination sites known as the axial positions. These are often occupied by smaller ligands like water. The axial positions are the catalytically active sites where the complex and substrates interact.[24] Whereas, the equatorial ligands generally remain inert and provide the steric environment for reaction. Preparing paddlewheel complexes is generally straightforward, achieved by ligand exchange between $Rh_2(OAc)_4$ **7** and an organic carboxylic acid.[25]

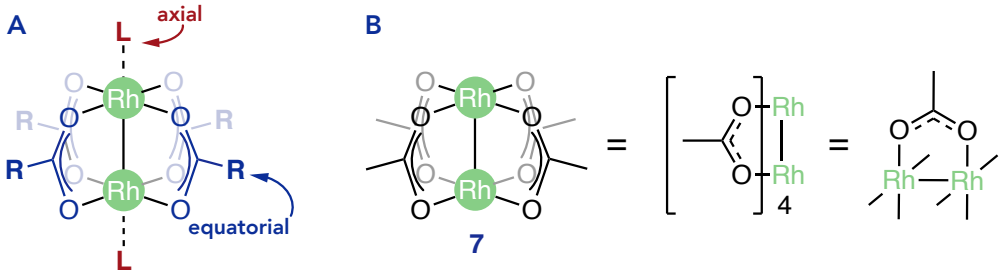

Figure 6: a) Generalised skeletal representation of a Rh(II) paddlewheel depicting the axial and equatorial ligands. b) $Rh_2(OAc)_4$ **7** and common simplified depictions of $Rh_2(OAc)_4$ found in the literature.

1.3.2 Symmetry

Rhodium complexes can become chiral if the coordinating atoms are different or a chiral ligand is used, which causes both Rh atoms to become stereocentres.[23] Using a racemic mixture of ligand will produce many diastereoisomers. If an enantiomerically pure ligand is used, then only one enantiomerically pure complex will be formed (Figure 7). The catalyst may possess higher symmetry than the ligands themselves, chiral paddlewheels can possess up to D_4 symmetry depending on the steric demands of the ligands.[24] Three common symmetry patterns are depicted in Figure 8. These patterns are closely linked to the way paddlewheel complexes behave in catalytic reactions.

Figure 7: Two diastereoisomers of a Rh(II) complex: left is comprised of a racemic mixture of a ligand whereas, right is comprised of enantiomerically pure ligands.

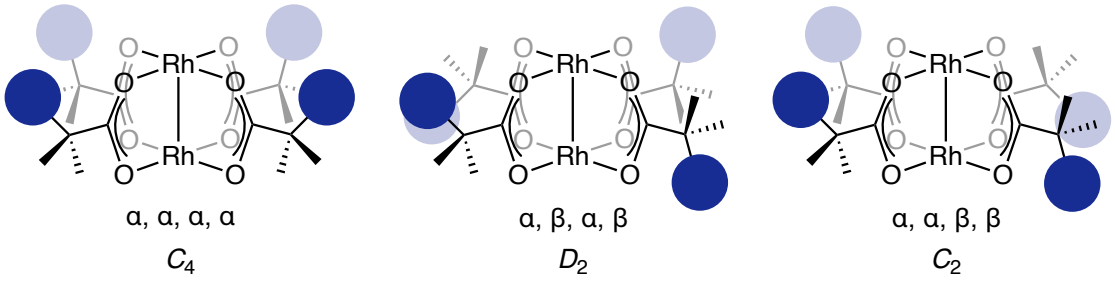

Figure 8: Common high symmetry patterns adopted by chiral Rh(II) paddlewheels. Orientation of the ligand is denoted as α for upwards and β for downwards.

1.3.3 Rhodium(II) catalysts for C-H activation

Rh(II) catalysts display high selectivity in carbene and nitrene transfer reactions. The best examples showcase unambiguous site-selectivity and stereoselectivity for both unactivated and activated C-H bonds alike.

1.3.3.1 Carbene insertion

Davies' group has pioneered a family of Rh(II) paddlewheels that facilitate the functionalisation of most general types of C-H bonds (Scheme 5a). Discrimination for activated sites is shown by Rh_2(*S*-TCPTAD)$_4$ **8** while sterically accessible sites are preferred by Rh_2(*S*-2-Cl-5-Br-TPCP)$_4$ **9** (Figure 5b-c). This selectivity was shown using benzylic substrates. Catalyst **8** functionalised the more reactive benzylic site and **9** targeted the more inert secondary methylene site, both with high enantioselectivity.[26] TPCP ligands are known to cause higher steric crowding at Rh compared to the TCPTAD ligands, forcing them to prefer more accessible C-H sites.[22] Although **8** is also sterically crowded, it shows a larger preference for activated C-H sites and attacks the benzylic site in preference to the unactivated methylene site.

Discrimination between C-H sites in alkanes is possible by changing the bulkiness of the catalyst. Functionalisation of the 3°, 2° and 1° C-H sites in 2-methylpentane was achieved

with three different catalysts (Scheme 5d).[27] Preference for the 3° site was shown by **8**, the 2° site by Rh_2[*R*-3,5-di(*p*-^{t}BuC_6H_4)TPCP]$_4$ **10**, and the 1° site by Rh_2[*R*-tris(*p*-^{t}BuC_6H_4)TPCP]$_4$ **11**. Each catalyst has C_4, D_2 and C_2 symmetry respectively, indicating the arrangement of ligands around the active site leads to very different selectivity.[22] The scope of primary C-H activation was further investigated using **11**, where wide substrate tolerance – especially in the presence of more activated sites was exhibited, additionally with high enantioselectivities. The bulkier catalysts **10** and **11** were also conveniently synthesised by a late-stage Suzuki coupling protocol. This was performed on the Rh(II) paddlewheels rather than the carboxylate ligands, greatly increasing the synthetic efficiency of catalyst synthesis.

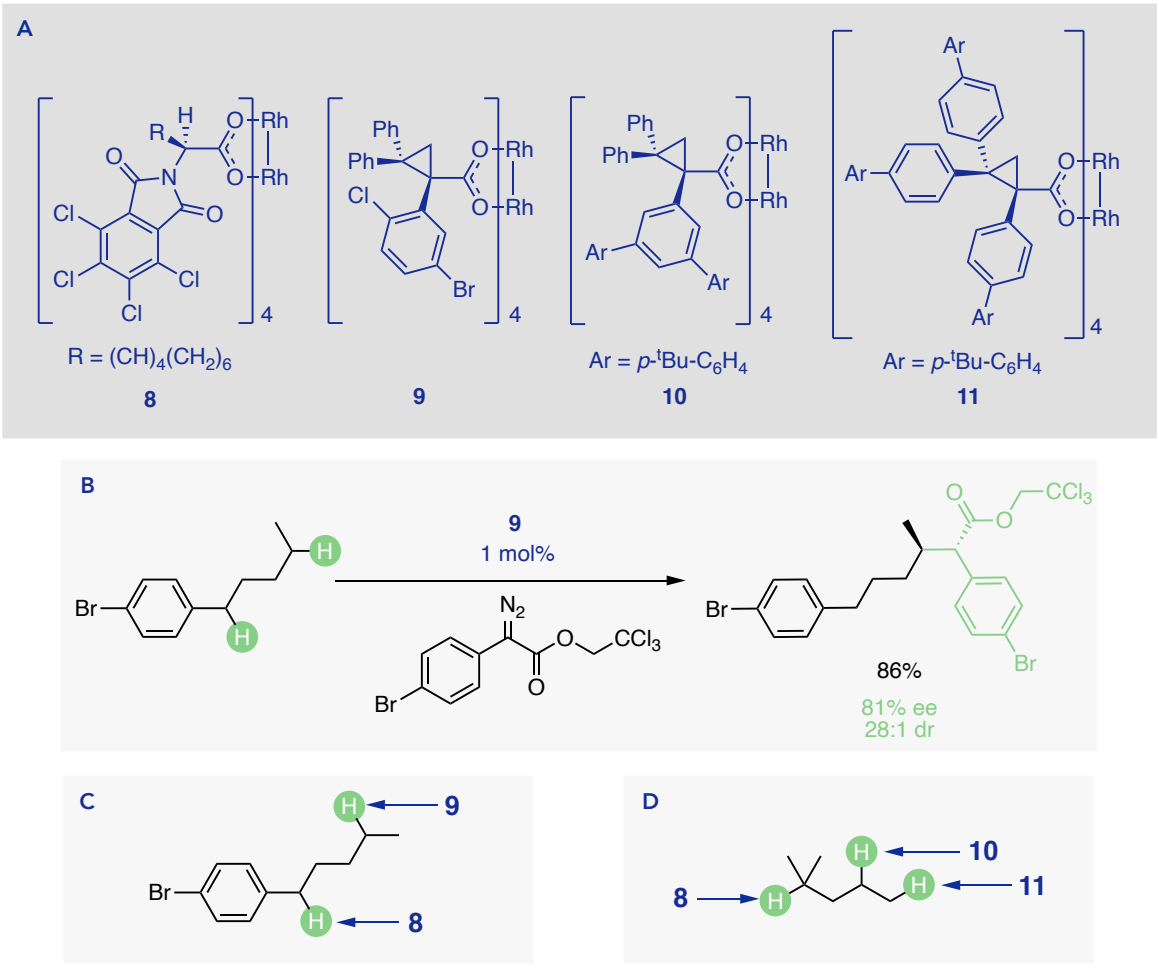

Scheme 5: a) Rh(II) paddlewheels developed by the Davies group for carbene insertion: Rh_2(*S*-TCPTAD)$_4$ **8**, Rh_2(*S*-2-Cl-5-Br-TPCP)$_4$ **9**, Rh_2[*R*-3,5-di(*p*-^{t}BuC_6H_4)TPCP]$_4$ **10** and Rh_2[*R*-tris(*p*-^{t}BuC_6H_4)TPCP]$_4$ **11**. b) Example of carbene insertion at the terminal methylene position using Rh_2(*S*-2-Cl-5-Br-TPCP)$_4$ **9**. c) C-H site preference for carbene insertion by catalysts **8** and **9**. d) C-H site preference for carbene insertion into 2-methylpentane by catalysts **8**, **10** and **11**.

1.3.3.2 Nitrene insertion

Rh(II) catalysed nitrene transfer reactions are not as developed as their carbene counterparts, fewer examples exist of enantioselective C-H bond amination, especially for unactivated C-H bonds. Selectivity of carbene insertion is known to be dependent on the nature of the carbene substituents, which has allowed chemists to optimise substrate and catalyst combinations to achieve the desired selectivity.[28] Such studies have not been performed for nitrene insertion reactions and the origin of selectivity is not common knowledge.

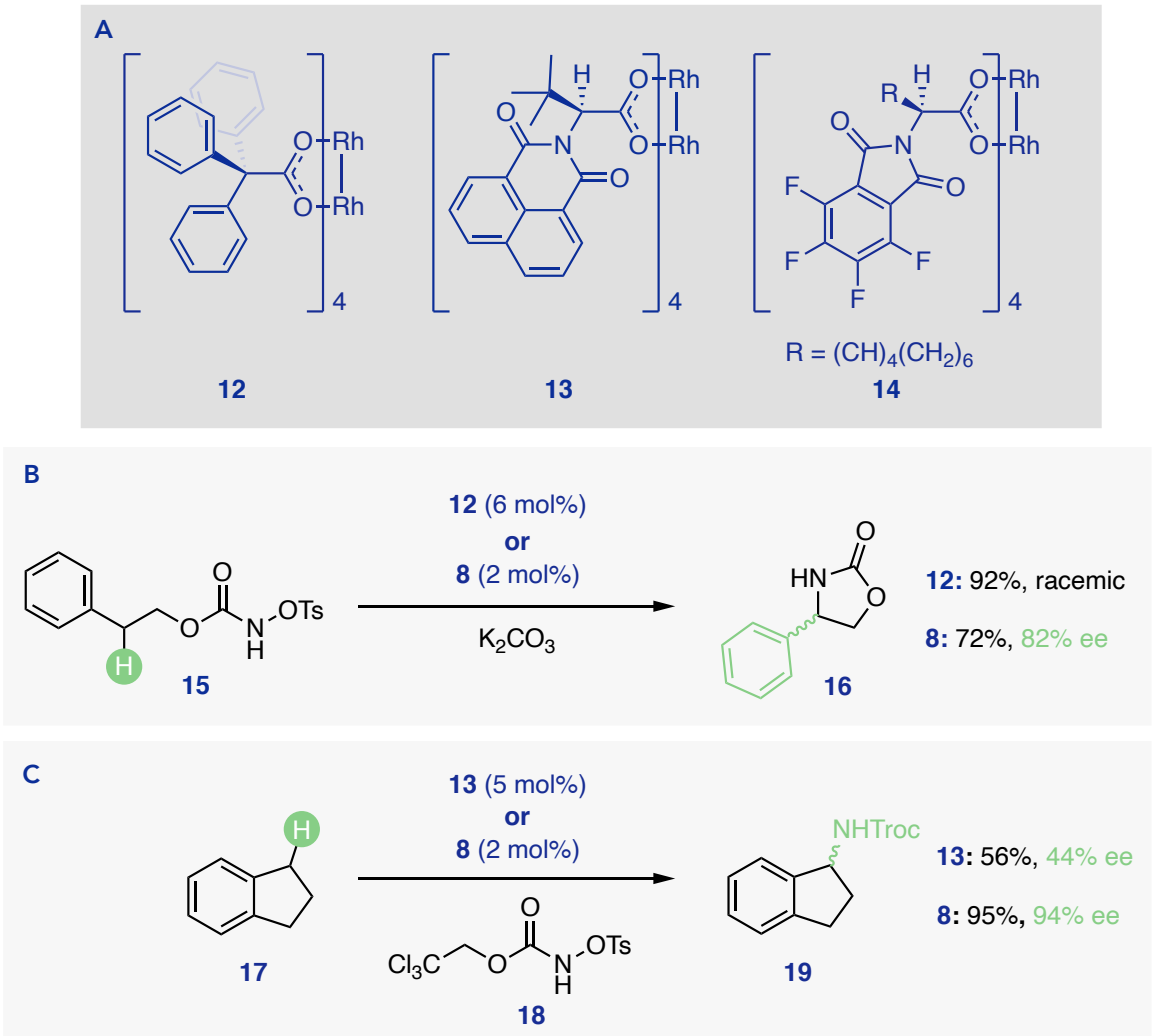

Scheme 6: a) Rh(II) paddlewheels developed for nitrene insertion: $Rh_2(TPA)_4$ **12**, $Rh_2(S\text{-NTTL})_4$ **13** and $Rh_2[TFPTAD]_4$ **14**. b) Intramolecular nitrene insertion of an *N*-tosyloxycarbamate performed by **8** or **12**. c) Intermolecular nitrene insertion of an *N*-tosyloxycarbamate by **8** or **13**.

Lebel demonstrated success of both intra- and intermolecular C-H bond amination using *N*-tosyloxycarbamates as the nitrene source.[29] Using achiral catalyst **12** to cyclise **15** to form **16** resulted in excellent yields, even when azide nitrene sources failed to produce any

reaction (Scheme 6b).[30] The enantioselectivity of the reaction was investigated by using a chiral Rh(II) catalyst: Rh_2[*S*-NTTL]$_4$ **13** that provided no enantioinduction for reaction of **15**, but a modest 44% ee for reaction between **17** and **18** (Scheme 6c). Davies further expanded on this set of reactions by using the carbene insertion catalyst **8**.[31] Improved yields and enantioselectivities for both intra- and intermolecular C-H aminations were observed in excellent yields. Increasing the enantioselectivity of nitrene insertion into benzylic bonds was investigated by Dauban using Rh_2[TFPTAD]$_4$ **14**. (Scheme 7a).[32] Benzylic, ethereal and unactivated methylene C-H sites were included within a single substrate but **14** remained consistent in targeting the methylene benzylic bond. Intermolecular nitrene insertion into 2,4-dimethylpentane was recently investigated using **14** (Scheme 7b).[33] Bias for amination at the 3° position over the 2° position was demonstrated in 20:1 excess, yet no enantioselectivity was shown.

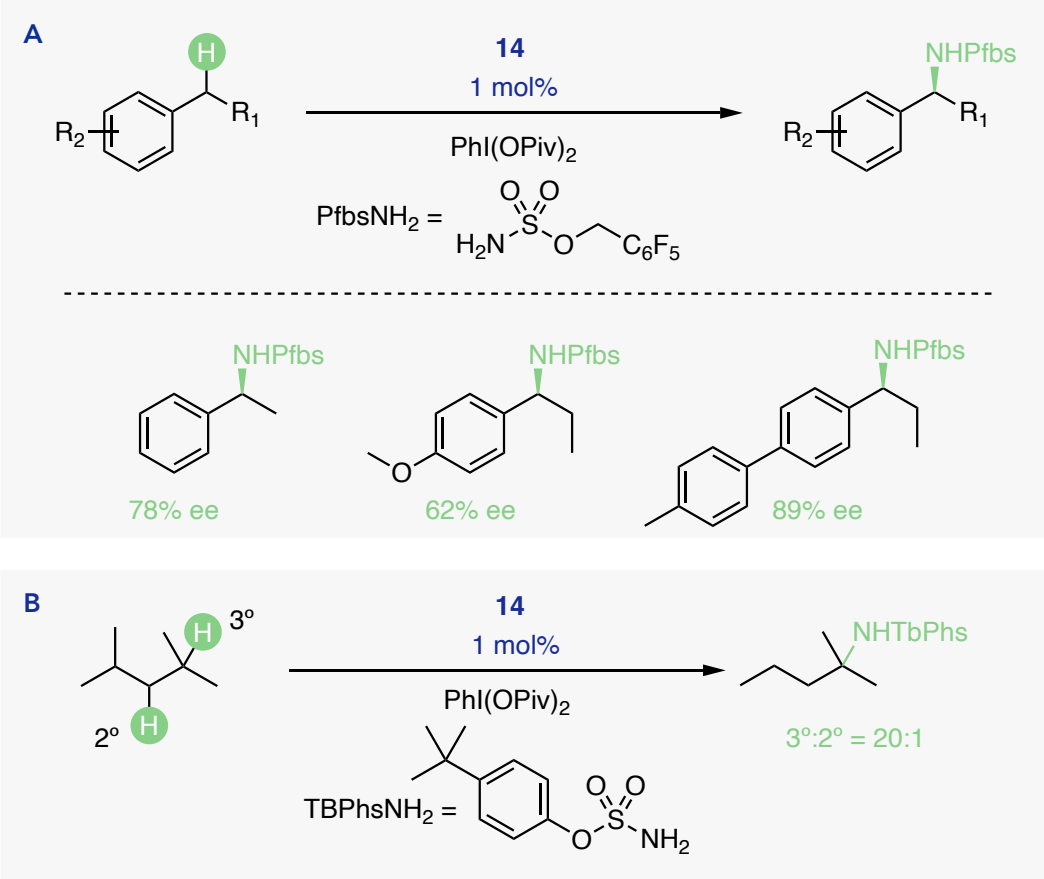

Scheme 7: a) Enantioselective nitrene insertion into benzylic C-H bonds using catalyst **14**. b) Nitrene insertion into unactivated C-H bonds using catalyst **14**.

The Rh(II) catalysts mentioned above show reliable carbene and nitrene insertion into a number of chemically distinct C-H sites, facilitating the functionalisation of molecules with no inherent functionality. Davies' class of Rh(II) catalysts appear to be the most promising

set of enantio- and site-selective catalysts. However, the enantiopure cyclopropane carboxylate ligands are made through cyclopropanation using another chiral Rh(II) catalyst, often $Rh_2[PTAD]_4$. This makes the cyclopropane class of Rh(II) catalysts expensive to make, as the enantiopure $Rh_2[PTAD]_4$ catalyst must be either purchased or synthesised. However, the late-stage Suzuki coupling for the synthesis of some catalysts demonstrates an efficient way to add variation to catalysts late in the synthetic route.

1.4 [2.2]Paracyclophane

[2.2]Paracyclophane ([2.2]PC) **20** is a small molecule belonging to the cyclophane family, it is the simplest but most studied cyclophane due to its unique structure and electronics. Cyclophanes are a class of macrocyclic molecules characterised by the inclusion of one or more aromatic rings into a cyclic hydrocarbon chain (Figure 9).[34]

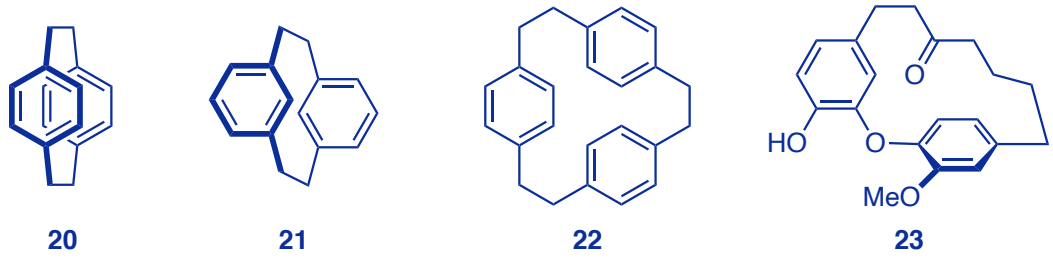

Figure 9: Cyclophane examples: [2.2]paracyclophane **20**, [2.2]metacyclophane **21**, [2.2.2]paracyclophane **22** and galeon **23**, a bioactive cyclophane extracted from bog-myrtle.[35]

1.4.1 [2.2]Paracyclophane structure and chemistry

[2.2]PC contains two benzene rings stacked parallel to one another, connected by two ethylene bridges at the *para* positions. The short length of the hydrocarbon bridges means rotation of the two rings is prohibited, the proximity of the rings allows their π orbitals to overlap.[36] This introduces significant strain into the molecule, distorting its bond lengths and angles from normal values. The length of the ethylene bridges are longer than the average C-C bond distance at 1.63 Å and the benzene rings are forced out of planarity into a 'boat-like' conformation (Figure 10).[36]

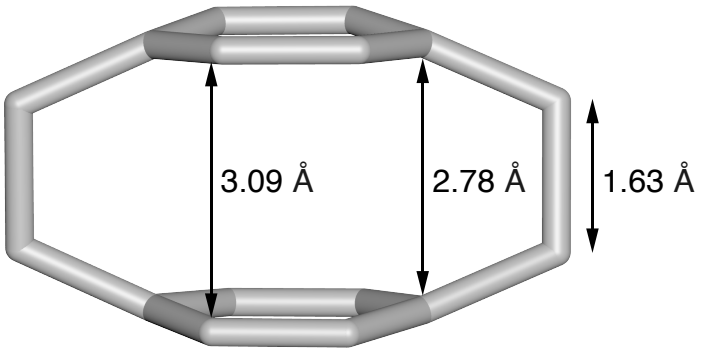

Figure 10: Molecular model of [2.2]paracyclophane depicting the shortened ethylene bridges and distorted benzene rings. Hydrogen atoms omitted for clarity.

The overlap of π orbitals from both rings increases the energy of the HOMO of [2.2]PC, rendering it more reactive towards electrophilic substitution than common alkyl benzene

derivatives.[37] Multiple substitution of both rings is therefore possible (Figure 11a), substituent patterns are affected by the 'transannular' phenomenon: a substituent on one aryl deck will affect the chemistry of the opposing deck.[38] Controlling the regiochemistry of substitution is well studied, making [2.2]PC an attractive scaffold for optical materials, surface coatings and asymmetric catalysts.[39,40]

1.4.2 Planar chirality and nomenclature

Restricted rotation of the two benzene rings renders [2.2]PC prochiral. When substituents are introduced on the rings, its symmetry can be broken, and the molecule becomes planar chiral. Not all substituent patterns are inherently chiral and are dependent on the nature of each substituent, for example if R_1=R_2 for the *pseudo-para* pattern, the molecule is achiral (Figure 11a). Numbering [2.2]PC derivatives and assigning them with planar chirality descriptors is performed according to Cahn-Ingold-Prelog (CIP) priority rules (Figure 11b-c).[41] Assignment is performed by identifying the chiral plane, which is the most highly substituted aromatic deck. A 'pilot atom' is chosen, which the first atom out of the chiral plane, connected to the highest priority substituent within the plane. The chiral plane is then viewed face on, by looking down the pilot atom, and the first three atoms in the plane are numbered according to CIP priority rules. If numbering occurs in a clockwise direction the derivative is R_p and for the anticlockwise direction, S_p.

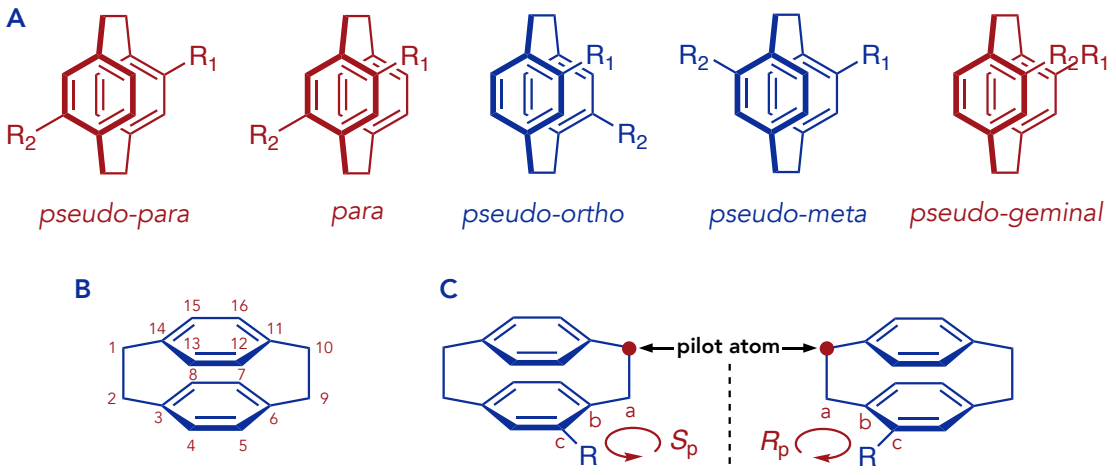

Figure 11: a) Selected substituent patterns of [2.2]PC derivatives, depictions in blue are inherently chiral patterns while those in red are only chiral if $R_1 \neq R_2$. b) Numbering convention used for [2.2]PC derivatives. c) Assignment of chiral [2.2]PC derivatives as S_p or R_p.

1.4.3 Applications in asymmetric catalysis

The quality of planar chirality has encouraged [2.2]PC's use in asymmetric catalysis. The first prominent success was with PHANEPHOS **24**, a bisphosphine ligand that delivered excellent enantiocontrol over Rh(I)-catalysed asymmetric hydrogenations (Scheme 8a).[42] The R_p enantiomer of the catalyst provided superior enantiocontrol compared with other chiral phosphine ligands that failed to breach >60% ee. Bräse and coworkers developed a class of ketimine ligand **25** for the asymmetric addition of alkenyl zinc reagents to aldehydes (Scheme 8b).[43] Each enantiomer of the ligand delivered alcohols with the opposite stereochemistry in good enantioselectivity, showing the influence of planar chirality on the alcohol's stereochemistry.[44, 43]

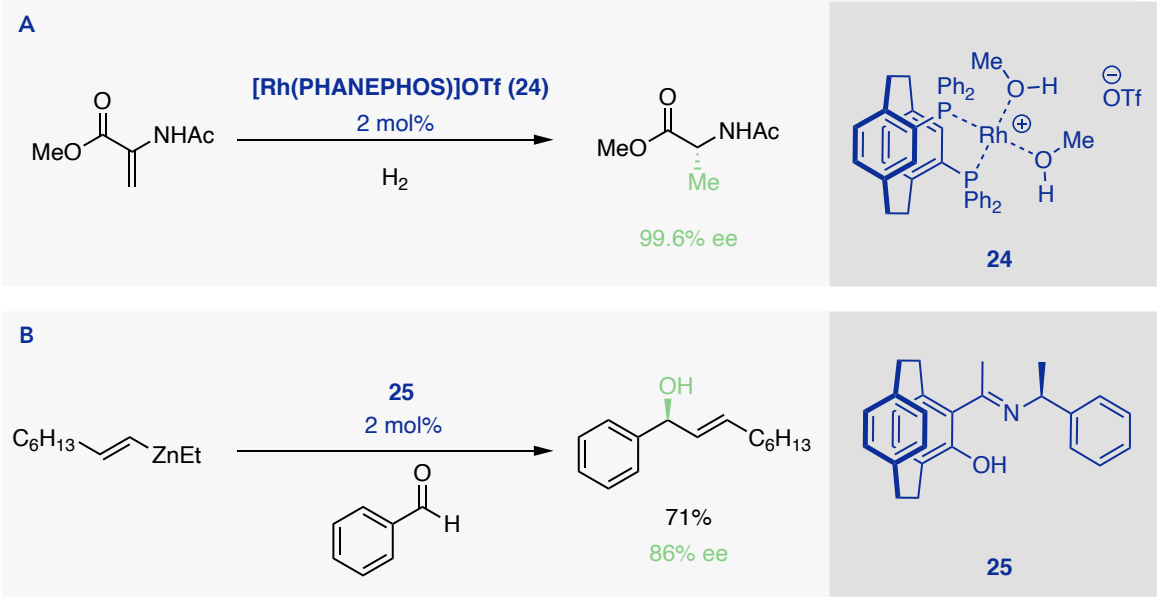

Scheme 8: a) [Rh(PHANEPHOS)]OTf catalysed asymmetric hydrogenation of alkenes b) Bräse's ketimine ligand for asymmetric addition of alkenyl zinc reagents to aldehydes.

Fewer examples exist of [2.2]PC ligands or catalysts for the functionalisation of C-H bonds. Fluorination of carboxylic acids was reported using a [2.2]PC isothiourea catalyst **26** (Scheme 9a).[45] Fluorination of the α-position and subsequent coupling with an alcohol in the one-pot process delivered α-fluorinated esters in both excellent yields and enantioselectivies up to 99.5%. Synthesis of the first [2.2]PC Rh(II) paddlewheel catalyst **27** was recently described by Bräse and coworkers for asymmetric cyclopropanation (Scheme 9b).[46] Addition of diazo carbenoid precursors to alkenes was demonstrated by the S_p enantiomer of the catalyst, delivering cyclopropanation products in moderate to good diasteroselectivity.

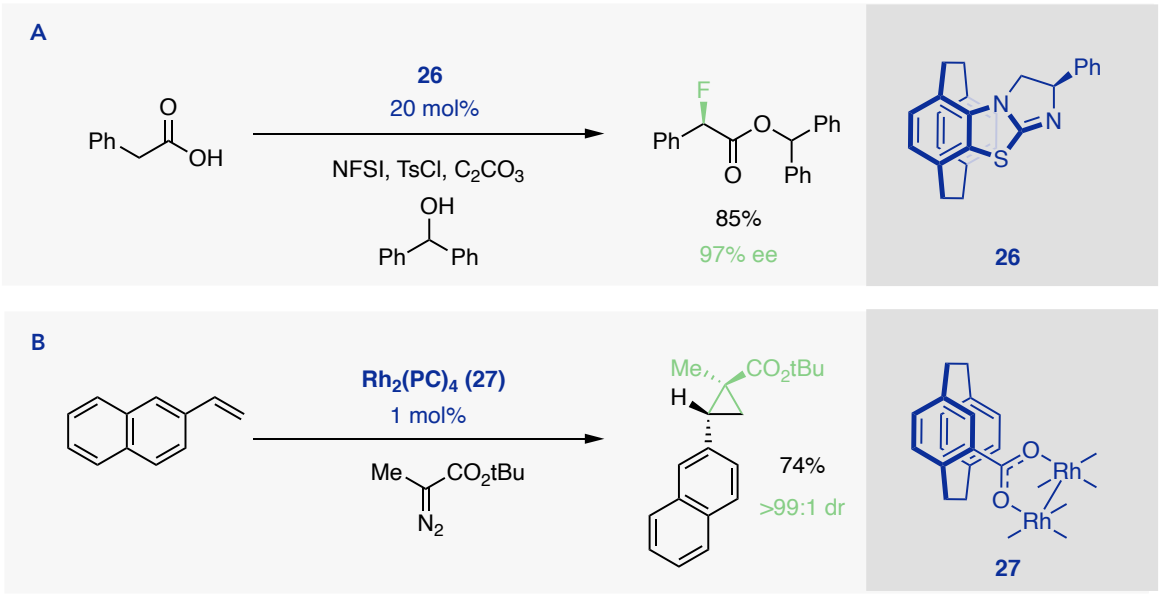

Scheme 9: a) Asymmetric α-fluorination of carboxylic acids catalysed by [2.2]PC isothiourea catalsyt **26**. b) Asymmetric cyclopropanation catalysed by $Rh_2(PC)_4$ **27**.

1.4.4 Resolution methods

Access to enantiomerically pure derivatives of [2.2]PC is essential for constructing site-selective and enantioselective catalysts. Resolution is accomplished by reacting a racemic mixture of [2.2]PC enantiomers with a chiral auxiliary to form two diastereoisomers. The differing chemical properties of diastereomers render them separable with generic purification methods like chromatography or recrystallisation. Afterwards, the auxiliary is removed to yield the two pure enantiomers (Scheme 10).

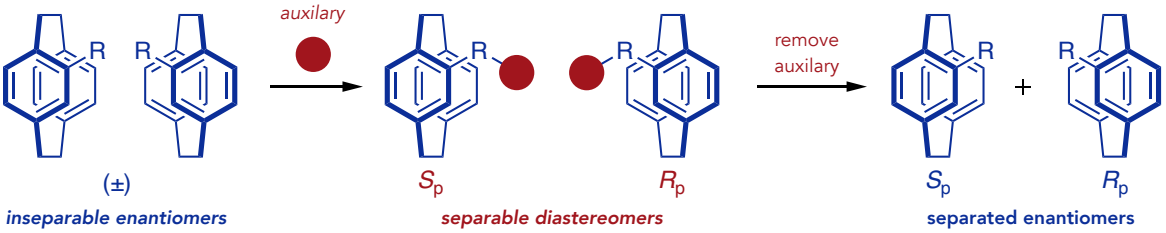

Scheme 10: Simplified schematic for the resolution of [2.2]PC enantiomers with chiral derivatisation.

Salt formation between 4-carboxy[2.2]paracyclophane **28** and (*S*)-NPEA **29** delivers diastereomeric salts separable through recrystallisation. The S_p,*S* salt crystallises from solution while the R_p,*S* salt is collected in the filtrate (Scheme 11).[47] Subsequent neutralisation of the salts delivers both enantiomers of the salt in 99% ee each. This technique relies on acid-base interactions to work, requiring the [2.2]PC derivative to possess an acidic or basic residue. When the right chiral auxiliary partner is chosen, salt formation can be

simple. However, purification relies solely on recrystallisation as diastereomeric salts can be difficult to separate by chromatography. This method is also based on luck that the two diastereomeric salts have vastly different solubilities. A range of chiral auxiliaries must therefore be tested to ensure a pure diastereomeric salt crystallises rather than the mixture.

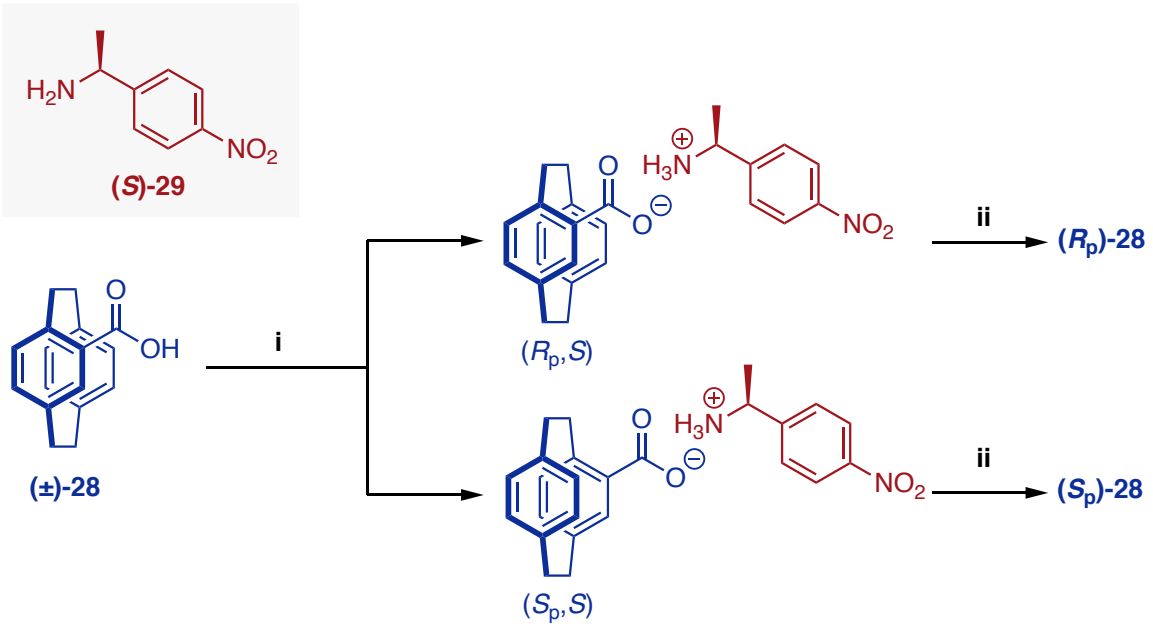

Scheme 11: Resolution method of **28**. i) Salt formation with (*S*)-NPEA **29** and recrystallisation. ii) Neutralisation with HCl.

Covalent derivatisation is also possible by esterification with chiral alcohols. Dicarboxylic acid derivative **30** can be resolved by esterification with an alcohol derivative of camphanic acid **31** (Scheme 12).[48] Esterification is achieved through formation of the acyl chloride derivative of **30** and coupling to **31**. Separation is performed with flash chromatography and the auxiliary is removed by de-esterification under basic conditions to yield the S_p diacid in 99% ee and the R_p diacid in 97% ee. This method makes purification more accessible as both chromatography and recrystallisation of the diastereoisomers is achievable. Returning the enantiomers is more difficult compared to salt formation, as harsher reaction conditions must be used to remove the auxiliary rather than a simple acid-base neutralisation reaction.

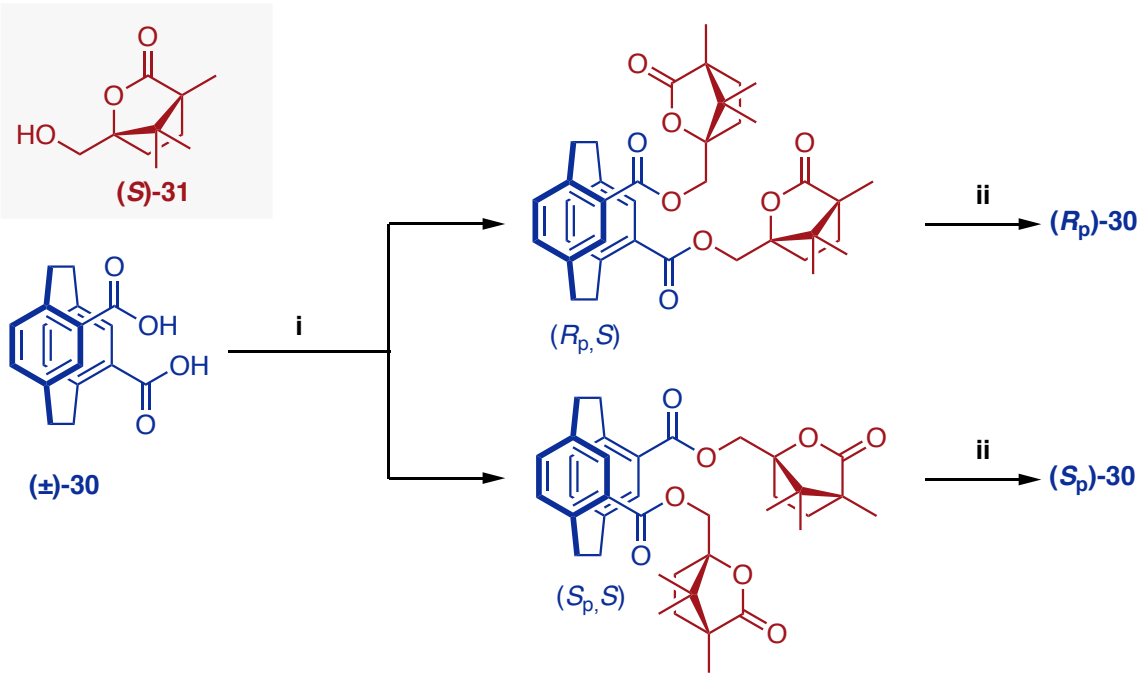

Scheme 12: Covalent resolution of **30**. i) Esterification with chiral alcohol **31** and separation via column chromatography. ii) Hydrolysis in *t*BuOK/H_2O/THF.

1.5 Aims of this research

Chiral Rh(II) paddlewheel catalysts provide a way to achieve highly selective C-H functionalisation in organic synthesis. Rh(II) catalysts possessing planar chiral ligands are scarce and the influence of planar chirality on Rh(II) catalysed C-H functionalisation is largely unexplored. This research will aim to prepare enantiopure [2.2]PC ligands for the synthesis of Rh(II) paddlewheel catalysts and investigate their activity and selectivity in C-H insertion using model reactions.

Known reactions were used to prepare the desired [2.2]PC regioisomers through bromination and subsequent Friedel-Crafts acylation to form (±)-**32** (Scheme 13). Resolution of the two [2.2]PC enantiomers was crucial prior to catalyst synthesis to ensure a single enantiomer of the catalyst is formed. This research attempted a covalent-style resolution (**i**). Oxidative hydrolysis of the quaternary ammonium salt was also attempted (**ii**), which would afford the enantioenriched carboxylic acid. Rh(II) paddlewheels were then prepared with the enantioenriched ligands to afford the first set of catalysts (**iii**). Catalyst functionalisation could then be explored using the aryl bromides for Suzuki coupling (**iv**), if unsuccessful this was performed on the ligand prior to complexation. Model nitrene insertion reactions such as the cyclisation of **15** were then used to determine if the catalysts were active and if any enantioselectivity was demonstrated.

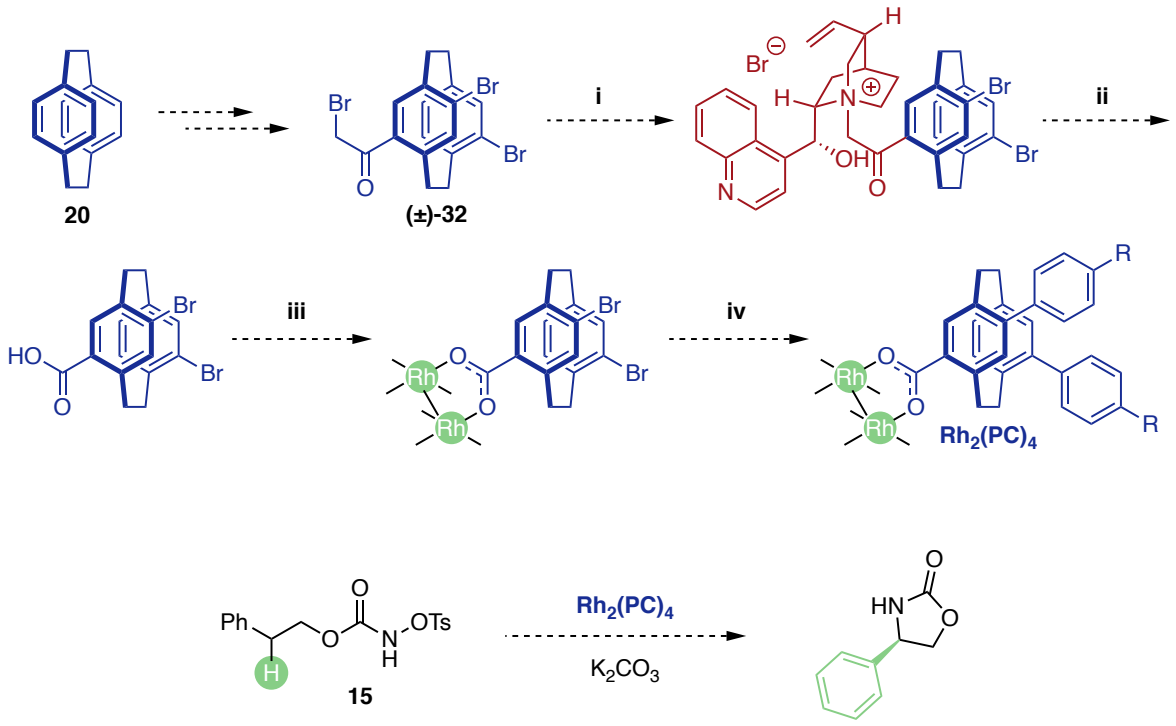

Scheme 13: Synthetic scheme for a [2.2]PC Rh(II) catalyst and its use in nitrene insertion.

Results and Discussion

2.1 Synthesis and resolution of [2.2]paracyclophane carboxylic acids

Our first objective was to synthesise enantiopure [2.2]PC carboxylic acid ligands **33**, **34** and **28** that we would use to prepare the Rh(II) catalysts. (Scheme 14). Two of these derivatives possess bromo substituents that would allow further derivatisation discussed in Section 2.3.

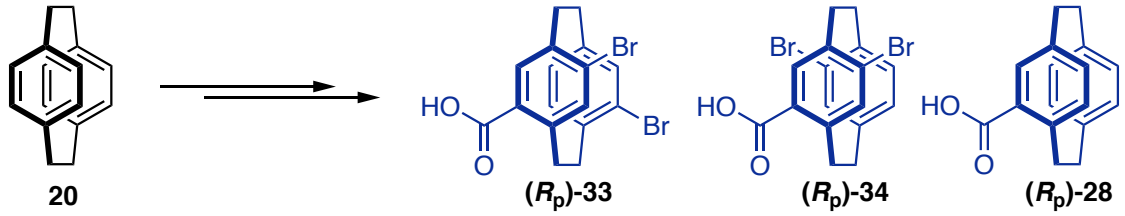

Scheme 14: Simplified synthetic scheme for ligand synthesis of carboxylic acids (R_p)-4,12-dibromo-7-carboxy[2.2]paracyclophane **33**, (R_p)-4,15-dibromo-7-carboxy[2.2]paracyclophane **34** and (R_p)-7-carboxy[2.2]paracyclophane **28**.

Resolution of (±)-**33** has been achieved before, by salt formation to make (S_p)-**35**, then recrystallisation, and neutralisation to afford (S_p)-**33** (Scheme 15).[49] We were interested if the carboxylic acid could instead be installed by attempting a covalent resolution on (±)-**32** with a chiral tertiary amine to yield **36**, then performing an oxidative cleavage of the chiral auxiliary to yield enantiopure **33** (Scheme 16). This route has not been attempted before and we hoped covalently linking our chiral resolving agent would increase our chances at separation as crystallisation and chromatographic methods are both possible. Both scaffolds (±)-**33** and (±)-**32** were therefore synthesised to compare methodologies.

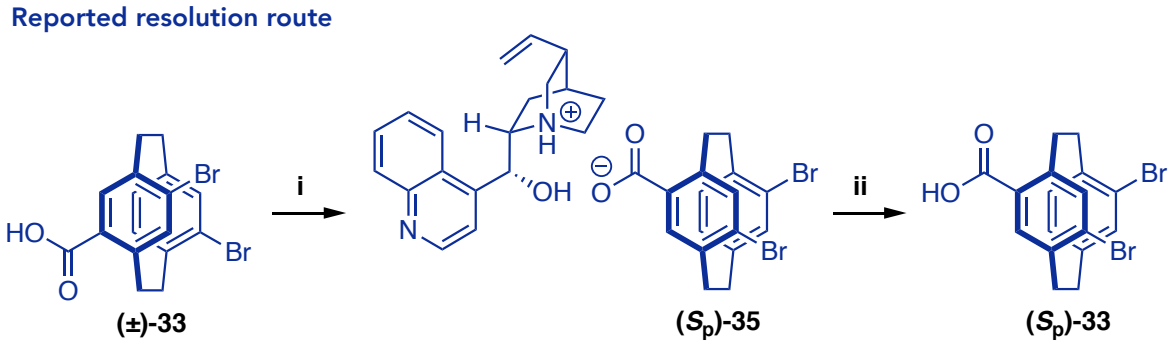

Scheme 15: Resolution of (±)-**33**. i) (–)-Cinchonidine, EtOH. ii) Aq. HCl.

Our proposed resolution route

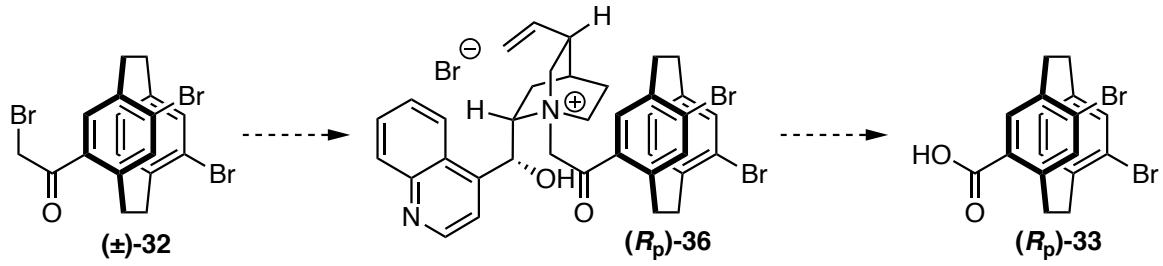

Scheme 16: Our proposed covalent resolution method for the separation of (R_p)-**36** through (±)-**32**.

Bromination

The first step of the synthetic route was bromination. Dibromination of [2.2]PC is a well-studied reaction that leads to three main regioisomers: *pseudo-para* **37**, *pseudo-ortho* (±)-**38** and *pseudo-meta* (±)-**39**.[50] Two literature methods exist that differ by the relative amounts of each regioisomer produced. Iron-catalysed bromination typically furnishes **37** in up to 38% yield, alongside (±)-**38** (16%) and (±)-**39** (6%).[51] Uncatalysed gives a mixture of **37** and (±)-**39** in 34% and 43% yield respectively.[52] Both regioisomers **37** and (±)-**39** were required for ligand synthesis, so the latter method was used (Scheme 17).

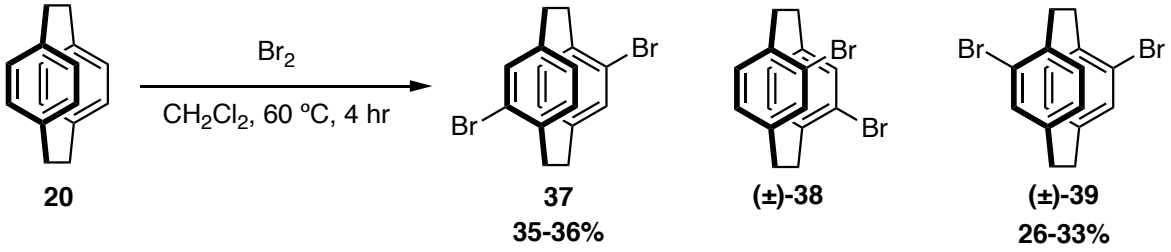

Scheme 17: Reaction conditions used to synthesise **37** and (±)-**39**.

Bromination was achieved by refluxing **20** with 4 equivalents of Br_2 in CH_2Cl_2 for 4 hours. Substitution begins by electrophilic attack on a molecule of Br_2 by the first deck followed by loss of a proton to restore aromaticity (Scheme 18). Attack of the second deck can occur with varying regiochemistry. Attack *pseudo-para* or *pseudo-ortho* is due to the transannular effect, as the first bromine substituent is *ortho*/*para* directing. Attack *pseudo-meta* occurs when the two aromatic decks behave as separate benzene rings, and no directing effects are present. Due to its low solubility, **37** can be isolated by cooling the reaction mixture and filtering off the white crystals to give **37** in 25-26% yield. Another crop of **37** and (±)-**39** are then isolated from the filtrate by a series of recrystallisation steps. Typically, mixtures of **37** and (±)-**39** can be purified by recrystallisation in 1,4-dioxane and crude mixtures of (±)-**39**

can be purified by recrystallisation in ethanol or isopropyl alcohol. Yields for **37** were consistent at 35-36%, however yields were lower for (±)-**39** at 26-33% if higher purity was desired. Recrystallisation of (±)-**39** always sacrifices some material in the filtrate, alongside (±)-**38** that could not be further separated from each other.

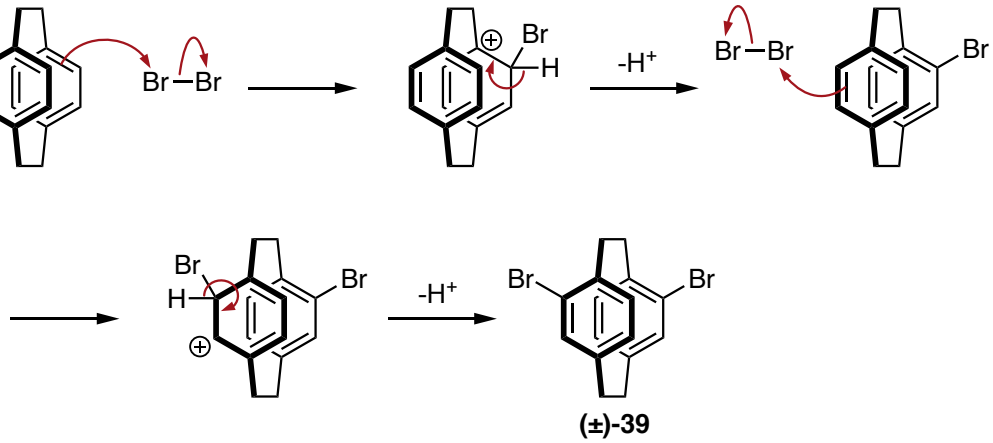

Scheme 18: Mechanism for bromination of **20** to afford (±)-**39**.

Isomerisation

As (±)-**38** is not easily isolated in appreciable yields from the bromination step, it must be produced through the isomerisation of **37**, which is achieved by heating it to temperatures >180 °C. The original method for isomerising **37** to (±)-**38** heats a suspension of **37** in triglyme to 230 °C for three hours, requiring (±)-**38** to be isolated from the filtrate by vacuum distillation. A more user-friendly microwave method was used instead, that simplifies workup and delivers similar yields to the triglyme method (Scheme 19).[53]

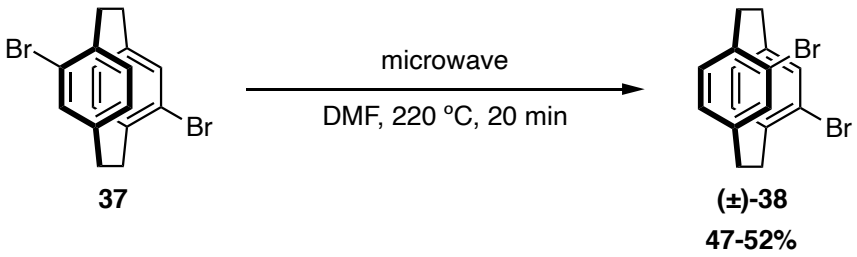

Scheme 19: Reaction conditions used for the preparation of (±)-**38**.

Heating a suspension of **37** in DMF at 220 °C for 20 minutes causes scission of the ethylene bridges, forming a diradical intermediate (Scheme 20).[54] This allows free rotation about the rings and interconversion between regioisomers **37** and (±)-**38** through an equilibrium process. Cooling the reaction mixture reforms the ethylene bridges and allows **37** to precipitate out while (±)-**38** remains in solution. Filtering off **37** and removing the DMF with

water washing cycles allows (±)-**38** to be isolated from the filtrate in 47-52% yield. Recovered **37** may then be used in further microwave cycles until fully converted to (±)-**38**.

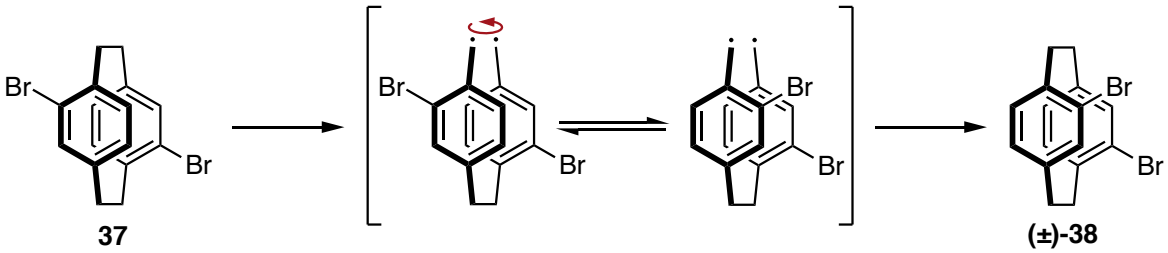

Scheme 20: Proposed mechanism for isomerisation of **37** to (±)-**38**.

Friedel-Crafts acylation

Friedel-Crafts acylation is another fundamental reaction of [2.2]PC derivatives that allows the direct installation of a carbonyl functionality onto a single deck. Direct preparation of the carboxylic acid (±)-**33** is achieved by reacting (±)-**38** with oxalyl chloride (Scheme 21). Regiochemistry of substitution is controlled by the bromine substituents that direct *para* on the same ring. Once substitution occurs on one ring, the system is sufficiently deactivated and doesn't undergo further reaction.

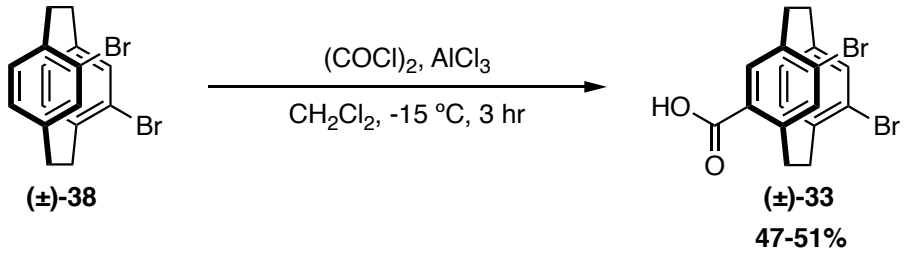

Scheme 21: Reaction conditions to prepare (±)-**33**.

Initially, the electrophile and $AlCl_3$ are premixed together in CH_2Cl_2 to form a highly electrophilic oxonium species, (±)-**38** is then added, and it attacks the electrophile (Scheme 22). A proton is lost to restore aromaticity and deliver a keto-acid species that decomposes to deliver the acyl chloride (±)-**40**.[55] Quenching the reaction with H_2O delivers the carboxylic acid (±)-**33** whereas, quenching with MeOH delivers the methyl ester. The crude mixture could not be purified by acid/base extraction and required silica-gel chromatography. Yields for this reaction were always poor, never reaching far above 50% yield.

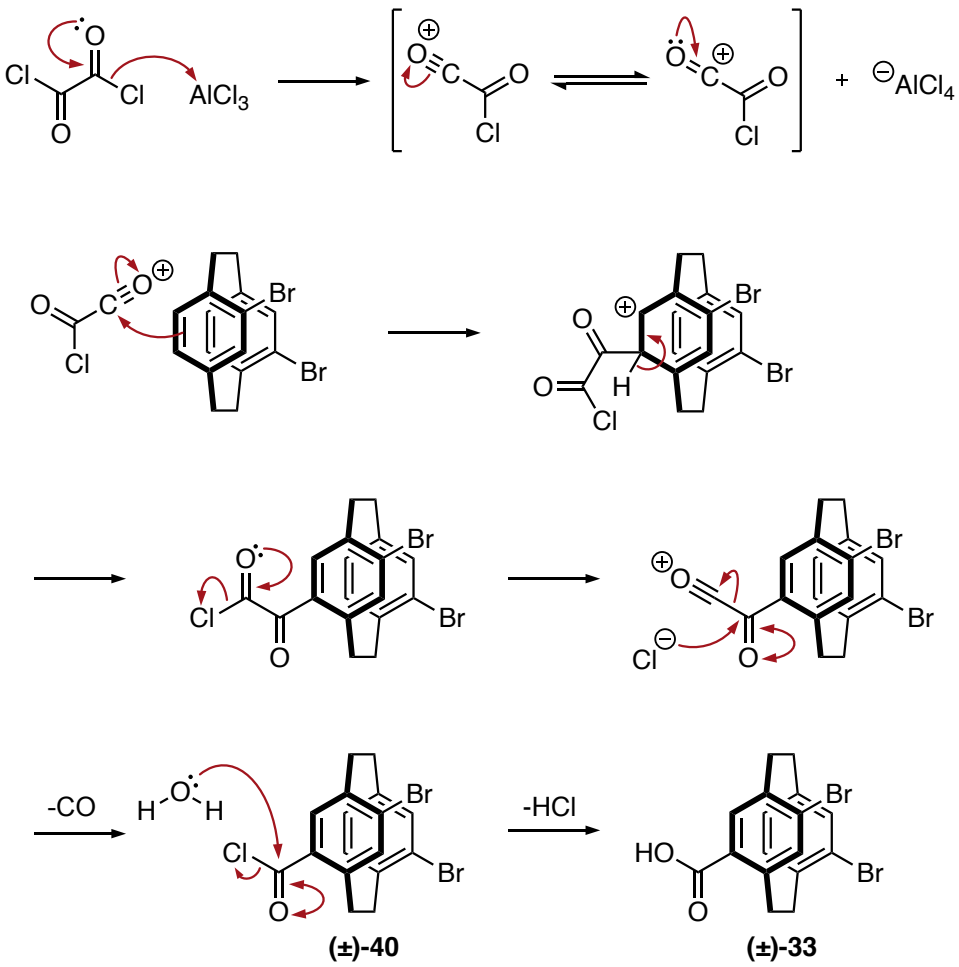

Scheme 22: Proposed mechanism for the formation of (±)-**33**.

It was expected the proton *pseudo-geminal* to the carboxyl group (H-16) would be one of the more deshielded signals in the ^{1}H NMR spectrum. This is due to the transannular effect that allows Lewis basic substituents on [2.2]PC to act as an internal base. This makes the proton *pseudo-geminal* to the substituent more acidic and deshields it. Unexpectedly, H-16 of (±)-**33** was one of the more shielded aromatic signals at 6.62 ppm. This is most likely due to the π cloud of the C=O group that shields H-16, rather than making it more acidic. An X-ray crystal structure of (±)-**33** was obtained that shows the correct orientation of the carboxyl group to allow the π cloud of the C=O to overlap with H-16 (Figure 12).

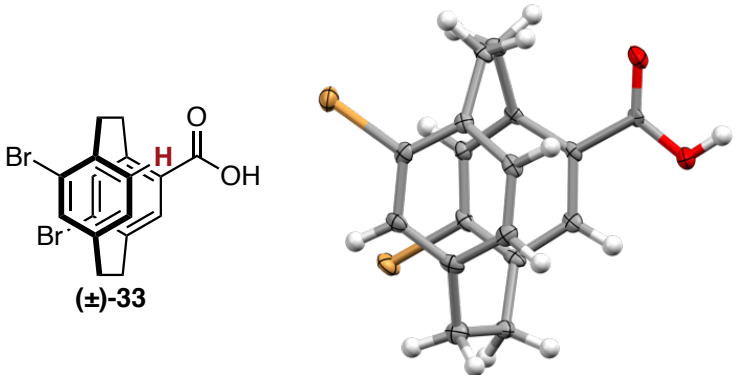

Figure 12: X-ray crystal structure of (±)-**33**, C = grey, H = white, O = red, Br = brown. Thermal ellipsoid probability level 50%.

We also wanted to prepare bromoacetyl derivative (±)-**32** that would allow us to investigate a covalent resolution step. Preparation is analogous to that of (±)-**33**, but the electrophile was changed to bromoacetyl bromide **41**, that installs an α-halogen carbonyl functionality rather than a carboxylic acid (Scheme 23).

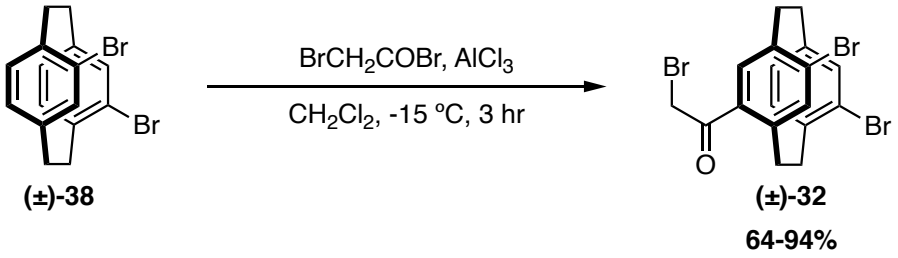

Scheme 23: Reaction conditions for the preparation of (±)-**32**.

This mechanism is simpler compared to the one for (±)-**33**, as once aromatic substitution occurs the reaction is complete and no keto-acid species is formed (Scheme 24). Purification is performed by recrystallisation in acetone delivering more satisfactory yields of 64-94%. This is possibly due to the nature of the electrophile **41**, which is much more reactive than oxalyl chloride. Preparation of (±)-**33** also requires an extra mechanistic step to decompose the keto-acid chloride into the acid chloride through loss of CO and HCl. While preparation of (±)-**32** only has three mechanistic steps.

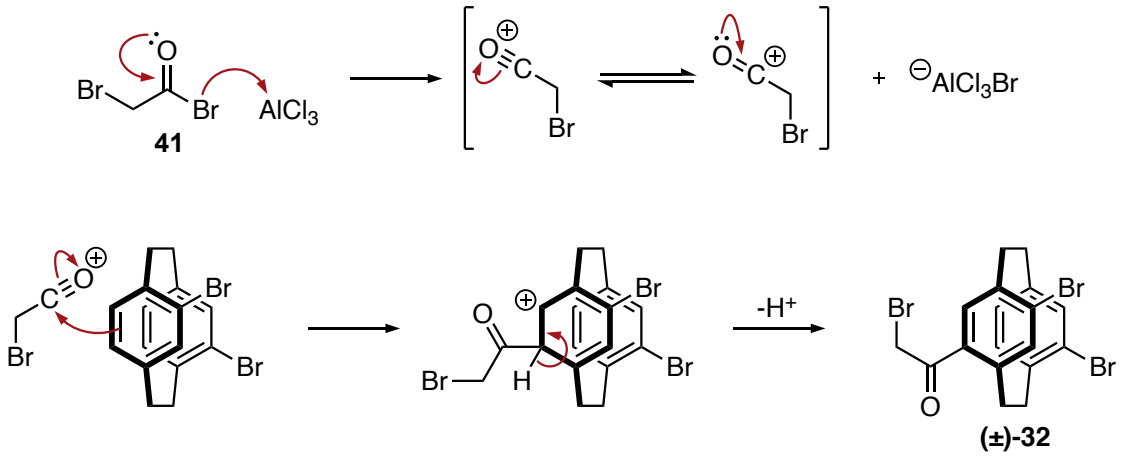

Scheme 24: Proposed mechanism for the synthesis of (±)-**32**.

Friedel-Crafts reactions were then attempted on (±)-**39** and **20** to deliver the next scaffolds (Scheme 25). Mechanistic details for these reactions are identical to that for (±)-**32**, but the reaction to produce (±)-**43** isn't directed by a bromo substituent. Synthesis of both scaffolds were as simple as the first and purification was achieved through simple silica-gel chromatography, delivering (±)-**42** in 65-77% yield and (±)-**43** in 51-77% yield.

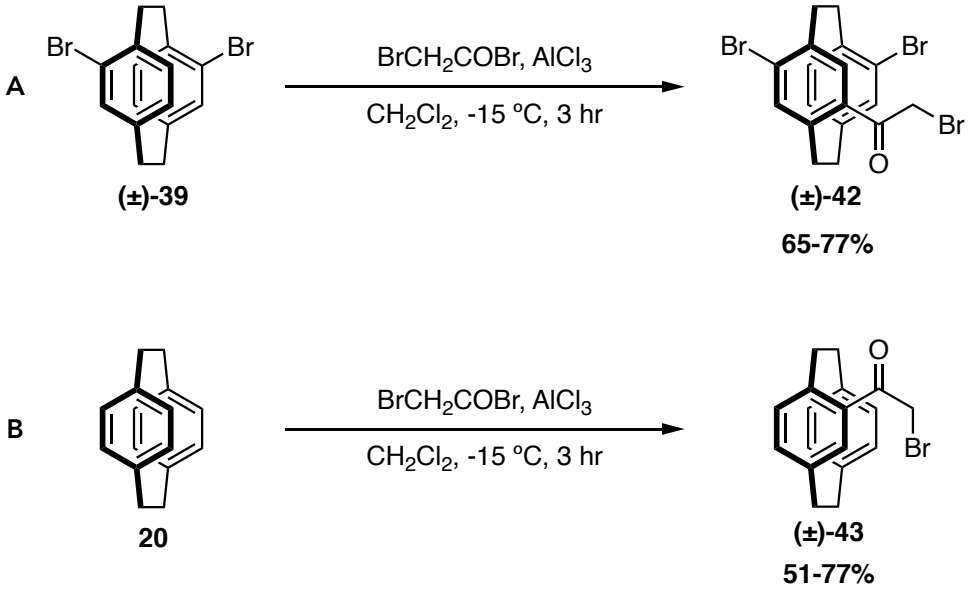

Scheme 25: a) Reaction conditions for the synthesis of (±)-**42**. b) Reaction conditions for the synthesis of (±)-**43**.

To extend this methodology, the reaction conditions were briefly attempted on a range of [2.2]PC derivatives previous members of our group had prepared. This would potentially allow the resolution of a range of different substituted [2.2]PCs. From the derivatives depicted in Scheme 26 only the mono substituted bromide (±)-**44h** underwent reaction. Changing the Lewis acid to $TiCl_4$ was also briefly tried for (±)-**44f** but this still provided no reaction.

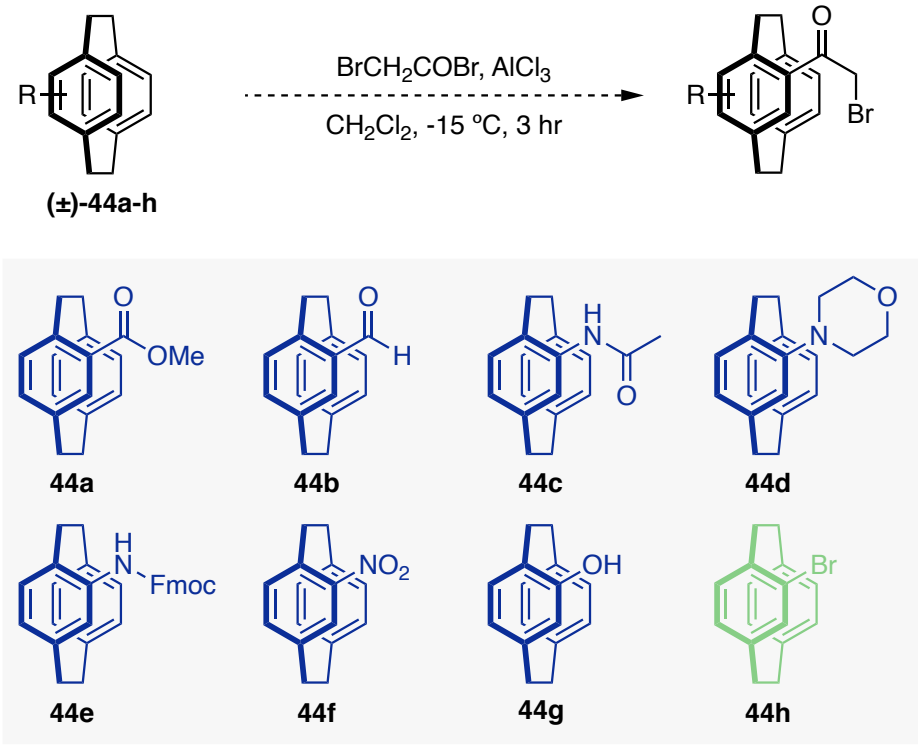

Scheme 26: Reaction conditions for Friedel-Crafts acylation of [2.2]PC derivatives (±)-**44a-h**.

The failure of electron withdrawing derivatives was understandable as they are deactivated. Lack of reaction of electron donating derivatives (±)-**44d** and (±)-**44g** was more surprising, especially since acylation using acetyl chloride has been reported for (±)-**44g**.[52] The lack of reaction could potentially be caused by the larger bromo substituent of the electrophile, that may hinder electrophilic attack, compared to smaller electrophiles like acetyl chloride. Introducing carbonyl functionalities onto substituted [2.2]PC derivatives is most commonly performed by Reiche formylation, which has been performed by our group on derivatives (±)-**44a** and (±)-**44f**.[56] The introduced aldehyde can then be used for the desired functional group interconversions. Only one set of conditions was tried for most scaffolds so it is highly likely substitution could be achieved by either increasing temperature or using different Lewis acid catalysts.

Although bromide (±)-**44h** did react, this produced a mixture of two products with identical R_f values, preventing their separation with silica-gel chromatography. The two derivatives could be partially separated by recrystallising in EtOAc, but never in high enough purity to be fully characterised. Due to successfully making derivatives (±)-**32**, (±)-**42** and (±)-**43**, these reactions were not investigated further.

Resolution

Resolving the two enantiomers of the carboxylic acids was the crucial step of this project. Enantiomerically pure ligands were required for Rh(II) paddlewheel synthesis, if a racemic ligand was used it could potentially create up to 64 diastereoisomers. Many different resolution methods exist for [2.2]PC as outlined in Section 1.4, however the focus was on salt formation of (±)-**33** or covalent resolution of (±)-**32** using the chiral amine auxiliaries depicted in Figure 13. Amines **45a-d** are alkaloids naturally derived from the same *Cinchona* tree, while **46a** and **46b** are derived from the *Nux vomica* plant. Each amine is enantiomerically pure and can be reacted with a racemic mixture of enantiomers to form one pair of diastereoisomers.

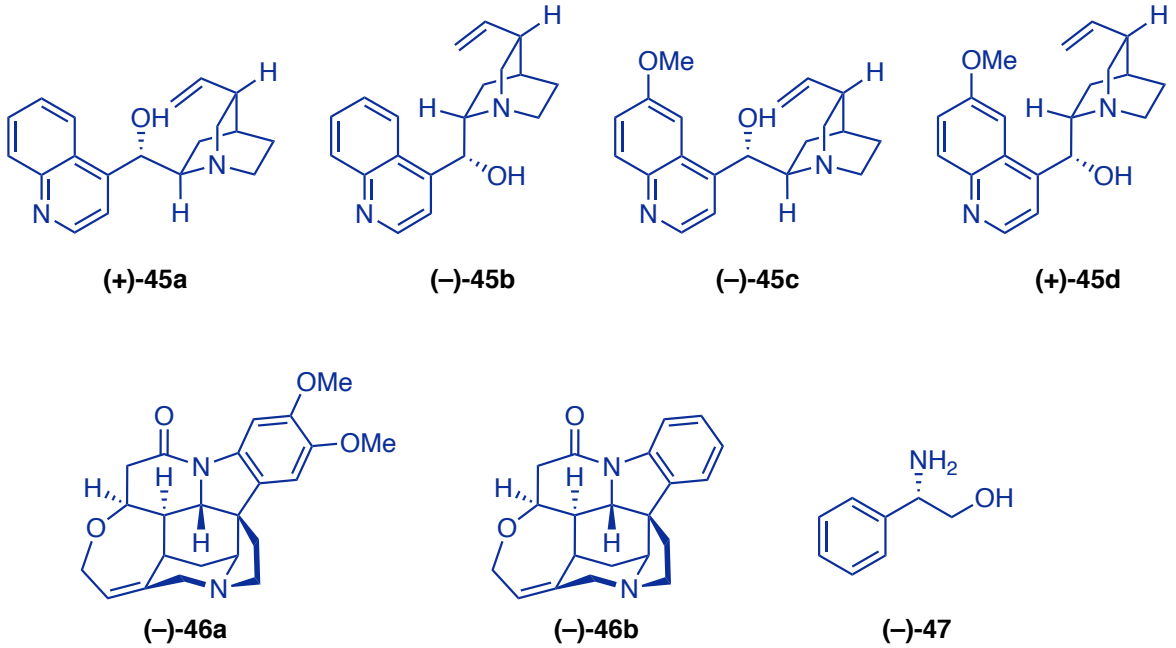

Figure 13: Common chiral amines used for chiral derivatisation: (+)-cinchonine **45a**, (–)-cinchonidine **45b**, (–)-quinidine **45c**, (+)-quinine **45d**, (–)-brucine **46a**, (–)-strychnine **46b**, (–)-phenylalaninol **47**.

Resolution of (±)-**33** was first attempted by salt formation with the chiral tertiary amine (–)-cinchonidine **45b** (Scheme 27). The [2.2]PC acid and amine were heated together in

EtOH and cooled to room temperature, however no precipitate formed. ^{1}H NMR showed diastereoisomer formation had occurred, but separation couldn't be achieved.

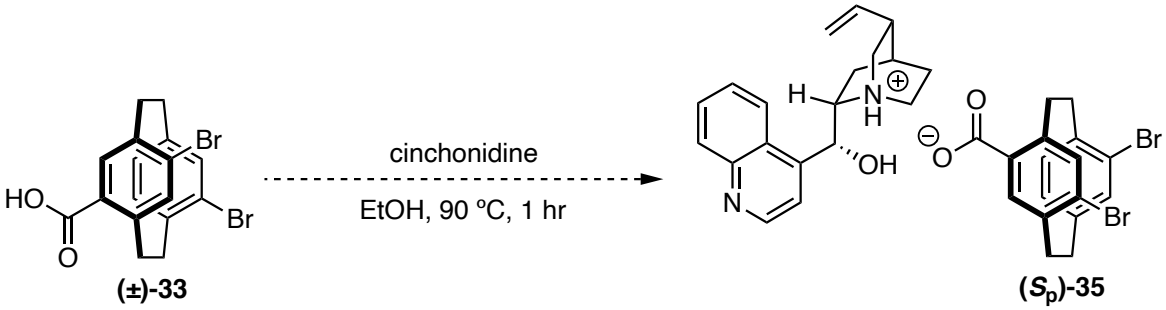

Scheme 27: Attempted reaction conditions to produce (S_p)-**35**.

Our group had created a resolution procedure for the covalent attachment of (+)-cinchonine **45a** to (±)-**43**, to yield two diastereoisomers separable through precipitation of a single quarternary ammonium salt (R_p)-**48** (Scheme 28). The salt was then used in a Bischler-Möhlau indole synthesis, showing the C-N bond could be cleaved and replaced with a C-C bond to produce (R_p)-**49**.[57] The goal was to perform this methodology on derivatives (±)-**32**, (±)-**42** and (±)-**43** but to instead oxidise the C-C bond of the carbonyl.

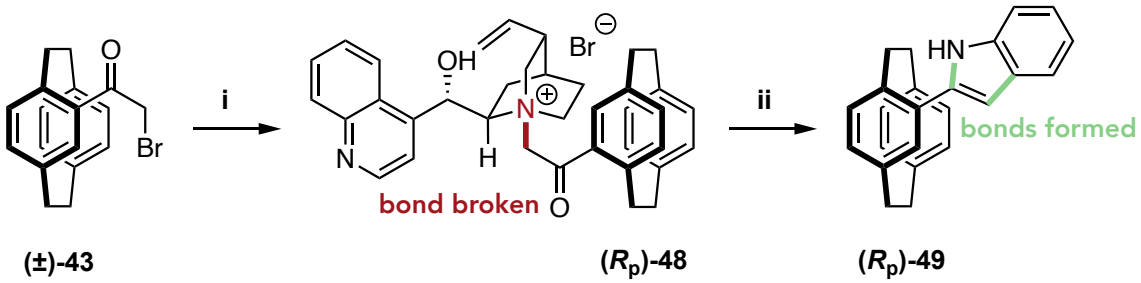

Scheme 28: Resolution of (±)-**43** for a Bischler-Möhlau indole synthesis. i) (+)-Cinchonine. ii) Aniline.

Refluxing a solution of (±)-**43**, and (–)-cinchonidine **45b** together in acetone led to the rapid formation of a white precipitate after a few minutes (Scheme 29). After filtering the solid material, the ^{1}H NMR revealed the solid was a single diasteroisomer (R_p)-**36**, while the filtrate was a mixture.

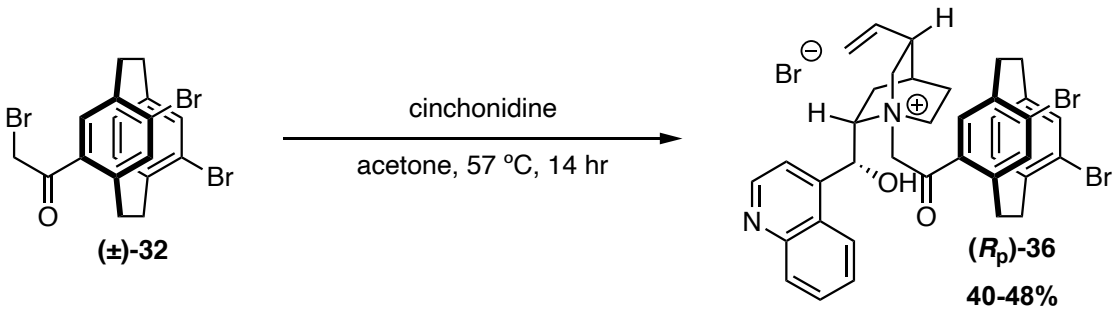

Scheme 29: Reaction conditions used for the resolution of (±)-**32** to form (R_p)-**36**.

The rapid substitution at saturated carbon rather than at the carbonyl is facilitated by the highly reactive α-halogen bond. Carbon-halogen bonds adjacent to carbonyl groups are highly reactive due an orbital mixing effect between the π^* of the C=O bond and σ^* of the C-Br bond (Scheme 30a). Overlap of these two molecular orbitals creates a new low energy LUMO that is highly electrophilic, encouraging substitution at saturated carbon.[58] The analogous mechanism for the synthesis of (R_p)-**36** is shown in Scheme 30b.

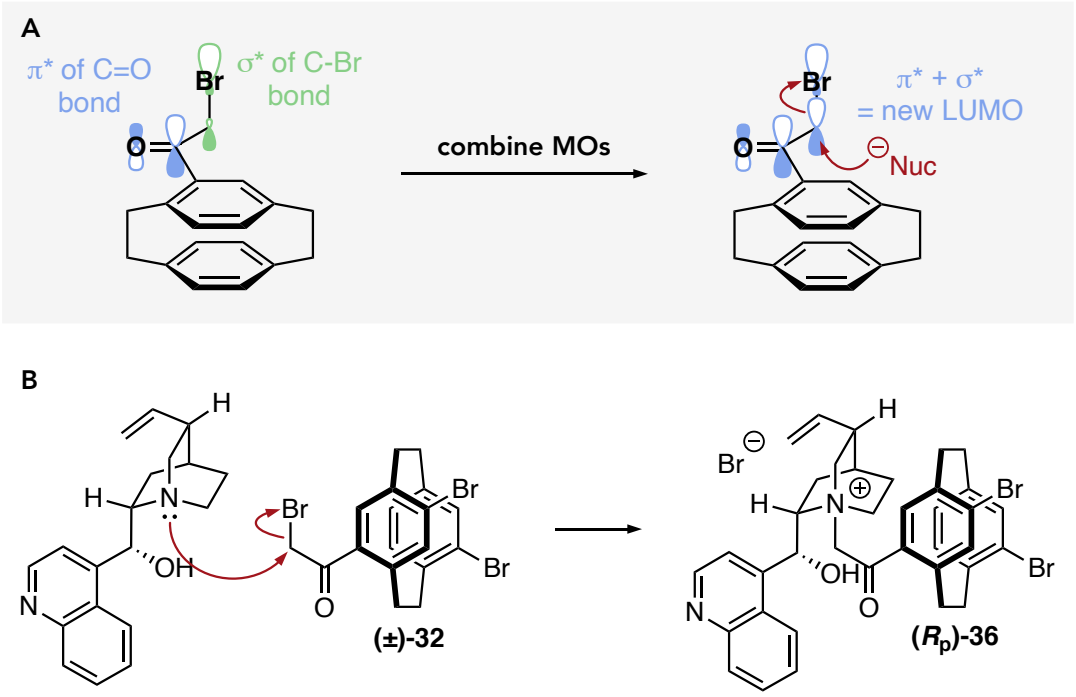

Scheme 30: a) Simplified representation of orbital mixing effects of α-halogen carbonyl compounds. b) Proposed reaction mechanism for the formation of (R_p)-**36**.

The diastereomeric ratio of each fraction could be easily determined by inspection of the aromatic region of the ^{1}H NMR spectrum (Figure 14). The aromatic proton *ortho* to nitrogen of cinchonidine (H2') appears as a doublet at 9.01 ppm for the diastereoisomer in the solid portion and 8.97 ppm for the diastereoisomer in the liquid portion. A further crop of the first

diastereoisomer could be obtained by adding Et_2O to the filtrate and letting it stand overnight. The relative stereochemistry of each diastereoisomer discussed in this section is inferred from the Rh(II) crystal structures discussed in Section 2.2.

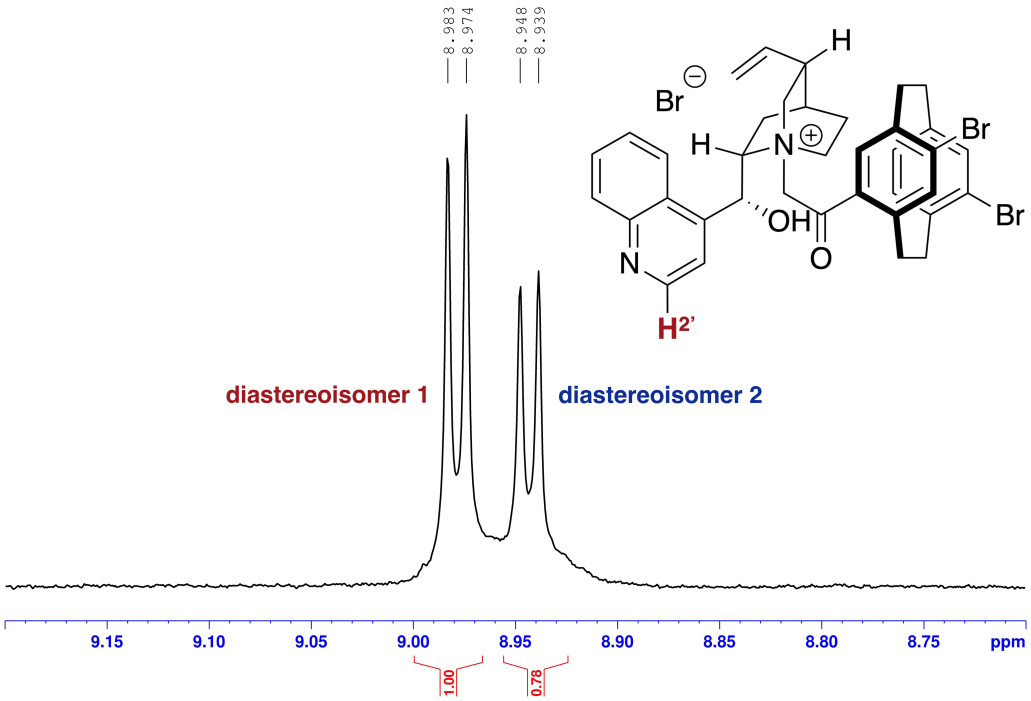

Figure 14: Region of a ^{1}H NMR spectrum depicting H2' for two diastereoisomers that was used to determine the diastereomeric ratio of (R_p)-**36** and (S_p)-**36**.

Repetition of the Rowlands' group method for covalent resolution of (±)-**43** was attempted (Scheme 31). The method for separation was different to the above as no precipitate formed from the reaction mixture overnight. Adding Et_2O and MeOH to the mixture was required to precipitate the first diastereoisomer (R_p)-**48** from solution. (–)-Cinchonidine was also briefly tried to resolve (±)-**43**, however no precipitate could be formed using the same conditions.

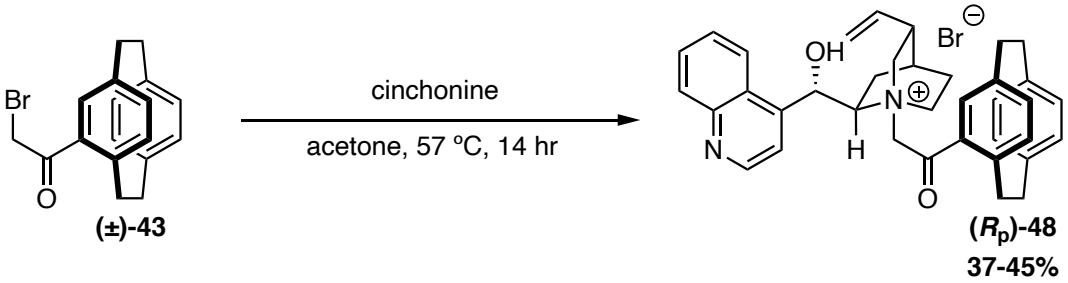

Scheme 31: Reaction conditions used to produce (R_p)-**48**.

The *pseudo-meta* regioisomer (±)-**42** was more problematic to resolve than the previous two compounds. Attempting resolution with (–)-cinchonidine produced a precipitate overnight but it was identified as a partially reacted mixture, containing unreacted (±)-**42**, (–)-cinchonidine and two diasteroisomers (Scheme 32). Reaction duration was then extended to 48 hours but still failed to reach completion. Changing the solvent to $CHCl_3$ to allow complete dissolution of all reagents was tried, also failing to improve the result. Changing the alkaloid was then investigated, (+)-cinchonine **45a**, (–)-quinidine **45c** and (+)-quinine **45d** were all tried garnering the same results of incomplete reaction.

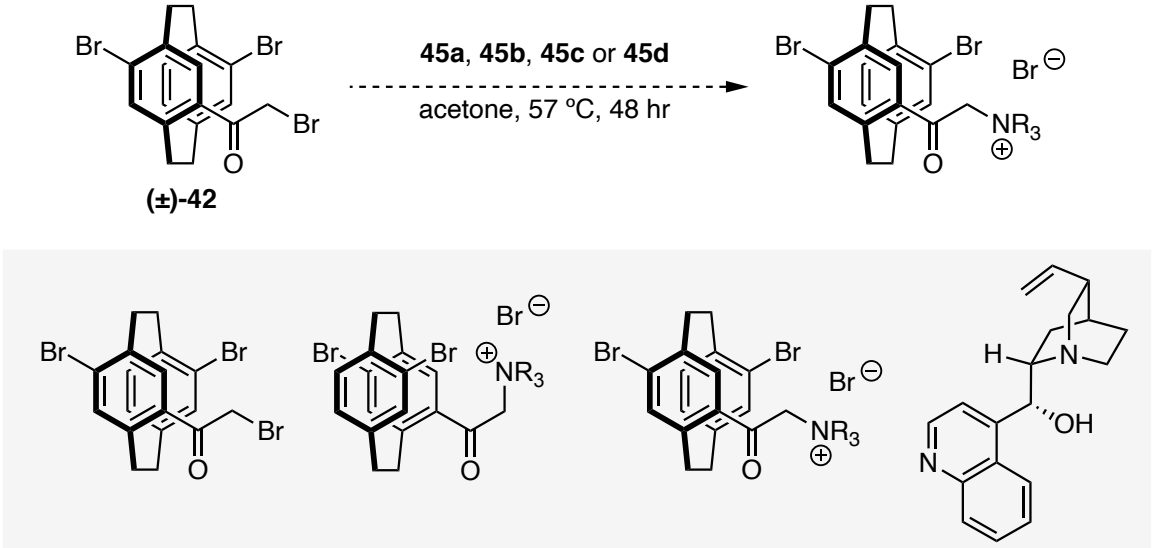

Scheme 32: Failed reaction conditions for resolving (±)-**42** (top) and the products commonly identified in each crude ^{1}H NMR spectrum (bottom).

Different chiral amines were then considered such as (–)-brucine **46a** and (–)-strychnine **46b**, these tertiary amines were preferred as they would form quarternary ammonium salts upon reaction with (±)-**42**. We believed the electron withdrawing effect of the cationic salts was necessary to facilitate cleavage of the C-N bond. We also considered primary amines such as (–)-phenylalaninol **47** but recognised this could potentially require treatment with iodomethane to form a tertiary amine for hydrolysis. Heating a solution of (±)-**42** and (–)-brucine together in $CHCl_3$ overnight then cooling the mixture formed a precipitate (Scheme 33).

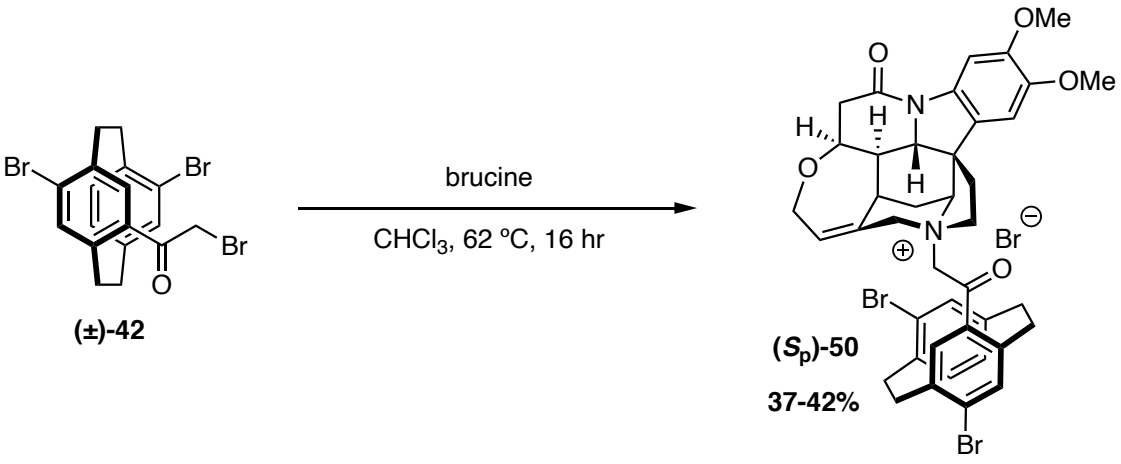

Scheme 33: Reaction conditions used for the synthesis of (S_p)-**50**.

^{1}H NMR revealed the reaction had gone to completion and all brucine had reacted. The precipitate was a 2:1 mixture of diastereoisomers, while the filtrate was also a mixture. An array of recrystallisation conditions were attempted with some providing inconsistent results, however hot DCE and the minimal MeOH provided consistent success with the first diastereoisomer (S_p)-**50** being isolated in 37-42% yield.

We believe the problem with the reactions above can be attributed to the bulk of the *pseudo-meta* derivative (±)-**42** and the sterically demanding *cinchona* alkaloids obstructing substitution. Substitution at saturated carbon is an S_N2 reaction, requiring the tertiary amine to attack the C-Br bond by 180° (Scheme 34). The increased bulk from the bromine substituent *pseudo-ortho* to the bromoacetate group blocks nucleophilic approach from the bottom face of [2.2]PC. This can be seen in a crystal structure obtained of (±)-**42** (Figure 15). As we couldn't change the sterics of (±)-**42**, we needed to change the sterics of the amine. The *cinchona* type alkaloids are more sterically demanding compared to (–)-brucine that has a more bowl-shaped structure and makes the tertiary amine more accessible.

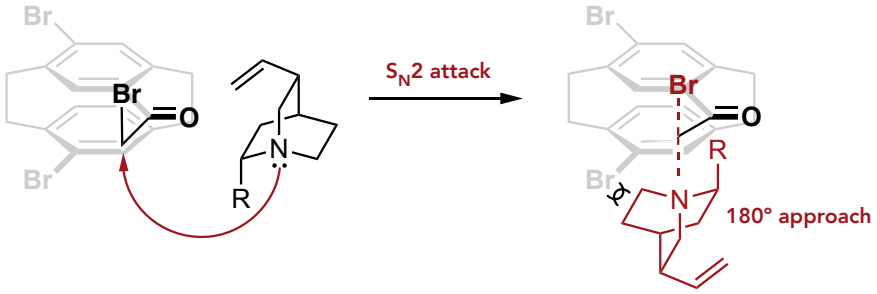

Scheme 34: Simplified schematic for S_N2 nucleophilic approach on (±)-**42**.

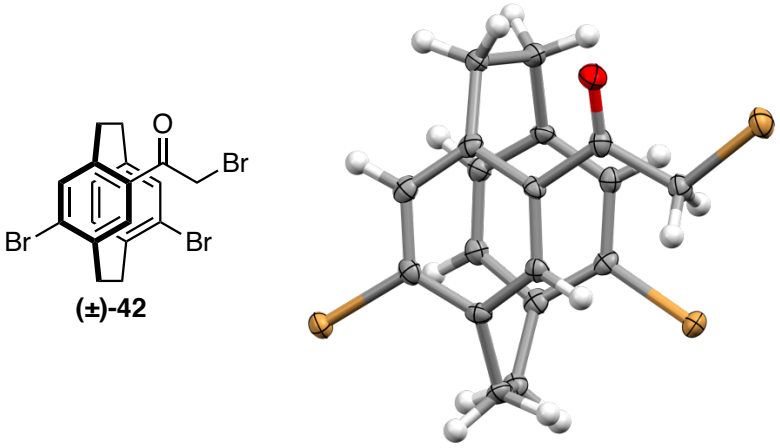

Figure 15: X-ray crystal structure of (±)-**42**, C = grey, H = white, O = red, Br = brown. Thermal ellipsoid probability level 50%.

Oxidation of the quarternary ammonium salts

Successfully resolving the [2.2]PC scaffolds allowed us to now investigate conditions to oxidise the resolved salts to obtain the enantioenriched carboxylic acids. We wanted to mimic a haloform reaction, which is a C-C bond cleavage reaction due to the over halogenation of an α-carbonyl (Scheme 35).[59] The reaction is performed under basic conditions to achieve multiple halogenation, as halogenation in acid only occurs once. When no α-hydrogens remain a hydroxide anion attacks the carbonyl, expelling a $^{-}CBr_3$ anion as the leaving group and delivering a carboxylate salt.

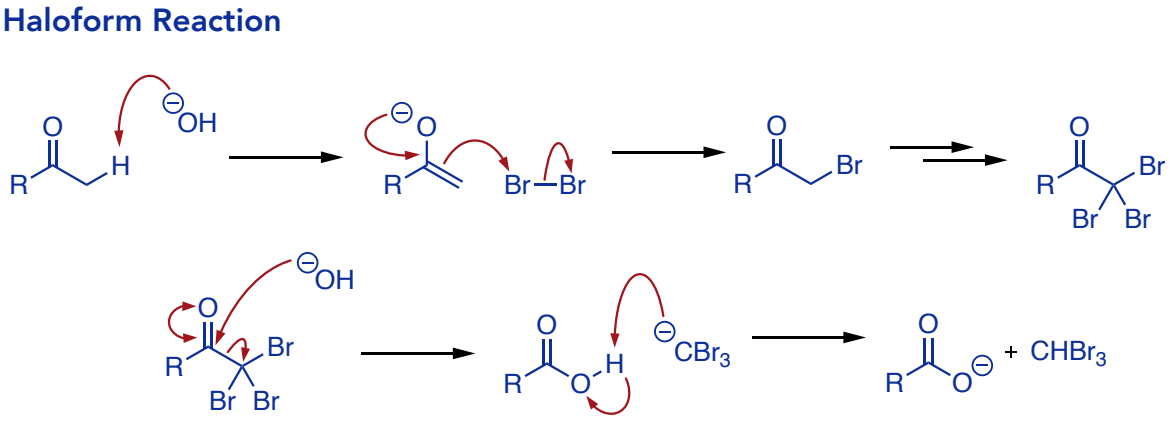

Scheme 35: General mechanism for the haloform reaction.

We opted for a green approach that avoided using organic solvents and instead used water as the reaction medium. The conditions used *t*-BuOOH as the oxidising agent rather than a halogen.[60] The oxidation of 4-acetyl[2.2]PC to 4-carboxy[2.2]PC has been performed using *t*-BuOOH before, suggesting this method would give us a higher chance of success.[61] The

original conditions used a reaction molarity of 8.3 M, which created issues with the viscosity of our reaction mixture. We opted to dilute the reaction to 1.0 M and monitor it with TLC. Heating salt (R_p)-**36** at 90 °C overnight in the presence of *t*-BuOOH resulted in complete reaction and the desired carboxylic acid (R_p)-**33** was obtained in excellent yield (Scheme 36).

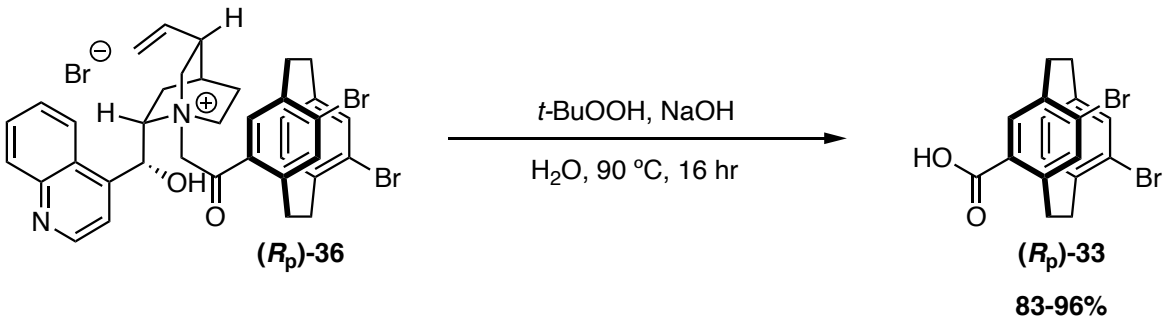

Scheme 36: Reaction conditions used for the synthesis of (R_p)-**33**.

We originally thought the reaction would work by a simple mechanism where hydroxide ion attacks the carbonyl position and expels methyl cinchonidine as the leaving group shown in Scheme 37.

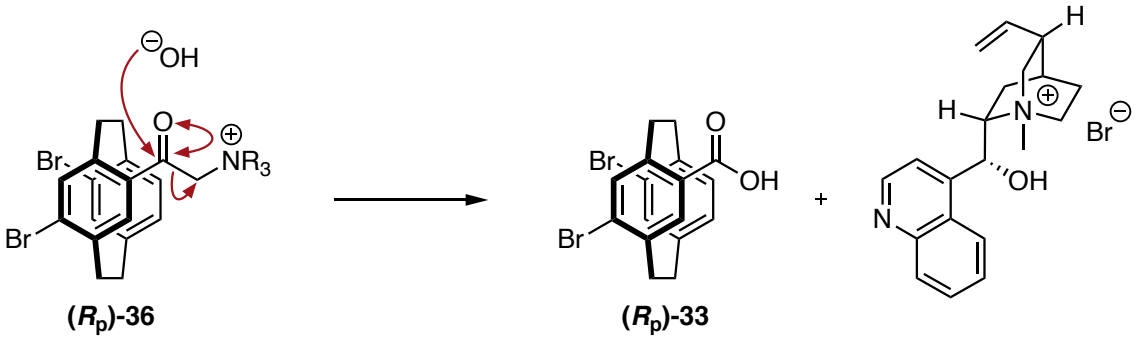

Scheme 37: First proposed mechanism for the synthesis of (R_p)-**33**.

However, the requirement for peroxide in the reaction suggests a more complex radical mechanism is responsible. The reaction begins with the formation of a radical peroxide species, then the abstraction of an α-hydrogen to yield a radical intermediate (Scheme 38). Radical recombination occurs to give a peroxide species that then oxidises the α-carbon further to give a keto-amide species. We then believe a mechanism similar to keto-acid chloride decomposition occurs. Formation of an oxonium species expels the tertiary amine, followed by attack of hydroxide ion and expulsion of CO to give the acid (R_p)-**33**.

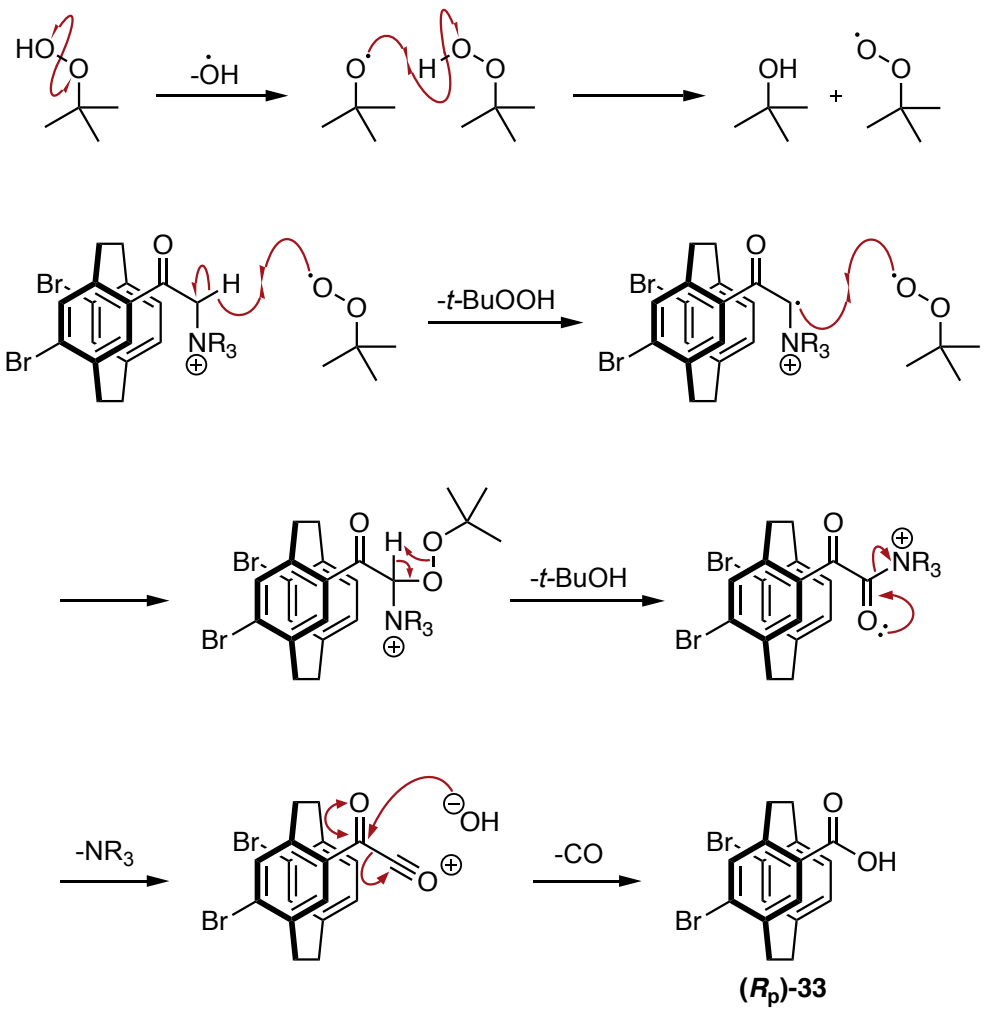

Scheme 38: An alternative proposed mechanism for synthesis of (R_p)-**33**.

Conveniently, the alkaloid is separated from the carboxylic acid, as the pyridine nitrogen is protonated during acidic workup, removing it with the aqueous layer. Using the above conditions on salt derivatives (S_p)-**50** and (R_p)-**48** garnered the same excellent results in both high yields and purity (Scheme 39). Not only had we obtained the enantioenriched acids, but we had developed a new method for a covalent resolution of [2.2]PC carboxylic acid derivatives. The molarity was further modified to 0.2 M for routine repetitions of the reaction, to ensure the reaction was homogenous. Higher yields were obtained if the reaction was run in multiple smaller-scale batches, rather than performing one large scale reaction as yields dropped when performed >1 g scale.

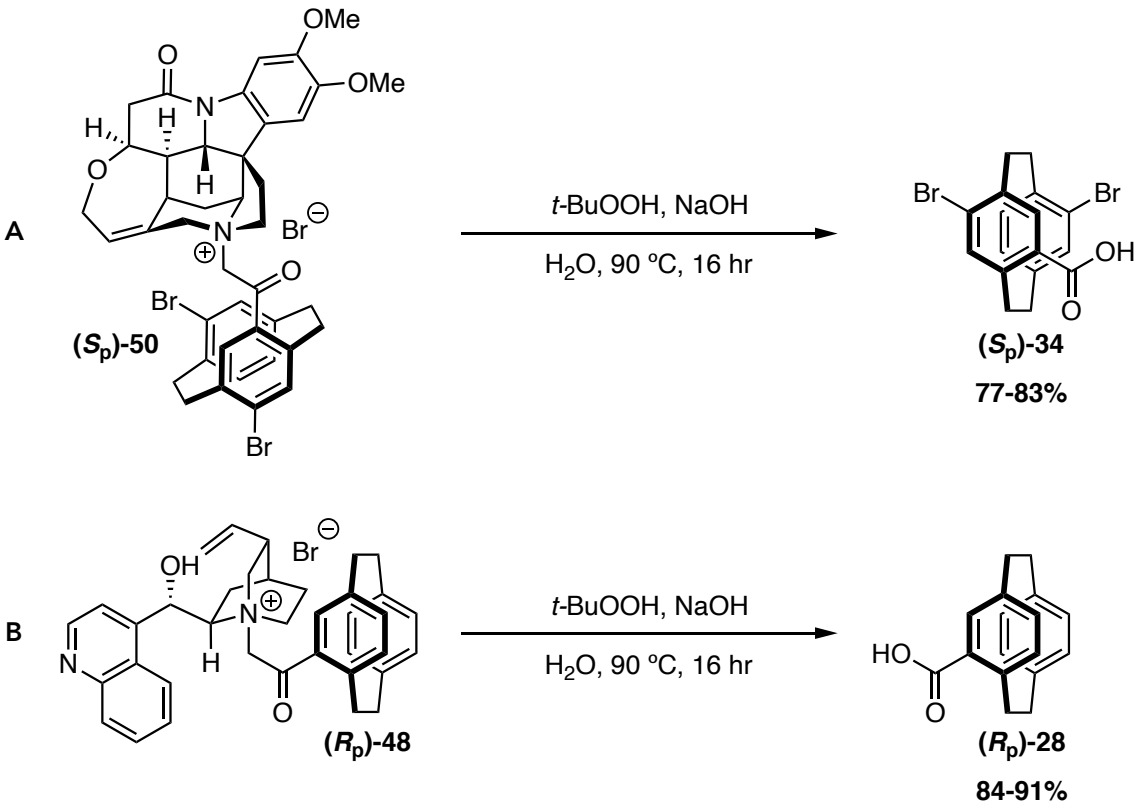

Scheme 39: a) Reaction conditions used for the synthesis of (S_p)-**34**. b) Reaction conditions used for the synthesis of (R_p)-**28**.

Enantiomeric excess measurements

Enantiomeric excess measurements were made using HPLC with a chiral column to determine if the resolution and oxidation had delivered the enantiopure carboxylic acids. The resolved carboxylic acids were converted into their corresponding methyl esters that were then analysed with HPLC (Scheme 40).

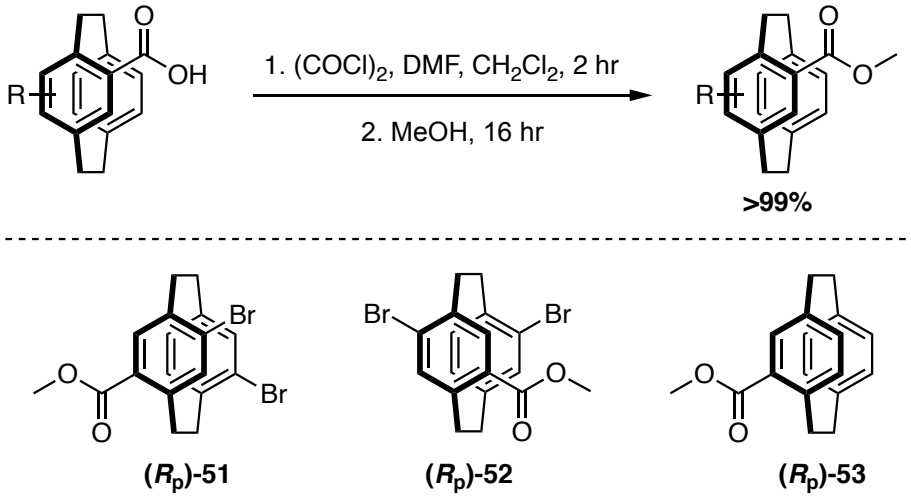

Scheme 40: General reaction conditions used for the synthesis of (R_p)-**51**, (S_p)-**52**, (R_p)-**53**.

Methyl ester conversion was performed as this improved solubility of the compounds in the HPLC solvents compared to that of the carboxylic acids. HPLC conditions for the methyl ester (±)-**51** have also been reported before using an OJ-H chiral column. The mechanism for acid chloride formation is shown in Scheme 41 and begins with formation of the electrophilic Vilsmeier reagent. Attack by (R_p)-**33** occurs, followed by the expulsion of chloride ion. Chloride ion then attacks the carbonyl eliminating DMF and producing the acyl chloride. Adding MeOH to the reaction converts the acid chloride into the desired methyl ester (R_p)-**51**.

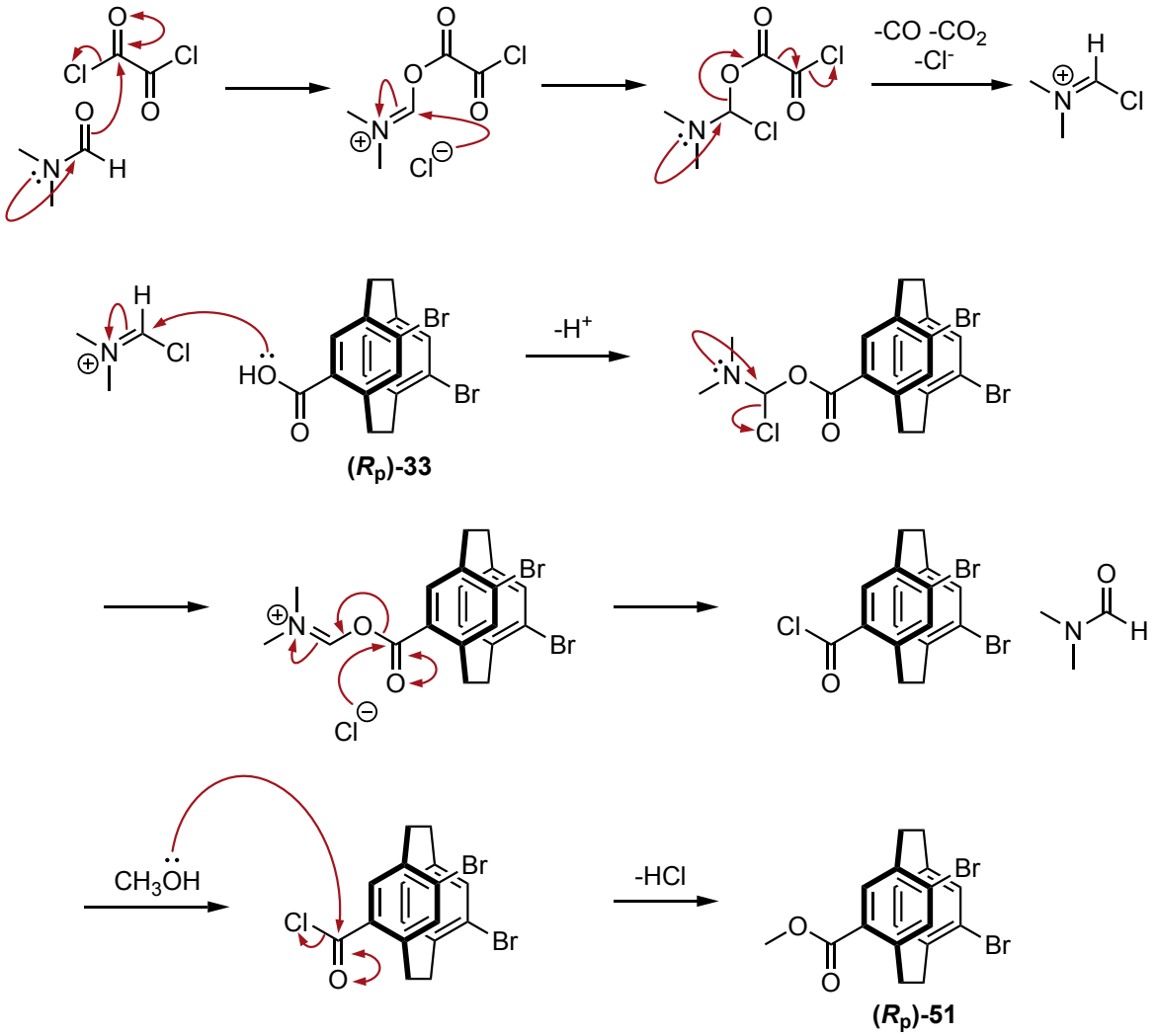

Scheme 41: Proposed mechanism of formation for the Vilsmeier reagent and synthesis of (R_p)-**51**.

Separation was found for esters (±)-**51** and (±)-**53** using an OD-H column with 95:5 *n*-hexane/*i*-PrOH, 1 mL/min and ester (±)-**52** with 99:1 *n*-hexane/*i*-PrOH, 1 mL/min. The highest ee obtained was for (S_p)-**52** in 88% ee, reflected by the purer diastereomeric ratio measured with ^{1}H NMR compared to the other two derivatives. Both (R_p)-**51** and (R_p)-**53** had lower ee of 80% and 73% respectively.

2.2 Synthesis of rhodium(II) paddlewheel catalysts

With the enantiomerically enriched carboxylic acid derivatives in hand, Rh(II) paddlewheel synthesis commenced. There are two routes to the desired complex: ligand exchange with $Rh_2(OAc)_4$[46] or a *de novo* synthesis from $RhCl_3$ and Li_2CO_3.[62] As Bräse has previously synthesised a [2.2]PC paddlewheel from $Rh_2(OAc)_4$ it was decided to attempt this method first.[46]

A mixture of $Rh_2(OAc)_4$ and excess acid (R_p)-**33** were heated together in chlorobenzene for 72 hours equipped with a condenser and Soxhlet extractor filled with K_2CO_3 (Scheme 42). As the reaction is an equilibrium process between the Rh(II) paddlewheel and (R_p)-**33**, it must be driven to completion. This is achieved by removing the acetic acid from the reaction by formation of potassium acetate in the Soxhlet thimble. Unfortunately, this attempt was nothing short of a complete disaster. The main issues were the high boiling point of chlorobenzene and the Soxhlet extraction apparatus.

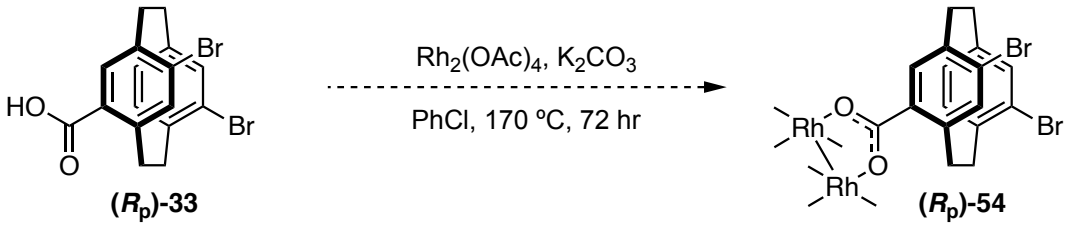

Scheme 42: Failed reaction conditions for synthesis of (R_p)-**54**.

Chlorobenzene possesses a boiling point of 132 °C, however temperatures >170 °C were required to allow solvent vapour to flow up the distillation path of the extractor. This was close to the temperature that racemisation occurs for [2.2]PC compounds, which was an especially valid concern for our ligands (R_p)-**33** and (S_p)-**34** as more highly substituted derivatives undergo racemisation at lower temperatures. The distillation path of the Soxhlet extractor was also too long, preventing any solvent condensate from reaching the K_2CO_3. ^1H NMR of the crude material could not be collected; however, X-ray quality crystals of the complex could be grown, and a crystal structure was collected (Figure 16). This revealed the four ligands had attached, but racemisation had occurred.

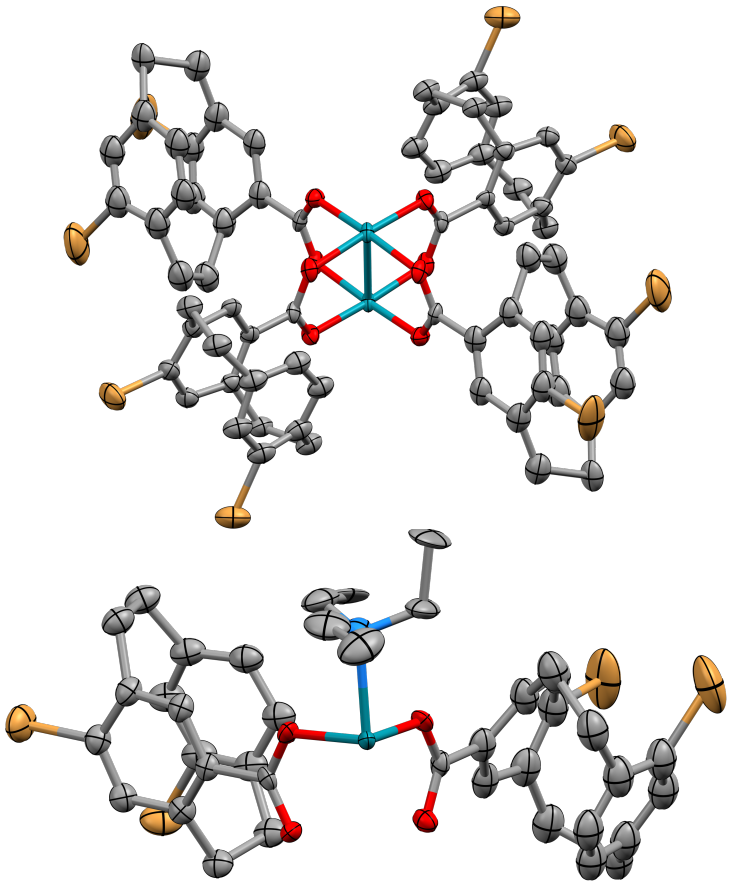

Figure 16: X-ray crystal structure of (±)-**54** depicting the unit cell, C = grey, O = red, Rh = teal, Br = brown. Thermal ellipsoid probability level 50%. Hydrogen atoms are omitted for clarity. Axial Et_3N ligands are omitted for clarity. Bottom: X-ray crystal structure of (±)-**54** depicting the asymmetric unit. Hydrogen atoms are omitted for clarity.

Learning from our first attempt, the Soxhlet extractor was swapped for a pressure equalising dropping funnel as this had a shorter path for the solvent to reach the K_2CO_3. Toluene, a lower boiling point solvent (110 °C) was also used to replace chlorobenzene. The new conditions only required heating to 125 °C to achieve solvent flow up the distillation path and into the reservoir containing K_2CO_3. The reaction reached completion after three days as judged by TLC and ^{1}H NMR showed the new complex had been successfully formed (Scheme 43).

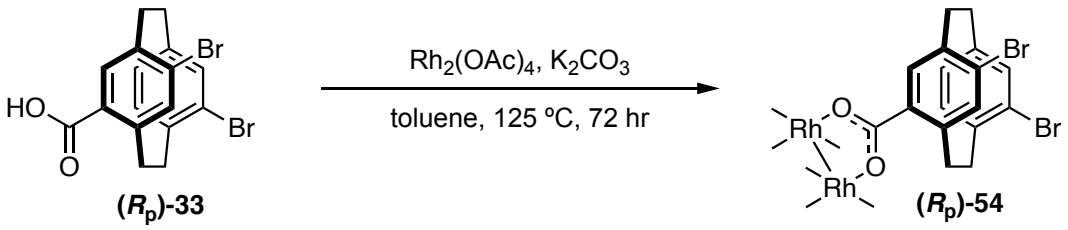

Scheme 43: Successful reaction conditions for synthesis of (R_p)-**54**.

Ligand exchange is best described as an equilibrium process.[23] The new carboxylate ligand first coordinates at the axial position of the complex and the acetate ligand is protonated to form a molecule of acetic acid (Scheme 44). The acetic acid is then lost and replaced by coordination of the new ligand in the equatorial position. Paddlewheel complexations are performed in high boiling point solvents such as toluene to distil the acetic acid out from the reaction mixture, shifting the equilibrium to the new complex.

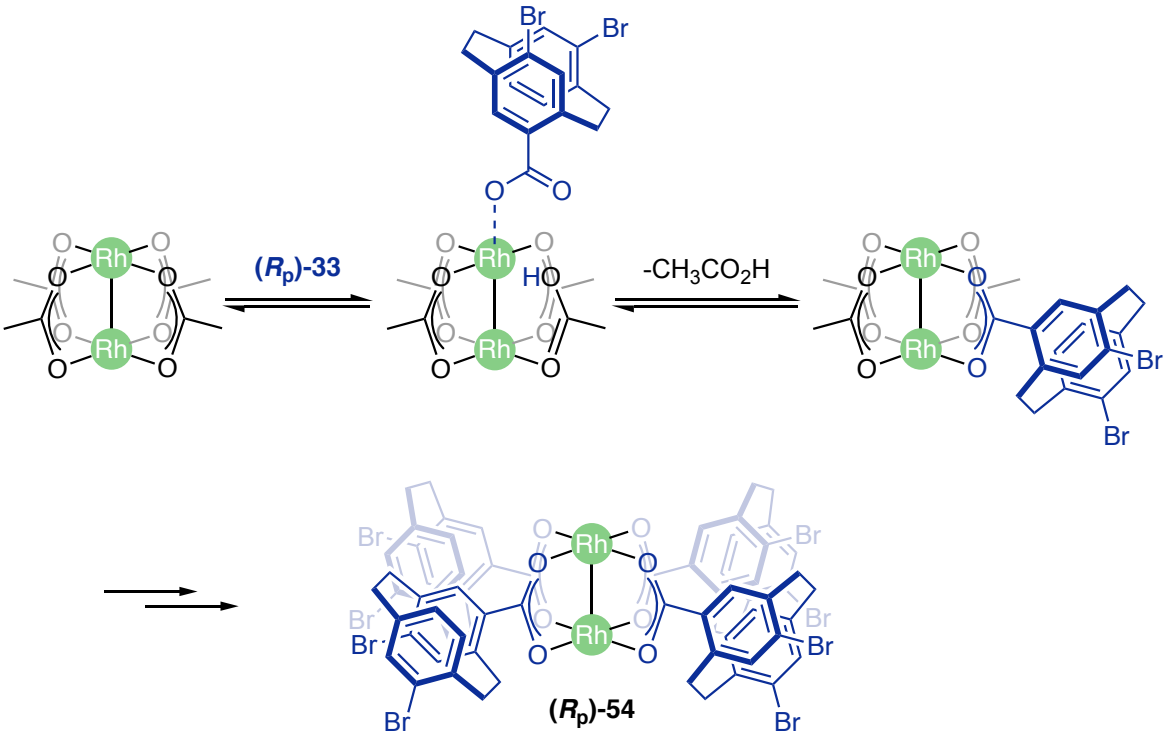

Scheme 44: Equilibrium process for the synthesis of (R_p)-**54**.

Separation from the excess [2.2]PC carboxylic acid was simple and achieved by passing through a plug of silica with 100% CH_2Cl_2. Despite this, there still appeared to be a small impurity in the ^{1}H NMR spectrum that was [2.2]PC based. There also appeared to be two green spots running in an EtOAc/*n*-hexane system with an R_f difference of ~0.1. Multiple attempts at purification ensued to separate the two green spots and most were unsuccessful.

The main issue was the solubility of the crude material that only dissolved in CH_2Cl_2 or THF. Recrystallisation was unsuccessful, as was column chromatography as the loading solvents were more polar than the eluent system, causing the mixture to streak. Preparatory TLC also failed as the compound was too insoluble to run with the solvent and stuck to the bottom of the plate. Eventually, a method was found for large-scale purification that involved loading the crude mixture onto celite, loading the mixture onto a silica plug and eluting it with a 15% EtAOc, 83.5% *n*-hexane, 1.5% THF mixture, using vacuum. Fortunately, a crystal structure could be obtained for catalyst (R_p)-**54** by slow evaporation of a 60% CH_2Cl_2, 39% CH_3CN, 1% THF mixture (Figure 17). This allowed the absolute configuration of the complex to be assigned as the R_p enantiomer. This also revealed the relative stereochemistry of the diastereomeric salt and the absolute stereochemistry of the carboxylic acid.

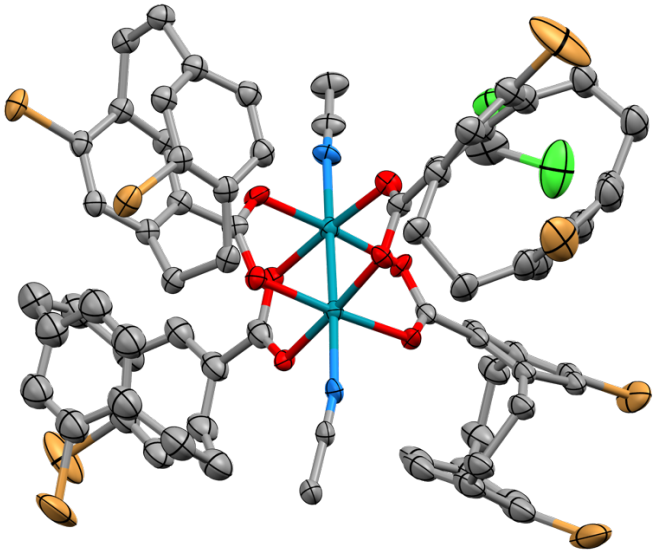

Figure 17: X-ray crystal structure of (R_p)-**54**, C = grey, N = blue, O = red, Rh = teal, Br = brown. Thermal ellipsoid probability level 50%. Hydrogens are omitted for clarity.

^{1}H NMR of the isolated impurity was similar to the desired complex, however the aromatic region possessed overlapping peaks with complex multiplets. We suspected it was either a complex containing a different regioisomer impurity or a diastereoisomer of the complex. To determine this, a sample of both the desired complex and the unknown impurity were hydrolysed in 6.0 M aqueous HCl to obtain the carboxylic acids (R_p)-**33** from the complex. ^{1}H NMR revealed only (R_p)-**33** was present, ruling out our first suspicion. The acids were converted to their methyl esters and analysed with HPLC, revealing the impurity was a diastereomeric complex comprised of a mixture of enantiomers with 37% ee, while the desired complex comprised of a >99% ee sample of the [2.2]PC acid (Figure 18).

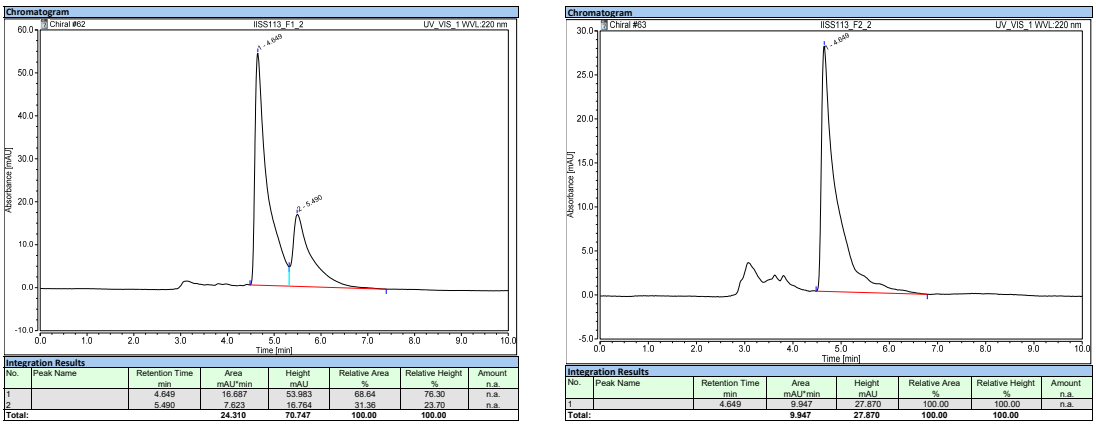

Figure 18: HPLC chiral chromatogram of recovered acid from the diastereoisomer impurity (left) and of the desired complex (R_p)-**54** (right).

We wondered if the 'self-sorting' behaviour of complexation observed was due to (R_p)-**33** reacting first, then the small amount of (S_p)-**33** reacting last. To determine this, the excess acid from complexation was isolated, converted to the methyl ester and analysed with HPLC. If (R_p)-**33** was used up in the complexation first, (S_p)-**33** should be the only compound detected. HPLC revealed the leftover acid was an 80% ee sample of the R_p enantiomer, which was a similar ee to the starting acid used for complexation. This potentially implies both complexes are formed at the same rate, or once the enantiomerically pure complex is formed, it epimerises over time to include the (S_p)-**33** enantiomer.

Once purification of (R_p)-**54** was sorted, the other two complexes (S_p)-**55** and (R_p)-**56** were synthesised (Scheme 45). Both possessed similar solubility issues but not to the extent of the *pseudo-ortho* Rh(II) complex (R_p)-**54**. Both (S_p)-**55** and (R_p)-**56** were readily soluble in toluene and could be loaded onto and eluted on a silica-gel column with no issues. After purification was sorted, all complexes were obtained in moderate to good yields: (S_p)-**55** in 71-80% yield and (R_p)-**56** in 50-70% yield.

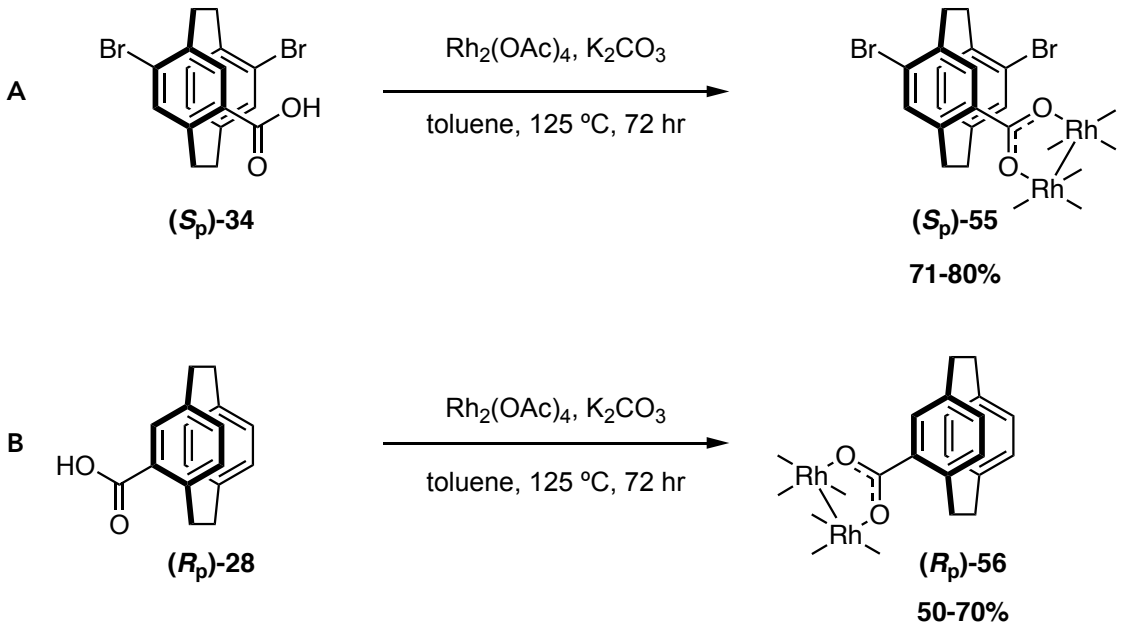

Scheme 45: a) Reaction conditions for the synthesis of (S_p)-**55**. b) Reaction conditions for the synthesis of (R_p)-**56**.

A crystal structure of catalyst (S_p)-**55** was obtained through slow evaporation of a 95% CH_2Cl_2, 5% THF mixture (Figure 19). This revealed the absolute configuration of the complex to be the S_p enantiomer.

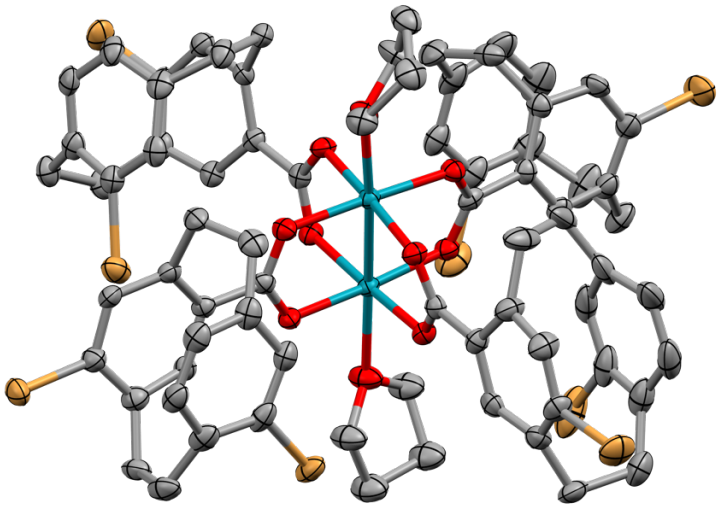

Figure 19: X-ray crystal structure of (S_p)-**55**, C = grey, O = red, Rh = teal, Br = brown. Thermal ellipsoid probability level 50%. Hydrogens and axial THF disorder omitted for clarity.

2.3 Late-stage catalyst functionalisation

With the Rh(II) catalysts in hand we wanted to functionalise them by attempting a Suzuki-Miyaura coupling on catalysts (R_p)-**54** and (S_p)-**55**. Introducing extra aromatic substituents onto the [2.2]PC backbone would create new catalysts with a different steric and electronic environment around the active site. Late stage functionalisation of the catalysts also increases synthetic efficiency and allows functional groups to be introduced that are incompatible with the prior complexation step.[63,23] We first followed a method developed by Davies that described a 12-fold Suzuki coupling of their $Rh_2[TPCP]_4$ catalysts.[64] 4-*tert*-Butylphenylboronic acid was chosen as the aryl coupling partner as an electron rich aryl ring should encourage a rapid transmetalation step while introducing extra bulk to the system.[65] The *tert*-butyl group would also provide a useful anchor-point in the ^{1}H NMR and should improve the solubility of the complex. The first set of coupling conditions are shown in Scheme 46, complete consumption of starting material was indicated by TLC, but the ^{1}H NMR of the crude reaction mixture was uninterpretable.

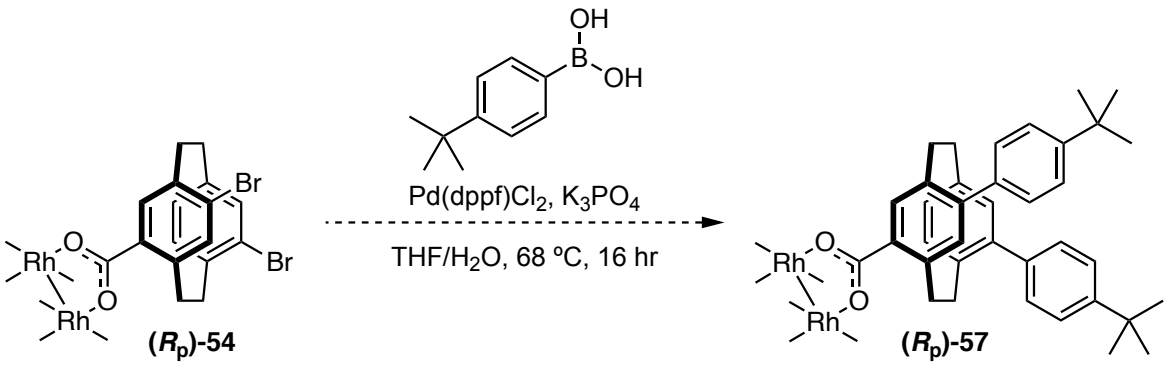

Scheme 46: Failed Suzuki coupling conditions for the synthesis of (R_p)-**57**.

When attempting to find purification conditions, it was discovered multiple Rh(II) products had formed. Attempting to isolate each product by preparatory TLC was unsuccessful as each spot isolated was revealed to still contain multiple compounds in the ^{1}H NMR. The reaction was repeated and run for 48 hours to see if an incomplete reaction was the issue, but still showed no improvement. We decided to attempt the reverse sequence: Suzuki coupling on the free acid, then complexation. This would provide a reference ^{1}H NMR spectrum to help identify the desired paddlewheel out of the complex mixture of Suzuki products. Conditions first attempted for the paddlewheel were attempted on (R_p)-**33** (Scheme 47). These conditions led to a more identifiable mixture of three products shown in the crude ^{1}H NMR spectrum, of which only two could be separated from one another.

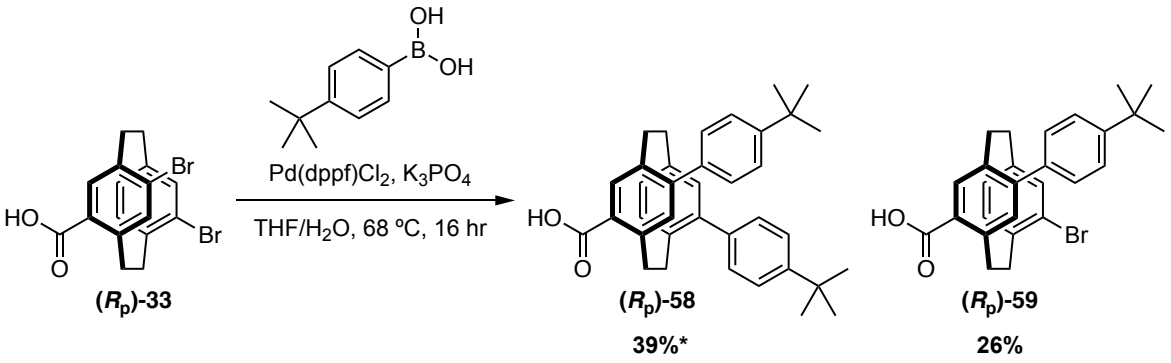

Scheme 47: Suzuki coupling conditions for the synthesis of (R_p)-**58** and (R_p)-**59**. *With inseparable (R_p)-**60** present.

Two samples were isolated, one was a 1:0.4 mixture of the desired product (R_p)-**58** and proto-debrominated (R_p)-**60**. These compounds had identical R_f values and were inseparable by preparatory TLC. The other was a single addition product (R_p)-**59**, the regioselectivity of coupling is most likely due to the electron withdrawing effect of the acid on the same ring. This removes electron density from the C-Br bond, weakening it and making oxidative addition easier. Different conditions were tried in parallel in hopes to quickly optimise the reaction for (R_p)-**58**. Conditions using $Pd(PPh_3)_4$ eliminated production of (R_p)-**59**, but produced a 1:1 mixture of (R_p)-**58** and (R_p)-**60** (Scheme 48). Isolation and characterisation of (R_p)-**60** was not achieved for this reaction but achieved for the reaction depicted in Scheme 50.

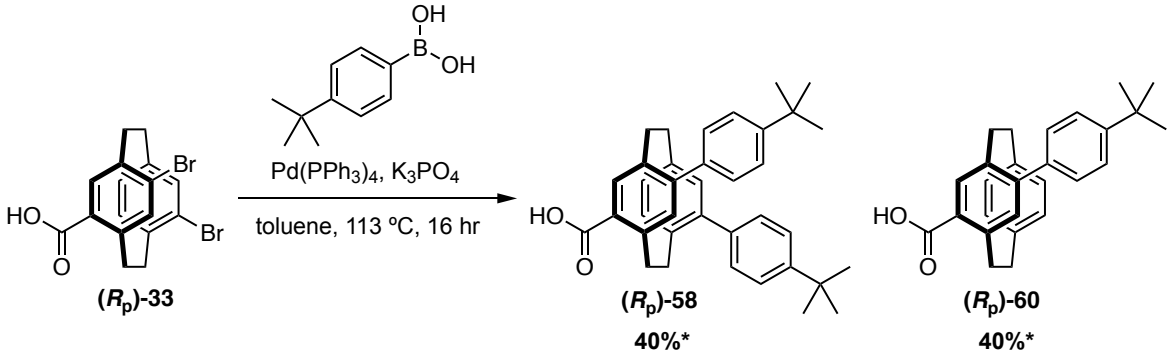

Scheme 48: Suzuki coupling conditions for the synthesis of (R_p)-**58** and (R_p)-**60**. *Determined by ^{1}H NMR integration.

Conditions using SPhos and $Pd(OAc)_2$ were found to be best, providing (R_p)-**58** as the main product in 69-70% yield with only 9% of (R_p)-**60** present in the ^{1}H NMR spectrum (Scheme 49).

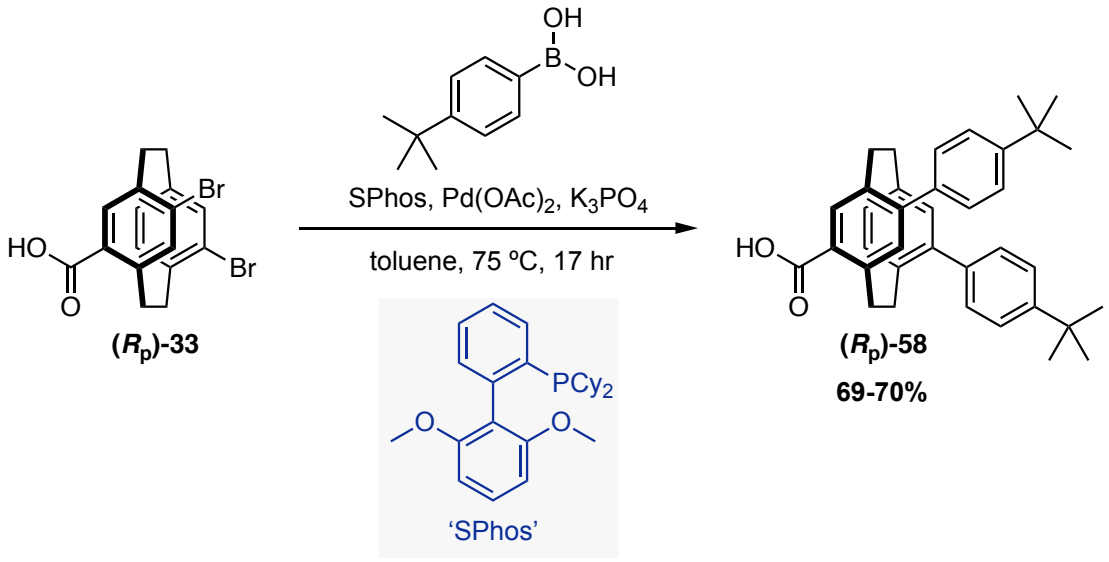

Scheme 49: Suzuki coupling conditions for the synthesis of (R_p)-**58**.

Suzuki coupling was also attempted on (S_p)-**34** before attempting coupling on the paddlewheel. Using the conditions that were successful to make (R_p)-**58** produced mediocre results. The desired compound (S_p)-**61** and proto-debrominated product (S_p)-**60** were both isolated in 38% and 41% yield, respectively.

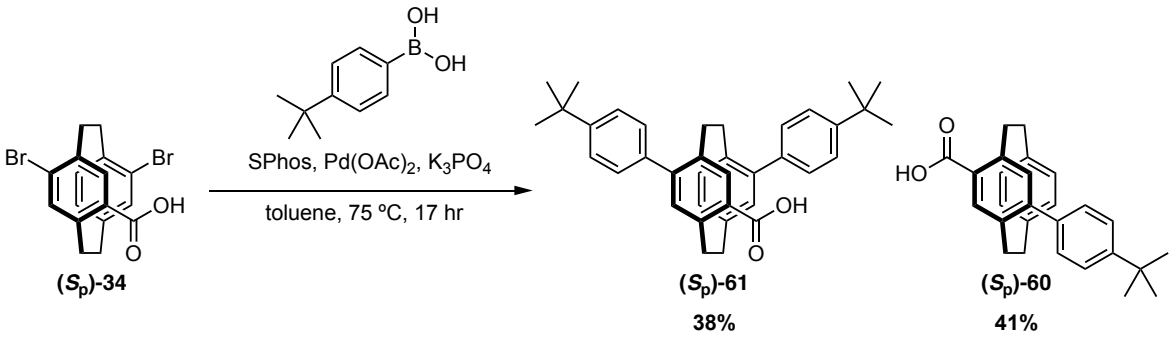

Scheme 50: Suzuki coupling conditions for the synthesis of (S_p)-**61** and (S_p)-**60**.

This was unsurprising due to the increased bulk of the acid substituent *pseudo-ortho* to the bromine substituent, that increased the incidence of proto-dehalogenation. One further set of conditions were tried by switching the phosphine ligand to XPhos but resulted in the same ratio of both products. Overlaying the ^{1}H NMR spectrum of (S_p)-**60** and the crude mixture of Scheme 48 now allowed us to identify the unknown product made alongside (R_p)-**58** was the opposite enantiomer of the proto-dehalogenated product (R_p)-**60**.

Suzuki-Miyaura coupling involves the classic palladium catalytic cycle.[66] The mechanism begins with the formation of the active palladium species by reduction of Pd^{II} to Pd^0 (Scheme

51). The Pd^0 species inserts into the C-Br bond of the aryl bromide, in turn becoming oxidised to Pd^{II}. Oxidative insertion can be accelerated by using electron rich ligands that increase the nucleophilicity of palladium, or using electron deficient aryl bromides that increase the electrophilicity of the halide. The boronic acid is thought to be preactivated through the addition of base, creating a more nucleophilic boronate species that facilitates a more rapid transmetalataion step. Transmetalation then occurs which is a ligand exchange step between the Pd^{II} and boronate species, leaving palladium with the two aryl coupling partners coordinated and eliminating a boronate species. Finally, reductive elimination results in C-C bond formation and reduction of Pd^{II} to Pd^0.[67]

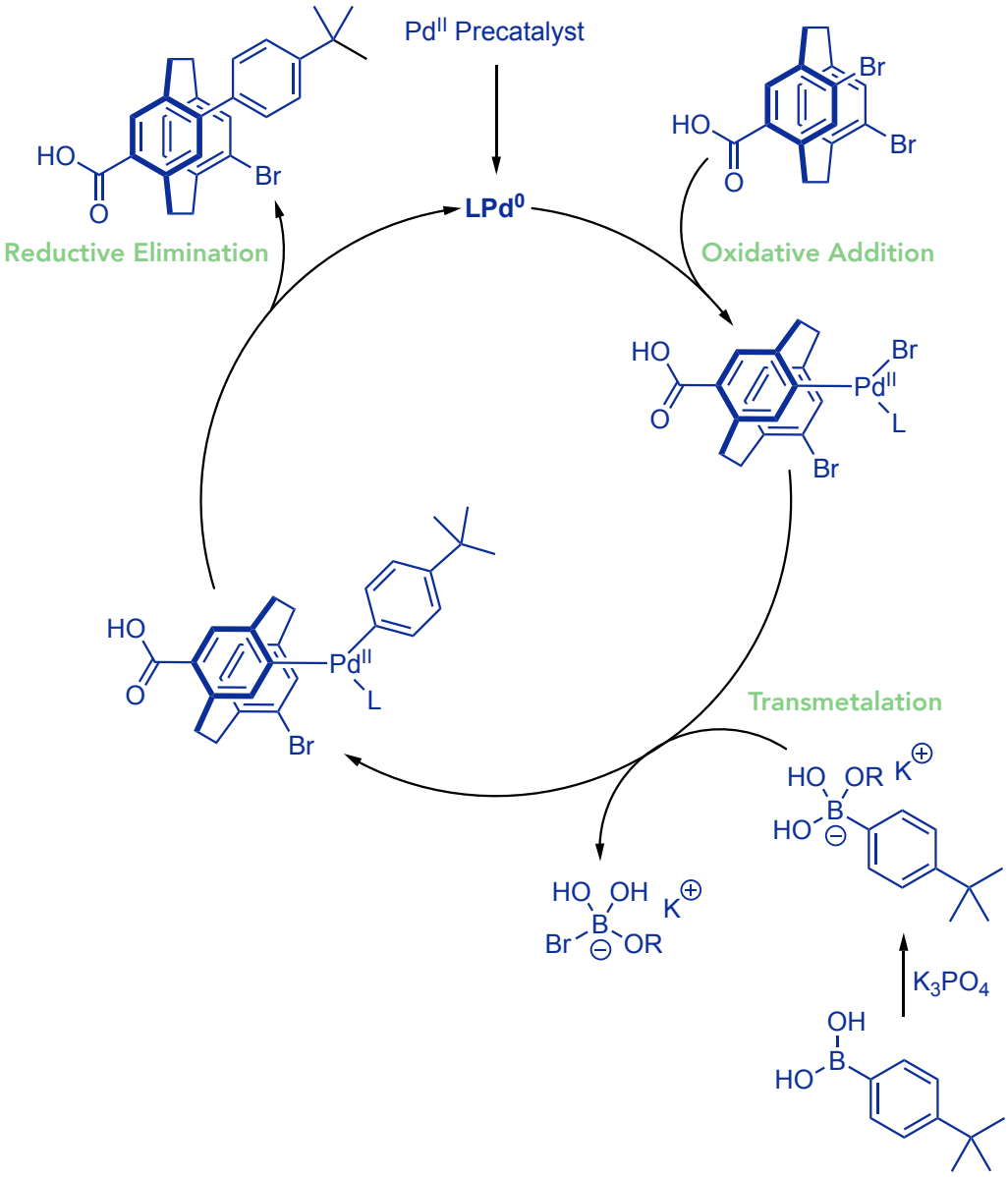

Scheme 51: Proposed mechanistic cycle of Suzuki coupling for [2.2]PC derivatives.

The proto-dehalogenation products produced from the initial reaction conditions indicate (R_p)-**33** could undergo the oxidative addition step but failed to undergo the remainder of the catalytic cycle. De-halogenation occurs after oxidative addition and involves the Pd^{II} species intercepting a proton from either the solvent or residual water in the reaction.[68] A proto-dehalogenated product is then eliminated from Pd, forming a C-H bond rather than a C-C bond. Proto-dehelogenation is a common side reaction that is most incident in sterically hindered aryl systems.[66] Changing the ligand to a more electron rich and bulky Buchwald phosphine ligand may have helped increase both the rate of the oxidative addition and reductive elimination, preventing the chance for proto-dehalogenation for the (R_p)-**33** system.[69] However, the sterics of the (S_p)-**34** system could not be overcome and proto-dehalogenation prevailed.

Refocusing on the paddlewheels, complexation was attempted with (R_p)-**58** using our new conditions. Reaction completion was reached within the same timeframe of 3 days and purification by chromatography delivered (R_p)-**57** in 68% yield (Scheme 52a). Attempting our optimised Suzuki coupling conditions on the Rh(II) paddlewheel also produced (R_p)-**57** in 66-72% yield, rather than the complex mixture observed before (Scheme 52b).

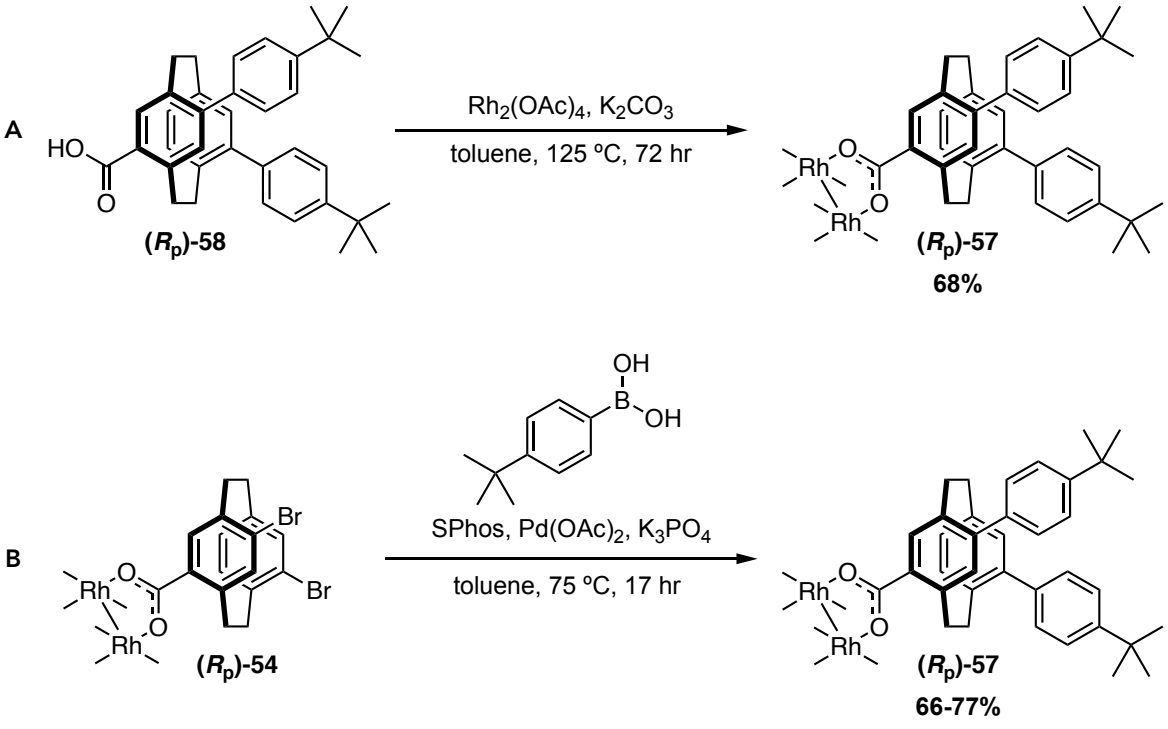

Scheme 52: a) Complexation conditions used to obtain (R_p)-**57**. b) Suzuki coupling conditions used to obtain (R_p)-**57**.

The battle with Suzuki conditions for the ligand alone now helped make sense of the complex mixture obtained when first trying the coupling on the paddlewheel. The $Pd(dppf)Cl_2$

conditions gave three different products, meaning paddlewheels with up to three different [2.2]PC derivatives attached could be made, resulting in the very messy crude mixture.

Although coupling conditions hadn't been fully optimised for (S_p)-**61**, coupling was tried on (S_p)-**55** anyway to see if a single product could be isolated (Scheme 53). Unfortunately, the same messy mixture of products was observed like the first attempt to make (R_p)-**57**. No single product could be isolated when performing a prep TLC on the mixture, confirming the coupling was unsuccessful.

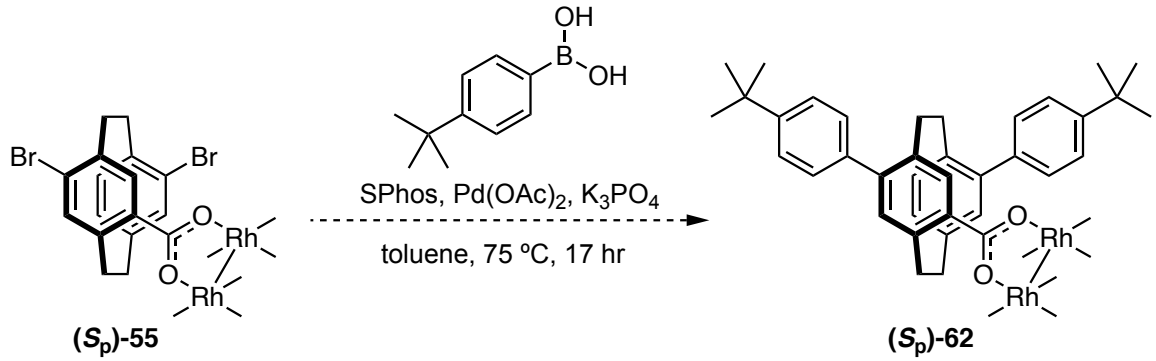

(S_p)-55 **(S_p)-62**

Scheme 53: Failed reaction conditions to produce (S_p)-**62**.

We then tried the reverse sequence, complexation of the free acid (S_p)-**61**. Due to the increased steric demands of this derivative the reaction was left to run for a longer duration of 6 days. Two samples were isolated from the crude reaction mixture, one was the desired complex (S_p)-**61** although in a poor 22% yield. The other sample isolated was unidentifiable, but we suspect it is a product of incomplete complexation. Due to time restraints, the above reaction was not optimised further.

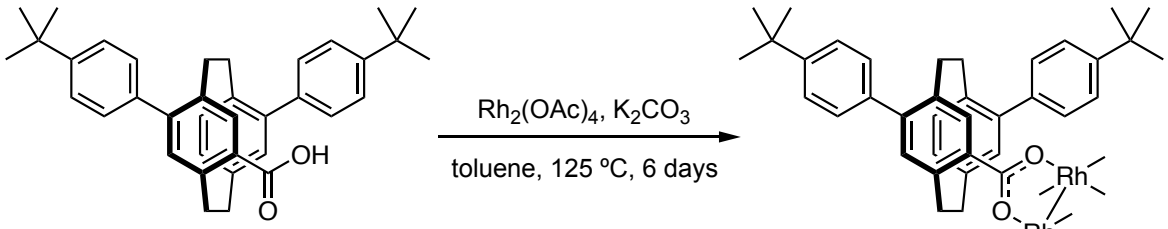

(S_p)-61 **(S_p)-62**
22%

Scheme 54: Successful reaction conditions to produce (S_p)-**62**.

Rh(II) catalyst synthesis concluded with five catalysts being synthesised. Synthesis of paddlewheels (R_p)-**54**, (S_p)-**55** and (R_p)-**56** was achieved in good yields. Synthesis of catalyst (R_p)-**57** could be performed in two ways: through complexation of (R_p)-**58** or Suzuki

coupling on the paddlewheel (R_p)-**54**, both in good yields. Catalyst (S_p)-**62** could unfortunately not be made through Suzuki coupling on the paddlewheel but could be made by complexation of the acid (S_p)-**61** though in poor yield. The complexation for this catalyst wasn't optimised further and was not made in large enough quantity to use for catalysis studies.

2.4 Nitrene insertion catalysis studies

Four of the catalysts could be made in large enough quantity to investigate their reactivity and selectivity in nitrene insertion reactions. Nitrene insertion was identified as a preferred model reaction rather than carbene insertion. C-H bond amination is a far less studied area compared to C-C bond formation and installing C-N bonds is synthetically useful, especially for the late-stage functionalisation of biologically active compounds. Diazo carbenoid precursors can be simple to make but difficult to handle as they are thermally unstable and explosive compounds.[70] Early nitrene sources were derived from explosive azide compounds, however significant work has resulted in a range of user-friendly bench stable nitrene sources, such as carbamates and sulfonamides (Figure 20).[71] To generate the nitrene precursor these reagents require the addition of (diacetoxyiodo)benzene into the reaction mixture to act as an external stoichiometric oxidant. However, this method is disadvantageous as it generates an equivalent of iodobenzene as waste.

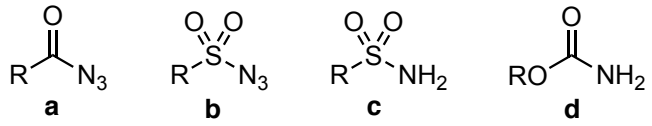

Figure 20: Nitrene precursors: a) Acyl azide. b) Sulfonyl azide. c) Sulfonamide. d) Carbamate.

Lebel developed a method that avoids hypervalent iodine reagents and instead uses *N*-tosyloxycarbamates that use a tosyl leaving group as the oxidant.[29] Although this method produces an equivalent of potassium tosylate as waste, this is easily removed during reaction workup. These reagents were easily synthesised in two steps from the corresponding alcohol to form the carbamate, then protection with tosyl chloride to give **15** and **18** (Scheme 55).

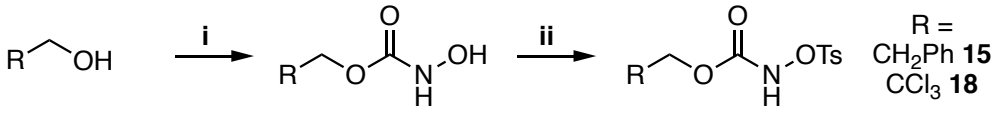

Scheme 55: General conditions for the synthesis of *N*-tosyloxycarbamates. i) CDI, $NH_2OH{\cdot}HCl$, imidazole. ii) TsCl, Et_3N.

Two test reactions were completed using catalysts (R_p)-**54**, (S_p)-**55**, (R_p)-**56**, and (R_p)-**57**: the cyclisation of **15** to form **16a** and the intermolecular reaction between **18** and THF to form **19b** (Scheme 56). The enantioselectivity of each reaction was analysed with HPLC.

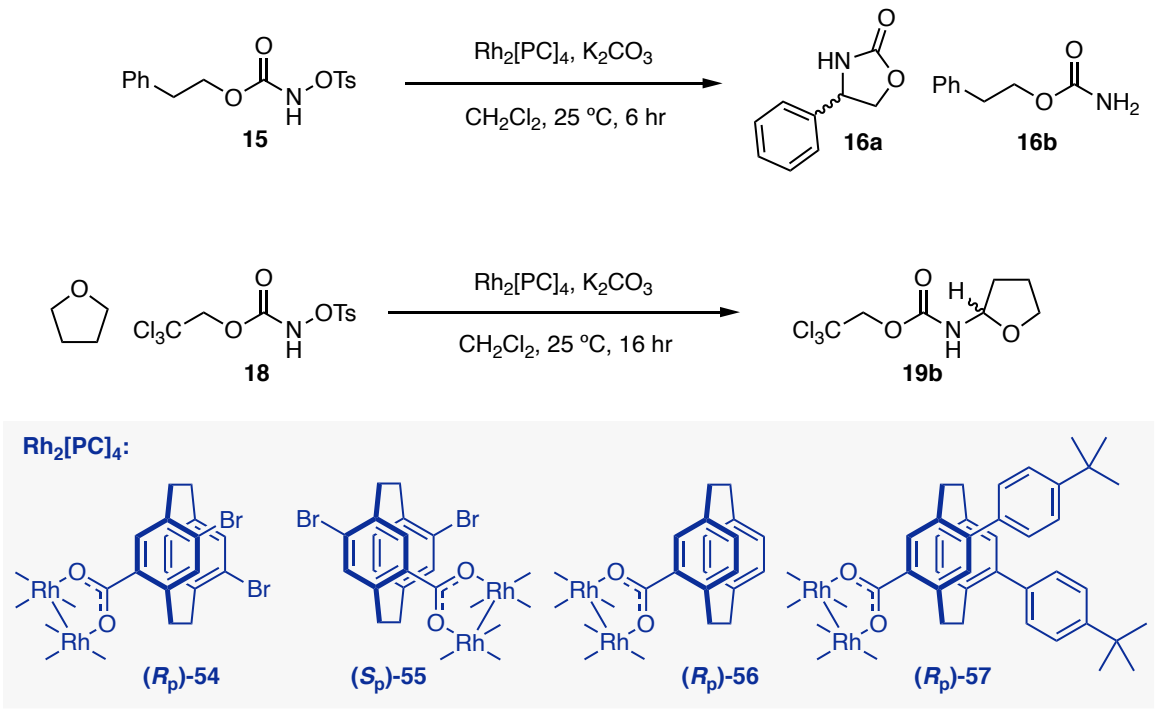

Scheme 56: Intramolecular reaction conditions for the synthesis of **16a** and **16b**, intermolecular reaction conditions for the synthesis of **19b** and catalysts (R_p)-**54**, (S_p)-**55**, (R_p)-**56**, and (R_p)-**57** used for each reaction.

Synthesis of **16a** was performed using 6 mol% of the Rh(II) catalyst in the presence of K_2CO_3 and run for six hours. All catalysts performed well to produce the oxazalidinone **16a** in moderate to good yields. All catalysts produced **16a** as the major product, while $Rh_2(OAc)_4$ produced the carbamate **16b** as the major product and **16a** as the minor product. Catalyst recovery was not possible, during the reaction a colour change from vibrant green to pale yellow was observed. This is a 'bleaching' effect attributed to catalyst degradation upon oxidation to Rh(II)/(III) and loss of the equatorial ligands.[72] Unfortunately, HPLC analysis of the catalysis product showed all catalysts provided no significant enantioinduction upon cyclisation (Table 1).

Intermolecular nitrene insertion was also performed with 6 mol% of catalyst but instead run for 16 hours overnight. The bleaching effect of the previous reaction was not observed, and the mixture remained a vibrant green. ^{1}H NMR of the crude mixture revealed both the product and the catalyst were present, indicating catalyst degradation had not occurred. All Rh(II) catalysts could be recovered in >70%. Yields of **19b** were moderate to excellent with (R_p)-**57** providing the best yield of 86%. HPLC analysis was difficult due to the lack of UV activity exhibited by the compound and meant impurities absent in the ^{1}H NMR were observed in the HPLC chromatogram. Adequate conditions were eventually found for

separation, however revealed no significant enantioinduction was shown for the intermolecular reaction as well.

Entry	Catalyst	Product	Yield%	ee%
1	$Rh_2(OAc)_4$	**16a**	13	-
2	(R_p)-**54**	**16a**	79	2
3	(S_p)-**55**	**16a**	51	4
4	(R_p)-**56**	**16a**	72	4
5	(R_p)-**57**	**16a**	74	4
6	$Rh_2(OAc)_4$	**19b**	61	-
7	(R_p)-**54**	**19b**	63	2
8	(S_p)-**55**	**19b**	69	2
9	(R_p)-**56**	**19b**	61	6
10	(R_p)-**57**	**19b**	86	10

Table 1: Intramolecular and intermolecular nitrene insertion catalysis results.

The mechanism of nitrene insertion is best viewed from the perspective of the Rh(II) paddlewheel catalyst. The *N*-tosyloxycarbamate coordinates to the Rh(II) catalyst in the axial position to give intermediate **A** (Scheme 57).[73] A proton is removed by a molecule of K_2CO_3 followed by elimination of the tosylate leaving group to give the active nitrenoid species **B**. Two methods for nitrene insertion are accepted, one is the stepwise pathway which involves a diradical intermediate, or a concerted pathway that involves simultaneous C-H bond cleavage and C-N bond formation.[74] The concerted pathway is generally accepted for *N*-tosyoxycarbamate substrates and is depicted by intermediate **C**.[29] Expulsion of nitrene insertion product regenerates the Rh(II) catalyst for another cycle.

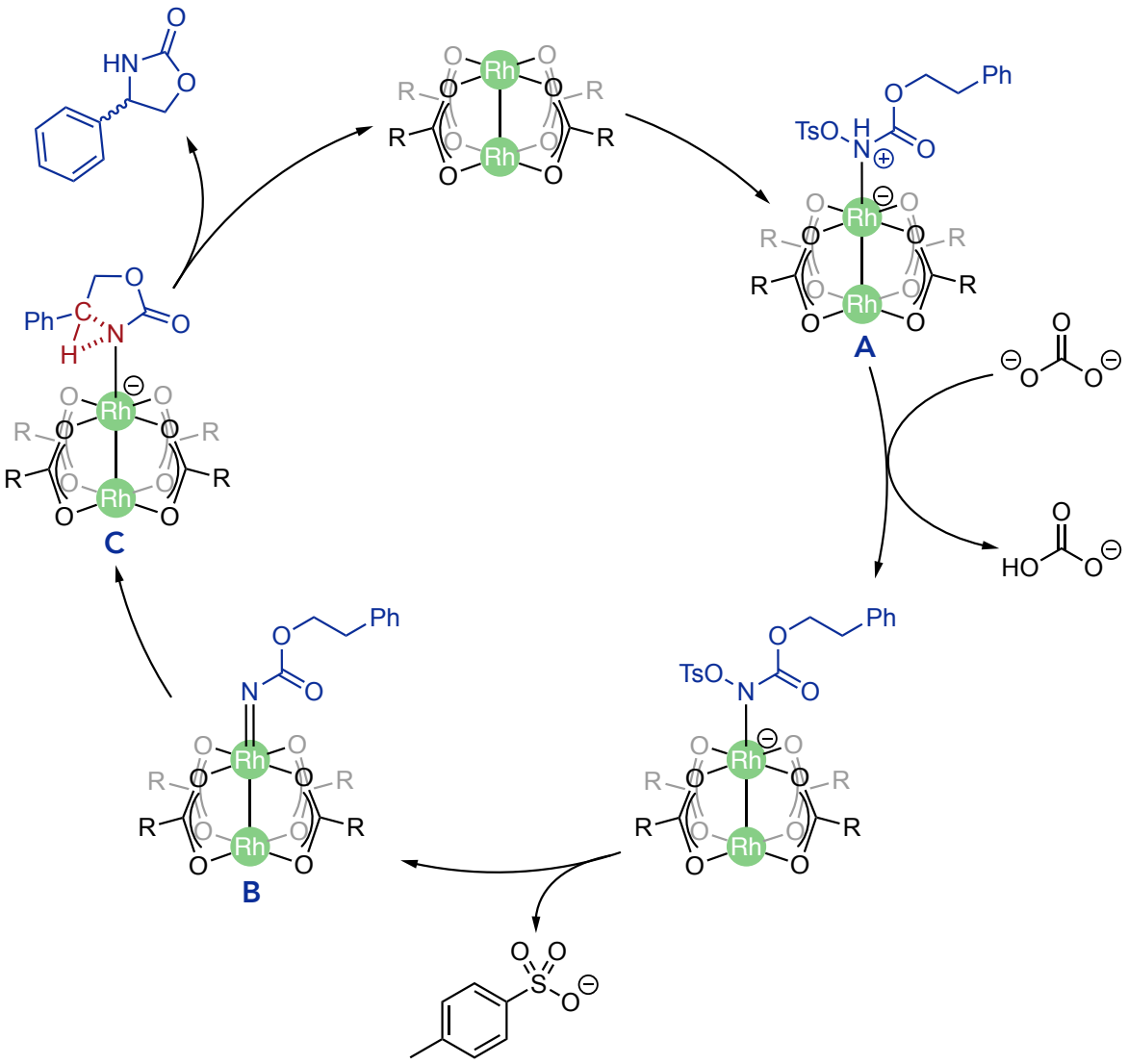

Scheme 57: Proposed catalytic cycle of Rh(II) catalysts for nitrene insertion.

It is not explicit why no enantioinduction was introduced into any of the above reactions. This is most likely due to the geometry of our Rh(II) catalysts revealed by their crystal structures in Figure 17 and 19 of Section 2.2. The conformation of (R_p)-**54** shows the bromine substituents point away from the axial position of both Rh atoms entirely. The bridgehead groups occupy the space closest to the axial position on one face of the catalyst, while the other face is completely open. We hoped the *pseudo-meta* arrangement of bromine substituents of (S_p)-**55** would hold bulk closer to the axial site and induce enantioselectivity. The crystal structure shows the bromine substituents occupy one of the axial sites and the bridgeheads the other site. However, this was not enough to influence the enantioselectivity of the reaction. Comparison with Davies' Rh_2[TCPTAD]$_4$ catalyst that demonstrated enantioinduction for the cyclisation of **16a** reveal our catalysts' active pockets are less crowded (Figure 21a-b).[31,75] In Davies' catalyst the adamantyl groups block substrate

approach from the bottom axial site completely (Figure 21c). The substrate must approach the top axial site that is hindered by the aryl chloride groups and can only coordinate in one orientation, forcing the reaction to occur on a single face (Figure 21d). Our catalysts have both axial positions accessible and a poorly defined chiral pocket. Another observation is common Rh(II) catalysts that display enantioselectivity are based around carboxylic acid ligands that are sp^3 hybridised in the α-position. This brings the sterically crowding groups closer to the Rh(II) dimer itself, whereas our acidic ligands are sp^2 hybridised, that inherently hold substituents further away from Rh(II). However, as few planar chiral catalysts have been investigated before, we hoped this would have shown some advantages. As only two sets of catalysis conditions were used, it is highly likely that altering parameters like the substrate, solvent and reaction temperature could provide different results.

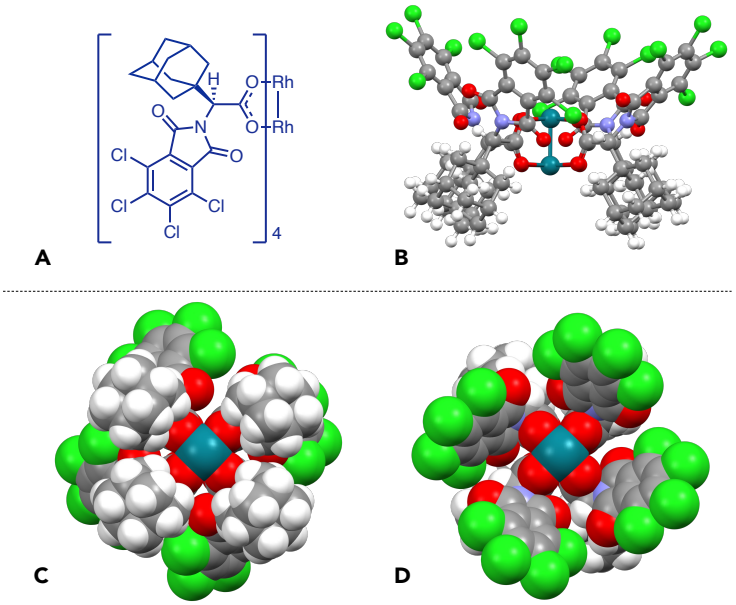

Figure 21: a) $Rh_2[TCPTAD]_4$ skeletal representation. b) $Rh_2[TCPTAD]_4$ crystal structure. c) $Rh_2[TCPTAD]_4$ space filling model bottom face. d) $Rh_2[TCPTAD]_4$ space filling model top face.

It was pleasing that our four catalysts were active for both intramolecular and intermolecular C-N bond formation in good yields. Although the lack of enantioselectivity displayed was disappointing, there are opportunities to alter the steric environment of our catalysts discussed in the previous section. Our four catalysts discussed above form the foundation of a larger catalyst library that could be constructed and investigated.

Conclusion and Future Perspective

This work developed a short synthesis of enantioenriched substituted [2.2]PC carboxylic acids, the utility of these acids was demonstrated by synthesising Rh(II) paddlewheel catalysts. Our resolution method should allow a range of substituted [2.2]PC derivatives to be prepared in enantioenriched form. We also showed substituted [2.2]PC Rh(II) paddlewheel catalysts could be synthesised and catalyst variation could be achieved with a late-stage Suzuki coupling on the paddlewheels. Four Rh(II) catalysts showed they were active for C-N bond formation, but unfortunately were not enantioselective. These results show further investigation is required in multiple areas and have provided a better perspective on how these could be approached.

The resolution step of [2.2]PC enantiomers can be highly tedious and time consuming, however our method for covalently resolving [2.2]PC acids shows an efficient way to access enantiopure derivatives. Expanding this resolution step to different [2.2]PC derivatives would be highly rewarding. The failure of the Friedel-Crafts reactions on multiple [2.2]PC derivatives prevented installation of the bromoacetyl functionality required for resolution. An alternative route to install this functionality could be acetylation (**i**) then α-bromination (**ii**) to obtain (±)-**63a** (Scheme 58). Alternatively, formylation (**iii**), nucleophilic addition (**iv**) and oxidation (**v**) to give the ketone, then α-bromination could also give (±)-**63a** (Scheme 58). Resolution using tertiary chiral amines and subsequent oxidation to obtain the acid (R_p) or (S_p)-**63b** could then be investigated.

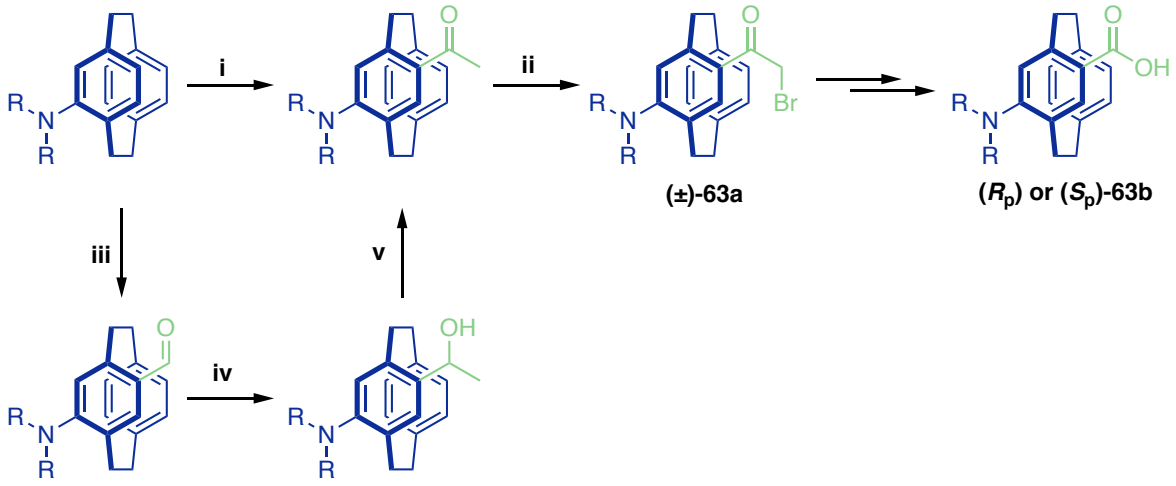

Scheme 58: Possible synthetic routes to obtain the bromoacetyl functionality on an amine derivative of [2.2]PC, then subsequent resolution and oxidation to obtain (R_p) or (S_p)-**63b**. i) CH_3COCl, $AlCl_3$. ii) Br_2. iii) Cl_2CHOCH_3, $TiCl_4$. iv) MeMgBr. v) PCC.

The late-stage catalyst functionalisation on the dibromide paddlewheels was successful to produce (R_p)-**57** however, failed for synthesis of (S_p)-**62** as Suzuki coupling on the free acid (S_p)-**34** had not been fully optimised. More coupling conditions must be screened on (S_p)-**34**, such as changing the phosphine ligand and palladium source, before attempting on the paddlewheel. Late-stage Suzuki coupling would allow different aryl substituted [2.2]PC Rh(II) paddlewheels to be made from the same common precursor (R_p)-**54**. This increases synthetic efficiency and allows rapid construction of a library of catalysts. (Scheme 59).

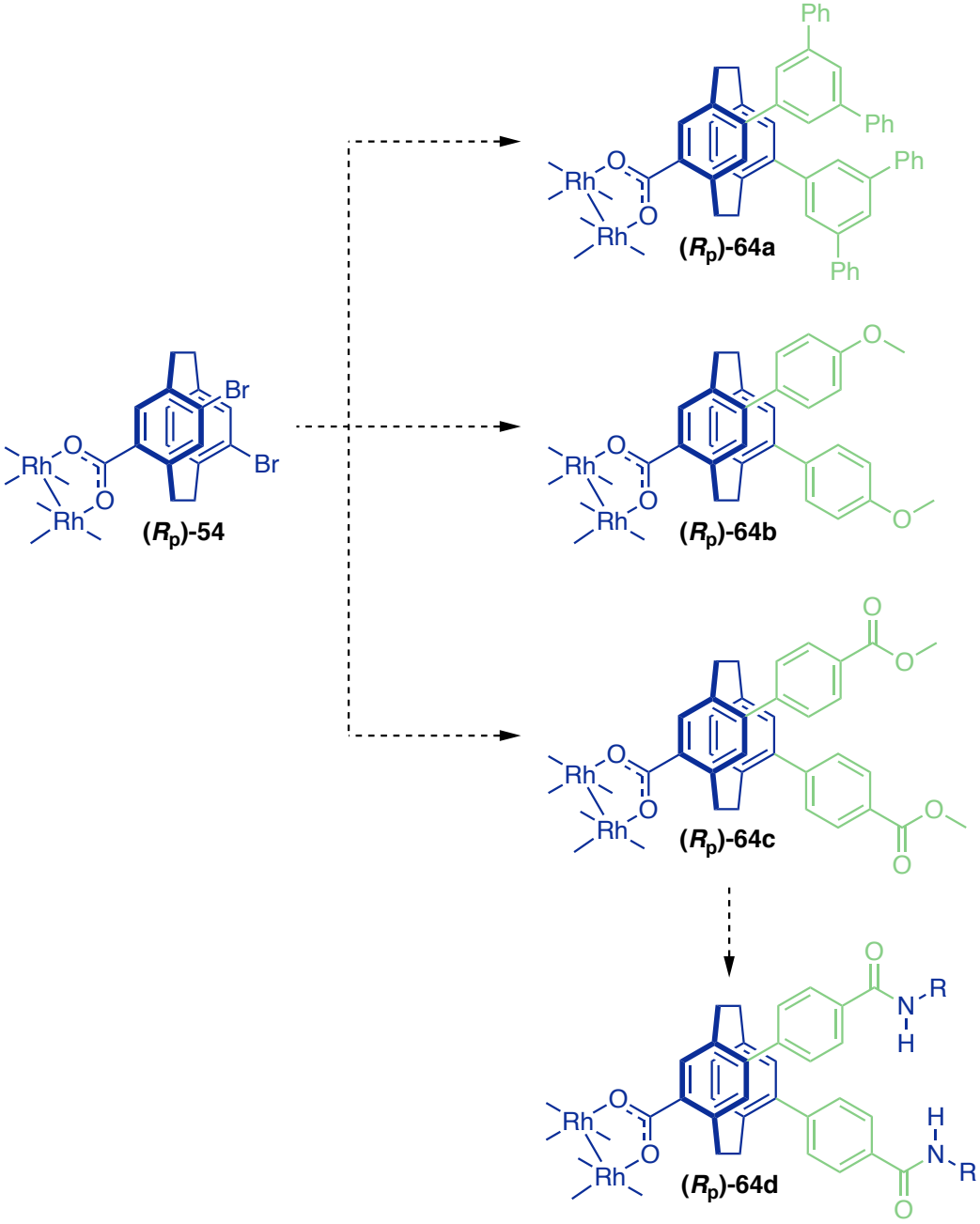

Scheme 59: Proposed catalysts **64a**-**d** derived from the same common precursor (R_p)-**54** from a late-stage catalyst functionalisation.

Derivatives such as (R_p)-**64a** could be made that alter the substitution pattern of the boronic acid to change the catalyst's steric environment. Derivatives such as (R_p)-**64c** could also further be used for an 8-fold substitution reaction to include directing groups on the catalyst. For example, amide groups could be installed that act as hydrogen bond donor and acceptor groups shown by (R_p)-**64d**. These could interact with the substrate through weak interactions, that could potentially direct the site of reaction.

The results from Rh(II) catalysed nitrene insertion reactions demonstrated our catalysts were active, but not enantioselective. We believe the main issue was that one axial site was readily accessible, allowing the reaction to occur on both faces of the substrate. The substitution pattern of catalyst (S_p)-**55** is more promising as both axial sites are more congested compared with catalyst (R_p)-**54** (Figure 22).

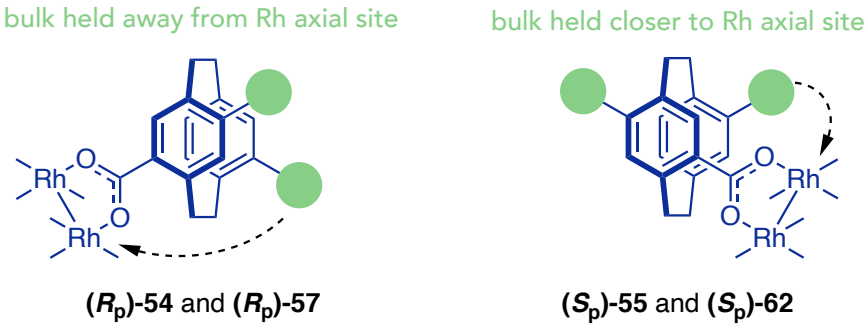

Figure 22: [2.2]PC catalyst substitution patterns that hold substituents away from the Rh(II) axial site (left) and closer to it (right).

It is a shame the biphenyl *pseudo-meta* catalyst (S_p)-**62** was not investigated in nitrene insertion as this would have provided the most sterically congested active site. [2.2]PC substituent patterns that possess a substituent either *pseudo-ortho* **a** or *ortho* **b** to the Rh(II) functionality should be investigated, as these place the substituents closest to the axial site of the Rh(II) catalyst (Figure 23).

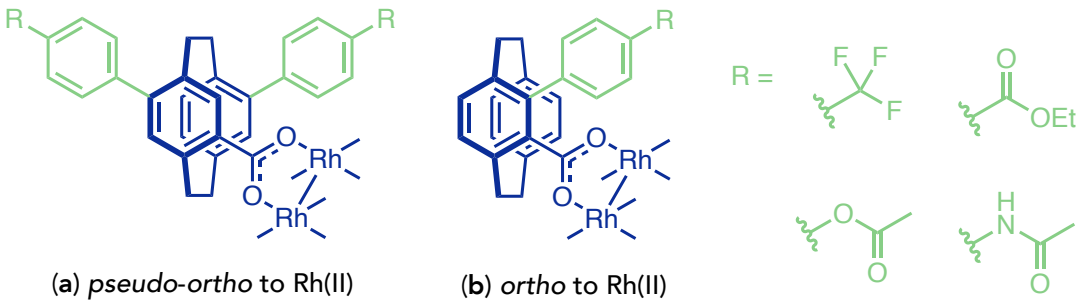

Figure 23: Proposed [2.2]PC Rh(II) catalysts that would create steric congestion around both axial sites to influence the enantioselectivity of C-H insertion.

The original goals for this work were achieved. We successfully developed a new resolution route for substituted [2.2]PC carboxylic acids. Substituted Rh(II) paddlewheels were also successfully made that were active for nitrene insertion. As the project progressed new synthetic struggles were encountered and new ideas to expand the project were gained. Overall, it has revealed the potential to extend our resolution procedure and a rapid route to a diverse family of catalysts. These are the foundations to extend this project to create more functionalised and potentially more selective catalysts.

Chapter 4

Experimental Methods

All chemicals were used as received without further purification. All reactions were performed in oven-dried glassware under atmospheric conditions unless otherwise stated. Solvents were dried over 4 Å molecular sieves. TLC was performed on aluminum backed silica-gel coated plates (Merk), visualisation methods included 254 nm UV light, $KMnO_4$ or iodine when applicable. Column chromatography was performed using silica-gel (60 Å, 40-63 micron, Scharlau).

NMR spectra were collected at room temperature using Bruker 500 MHz or Bruker 700 MHz spectrometers. High resolution mass spectrometry was performed on a ThermoScientific Q Exactive Focus Hybrid Quadripole-Orbitrap Mass Spectrometer using either an EI or APCI probe head. Infrared spectroscopy was performed on a ThermoFisher Nicolet iS5 with an ATR accessory. Analytical chiral HPLC was performed on a ThermoFisher Dionex Ultimate 3000 system equipped with a UV detector. Normal-phase elution was used either with an OD-H or AD column. Melting points were recorded on a Gallenkamp melting point instrument.

X-ray crystallography was performed on a Bruker D8 Venture diffractometer equipped with a Photon III detector and an IμS Diamond microfocus X-ray source, emitting Cu K_α radiation (λ = 1.54178 Å). MiTeGen mylar loops and Fomblin® Y oil were used to mount single crystals and cooled to 100 K using an Oxford Cryostream 800. Data was collected, integrated, scaled, and averaged using the APEX4 software package. The space group was determined and data merged by XPREP.[76] All structures were solved by SHELXT[77] and refined with SHELXL,[76] as implements in Olex2.[78] All non-hydrogen atoms were found in the electron density difference map, and refined anisotropically. All hydrogen atoms were calculated to their ideal positions, unless otherwise stated, and refined using a riding model with fixed isotropic U_{iso} values.

Planar chirality descriptors are assigned to [2.2]PC derivatives according to CIP rules (Figure 24). Assignment is performed by identifying the chiral plane – which is the most highly substituted aromatic deck. A 'pilot atom' is chosen, which the first atom out of the chiral plane, connected to the highest priority substituent within the chiral plane. The chiral plane is then viewed face on, by looking down the pilot atom, and the first three atoms in the plane are numbered according to CIP priority rules. If numbering occurs in a clockwise direction the derivative is R_p and for the anticlockwise direction, S_p.

When assigning ^{1}H resonances [2.2]PC derivatives are numbered according to CIP priority rules shown in Figure 24. When viewed from the pilot atom, bridgehead protons that extend left are labelled **a** and those extending right are labelled **b** as shown. Extra substituents are numbered starting from 17 unless otherwise depicted. For diastereomeric salts, ^{1}H resonances that belong to [2.2]PC are labelled with the subscript H_{22PC}.

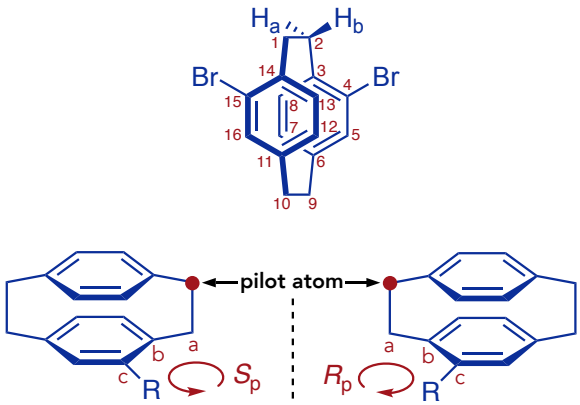

Figure 24: 4,15-Dibromo[2.2]paracyclophane numbered according to CIP rules (top) and simplified depiction for assigning planar chirality descriptors to [2.2]PC derivatives (bottom).

Synthesis of 4,16-dibromo[2.2]paracyclophane **37** and (±)-4,15-dibromo[2.2]paracyclophane **39**

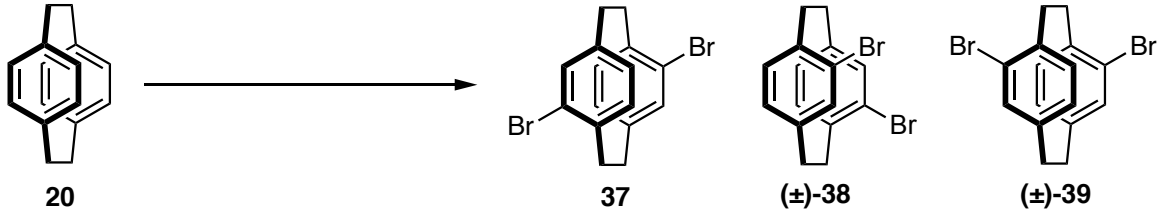

20 **37** **(±)-38** **(±)-39**

To a suspension of [2.2]paracyclophane (10.0 g, 48.0 mmol, 1.0 eq) in CH_2Cl_2 (150 mL) stirring vigorously at 60 °C, a solution of Br_2 (9.8 mL, 192 mmol, 4.0 eq) in CH_2Cl_2 (15 mL) was added dropwise. The reaction was refluxed at this temperature for a further 4 hours, then cooled to room temperature. The reaction mixture was filtered through filter paper to yield **37** as white crystals (4.50 g, 12.3 mmol, 26% yield). The filtrate was washed with saturated aqueous $Na_2S_2O_3$ solution and passed through filter paper again. The filtrate was washed with brine, dried over $MgSO_4$ and removed under reduced pressure to yield a yellow oily solid. The solid was washed with cold $CHCl_3$ (2 × 20 mL), to yield a mixture of **37** and (±)-**39** as a white solid. The filtrate was removed under reduced pressure to yield a mixture of (±)-**39** and (±)-**38** as a yellow solid. The mixture of **37** and (±)-**39** was recrystallised in 1,4-dioxane to afford **37** as a white powder (1.60 g, 4.37 mmol, 9% yield), while the filtrate was reduced to yield (±)-**39** as an off-white solid (2.20 g, 6.01 mmol, 13% yield). The mixture of (±)-**39** and (±)-**38** could be partially purified by recrystallisation in hot isopropyl alcohol, to yield (±)-**39** as white crystals (3.50 g, 9.56 mmol, 20% yield), while the filtrate was removed under reduced pressure to yield a mixture of (±)-**39** and (±)-**38** (4.10 g, 11.2 mmol, 23% yield).

4,16-dibromo[2.2]paracyclophane 37

^{1}H NMR (500 MHz, $CDCl_3$) δ (ppm) = 7.14, (2H, dd, J = 7.8, 1.6 Hz, H-13, H-7), 6.51 (2H, d, J = 1.6 Hz, H-15, H-5), 6.44 (2H, d, J = 7.8 Hz, H-12, H-8), 3.49 (2H, ddd, J = 13.5, 10.1, 2.3 Hz, H-10a, H-2b), 3.17 (1H, dd, J = 10.6, 5.0 Hz, H-1b), 3.14 (1H, dd, J = 10.3, 4.9 Hz, H-9a), 2.94 (2H, td, J = 10.9, 2.5 Hz, H-9b, H-1a), 2.86 (1H, dd, J = 13.2, 4.9 Hz, H-2a), 2.83 (1H, dd, J = 13.0, 5.1 Hz, H-10b).

^{13}C NMR (126 MHz, $CDCl_3$): δ (ppm) = 141.2, 138.5, 137.3, 134.1, 128.3, 126.8, 35.4, 32.8.

IR: 2950, 1391, 1032, 900, 707 cm^{-1}.

R_f: 0.45 (*n*-hexane).

Data comparable to that in the literature.[50]

(±)-4,15-dibromo[2.2]paracyclophane 39

^{1}H NMR (500 MHz, $CDCl_3$) δ (ppm) = 7.17 (2H, d, J = 7.8 Hz, H-13, H-8), 6.59 (2H, d, J = 1.6 Hz, H-16, H-5), 6.48 (2H, dd, J = 7.9, 1.6 Hz, H-12, H-7), 3.36-3.27 (2H, m, H-2b, H1a), 3.12-3.01 (4H, m, H-10b, H-9a, H-2a, H-1b), 2.95-2.86 (2H, m, H-10a, H-9b).

^{13}C NMR (126 MHz, $CDCl_3$): δ (ppm) = 141.2, 139.1, 136.9, 131.0, 130.4, 127.7, 34.7, 33.6.

IR: 2952, 2929, 1392, 1032, 842, 706 cm^{-1}.

R_f: 0.39 (*n*-hexane).

Data comparable to that in the literature.[50]

Synthesis of (±)-4,12-dibromo[2.2]paracyclophane **38**

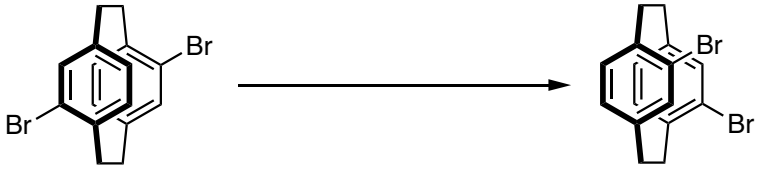

37 **(±)-38**

Five microwave tubes, each containing a suspension of **37** (0.500 g, 1.37 mmol, 1.0 eq) in DMF (4 mL) were heated by microwave irradiation to 220 °C for 20 minutes, twice. The reaction mixtures were combined and the solid was filtered to recover remaining **37** (1.14 g, 3.11 mmol, 46% yield). The filtrate was diluted with EtOAc (10 mL) and the organic layer was washed with water (6 × 10 mL), brine and dried over $MgSO_4$. The organic layer was removed under reduced pressure to yield (±)-**38** as an off-white solid (1.30 g, 3.55 mmol, 52% yield).

^{1}H NMR (500 MHz, $CDCl_3$): δ (ppm) = 7.19 (2H, d, J = 1.3 Hz, H-13, H-5), 6.55 (2H, d, J = 7.9 Hz, H-16, H-8), 6.51 (2H, dd, J = 7.9, 1.3 Hz, H-15, H-7), 3.45 (2H ddd, J = 13.5, 9.9, 1.8 Hz, H-10b, H-2b), 3.12-2.98 (4H, m, H-9, H-1), 2.81 (2H, ddd, J = 13.5, 10.5, 6.9 Hz, H-10a, H-2a).

^{13}C NMR (126 MHz, $CDCl_3$): δ (ppm) = 141.4, 138.9, 135.1, 132.9, 131.8, 126.8, 35.9, 32.6.

IR: 2935, 1391, 1032, 707 cm^{-1}.

R_f :0.33 (*n*-hexane).

Data comparable to that in the literature.[50]

Synthesis of (±)-4,12-dibromo-7-bromoacetyl[2.2]paracyclophane **32**

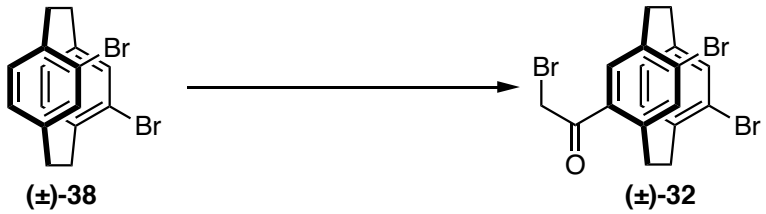

(±)-38 **(±)-32**

To a suspension of $AlCl_3$ (1.93 g, 14.5 mmol, 2.0 eq) in dry CH_2Cl_2 (14.5 mL) at 0 °C under Ar, bromoacetyl bromide (2.5 mL, 29.1 mmol, 4.0 eq) was added dropwise. The reaction was warmed to room temperature and stirred for 20 minutes which caused a colour change from clear to orange. The reaction was cooled to –15 °C and a solution of (±)-**38** (2.66 g, 7.27 mmol, 1.0 eq) in CH_2Cl_2 (14.5 mL) was added slowly which caused a colour change from orange to dark red. The reaction was stirred at –15 °C for a further 30 minutes, then warmed to room temperature for 3 hours. The reaction mixture was poured onto ice water slowly and stirred until it became clear. The organic layer was separated, washed with saturated $NaHCO_3$ solution, brine, dried over $MgSO_4$ and removed under reduced pressure to yield a yellow solid. The crude material was purified by recrystallisation in acetone to yield (±)-**32** as an off-white solid (3.30 g, 6.78 mmol, 94% yield).

^{1}H NMR (500 MHz, $CDCl_3$): δ (ppm) = 7.28 (1H, s, H-5), 7.17 (1H, d, J = 1.6 Hz, H-13), 7.04 (1H, s, H-8), 6.56 (1H, d, J = 7.9 Hz, H-16), 6.42 (1H, dd, J = 7.9, 1.6 Hz, H-15), 4.31 (1H, d, J = 12.0 Hz, H-17a), 4.10 (1H, d, J = 12.0 Hz, H-17b), 3.67 (1H, dd, J = 12.3, 9.8 Hz, H-9a), 3.48 (1H, ddd, J = 13.5, 7.4, 4.4 Hz, H-2b), 3.40 (1H, dd, J = 12.9, 9.5 Hz, H-10b), 3.15 (1H, ddd, J = 13.1, 9.4, 7.6 Hz, H-10a), 3.09-3.04 (2H, m, H-1), 3.00 (1H, ddd, J = 12.5, 9.3, 7.8 Hz, H-9b), 2.83 (1H, ddd, J = 13.5, 9.7, 8.2 Hz, H-2a).

^{13}C NMR (126 MHz, $CDCl_3$): δ (ppm) = 192.5, 144.5, 140.8, 139.5, 139.4, 135.8, 135.2, 134.4, 133.1, 132.8, 132.1, 131.3, 126.9, 35.6, 35.5, 32.9, 32.4, 32.1.

HRMS-APCI: m/z found: $[M]^+$, 484.8743. $C_{18}H_{15}Br_3O + H^+$ requires $[M]^+$, 484.8746.

IR: 2934, 1689, 1524, 1213, 1008, 710 cm^{-1}.

Mp: 145-146 °C.

R_f: 0.37 (5% EtOAc, 95% *n*-hexane).

Synthesis of (±)-4,15-dibromo-7-bromoacetyl[2.2]paracyclophane **42**

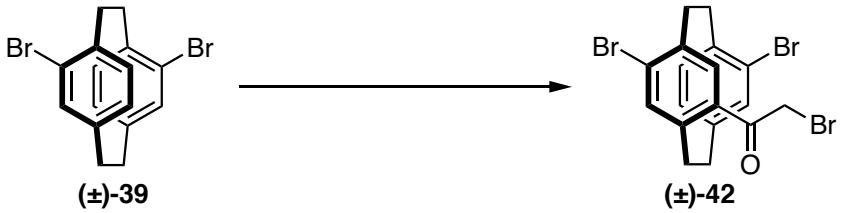

(±)-39 **(±)-42**

To a suspension of $AlCl_3$ (0.720 g, 5.39 mmol, 2.0 eq) in dry CH_2Cl_2 (5.4 mL) at 0 °C under Ar, bromoacetyl bromide (0.94 mL, 1.09 mmol, 4.0 eq) was added dropwise. The reaction was warmed to room temperature and stirred for 20 minutes which caused a colour change from clear to orange. The reaction was cooled to –15 °C and a solution of (±)-**39** (0.990 g, 2.69 mmol, 1.0 eq) in CH_2Cl_2 (5.39 mL) was added slowly which caused a colour change from orange to brown. The reaction was stirred at –15 °C for a further 30 minutes, then warmed to room temperature for 3 hours. The reaction mixture was poured onto ice water slowly and stirred until it became clear. The organic layer was separated, washed with saturated $NaHCO_3$ solution, brine, dried over $MgSO_4$ and removed under reduced pressure to yield a brown oil. The crude material was purified by silica-gel chromatography (2.5% EtOAc, 97.5% *n*-hexane) to yield (±)-**42** as a white oily solid (1.01 g, 2.07 mmol, 77% yield).

^{1}H NMR (500 MHz, $CDCl_3$): δ (ppm) = 7.56 (1H, s, H-8), 7.14 (1H, d, J = 7.5 Hz, H-13), 6.70 (1H, s, H-5), 6.56-6.52 (2H, m, H-16, H-12), 4.44 (1H, d, J = 12.9 Hz, H-17a), 4.40 (1H, d, J = 12.9 Hz, H-17b), 3.82 (1H, ddd, J = 12.8, 10.2, 2.5 Hz, H-9a), 3.38-3.29 (2H, m, H-2b, H-1a), 3.18-3.02 (4H, m, H-10, H-2a, H-1b), 2.71 (1H, ddd, J = 12.6, 9.0, 7.6 Hz, H-9b).

^{13}C NMR (126 MHz, $CDCl_3$): δ (ppm) = 192.4, 143.9, 142.0, 140.0, 139.5, 138.5, 135.0, 133.5, 32.8, 130.8, 130.6, 130.6, 127.4, 35.4, 34.1, 33.4, 33.2, 33.1.

HRMS-APCI: *m/z* found: $[M]^+$, 484.8742. $C_{18}H_{15}Br_3O + H^+$ requires $[M]^+$, 484.8746.

IR: 2931, 1685, 1524, 1006, 859 cm^{-1}.

Mp: 104-105 °C.

R_f: 0.62 (5% EtOAc, 95% *n*-hexane).

Synthesis of (±)-4-bromoacetyl[2.2]paracyclophane **43**

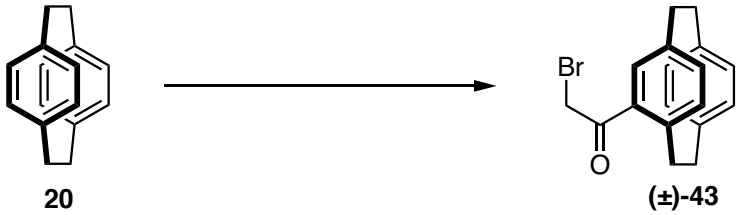

20 **(±)-43**

To a suspension of $AlCl_3$ (3.84 g, 28.8 mmol, 2.0 eq) in dry CH_2Cl_2 (28 mL) at 0 °C under Ar, bromoacetyl bromide (5.02 mL, 57.6 mmol, 4.0 eq) was added dropwise. The reaction was warmed to room temperature and stirred for 20 minutes which caused a colour change from clear to orange. In a separate flask, a suspension of **20** (3.00 g, 14.4 mmol, 1.0 eq) in dry CH_2Cl_2 (28 mL) under Ar, was cooled to –15 °C. The orange $AlCl_3$ solution was transferred by syringe to the flask containing **20** and added slowly, which caused a colour change from orange to bright red. The reaction was stirred at –15 °C for a further 30 minutes, then warmed to room temperature for 3 hours. The reaction mixture was poured onto ice water slowly and stirred until it became clear. The organic layer was separated, washed with saturated $NaHCO_3$ solution, brine, dried over $MgSO_4$ and removed under reduced pressure to yield a brown oil. The crude material was purified by silica-gel chromatography (5% EtOAc, 95% *n*-hexane) to yield (±)-**43** as a white solid (3.01 g, 9.14 mmol, 64% yield).

^{1}H NMR (700 MHz, $CDCl_3$): δ (ppm) = 6.97 (1H, d, J = 1.6 Hz, H-5), 6.71 (1H, dd, J = 7.6, 1.6 Hz, H-7), 6.57 (1H, dd, J = 7.6, 1.9 Hz, H-15), 6.56 (1H, d, J = 7.8 Hz, H-8), 6.52 (1H, dd, J = 7.7, 1.8 Hz, H-13), 6.52 (1H, dd, J = 7.8, 1.8 Hz, H-16), 6.39 (1H, dd, J = 7.9, 1.7 Hz, H-12), 4.37 (1H, d, J = 12.3 Hz, H-17a), 4.17 (1H, d, J = 12.3 Hz, H-17b), 3.88 (1H, ddd, J = 12.9, 11.6, 1.5 Hz, H-2b), 3.28-3.15 (4H, m, H-10b, H-9a, H-1), 3.15-2.99 (2H, m, H-10a, H-9b), 2.87 (1H, ddd, J = 12.8, 9.5, 6.7 Hz, H-2a).

^{13}C NMR (176 MHz, $CDCl_3$): δ (ppm) = 193.0, 143.1, 140.3, 140.2, 139.3, 137.5, 136.8, 134.9, 133.8, 133.0, 133.0 132.5, 131.4, 36.2, 35.3, 35.3, 35.0, 33.3.

HRMS-APCI: *m/z* found: $[M]^+$, 329.0534. $C_{18}H_{17}BrO + H^+$ requires $[M]^+$, 329.0534.

IR: 2930, 2855, 1697, 1213, 994, 721 cm^{-1}.

Mp: 120-121 °C.

R_f: 0.47 (5% EtOAc, 95% *n*-hexane).

Data comparable to that in the literature.[57]

Synthesis of (R_p)-4,12-dibromo-7-acetyl[2.2]paracyclophane cinchonidinium bromide **36**

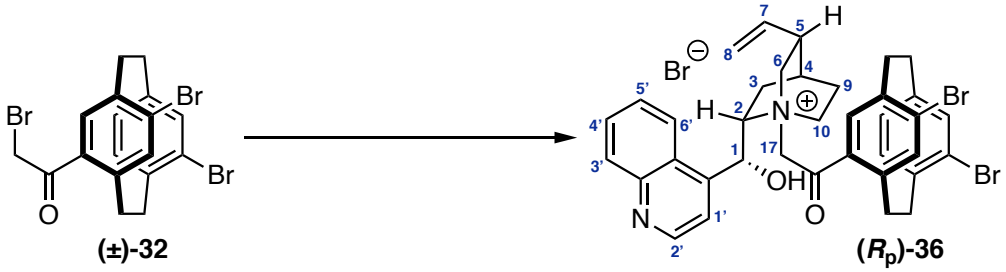

To a suspension of (–)-cinchonidine (0.605 g, 2.05 mmol, 1.0 eq) in acetone (5.2 mL) a solution of (±)-**32** (1.00 g, 2.05 mmol, 1.0 eq) in acetone (3 mL) was added. The reaction was heated to 57 °C and stirred for 14 hours, which caused a colour change from yellow to orange and a white precipitate to form. The reaction was cooled to room temperature, diluted with MeOH (6.0 mL) and Et_2O (6.0 mL) and stirred for 2 hours. The reaction mixture was filtered through a Büchner funnel and washed with acetone to yield (R_p)-**36** as a cream-coloured powder (0.703 g, 0.898 mmol, 44% yield). The filtrate was reduced to a volume of 6 mL, Et_2O (4 drops) was added, and the solution was left overnight. The mixture was filtered to yield a second crop of (R_p)-**36** as a cream-coloured powder (60.0 mg, 0.0767 mmol, 4% yield).

^{1}H NMR (500 MHz, $CDCl_3$): δ (ppm) = 9.00 (1H, d, J = 4.7 Hz, H-2'), 8.30 (1H, s, H-8_{22PC}), 8.27-8.24 (1H, m, H-6'), 8.22-8.18 (1H, m, H-3'), 7.96 (1H, d, J = 4.4 Hz, H-1'), 7.79-7.75 (2H, m, H-5', H-4'), 7.28 (1H, s, H-5_{22PC}), 7.14 (1H, d, J = 1.6 Hz, H-13_{22PC}), 6.90 (1H, dd, J = 7.9, 1.6 Hz, H-15_{22PC}), 6.78 (1H, d, J = 18.6 Hz, H-$17a_{22PC}$), 6.59 (1H, d, J = 6.6 Hz, OH), 6.50 (1H, d, J = 8.0 Hz, H-16_{22PC}), 6.18 (1H, dd, J = 6.6, 1.6 Hz, H-1), 5.66 (1H, ddd, J = 17.2, 10.4, 6.3 Hz, H-7), 5.26 (1H, dd, J = 17.3, 1.3 Hz, H-$8a_{trans}$), 5.13 (1H, dd, J = 10.7, 1.3 Hz, H-$8b_{cis}$), 5.11-5.06 (1H, m, H-2), 5.04-4.95 (1H, m, H-10a), 4.53 (1H, d, J = 18.7 Hz, H-$17b_{22PC}$), 4.36 (1H, dt, J = 12.5, 3.1 Hz, H-6a), 3.73 (1H, dd, J = 12.6, 9.8 Hz, H-$9b_{22PC}$), 3.69-3.58 (3H, m, H-10b, H-6b, H-$2a_{22PC}$), 3.41-3.30 (3H, m, H-10_{22PC}, H-$2b_{22PC}$), 3.20-3.09 (2H, m, H-$9a_{22PC}$, H-$1b_{22PC}$), 2.98 (1H, ddd, J = 13.3, 9.5, 7.4 Hz, H-$1a_{22PC}$), 2.81 (1H, s, H-5), 2.17-2.13 (2H, m, H-9a, H-4), 2.04 (1H, t, J = 13.0 Hz, H-3a), 2.01-1.95 (1H, m, H-9b), 1.35-1.27 (1H, m, H-3b).

^{13}C NMR (126 MHz, $CDCl_3$): δ (ppm) = 194.2, 150.6, 148.4, 144.5, 144.2, 141.7, 141.5, 138.3, 136.8, 135.8, 135.6, 134.1, 133.2, 133.1, 132.8, 132.7, 131.1, 129.6, 127.4, 126.2, 125.0, 122.3, 120.8, 117.7, 65.4, 64.4, 61.6, 58.4, 38.0, 35.9, 34.6, 33.1, 31.9, 31.1, 26.5, 26.0, 22.1.

HRMS-EI: m/z found: $[M-Br]^+$, 699.1198. $C_{37}H_{37}Br_2N_2O_2$ requires $[M-Br]^+$, 699.1216.

IR: 3136, 2935, 1677, 1248, 1012, 776 cm^{-1}.

Mp: 223 °C (decomposes).

R_f: 0.17 (5% MeOH, 95% CH_2Cl_2).

Synthesis of (S_p)-4,15-dibromo-7-acetyl[2.2]paracyclophane brucinium bromide **50**

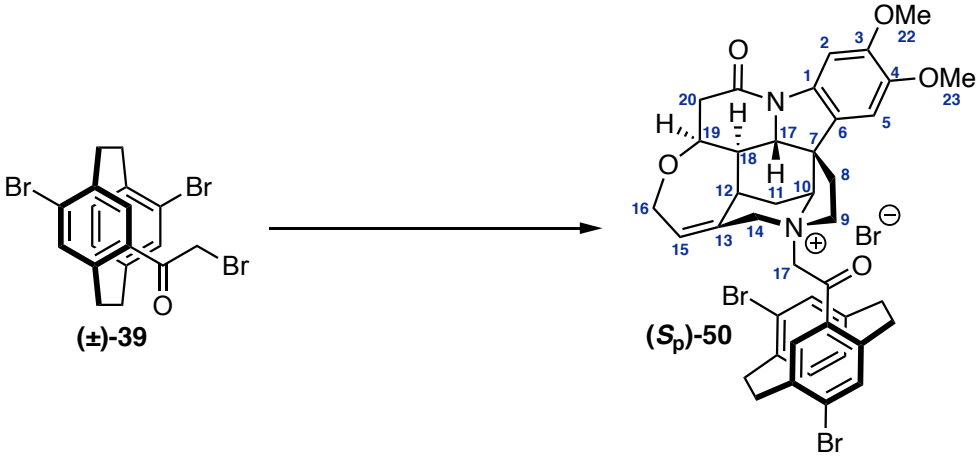

(–)-Brucine (65.0 mg, 0.164 mmol, 1.0 eq) and (±)-**39** (80.0 mg, 0.164 mmol, 1.0 eq) were dissolved in $CHCl_3$ (0.82 mL), heated to 62 °C and stirred for 16 hours. The reaction was cooled to room temperature and the solvent was removed under reduced pressure. Hot 1,2-dichloroethane (1 mL) was added to suspend the solid and MeOH was added dropwise until all solid dissolved. The solution was left to stand overnight which caused a white solid to form. The mixture was filtered through a Büchner funnel to yield (S_p)-**50** as white crystals (53.5 mg, 0.0607 mmol, 37% yield).

^{1}H NMR (700 MHz, $CDCl_3$): δ (ppm) = 8.42 (1H, s, H-8$_{22PC}$), 7.81 (1H, s, H-2), 7.71 (1H, s, H-5), 7.07 (1H, d, J = 7.9 Hz, H-13$_{22PC}$), 6.50 (1H, dd, J = 7.6, 1.6 Hz, H-12$_{22PC}$), 6.50 (1H, s, H-5$_{22PC}$), 6.46 (1H, d, J = 1.6 Hz, H-16$_{22PC}$), 6.42 (1H, d, J = 18.0 Hz, H-17a$_{22PC}$), 6.33 (1H, s, H-15), 6.11 (1H, d, J = 18.0 Hz, H-17b$_{22PC}$), 5.21 (1H, s, H-10), 4.83 (1H, d, J = 12.5 Hz, H-14a), 4.47 (1H, d, J = 13 Hz, H-14b), 4.34 (2H, dt, J = 14.2, 2.8 Hz, H-19, H-9a), 4.24 (1H, dd, J = 14.2, 6.8 Hz, H-16a), 4.06 (1H, dd, J = 14.0, 6.4 Hz, H-16b), 4.04 (3H, s, H-23), 3.95 (1H, d, J = 11.0 Hz, H-17), 3.94 (3H, s, H-22), 3.72-3.65 (2H, m, H-9a$_{22PC}$, H-9b), 3.33-3.25 (3H, m, H-11a, H-2a$_{22PC}$, H-1a$_{22PC}$), 3.22 (1H, s, H-12), 3.15 (1H, dd, J = 17.8, 8.4 Hz, H-20a), 3.09 (2H, t, J = 7.8 Hz, H-10$_{22PC}$), 2.99-2.91 (2H, m, H-2b$_{22PC}$, H-1b$_{22PC}$), 2.70 (1H, dd, J = 17.8, 2.8 Hz, H-20b), 2.68 (2H, ddd, J = 14.0, 10.6, 8.4 Hz, H-9b$_{22PC}$, H-8a), 1.91 (1H, s, H-8b), 1.43 (1H, d, J = 13.9 Hz, H-11a), 1.38 (1H, dt, J = 10.5, 3.0 Hz, H-18).

^{13}C NMR (176 MHz, $CDCl_3$): δ (ppm) = 194.5, 168.5, 150.3, 147.2, 143.6, 141.6, 140.5, 139.7, 138.9, 136.6, 135.4, 134.4, 133.4, 133.4, 133.1, 132.1, 130.9, 130.7, 127.7, 119.1, 107.1, 100.8, 71.3, 64.4, 59.6, 57.8, 56.5, 53.0, 47.1, 43.6, 42.1, 40.1, 35.0, 34.3, 33.1, 32.7, 30.3, 29.8.

HRMS-EI: m/z found: $[M\text{-}Br]^+$, 799.1359. $C_{41}H_{41}Br_2N_2O_5$ requires $[M\text{-}Br]^+$, 799.1377.

IR: 2930, 1670, 1503, 1392, 1282, 848 cm^{-1}.

Mp: 236 °C (decomposes).

R_f: 0.21 (5% MeOH, 95% CH_2Cl_2).

Synthesis of (R_p)-4-acetyl[2.2]paracyclophane cinchonium bromide **48**

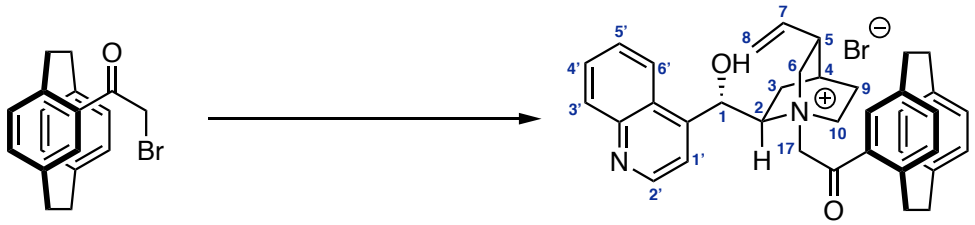

(+)-Cinchonine (0.180 g, 0.611 mmol, 1.0 eq) and (±)-**43** (0.200 g, 0.611 mmol, 1.0 eq) were suspended in acetone (2.4 mL), heated to 57 °C and stirred for 14 hours, causing all solid to dissolve. The reaction was cooled to room temperature, MeOH (2 mL) and Et_2O (3 mL) were added, and the reaction mixture was stirred for 2 hours, causing a precipitate to form. The reaction mixture was filtered through a Büchner funnel to yield (R_p)-**48** as a cream-coloured powder (141 mg, 0.226 mmol, 37% yield).

^{1}H NMR (700 MHz, $CDCl_3$): δ (ppm) = 8.94 (1H, d, J = 4.4 Hz, H-2'), 8.17 (1H, d, J = 8.3 Hz, H-6'), 7.95 (1H, s, H-5_{22PC}), 7.88 (1H, d, J = 7.8 Hz, H-3'), 7.85 (1H, d, J = 4.5 Hz, H-1'), 7.78 (1H, ddd, J = 8.0, 6.8, 1.0 Hz, H-5'), 7.66 (1H, ddd, J = 8.0, 6.8, 0.9 Hz, H-4'), 6.81 (1H, dd, J = 7.8, 1.6 Hz, H-13_{22PC}), 6.66 (1H, dd, J = 7.8, 1.3 Hz, H-7_{22PC}), 6.54 (1H, dd, J = 7.8, 1.8 Hz, H-15_{22PC}), 6.52 (1H, d, J = 7.8 Hz, H-8_{22PC}), 6.46 (1H, dd, J = 7.6, 1.7 Hz, H-16_{22PC}), 6.42 (1H, d, J = 18.0 Hz, H-$17a_{22PC}$), 6.38 (1H, dd, J = 7.8, 1.7 Hz, H-12_{22PC}), 5.99 (1H, s, H-1), 5.97 (1H, ddd, J = 17.3, 10.2, 7.2 Hz, H-7), 5.74 (1H, s, OH), 5.32 (1H, d, J = 17 Hz, H-$8a_{trans}$), 5.30 (1H, d, J = 10.8 Hz, H-$8b_{cis}$), 5.09 (1H, d, J = 17.8 Hz, H-$17b_{22PC}$), 4.72 (1H, t, J = 11.0 Hz, H-6a), 4.53 (1H, t, J = 11.0 Hz, H-6b), 4.47 (1H, t, J = 10.4 Hz, H-2), 4.22 (2H, t, J = 8.3 Hz, H-10), 4.02 (1H, ddd, J = 13.0, 9.1, 1.8 Hz, H-$2b_{22PC}$), 3.30-3.21 (3H, m, H-$10b_{22PC}$, H-1_{22PC}), 3.16-3.11 (1H, m, H-$9b_{22PC}$), 2.92 (2H, ddd, J = 12.8, 7.9, 7.3 Hz, H-5, H-$2a_{22PC}$), 2.88-2.81 (2H, m, H-$10a_{22PC}$, H-$9a_{22PC}$), 2.37 (1H, t, J = 12.0 Hz, H-3a), 2.14-2.08 (1H, m, H-9a), 2.06 (1H, t, J = 4.8 Hz, H-4), 1.94 (1H, dd, J = 22.0, 10.0 Hz, H-9b), 1.02-0.97 (1H, m, H-3b).

^{13}C NMR (176 MHz, $CDCl_3$): δ (ppm) = 193.9, 150.5, 148.3, 144.1, 143.1, 142.2, 140.4, 139.3, 139.1, 137.1, 135.2, 135.2, 133.7, 133.4, 133.2, 132.6, 131.0, 130.9, 129.6, 127.3, 124.6, 122.7, 120.3, 118.8, 66.1, 64.4, 56.9, 38.4, 36.7, 35.0, 34.9, 34.6, 27.3, 24.3, 21.2.

HRMS-EI: m/z found: $[M\text{-}Br]^+$, 543.2993. $C_{37}H_{39}N_2O_2$ requires $[M\text{-}Br]^+$, 543.3006.

IR: 3340, 2928, 2850, 1667, 1239, 995, 799 cm^{-1}.

Mp: 199 °C (decomposes).

R_f: 0.20 (5% MeOH, 95% CH_2Cl_2).

Data comparable to that in the literature.[57]

Synthesis of (±)-4,12-dibromo-7-carboxy[2.2]paracyclophane **33**

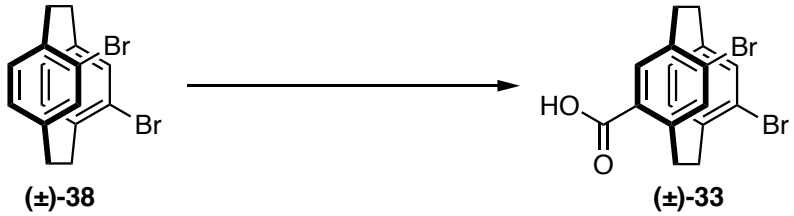

(±)-38 **(±)-33**

To a suspension of $AlCl_3$ (0.150 g, 1.10 mmol, 2.0 eq) in dry CH_2Cl_2 (1.1 mL) at 0 °C under Ar, oxalyl chloride (0.19 mL, 2.20 mmol, 4.0 eq) was added dropwise. The reaction was warmed to room temperature and stirred for 1 hour which caused a colour change from clear to yellow. The reaction was cooled to –15 °C and a solution of (±)-**38** (0.200 g, 0.546 mmol, 1.0 eq) in CH_2Cl_2 (1.1 mL) was added slowly, which caused a colour change from yellow to brown. The reaction was stirred at –15 °C for a further 30 minutes, then warmed to room temperature for 3 hours. The volatiles were removed under reduced pressure to yield the crude acyl chloride as a sticky brown solid. The solid was dissolved in dry THF (1.1 mL), H_2O (0.55 mL) was added, and the reaction was stirred overnight at room temperature. The reaction mixture was diluted with EtOAc (5 mL), and the organic layer was separated, washed with H_2O, brine and dried over $MgSO_4$. The organic layer was removed under reduced pressure to yield a yellow oil that was purified by silica-gel chromatography (2.5% MeOH, 97.5% CH_2Cl_2) to yield (±)-**33** as an off-white powder (0.114 g, 0.278 mmol, 51% yield).

^{1}H NMR (700 MHz, $CDCl_3$): δ (ppm) = 7.32 (1H, s, H-8), 7.29 (1H, s, H-5), 7.18 (1H, d, J = 1.7 Hz, H-13) 6.62 (1H d, J = 7.8 Hz, H-16), 6.51 (1H, dd, J = 7.8, 1.7 Hz, H-15), 4.00-3.93 (1H, m, H-9a), 3.48-3.39 (2H, m, H-10b, H-2b), 3.10-3.01 (4H, m, H10a, H9b, H1), 2.87 (1H, ddd, J = 13.3, 9.4, 7.8 Hz, H2a).

^{13}C NMR (176 MHz, $CDCl_3$): δ (ppm) = 170.3, 145.2, 141.2, 139.6, 139.3, 137.7, 135.6, 133.5, 133.0, 132.3, 131.3, 129.2, 126.8, 35.6, 35.5, 32.9, 32.3.

R_f: 0.26 (2.5% MeOH, 97.5% CH_2Cl_2).

Data comparable to that in the literature.[49]

Synthesis of (R_p)-4,12-dibromo-7-carboxy[2.2]paracyclophane **33**

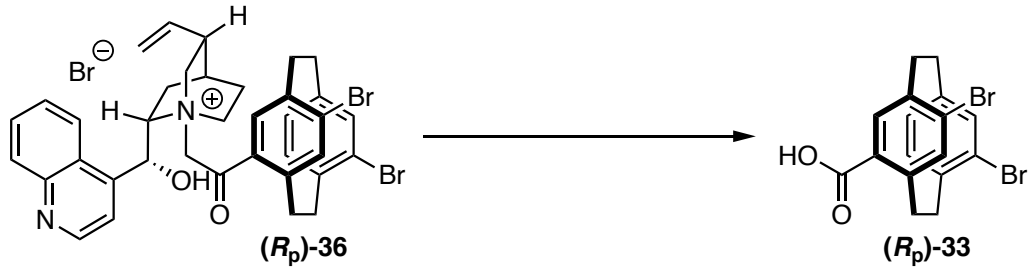

To a suspension of (R_p)-**36** (0.800 g, 1.02 mmol, 1.0 eq) and ground NaOH pellets (0.164 g, 4.09 mmol, 4.0 eq) in H_2O (5.1 mL), *tert*-butyl hydroperoxide (0.50 mL, 5.11 mmol, 5.0 eq) was added. The reaction mixture was heated to 90 °C and stirred for 16 hours, which caused all solid to dissolve. The reaction mixture was neutralised with aqueous 1 M HCl solution, and the aqueous layer was extracted with EtOAc (3 × 10 mL). The combined organics were washed with brine, dried over $MgSO_4$, and removed under reduced pressure to yield (R_p)-**33** as a light yellow solid (0.360 g, 0.880 mmol, 86% yield).

^{1}H NMR (700 MHz, $CDCl_3$): δ (ppm) = 7.32 (1H, s, H-8), 7.29 (1H, s, H-5), 7.18 (1H, d, J = 1.7 Hz, H-13), 6.62 (1H d, J = 7.8 Hz, H-16), 6.51 (1H, dd, J = 7.8, 1.7 Hz, H-15), 4.00-3.93 (1H, m, H-9a), 3.48-3.39 (2H, m, H-10b, H-2b), 3.10-3.01 (4H, m, H10a, H9b, H1), 2.87 (1H, ddd, J = 13.3, 9.4, 7.8 Hz, H2a).

^{13}C NMR (176 MHz, $CDCl_3$): δ (ppm) = 170.3, 145.2, 141.2, 139.6, 139.3, 137.7, 135.6, 133.5, 133.0, 132.3, 131.3, 129.2, 126.8, 35.6, 35.5, 32.9, 32.3.

HRMS-EI: m/z found: $[M]^-$, 406.9284. $C_{17}H_{13}Br_2O_2$ requires $[M]^-$, 406.9277.

IR: 2934, 1678, 1537, 1268, 1091, 878 cm^{-1}.

Mp: 172-173 °C.

R_f: 0.37 (45% EtOAc, 55% *n*-hexane).

Data comparable to that in the literature.[49]

Synthesis of (S_p)-4,15-dibromo-7-carboxy[2.2]paracyclophane **34**

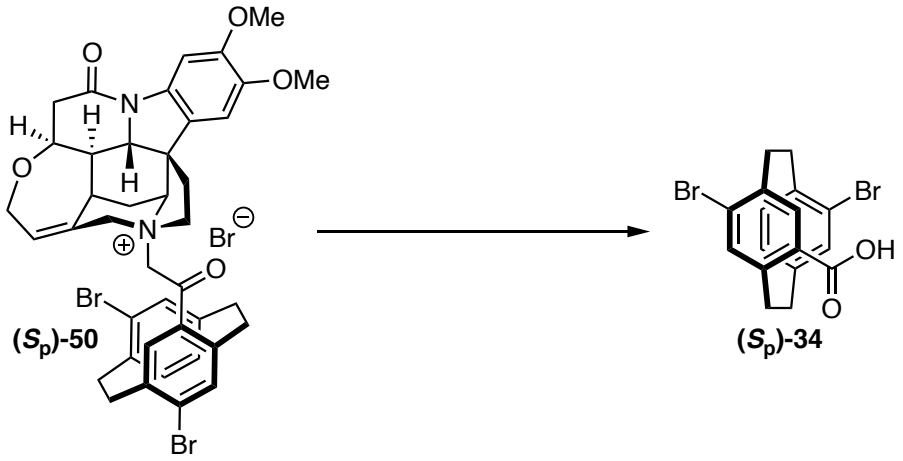

To a suspension of (S_p)-**50** (396 mg, 0.449 mmol, 1.0 eq) and ground NaOH pellets (71.0 mg, 1.78 mmol, 4.0 eq) in H_2O (2.2 mL), *tert*-butyl hydroperoxide (0.23 mL, 2.25 mmol, 5.0 eq) was added. The reaction mixture was heated to 90 °C and stirred for 16 hours, which caused all solid to dissolve. The reaction mixture was neutralised with aqueous 1 M HCl solution, and the aqueous layer was extracted with EtOAc (3 × 5 mL). The combined organics were washed with brine, dried over $MgSO_4$, and removed under reduced pressure to yield (S_p)-**34** as a light yellow solid (0.160 g, 0.390 mmol, 87% yield).

^{1}H NMR (500 MHz, $CDCl_3$): δ (ppm) = 7.90 (1H, s, H-8), 7.15 (1H, d, J = 7.8 Hz, H-13), 6.72-6.69 (2H, m, H-16, H-5), 6.55 (1H, dd, J = 7.8, 1.3 Hz, H-12), 4.09 (1H, dd, J = 13.2, 10.7 Hz, H-9a), 3.38-2.29 (2H, m, H-2b, H-1a), 3.20-3.13 (2H, m, H-10b, H-2a), 3.12-3.03 (2H, m, H-10a, H-1b), 2.73 (1H, ddd, J = 12.9, 9.5, 7.6 Hz, H-9b).

^{13}C NMR (126 MHz, $CDCl_3$): δ (ppm) = 171.1, 144.7, 141.7, 139.8, 139.7, 138.9, 135.7, 133.4, 133.0, 130.6, 130.6, 128.7, 127.4, 35.7, 34.3, 33.4, 33.1.

HRMS-EI: m/z found: $[M]^-$, 406.9283. $C_{17}H_{13}Br_2O_2$ requires $[M]^-$, 406.9277.

IR: 2934, 1682, 1538, 1269, 915 cm^{-1}.

Mp: 161-163 °C.

R_f: 0.53 (45% EtOAc, 55% *n*-hexane).

Synthesis of (R_p)-4-carboxy[2.2]paracyclophane **28**

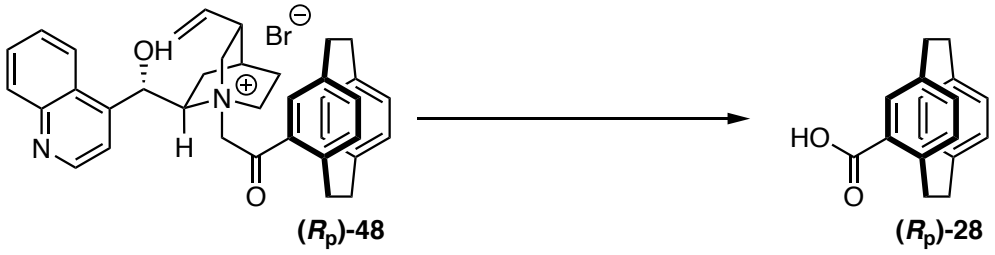

(R_p)-48 **(R_p)-28**

To a suspension of (R_p)-**48** (0.150 g, 0.241 mmol, 1.0 eq) and ground NaOH pellets (38.5 mg, 0.964 mmol, 4.0 eq) in H_2O (2.4 mL), *tert*-butyl hydroperoxide (0.12 mL, 1.21 mmol, 5.0 eq) was added. The reaction mixture was heated to 90 °C and stirred for 16 hours, which caused all solid to dissolve. The reaction mixture was neutralised with aqueous 1 M HCl solution, and the aqueous layer was extracted with EtOAc (3 × 5 mL). The combined organics were washed with brine, dried over $MgSO_4$, and removed under reduced pressure to yield (R_p)-**28** as a light yellow solid (51.0 mg, 0.202 mmol, 84% yield).

^{1}H NMR (500 MHz, $CDCl_3$): δ (ppm) = 7.28 (1H, d, J = 1.6 Hz, H-5), 6.70 (1H, dd, J = 7.6, 1.6 Hz, H-13), 6.60-6.56 (3H, m, H-7, H-8, H-15), 6.53-6.48 (2H, m, H-16, H-12), 4.19 (1H, t, J = 11.5 Hz, H-2b), 3.24-2.99 (6H, m, H-10, H-9, H-1), 2.89 (1H, ddd, J = 13.0, 9.3, 7.4 Hz, H-2a).

^{13}C NMR (126 MHz, $CDCl_3$): δ (ppm) = 172.2, 143.8, 140.1, 140.0, 139.5, 137.4, 136.4, 136.2, 133.2, 132.8, 132.3, 131.8, 129.6, 36.3, 35.3, 35.1, 34.9.

HRMS-EI: *m/z* found: $[M]^-$, 251.1075. $C_{17}H_{15}O_2$ requires $[M]^-$, 251.1067.

IR: 2924, 2853, 1679, 1303, 798 cm^{-1}.

Data comparable to that in the literature. [47]

Synthesis of (±)-4,12-dibromo-7-methylcarboxylate[2.2]paracyclophane **51**

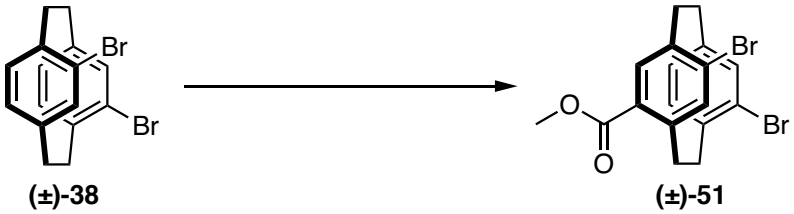

(±)-38 **(±)-51**

To a suspension of $AlCl_3$ (0.360 g, 2.73 mmol, 2.0 eq) in dry CH_2Cl_2 (2.7 mL) at 0 °C under Ar, oxalyl chloride (0.47 mL, 5.46 mmol, 4.0 eq) was added dropwise. The reaction was warmed to room temperature and stirred until all solid had dissolved which caused a colour change from clear to yellow. The reaction was cooled to –15 °C and a solution of (±)-**38** (0.500 g, 1.37 mmol, 1.0 eq) in CH_2Cl_2 (2.7 mL) was added slowly, which caused a colour change from yellow to brown. The reaction was stirred at –15 °C for a further 30 minutes, then warmed to room temperature for 3 hours. The volatiles were removed under reduced pressure to yield the crude acyl chloride as a sticky brown solid. The solid was dissolved in dry CH_2Cl_2 (3.4 mL) and MeOH (3.4 mL), and the reaction was stirred overnight at room temperature. The reaction mixture was diluted with CH_2Cl_2 (10 mL) washed with H_2O, brine and dried over $MgSO_4$. The organic layer was removed under reduced pressure to yield a yellow oil that was purified by silica-gel chromatography (5% EtOAc, 95% *n*-hexane) to yield (±)-**51** as a white solid (0.220 g, 0.519 mmol, 38% yield).

^{1}H NMR (500 MHz, $CDCl_3$): δ (ppm) = 7.24 (1H, s, H-5), 7.18 (1H, s, H-8), 7.17 (1H, d, J = 1.6 Hz, H-13), 6.51 (1H, d, J = 7.8 Hz, H-16), 6.46 (1H, dd, J = 7.8, 1.6 Hz, H-15), 3.91 (3H, s, H-17), 3.90-8.83 (1H, m, H-9a), 3.46-3.35 (2H, m, H-10b, H-2b), 3.08-2.93 (4H, m, H-10a, H-9b, H-1), 2.83 (1H, ddd, J = 13.3, 9.4, 7.8 Hz, H-2a).

^{13}C NMR (126 MHz, $CDCl_3$): δ (ppm) = 166.9, 144.2, 141.1, 139.3, 139.3, 137.0, 135.3, 133.4, 132.9, 131.3, 131.2, 130.5, 126.7, 52.2, 35.6, 35.5, 32.8, 32.3.

R_f: 0.54 (20% EtOAc, 80% *n*-hexane).

Data comparable to that in the literature.[49]

Synthesis of (R_p)-4,12-dibromo-7-methylcarboxylate[2.2]paracyclophane **51**

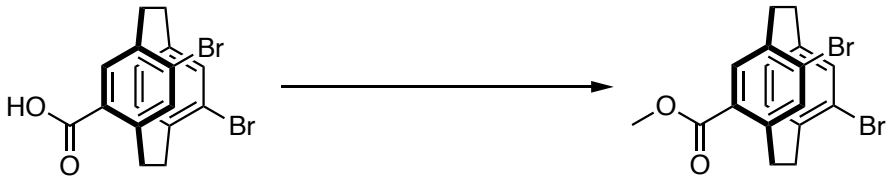

(R_p)-33 **(R_p)-51**

To a solution of (R_p)-**33** (14.0 mg, 0.0341 mmol, 1.0 eq) in dry CH_2Cl_2 (0.17 mL) at 0 °C under Ar, oxalyl chloride (0.005 mL, 0.0683 mmol, 2.0 eq) was added. One drop of a DMF stock solution (2 drops of DMF in 2 mL of CH_2Cl_2) was added which caused the solution to bubble. The reaction was warmed to room temperature and stirred for 30 minutes. The volatiles were removed under reduced pressure to yield the crude acyl chloride as a yellow solid. The solid was dissolved in dry CH_2Cl_2 (0.17 mL) and MeOH (0.17 mL), and the reaction was stirred at 50 °C overnight. The solvent was removed under reduced pressure to yield (R_p)-**51** an off-white solid (16.0 mg, 0.0377 mmol, >99% yield).

Enantiomeric excess measurements were carried out using HPLC. A Chiralcel OD-H 25 cm column was used, eluting 5% *i*PrOH, 95% *n*-hexane for 20 minutes, 1 mL/min at 25 °C, detecting at 220 nm. Retention times: (R_p)-**51** 5.1 min, (S_p)-**51** 6.2 min.

^{1}H NMR (500 MHz, $CDCl_3$): δ (ppm) = 7.24 (1H, s, H-5), 7.18 (1H, s, H-8), 7.17 (1H, d, J = 1.6 Hz, H-13), 6.51 (1H, d, J = 7.8 Hz, H-16), 6.46 (1H, dd, J = 7.8, 1.6 Hz, H-15), 3.91 (3H, s, H-17), 3.90-8.83 (1H, m, H-9a), 3.46-3.35 (2H, m, H-10b, H-2b), 3.08-2.93 (4H, m, H-10a, H-9b, H-1), 2.83 (1H, ddd, J = 13.3, 9.4, 7.8 Hz, H-2a).

^{13}C NMR (126 MHz, $CDCl_3$): δ (ppm) = 166.9, 144.2, 141.1, 139.3, 139.3, 137.0 135.3, 133.4, 132.9, 131.3, 131.2, 130.5, 126.7, 52.2, 35.6, 35.5, 32.8, 32.3.

HRMS-APCI: m/z found: $[M]^+$, 422.9589. $C_{18}H_{16}Br_2O_2$ $+H^+$ requires $[M]^+$, 422.9589.

IR: 2988, 1712, 1408, 1265, 1086 cm^{-1}.

Mp: 111-113 °C.

R_f: 0.54 (20% EtOAc, 80% *n*-hexane).

Data comparable to that in the literature.[49]

Synthesis of (S_p)-4,15-dibromo-7-methylcarboxylate[2.2]paracyclophane **52**

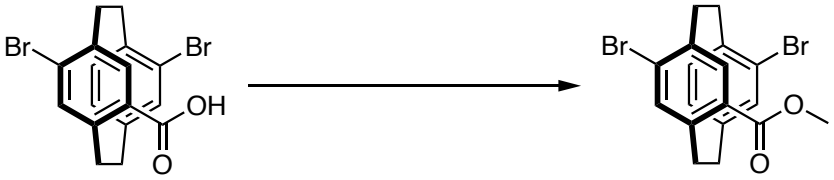

(S_p)-34 **(S_p)-52**

To a solution of (S_p)-**34** (16.0 mg, 0.0390 mmol, 1.0 eq) in dry CH_2Cl_2 (0.20 mL) at 0 °C under Ar, oxalyl chloride (0.007 mL, 0.0780 mmol, 2.0 eq) was added. One drop of a DMF stock solution (2 drops of DMF in 2 mL of CH_2Cl_2) was added which caused the solution to bubble. The reaction was warmed to room temperature and stirred for 30 minutes. The volatiles were removed under reduced pressure to yield the crude acyl chloride as a yellow solid. The solid was dissolved in dry CH_2Cl_2 (0.2 mL) and MeOH (0.2 mL), and the reaction was stirred at 50 °C overnight. The solvent was removed under reduced pressure to yield (S_p)-**52** an off-white solid (16.9 mg, 0.0400 mmol, >99% yield).

Enantiomeric excess measurements were carried out using HPLC. A Chiralcel OD-H 25 cm column was used, eluting 1% *i*PrOH, 99% *n*-hexane for 15 minutes, 1 mL/min at 25 °C, detecting at 220 nm. Retention times: (R_p)-**52** 5.6 min, (S_p)-**52** 7.6 min.

^{1}H NMR (500 MHz, $CDCl_3$): δ (ppm) = 7.75 (1H, s, H-8), 7.13 (1H, d, J = 7.8 Hz, H-13), 6.66 (1H, s, H-5), 6.59 (1H, d, J = 1.8 Hz, H-16), 6.52 (1H, dd, J = 7.8, 1.8 Hz, H-12), 4.00 (1H, dd, J = 12.5, 10.1 Hz, H-9a), 3.93 (3H, s, H-17), 3.32 (1H, dd, J = 12.1, 9.3 Hz, H-2b), 3.30 (1H, dd, J = 12.5, 9.9 Hz, H-1a) , 3.15-2.98 (4H, m, H-10, H-2a, H-1b), 2.69 (1H, ddd, J = 12.8, 9.4, 7.4 Hz, H-9b).

^{13}C NMR (126 MHz, $CDCl_3$): δ (ppm) = 167.0, 143.9, 141.8, 139.5, 139.5, 138.8, 135.5, 132.5, 131.9, 130.7, 130.6, 129.8, 127.3, 52.1, 35.4, 34.2, 33.4, 33.1.

HRMS-APCI: m/z found: $[M]^+$, 422.9589. $C_{18}H_{16}Br_2O_2$ $+H^+$ requires $[M]^+$, 422.9589.

IR: 2933, 1710, 1286, 1116, 833 cm^{-1}.

Mp: 112-113 °C.

R_f: 0.35 (5% EtOAc, 95% *n*-hexane).

Synthesis of (R_p)-4-methylcarboxylate[2.2]paracyclophane **53**

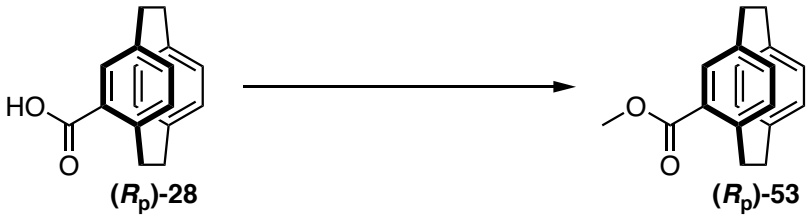

(R_p)-**28** (R_p)-**53**

To a solution of (R_p)-**28** (34.8 mg, 0.138 mmol, 1.0 eq) in dry CH_2Cl_2 (0.69 mL) at 0 °C under Ar, oxalyl chloride (0.024 mL, 0.276 mmol, 2.0 eq) was added. One drop of a DMF stock solution (2 drops of DMF in 2 mL of CH_2Cl_2) was added which caused the solution to bubble. The reaction was warmed to room temperature and stirred for 30 minutes. The volatiles were removed under reduced pressure to yield the crude acyl chloride as a yellow solid. The solid was dissolved in dry CH_2Cl_2 (0.69 mL) and MeOH (0.69 mL), and the reaction was stirred at 50 °C overnight. The solvent was removed under reduced pressure to yield (R_p)-**53** an off-white solid (37.2 mg, 0.140 mmol, >99% yield).

Enantiomeric excess measurements were carried out using HPLC. A Chiralcel OD-H 25 cm column was used, eluting 5% *i*PrOH, 95% *n*-hexane for 20 minutes, 1 mL/min at 25 °C, detecting at 220 nm. Retention times: (R_p)-**53** 7.2 min, (S_p)-**51** 9.3 min.

^{1}H NMR (500 MHz, $CDCl_3$): δ (ppm) = 7.13 (1H, d, J = 1.8 Hz, H-5), 6.66 (1H, dd, J = 7.9, 1.9 Hz, H-13), 6.56-6.52 (2H, m, H-12, H-7), 6.51-6.43 (3H, m, H-16, H-15, H-8), 4.08 (1H, ddd, J = 13.0, 10.9, 1.5 Hz, H-2b), 3.91 (3H, s, H-17), 3.21-2.98 (6H, m, H-10, H-9, H-1), 2.86 (1H, ddd, J = 12.9, 9.5, 7.0 Hz, H-2a).

^{13}C NMR (126 MHz, $CDCl_3$): δ (ppm) = 167.8, 142.8, 140.1, 140.0, 139.5, 136.6, 136.3, 135.4, 133.3, 132.9, 132.4, 131.7, 130.8, 51.9, 36.3, 35.4, 35.2, 35.1.

HRMS-EI: *m/z* found: $[M]^+$, 267.1380. $C_{18}H_{18}O_2$ +H^+ requires $[M]^+$, 267.1379.

IR: 2988, 1708, 1270, 1077, 863 cm^{-1}.

R_f: 0.32 (5% EtOAc, 95% *n*-hexane).

Data comparable to that in the literature.[79]

Synthesis of dirhodium(II) tetrakis[(R_p)-4,12-dibromo-7-carboxy[2.2]paracyclophane] **54**

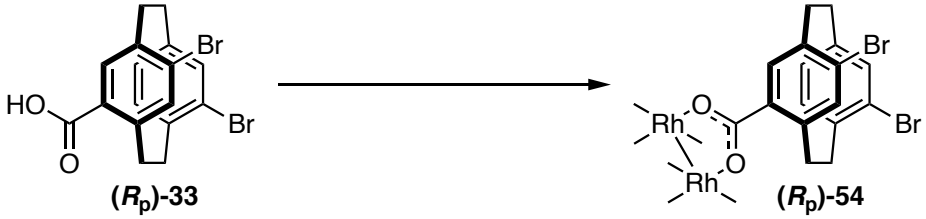

A round bottom flask containing (R_p)-**33** (226 mg, 0.551 mmol, 1.0 eq) and $Rh_2(OAc)_4$ (41.4 mg, 0.0937 mmol, 0.17 eq) was fitted with a dropping funnel filled with K_2CO_3 (8.0 g) and a reflux condenser. The system was put under Ar, then dry toluene (36.7 mL) was added. The reaction was heated to 125 °C for 72 hours, causing solvent to pass into the dropping funnel. The reaction was cooled to room temperature and the solvent removed under reduced pressure to yield a light green solid. The crude material was purified by silica-gel chromatography (1% THF, 15% EtOAc, 84% *n*-hexane). to yield (R_p)-**54** as a dark green solid (144 mg, 0.0782 mmol, 83% yield).

^{1}H NMR (700 MHz, $CDCl_3$): δ (ppm) = 7.14 (1H, s, H-8), 7.08 (1H, s, H-5), 7.03 (1H, d, J = 1.0 Hz, H-13), 6.07 (1H, dd, J = 7.8, 0.9 Hz, H-15), 6.05 (1H, d, J = 7.7 Hz, H-16), 3.80 (1H, dd, J = 12.1, 9.8 Hz, H-9a), 3.32 (1H, t, J = 11.0 Hz, H-2b), 3.25 (1H, dd, J = 12.8, 9.5 Hz, H-10b), 2.96-2.87 (3H, m, H-9b, H-1), 2.76-2.68 (2H, m, H-10a, H-2a).

^{13}C NMR (176 MHz, $CDCl_3$): δ (ppm) = 186.3, 142.7, 141.0, 139.1, 138.9, 136.5, 135.1, 132.9, 132.8, 130.9, 126.6, 35.5, 35.4, 33.3, 32.2.

HRMS-EI: *m/z* found: $[M]^+$, 1892.5334. $C_{68}H_{56}Br_8O_{10}Rh_2$ $+Na^+$ requires $[M]^+$, 1892.5343.

IR: 2929, 1560, 1391, 1033, 879, 562 cm^{-1}.

Mp: 197 °C (decomposes).

R_f: 0.15 (20% EtOAc, 78.5% *n*-hexane, 1.5% THF).

Synthesis of dirhodium(II) tetrakis[(S_p)-4,15-dibromo-7-carboxy[2.2]paracyclophane] **55**

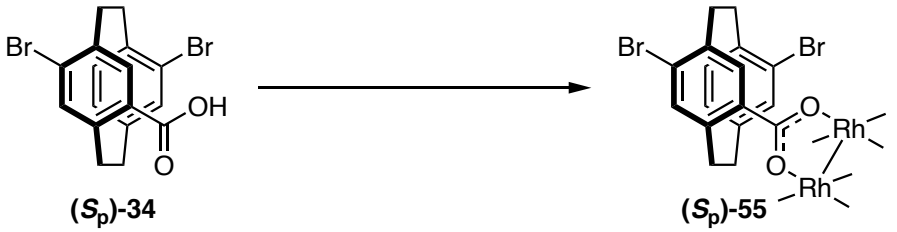

(S_p)-34 **(S_p)-55**

A round bottom flask containing (S_p)-**34** (141 mg, 0.344 mmol, 1.0 eq) and $Rh_2(OAc)_4$ (25.6 mg, 0.0579 mmol, 0.17 eq) was fitted with a dropping funnel filled with K_2CO_3 (8.0 g) and a reflux condenser. The system was put under Ar, then dry toluene (22.9 mL) was added. The reaction was heated to 125 °C for 72 hours, causing solvent to pass into the dropping funnel. The reaction was cooled to room temperature and the solvent removed under reduced pressure to yield a light green solid. The crude material was purified by silica-gel chromatography (1% THF, 40% toluene 59% *n*-hexane) to yield (R_p)-**55** as a dark green solid (82.1 mg, 0.0446 mmol, 77% yield).

^{1}H NMR (700 MHz, $CDCl_3$): δ (ppm) = 7.79 (1H, s, H-8), 6.97 (1H, d, J = 7.8 Hz, H-13), 6.49 (1H, s, H-5), 6.35 (1H, dd, J = 7.8, 1.6 Hz, H-12), 6.12 (1H, d, J = 1.3 Hz, H-16), 3.95 (1H, dd, J = 11.8, 9.8 Hz, H-10a), 3.20 (1H, dd, J = 12.9, 9.9 Hz, H-1a), 3.70 (1H, dd, J = 12.8, 9.9 Hz, H-2b), 3.05-2.99 (1H, m, H-2a), 2.96-2.89 (2H, m, H-10b, H-1b), 2.65-2.59 (1H, m, H-10a), 2.59-2.53 (1H, m, H-9b).

^{13}C NMR (126 MHz, $CDCl_3$): δ (ppm) = 185.8, 142.0, 141.3, 139.1, 139.0, 138.8, 135.2, 132.8, 132.1, 131.1, 130.4, 130.4, 127.1, 36.2, 34.2, 33.4, 33.1.

HRMS-EI: *m/z* found: $[M]^+$, 1890.4977. $C_{68}H_{54}Br_8O_9Rh_2 + K^+$ requires $[M]^+$, 1890.4977.

IR: 2927, 2852, 1589, 1399, 1350, 1098, 565 cm^{-1}.

Mp: 187 °C (decomposes).

R_f: 0.19 (20% EtOAc, 78.5% *n*-hexane, 1.5% THF).

Synthesis of dirhodium(II) tetrakis[(R_p)-4-carboxy[2.2]paracyclophane] **56**

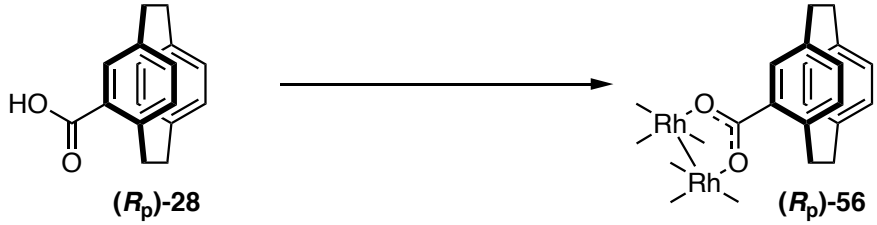

(R_p)-28 **(R_p)-56**

A round bottom flask containing (R_p)-**28** (100 mg, 0.397 mmol, 1.0 eq) and $Rh_2(OAc)_4$ (29.8 mg, 0.0674 mmol, 0.17 eq) was fitted with a dropping funnel filled with K_2CO_3 (8.0 g) and a reflux condenser. The system was put under Ar, then dry toluene (26.4 mL) was added. The reaction was heated to 125 °C for 72 hours, causing solvent to pass through the dropping funnel. The reaction was cooled to room temperature and the solvent removed under reduced pressure to yield a light green solid. The crude material was purified by silica-gel chromatography (1.5% THF, 48.5% CH_2Cl_2 50% *n*-hexane) to yield (R_p)-**56** as a dark green solid (56.7 mg, 0.0468 mmol, 70% yield).

^{1}H NMR (700 MHz, $CDCl_3$): δ (ppm) = 7.06 (1H, d, J = 1.4 Hz, H-5), 6.48 (1H, dd, J = 7.6, 1.7 Hz, H-7), 6.40 (1H, dd, J = 7.6, 1.6 Hz, H-13), 6.37-6.34 (2H, m, H-15, H-8), 6.18 (1H, dd, J = 7.9, 1.3 Hz, H-16), 6.09 (1H, dd, J = 7.8, 1.6 Hz, H-12), 4.04-3.98 (1H, m, H-2a), 3.05-2.96 (3H, m, H-10b, H-9a, H-1b), 2.94-2.85 (3H, m, H-10a, H-9b, H-1a), 2.74 (1H, ddd, J = 12.7, 9.6, 7.1 Hz, H-2b).

^{13}C NMR (176 MHz, $CDCl_3$): δ (ppm) = 187.1, 141.1, 140.0, 139.6, 139.3, 135.9, 135.9, 134.9, 133.1, 132.9, 132.6, 132.2, 131.5, 36.7, 35.3, 35.2, 35.1.

HRMS-EI: *m/z* found: $[M]^+$, 1315.2809. $C_{72}H_{66}O_8N_2Rh_2$ +Na^+ requires $[M]^+$, 1315.2821.

IR: 2925, 2851, 1565, 1374, 803 cm^{-1}.

Mp: 231 °C (decomposes).

R_f: 0.18 (20% EtOAc, 78.5% *n*-hexane, 1.5% THF).

Data comparable to that in the literature.[46]

Synthesis of (R_p)-4-carboxy-7,15-(4'-*tert*-butyl)diphenyl[2.2]paracyclophane **58**

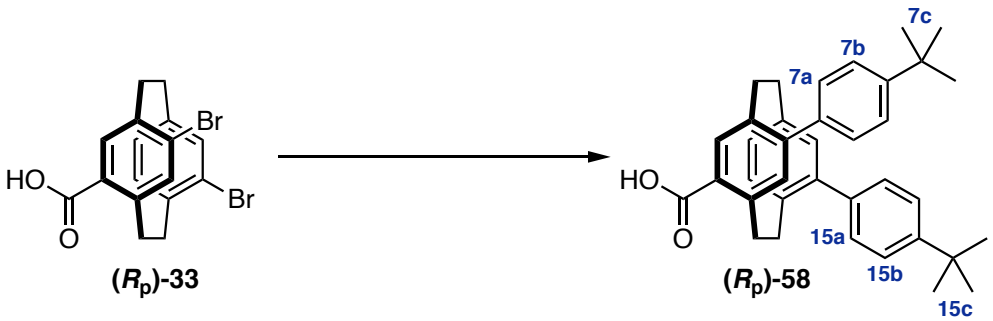

To a 4 mL vial (R_p)-**33** (42.0 mg, 0.102 mmol, 1.0 eq), $Pd(OAc)_2$ (2.3 mg, 0.0102 mmol, 0.1 eq), 2-dicyclohexylphosphino-2',6'-dimethoxybiphenyl ('SPhos') (8.4 mg, 0.0205 mmol, 0.2 eq), K_3PO_4 (108 mg, 0.512 mmol, 5.0 eq) and 4-*tert*-butylphenylboronic acid (73.0 mg, 0.410 mmol, 4.0 eq) were added. The vial was flushed with Ar and capped, then degassed toluene (1.5 mL) was added by syringe. The reaction was heated to 75 °C and stirred for 17 hours, then cooled to room temperature and neutralised with aqueous 1 M HCl solution. The aqueous layer was extracted with EtOAc (2 × 5 mL), the combined organics were washed with brine, dried over $MgSO_4$ and removed under reduced pressure to yield a yellow oil. The crude material was purified by silica-gel chromatography (20% EtOAc, 80% *n*-hexane) to yield (R_p)-**58** as a clear oil (37.0 mg, 0.0710 mmol, 70% yield).

^{1}H NMR (500 MHz, $CDCl_3$): δ (ppm) = 7.54 (1H, s, H-5), 7.47 (2H, d, J = 8.4 Hz, H-7b), 7.39 (4H, d, J = 8.4 Hz, H-15b, H-7a), 7.29 (2H, d, J = 8.3 Hz, H-15a), 6.83 (1H, d, J = 7.9 Hz, H-13), 6.76 (1H, s, H-8), 6.70 (1H, d, J = 1.5 Hz, H-16), 6.64 (1H, dd, J = 7.5, 1.4 Hz, H-12), 4.03 (1H, dd, J = 12.8, 9.7 Hz, H-2b), 3.59 (2H, dd, J = 13.6, 10.1 Hz, H-9a, H-1a), 3.22-3.14 (2H, m, H-10b, H-1b), 3.03 (1H, ddd, J = 13.7, 10.5, 6.7 Hz, H-9b), 2.80 (1H, ddd, J = 13.6, 10.3, 6.8 Hz, H-10a), 2.60 (1H, ddd, J = 12.7, 8.9, 8.4 Hz, H-2a), 1.41 (9H, s, H-15c), 1.38 (9H, s, H-7c).

^{13}C NMR (126 MHz, $CDCl_3$): δ (ppm) = 172.1, 150.8, 149.8, 145.5, 144.2, 141.1, 139.6, 138.3, 138.2, 137.7, 137.6, 137.1, 133.9, 133.5, 131.4, 130.3, 128.8, 128.7, 125.7, 125.5, 35.3, 34.8, 34.6, 34.5, 34.3, 34.2, 31.5, 31.5.

HRMS-EI: *m/z* found: $[M]^-$, 515.2950. $C_{37}H_{39}O_2$ requires $[M]^-$, 515.2945.

IR: 2962, 1678, 1393, 1268, 1027 cm^{-1}.

Mp: 142 °C (decomposes).

R_f: 0.20 (20% EtOAc, 80% *n*-hexane).

Synthesis of dirhodium(II) tetrakis[(R_p)-4-carboxy-7,15-(4'-*tert*-butyl)diphenyl [2.2]paracyclophane] **57**

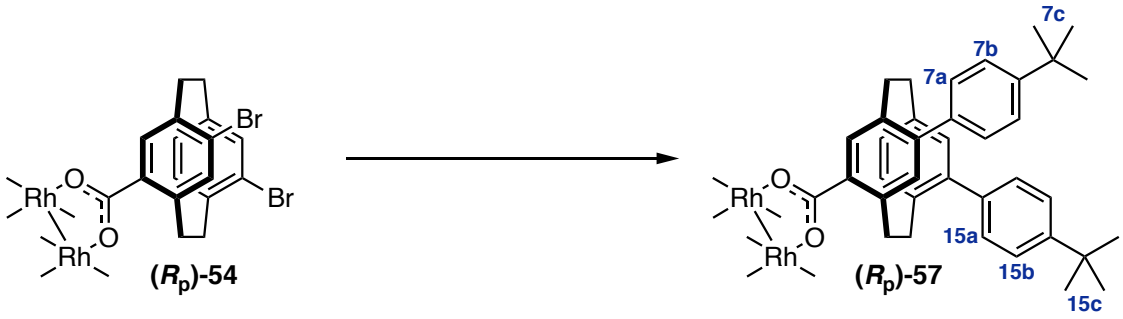

To a 4 mL vial (R_p)-**54** (20.5 mg, 0.0111 mmol, 1.0 eq), $Pd(OAc)_2$ (1.0 mg, 0.00445 mmol, 0.1 eq), 2-dicyclohexylphosphino-2',6'-dimethoxybiphenyl ('SPhos') (3.7 mg, 0.008902 mmol, 0.2 eq), K_3PO_4 (47.3 mg, 0.233 mmol, 5.0 eq) and 4-*tert*-butylphenylboronic acid (32.0 mg, 0.178 mmol, 4.0 eq) were added. The vial was flushed with Ar and capped, then degassed toluene (0.56 mL) was added by syringe. The reaction was heated to 75 °C and stirred for 17 hours, then cooled to room temperature and diluted with EtOAc (2 mL). The organic layer was washed with H_2O, brine, dried over $MgSO_4$ and removed under reduced pressure to yield a dark green solid. The crude material was purified by preparatory TLC (1.5% THF, 5% EtOAc, 93.5% *n*-hexane) to yield (R_p)-**57** as a translucent green solid (19.4 mg, 0.00855 mmol, 77% yield).

^{1}H NMR (700 MHz, $CDCl_3$): δ (ppm) = 7.35 (2H, d, J = 8.5 Hz, H-7b), 7.33 (1H, s, H-5), 7.31 (2H, d, J = 8.3 Hz, H-15b), 7.25 (2H, d, J = 8.5 Hz, H-7a), 7.18 (2H, d, J = 8.2 Hz, H-15a), 6.54 (1H, d, J = 1.7 Hz, H-16), 6.52 (1H, s, H-8), 6.50 (1H, d, J = 7.6 Hz, H-13), 6.21 (1H, dd, J = 7.7 Hz, 1.6 Hz, H-12), 3.90 (1H, dd, J = 12.3, 10.4 Hz, H-2b), 3.46 (1H, t, J = 11.3 Hz, H-9a), 3.43 (1H, dd, J = 12.6, 9.5 Hz, H-1a), 3.05 (1H, ddd, J = 12.5, 9.0, 8.3 Hz, H-1b), 2.98 (1H, t, J = 11.4 Hz, H-10b), 2.87 (1H, ddd, J = 13.7, 10.5, 6.9 Hz, H-9b), 2.62 (1H, ddd, J = 13.7, 9.9, 6.9 Hz, H-10a), 2.48 (1H, ddd, J = 12.0, 8.6, 7.9 Hz, H-2a), 1.34 (9H, s, H-15c), 1.33 (9H, s, H-7c).

^{13}C NMR (176 MHz, $CDCl_3$): δ (ppm) = 187.0, 150.2, 149.5, 143.8, 141.4, 140.5, 139.2, 138.4, 137.5, 137.4, 137.0, 136.8, 133.6, 132.9, 132.1, 131.4, 129.9, 128.8, 128.8, 125.7, 125.4, 125.3, 35.7, 34.6, 34.6, 34.3, 34.2, 34.1, 31.5, 31.5.

HRMS-EI: *m/z* found: $[M]^+$, 2289.978. $C_{148}H_{156}O_8Rh_2$ $+Na^+$ requires $[M]^+$, 2289.980.

IR: 2957, 1563, 1393, 1362, 834 cm^{-1}.

Mp: 192 °C (decomposes).

R_f: 0.35 (20% EtOAc, 78.5% *n*-hexane, 1.5% THF).

Synthesis of (S_p)-4-carboxy-7,12-(4'-*tert*-butyl)diphenyl[2.2]paracyclophane **61** and (S_p)-4-carboxy-7-(4'-*tert*-butyl)phenyl[2.2]paracyclophane **60**

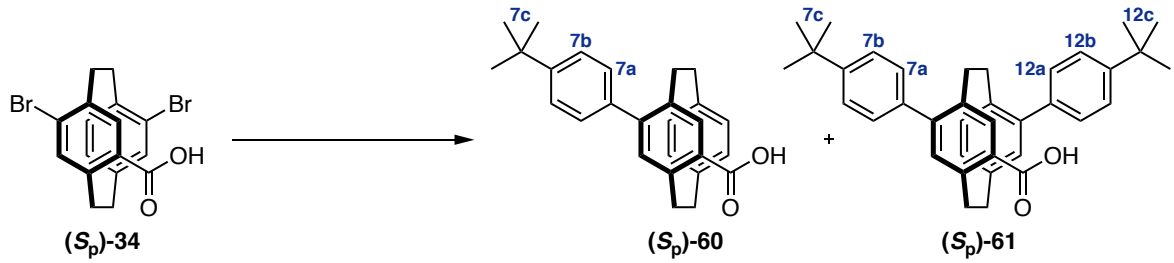

(S_p)-34 (S_p)-60 (S_p)-61

To a 4 mL vial (S_p)-**34** (20.0 mg, 0.0488 mmol, 1.0 eq), $Pd(OAc)_2$ (1.1 mg, 0.00488 mmol, 0.1 eq), 2-dicyclohexylphosphino-2',6'-dimethoxybiphenyl ('SPhos') (4.0 mg, 0.00976 mmol, 0.2 eq), K_3PO_4 (51.8 mg, 0.244 mmol, 5.0 eq) and 4-*tert*-butylphenylboronic acid (34.7 mg, 0.195 mmol, 4.0 eq) were added. The vial was flushed with Ar and capped, then degassed toluene (0.70 mL) was added by syringe. The reaction was heated to 75 °C and stirred for 17 hours, then cooled to room temperature and neutralised with aqueous 1 M HCl solution. The aqueous layer was extracted with EtOAc (2 × 5 mL), the combined organics were washed with brine, dried over $MgSO_4$ and removed under reduced pressure to yield a yellow oil. The crude material was purified by silica-gel chromatography (15% EtOAc, 85% *n*-hexane) to yield (S_p)-**61** as a clear oil (9.6 mg, 0.0186 mmol, 38% yield) and (S_p)-**60** as a yellow oil (7.7 mg, 0.0200 mmol, 41% yield).

(S_p)-4-carboxy-7,12-(4'-*tert*-butyl)diphenyl[2.2]paracyclophane 61

^{1}H NMR (700 MHz, $CDCl_3$): δ (ppm) = 7.48 (1H, s, H-5), 7.44 (2H, d, J = 8.4 Hz, H-7b), 7.41 (2H, d, J = 8.4 Hz, H-7a), 7.40 (2H, d, J = 8.4 Hz, H-12a), 7.37 (2H, d, J = 8.4 Hz, H-12b), 6.77 (1H, d, J = 7.6 Hz, H-16), 6.67 (1H, s, H-8), 6.63 (1H, d, J = 1.7 Hz, H-13), 6.59 (1H, dd, J = 7.6, 1.5 Hz, H-15), 4.19 (1H, dd, J = 12.7, 9.3 Hz, H-2b), 3.29-3.21 (3H, m, H-10b, H-9a, H-1a), 3.11 (1H, ddd, J =13.1, 9.4, 8.4 Hz, H-1b), 2.85 (1H, ddd, J = 12.9, 9.1, 8.4 Hz, H-2a), 2.32-2.23 (2H, H-10a, H-9b), 1.33 (9H, s, H-7c), 1.28 (9H, s, H-12c).

^{13}C NMR (176 MHz, $CDCl_3$): δ (ppm) = 169.3, 151.0, 149.9, 147.0, 144.1, 142.3, 140.0, 137.9, 137.8, 137.2, 137.1, 135.9, 135.6, 132.4, 131.2, 130.4, 129.1, 129.1, 127.0, 126.6, 125.8, 125.7, 36.7, 34.8, 34.7, 34.5, 33.6, 33.3, 31.6, 31.5.

HRMS-EI: m/z found: $[M]^-$, 515.2952. $C_{37}H_{39}O_2$ requires $[M]^-$, 515.2945.

IR: 2959, 2918, 1673, 1514, 1267, 833 cm^{-1}

Mp: 106-108 °C.

R_f: 0.43 (45% EtOAc, 55% *n*-hexane).

(S_p)-4-carboxy-7-(4'-*tert*-butyl)phenyl[2.2]paracyclophane 60

^{1}H NMR (700 MHz, $CDCl_3$): δ (ppm) = 7.51 (2H, d, J = 8.4 Hz, H-7b), 7.45 (2H, d, J = 8.4 Hz, H-7a), 7.39 (1H, s, H-5), 6.73 (1H, dd, J = 7.8, 1.8 Hz, H-13), 6.70 (1H, dd, J = 7.8, 1.7 Hz, H-16), 6.65 (1H, dd, J = 8.0, 1.7 Hz, H-15), 6.63 (1H, s, H-8), 6.58 (1H, dd, J = 7.8, 1.7 Hz, H-12), 4.23 (1H, ddd, J = 13.3, 10.7, 1.1 Hz, H-2b), 3.60-3.55 (1H, m, H-9a), 3.32-

3.21(2H, m, H-1), 2.98-2.89 (2H, m, H-10b, H-9b), 2.87 (1H, ddd, J = 13.2, 9.3, 7.6 Hz, H-2a), 2.59 (1H, ddd, J = 12.7, 10.2, 6.0 Hz, H-10a), 1.40 (9H, s, H-7c).

^{13}C NMR (176 MHz, $CDCl_3$): δ (ppm) = 171.2, 150.9, 146.7, 144.1, 140.0, 139.8, 139.0, 137.5, 137.1, 135.8, 132.5, 131.9, 131.5, 130.2, 129.3, 129.1, 128.3, 125.8, 36.4, 35.0, 34.8, 34.4, 34.3, 31.5.

HRMS-EI: m/z found: $[M]^-$, 383.2014. $C_{27}H_{27}O_2$ requires $[M]^-$, 383.2006.

IR: 2960, 2926, 1674, 1249, 836 cm^{-1}.

Mp: 140-141 °C.

R_f: 0.53 (45% EtOAc, 55% n-hexane).

Synthesis of dirhodium(II) tetrakis[(S_p)-4-carboxy-7,12-(4'-*tert*-butyl)diphenyl [2.2]paracyclophane] **62**

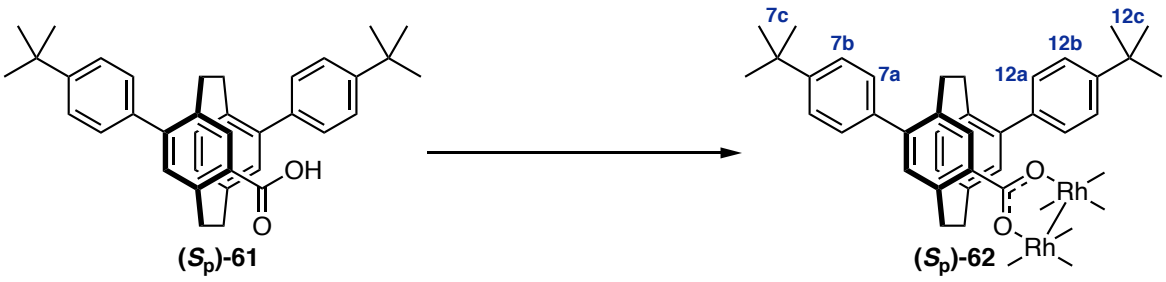

A round bottom flask containing (S_p)-**61** (26.0 mg, 0.0480 mmol, 1.0 eq) and $Rh_2(OAc)_4$ (3.6 mg, 0.00814 mmol, 0.17 eq) was fitted with a dropping funnel filled with K_2CO_3 (8.0 g) and a reflux condenser. The system was put under Ar, then dry toluene (3.6 mL) was added. The reaction was heated to 125 °C for 72 hours, causing solvent to pass through the dropping funnel. The reaction was cooled to room temperature and the solvent removed under reduced pressure to yield a light green solid. The crude material was purified by preparatory TLC (1.5% THF, 5% EtOAc, 93.5% *n*-hexane) to yield (S_p)-**62** as a translucent green solid (4.00 mg, 0.00177 mmol, 22% yield).

^{1}H NMR (700 MHz, $CDCl_3$): δ (ppm) = 7.57 (2H, d, J = 8.2 Hz, H-16b), 7.48 (1H, s, H-5), 7.36 (2H, d, J = 8.1 Hz, H-16a), 7.28 (1H, d, J = 8.6 Hz, H-7b), 7.08 (2H, d, J = 8.7 Hz, H-7a), 6.56 (1H, d, J = 8.0 Hz, H-16), 6.43 (1H, s, H-8), 6.34 (1H, dd, J = 7.7, 1.5 Hz, H-15), 5.81 (1H, s, H-13), 4.43 (1H, dd, J = 12.0, 9.6 Hz, H-2b), 3.08 (1H, dd, J = 12.9, 9.5 Hz, H-10b), 2.92 (1H, dd, J = 11.4, 8.3 Hz, H-1a), 2.84 (1H, dd, J = 12.6, 9.3 Hz, H-9a), 2.75-2.66 (2H, m, H-2a, H-1b), 2.01 (1H, ddd, J = 13.4, 8.9. 8.8 Hz, H-10a), 1.87 (1H, ddd, J = 12.8, 9.1, 8.2 Hz, H-9b), 1.43 (9H, s, H-16c), 1.28 (9H, s, H-7c).

^{13}C NMR (176 MHz, $CDCl_3$): δ (ppm) = 185.8, 150.0, 149.0, 145.1, 142.2, 141.8, 139.5, 137.6, 137.1, 136.4, 136.2, 135.9, 134.7, 131.5, 131.5, 129.7, 129.6, 129.3, 128.7, 125.2, 125.2, 37.2, 34.6, 34.5, 33.2, 32.7, 31.8, 31.3, 29.7.

HRMS-EI: *m/z* found: $[M]^+$, 2331.0077. $C_{150}H_{159}O_8NRh_2$ $+Na^+$ requires $[M]^+$, 2331.0068.

IR: 2953, 2858, 1567, 1391, 1364, 836 cm^{-1}.

R_f: 0.46 (20% EtOAc, 78.5% *n*-hexane, 1.5% THF).

Synthesis of phenylethyl hydroxycarbamate

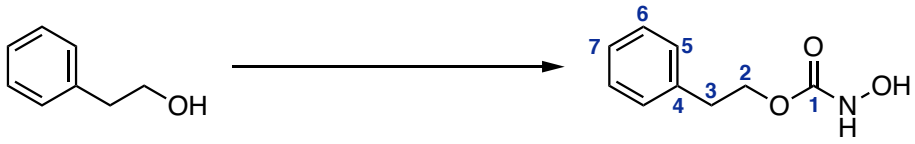

To a solution of 1,1′-carbonyldiimidazole (2.90 g, 13.50 mmol, 1.1 eq) in CH_3CN (61.4 mL) under Ar at 0 ºC, 1-phenylethanol (1.50 g, 12.3 mmol, 1.0 eq) was added slowly. The reaction was warmed to room temperature and stirred for 2 hours. Imidazole (2.50 g, 36.8 mmol, 3.0 eq) was added and allowed to dissolve, then hydroxylamine hydrochloride (3.40 g, 49.1 mmol, 4.0 eq) was added and the reaction was stirred for a further 15 hours. Aqueous 1.0 M HCl solution (50 mL) was added, and the aqueous layer was extracted with EtOAc (3 × 30 mL). The combined organics were washed with water and brine, dried over $MgSO_4$, and removed under reduced pressure to yield a light blue solid. The crude material was purified by recrystallisation in CH_2Cl_2 to yield phenylethyl hydroxycarbamate as a white powder (1.40 g, 7.73 mmol, 61% yield).

^{1}H NMR (500 MHz, $CDCl_3$): δ (ppm) = 7.33-7.28 (2H, m, H-6), 7.26-7.20 (3H, m, H-7, H-5), 7.10 (1H, s, NH), 5.92 (1H, s, OH), 4.39 (2H, t, J = 7.0 Hz, H-2), 2.97 (2H, t, J = 6.9 Hz, H-3).

^{13}C NMR (126 MHz, $CDCl_3$): δ (ppm) = 159.2, 137.3, 128.9, 128.6, 126.7, 66.6, 35.3.

IR: 3316, 2956, 1683, 1526, 1281, 1135, 753 cm^{-1}.

Data comparable to that in the literature.[29]

Synthesis of phenylethyl tosyloxycarbamate

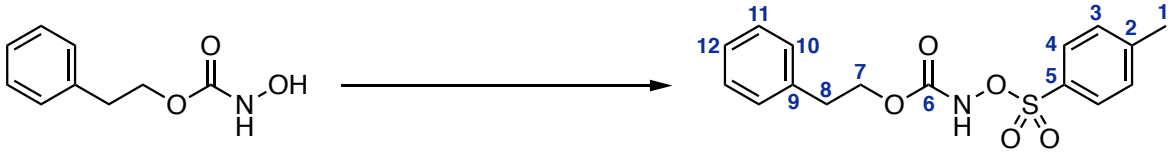

To a solution of phenylethyl hydroxycarbamate (0.250 g, 1.38 mmol, 1.0 eq) in dry Et_2O (13.8 mL) under Ar at 0 ºC, 4-toluenesulfonyl chloride (0.290 g, 1.52 mmol, 1.1 eq) in Et_2O (2.0 mL) was added. Et_3N (0.20 mL, 1.41 mmol, 1.0 eq) was then added slowly causing a white precipitate to form. The reaction was warmed to room temperature and stirred for 2 hours. The reaction mixture was then washed with water (2 × 20 mL) and brine, then dried over $MgSO_4$. The organic layer was then removed under reduced pressure to yield a clear oil that was purified by silica-gel chromatography (20% *n*-hexane, 80% CH_2Cl_2) to yield phenylethyl tosyloxycarbamate as a white solid (0.280 g, 0.835 mmol, 61% yield).

^{1}H NMR (500 MHz, $CDCl_3$): δ (ppm) = 7.85 (2H, d, J = 8.3 Hz, H-4), 7.78 (1H, s, NH), 7.34 (2H, d, J = 8.3 Hz, H-2), 7.32-7.28 (2H, m, H-11), 7.26-7.22 (1H, m, H-12), 7.14 (2H, d, J = 7.0 Hz, H-10), 4.22 (2H, t, J = 7.3 Hz, H-7), 2.81 (2H, t, J = 7.3 Hz, H-8), 2.45 (3H, s, H-1).

^{13}C NMR (126 MHz, $CDCl_3$): δ (ppm) = 155.4, 146.3, 137.0, 130.5, 129.9, 129.7, 129.0, 128.7, 127.0, 67.5, 35.0, 21.9.

IR: 3218, 1733, 1384, 1268, 1192, 1094 cm^{-1}.

Data comparable to that in the literature.[29]

Synthesis of 2,2,2-trichloroethyl hydroxycarbamate

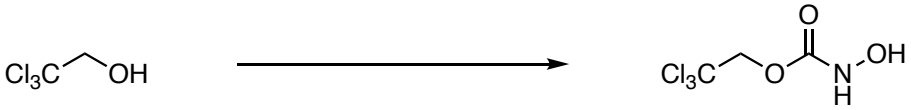

To a solution of 1,1′-carbonyldiimidazole (0.597 g, 3.68 mmol, 1.1 eq) in CH_3CN (16.8 mL) under Ar at 0 ºC, 2,2,2-trichloroethanol (0.500 g, 3.35 mmol, 1.0 eq) was added slowly. The reaction was warmed to room temperature and stirred for 2 hours. Imidazole (0.684 g, 10.05 mmol, 3.0 eq) was added and allowed to dissolve, then hydroxylamine hydrochloride (0.931 g, 13.4 mmol, 4.0 eq) was added and the reaction was stirred for 15 hours. Aqueous 1.0 M HCl solution (15 mL) was added, and the aqueous layer was extracted with EtOAc (3 × 15 mL). The combined organics were washed with water and brine, dried over $MgSO_4$, and removed under reduced pressure to yield a light purple solid. The crude material was purified by recrystallisation in CH_2Cl_2 to yield 2,2,2-trichloroethyl hydroxycarbamate as a white powder (0.483 g, 2.32 mmol, 69% yield).

^{1}H NMR (500 MHz, $CDCl_3$): δ (ppm) = 4.79 (2H, s, H-1).

^{13}C NMR (126 MHz, $CDCl_3$): δ (ppm) = 156.0, 94.9, 75.1.

IR: 3363, 3263, 1709, 1505, 1291, 1140 cm^{-1}.

Data comparable to that in the literature.[29]

Synthesis of 2,2,2-trichloroethyl tosyloxycarbamate

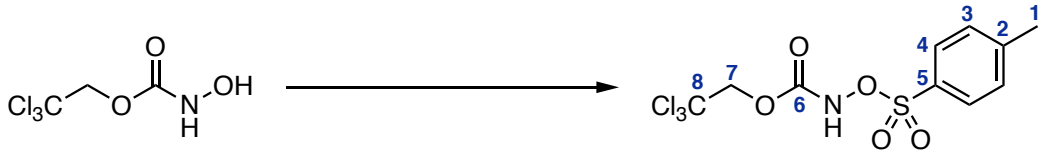

To a solution of 2,2,2-trichloroethyl hydroxycarbamate (0.240 g, 1.13 mmol, 1.0 eq) in dry Et_2O (11.3 mL) under Ar at 0 ºC, 4-toluenesulfonyl chloride (0.260 g, 1.36 mmol, 1.1 eq) in Et_2O (2.0 mL) was added. Et_3N was then added slowly (0.16 mL, 1.02 mmol, 1.0 eq) causing a white precipitate to form, the reaction was then warmed to room temperature and stirred for 2 hours. The reaction mixture was then washed with water (2 × 20 mL) and brine, then dried over $MgSO_4$. The organic layer was then removed under reduced pressure to yield a clear oil that was purified by silica-gel chromatography (20% *n*-hexane, 80% CH_2Cl_2) to yield 2,2,2-trichloroethyl tosyloxycarbamate as a white solid (0.180 g, 0.496 mmol, 44% yield).

^{1}H NMR (500 MHz, $CDCl_3$): δ (ppm) = 8.12 (1H, s, NH), 7.90 (2H, d, J = 8.3 Hz, H-4), 7.36 (2H, d, J = 8.3 Hz, H-3), 4.65 (2H, s, H-7), 2.46 (3H, s, H-1).

^{13}C NMR (126 MHz, $CDCl_3$): δ (ppm) = 153.5, 146.5, 129.9, 129.9, 129.7, 94.1, 75.1, 21.8.

IR: 3563, 1766, 1379, 1192, 762 cm^{-1}.

Data comparable to that in the literature.[29]

General procedure for intramolecular C-H amination

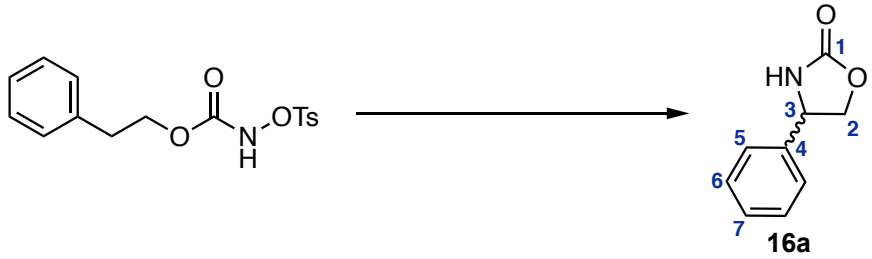

To a 2 mL vial phenylethyl tosyloxycarbamate (30.0 mg, 0.0890 mmol, 1.0 eq), Rh(II) catalyst (5.34 μmol, 0.06 eq) and K_2CO_3 (37.0 mg, 0.268 mmol, 3.0 eq) were added. The vial was flushed with argon and capped, then degassed CH_2Cl_2 (0.89 mL) was added by syringe. The vial was sonicated, and the reaction was stirred at room temperature for 6 hours, causing a colour change from green to yellow. The reaction mixture was diluted with CH_2Cl_2 (1 mL) and filtered through cotton wool. The solvent was removed under reduced pressure to yield a yellow solid that was purified by silica-gel chromatography (30% EtOAc, 70% *n*-hexane to 45% EtOAc, 55% *n*-hexane) to yield **16a** as a white solid.

Enantiomeric excess measurements were carried out using HPLC. A Chiralpak AD 25 cm column was used, eluting 10% *i*PrOH, 90% *n*-hexane for 30 minutes, 1 mL/min at 25 °C, detecting at 220 nm. Retention times: enantiomer 1: 19.0 min, enantiomer 2: 22.2 min.

^{1}H NMR (500 MHz, $CDCl_3$): δ (ppm) = 7.43-7.39 (2H, m, H-6), 7.38-7.33 (3H, m, H-7, H-5), 5.60 (1H, s, NH), 4.96 (1H, t, J = 8.0 Hz, H-3), 4.74 (1H, t, J = 8.7 Hz, H-2a), 4.20 (1H, dd, J = 8.7, 7.0 Hz, H-2b).

^{13}C NMR (126 MHz, $CDCl_3$): δ (ppm) = 159.6, 139.5, 129.4, 129.1, 126.2, 72.7, 56.5.

HRMS-EI: *m/z* found: $[M]^+$, 186.0523. $C_9H_9NO_2$ +Na^+ requires $[M]^+$, 186.0525.

IR: 3265, 1918, 1742, 1721, 1236, 1036, 764 cm^{-1}.

R_f: 0.22 (45% EtOAc, 55% *n*-hexane).

Data comparable to that in the literature.[29]

General procedure for intermolecular C-H amination

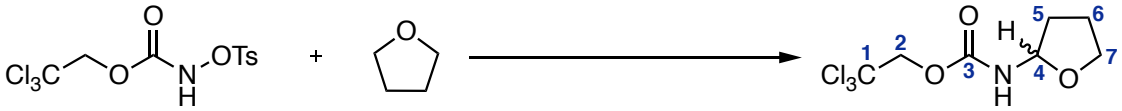

19b

To a 2 mL vial 2,2,2-trichloroethyl tosyloxycarbamate (40 mg, 0.110 mmol, 1.0 eq), Rh(II) catalyst (6.60 μmol, 0.06 eq) and K_2CO_3 (46 mg, 0.330 mmol, 3.0 eq) were added. The vial was flushed with argon and capped, then degassed THF (39.7 mg, 0.550 mmol, 5.0 eq) and degassed CH_2Cl_2 (0.22 mL) was added by syringe. The vial was sonicated and the reaction was stirred at room temperature for 16 hours. The reaction mixture was diluted with CH_2Cl_2 (1 mL) and filtered through cotton wool. The solvent was removed under reduced pressure to yield a green solid that was purified by silica-gel chromatography (50% toluene, 50% CH_2Cl_2 to 100% CH_2Cl_2) to yield **19b** as a white solid.

Enantiomeric excess measurements were carried out using HPLC. A Chiralpak AD 25 cm column was used, eluting 7% *i*PrOH, 93% *n*-hexane for 20 minutes, 1 mL/min at 25 °C, detecting at 210 nm. Retention times: enantiomer 1: 12.2 min, enantiomer 2: 15.0 min.

^{1}H NMR (500 MHz, $CDCl_3$): δ (ppm) = 5.58 (1H, ddd, J = 9.0, 6.5, 4.8 Hz, H-4), 5.41 (1H, s, NH), 4.78 (1H, d, J = 12.1 Hz, H-2a), 4.67 (1H, d, J = 12.1 Hz, H-2b), 3.97-3.93 (1H, m, H-7a), 3.86-3.82 (1H, m, H-7b), 2.27-2.21 (1H, m, H-5a), 2.01-1.92 (2H, m, H-6), 1.80-1.74 (1H, m, H-5b).

^{13}C NMR (126 MHz, $CDCl_3$): δ (ppm) = 153.7, 95.3, 82.9, 74.6, 67.5 31.9, 24.6.

HRMS-EI: m/z found: $[M]^+$, 283.9615. $C_7H_{10}Cl_3NO_3$ $+Na^+$ requires $[M]^+$, 283.9618.

IR: 3349, 2960, 1733, 1713, 1520, 1052, 814 cm^{-1}.

R_f: 0.31 (100% CH_2Cl_2).

Data comparable to that in the literature.[29]

References

(1) Huang, Z.; Dong, G. Site-Selectivity Control in Organic Reactions: A Quest to Differentiate Reactivity among the Same Kind of Functional Groups. *Acc. Chem. Res.* **2017**, *50* (3), 465–471. https://doi.org/10.1021/acs.accounts.6b00476.

(2) Hartwig, J. F. Catalyst-Controlled Site-Selective Bond Activation. *Acc. Chem. Res.* **2017**, *50* (3), 549–555. https://doi.org/10.1021/acs.accounts.6b00546.

(3) Davis, H. J.; Phipps, R. J. Harnessing Non-Covalent Interactions to Exert Control over Regioselectivity and Site-Selectivity in Catalytic Reactions. *Chem. Sci.* **2017**, *8* (2), 864–877. https://doi.org/10.1039/C6SC04157D.

(4) Meng, G.; Lam, N. Y. S.; Lucas, E. L.; Saint-Denis, T. G.; Verma, P.; Chekshin, N.; Yu, J.-Q. Achieving Site-Selectivity for C–H Activation Processes Based on Distance and Geometry: A Carpenter's Approach. *J. Am. Chem. Soc.* **2020**, *142* (24), 10571–10591. https://doi.org/10.1021/jacs.0c04074.

(5) Jiao, Y.; Chen, X.-Y.; Stoddart, J. F. Weak Bonding Strategies for Achieving Regio- and Site-Selective Transformations. *Chem.* **2022**, *8* (2), 414–438. https://doi.org/10.1016/j.chempr.2021.12.012.

(6) Docherty, J. H.; Lister, T. M.; Mcarthur, G.; Findlay, M. T.; Domingo-Legarda, P.; Kenyon, J.; Choudhary, S.; Larrosa, I. Transition-Metal-Catalysed C–H Bond Activation for the Formation of C–C Bonds in Complex Molecules. *Chem. Rev.* **2023**, *123* (12), 7692–7760. https://doi.org/10.1021/acs.chemrev.2c00888.

(7) Altus, K. M.; Love, J. A. The Continuum of Carbon–Cydrogen (C–H) Activation Mechanisms and Terminology. *Commun. Chem.* **2021**, *4* (1), 1–11. https://doi.org/10.1038/s42004-021-00611-1.

(8) Tadross, P. M.; Jacobsen, E. N. Remodelling by Diversity and Design. *Nat. Chem.* **2012**, *4* (12), 963–965. https://doi.org/10.1038/nchem.1509.

(9) Wang, R.; Yu, Y. Site-Selective Reactions Mediated by Molecular Containers. *Beilstein J. Org. Chem.* **2022**, *18* (1), 309–324. https://doi.org/10.3762/bjoc.18.35.

(10) Dalton, T.; Faber, T.; Glorius, F. C–H Activation: Toward Sustainability and Applications. *ACS Cent. Sci.* **2021**, *7* (2), 245–261. https://doi.org/10.1021/acscentsci.0c01413.

(11) Hartwig, J. F.; Larsen, M. A. Undirected, Homogeneous C–H Bond Functionalisation: Challenges and Opportunities. *ACS Cent. Sci.* **2016**, *2* (5), 281–292. https://doi.org/10.1021/acscentsci.6b00032.

(12) Wang, G.-W.; Wheatley, M.; Simonetti, M.; Cannas, D. M.; Larrosa, I. Cyclometalated Ruthenium Catalyst Enables *Ortho*-Selective C–H Alkylation with Secondary Alkyl Bromides. *Chem.* **2020**, *6* (6), 1459–1468. https://doi.org/10.1016/j.chempr.2020.04.006.

(13) Carestia, A. M.; Ravelli, D.; Alexanian, E. J. Metal Carbenoid and Nitrenoid Insertion. *Chem. Sci.* **2018**, *9* (24), 5360–5365. https://doi.org/10.1039/C8SC01756E.

(14) Davies, H. M. L.; Manning, J. R. Catalytic C–H Functionalization by Metal Carbenoid and Nitrenoid Insertion. *Nature*. **2008**, *451* (7177), 417–424. https://doi.org/10.1038/nature06485.

(15) Chu, J. C. K.; Rovis, T. Complementary Strategies for Directed C(Sp3)–H Functionalization: A Comparison of Transition-Metal-Catalyzed Activation, Hydrogen Atom Transfer, and Carbene/Nitrene Transfer. *Angew. Chem. Int. Ed.* **2018**, *57* (1), 62–101. https://doi.org/10.1002/anie.201703743.

(16) Ju, M.; Schomaker, J. M. Nitrene Transfer Catalysts for Enantioselective C–N Bond Formation. *Nat. Rev. Chem.* **2021**, *5* (8), 580–594. https://doi.org/10.1038/s41570-021-00291-4.

(17) Yamakawa, Y.; Ikuta, T.; Hayashi, H.; Hashimoto, K.; Fujii, R.; Kawashima, K.; Mori, S.; Uchida, T.; Katsuki, T. Iridium(III)-Catalysed Asymmetric Site-Selective Carbene C–H Insertion during Late-Stage Transformation. *J. Org. Chem.* **2022**, *87* (10), 6769–6780. https://doi.org/10.1021/acs.joc.2c00470.

(18) Weldy, N. M.; Schafer, A. G.; Owens, C. P.; Herting, C. J.; Varela-Alvarez, A.; Chen, S.; Niemeyer, Z.; Musaev, D. G.; Sigman, M. S.; Davies, H. M. L.; Blakey, S. B. Iridium(III)-Bis(Imidazolinyl)Phenyl Catalysts for Enantioselective C–H Functionalization with Ethyl Diazoacetate. *Chem. Sci.* **2016**, *7* (5), 3142–3146. https://doi.org/10.1039/C6SC00190D.

(19) Ichinose, M.; Suematsu, H.; Yasutomi, Y.; Nishioka, Y.; Uchida, T.; Katsuki, T. Enantioselective Intramolecular Benzylic C-H Bond Amination: Efficient Synthesis of Optically Active Benzosultams. *Angew. Chem. Int. Ed.* **2011**, *50* (42), 9884–9887. https://doi.org/10.1002/anie.201101801.

(20) Álvarez, M.; Molina, F.; Pérez, P. J. Carbene-Controlled Regioselective Functionalisation of Linear Alkanes under Silver Catalysis. *J. Am. Chem. Soc.* **2022**, *144* (51), 23275–23279. https://doi.org/10.1021/jacs.2c11707.

(21) Gómez-Emeterio, B. P.; Urbano, J.; Díaz-Requejo, M. M.; Pérez, P. J. Easy Alkane Catalytic Functionalisation. *Organometallics*. **2008**, *27* (16), 4126–4130. https://doi.org/10.1021/om800218d.

(22) Davies, H. M. L.; Liao, K. Dirhodium Tetracarboxylates as Catalysts for Selective Intermolecular C–H Functionalization. *Nat. Rev. Chem.* **2019**, *3* (6), 347–360. https://doi.org/10.1038/s41570-019-0099-x.

(23) Hrdina, R. Dirhodium(II,II) Paddlewheel Complexes. *Eur. J. of Inorg. Chem.* **2021**, *2021* (6), 501–528. https://doi.org/10.1002/ejic.202000955.

(24) Hansen, J.; Davies, H. M. L. High Symmetry Dirhodium(II) Paddlewheel Complexes as Chiral Catalysts. *Coord. Chem. Rev.* **2008**, *252* (5), 545–555. https://doi.org/10.1016/j.ccr.2007.08.019.

(25) Felthouse, T. R. The Chemistry, Structure, and Metal-Metal Bonding in Compounds of Rhodium(II). In *Progress in Inorganic Chemistry*; John Wiley & Sons, Ltd, 1982; pp 73–166. https://doi.org/10.1002/9780470166307.ch2.

(26) Liu, W.; Ren, Z.; Bosse, A. T.; Liao, K.; Goldstein, E. L.; Bacsa, J.; Musaev, D. G.; Stoltz, B. M.; Davies, H. M. L. Catalyst-Controlled Selective Functionalization of Unactivated C–H Bonds in the Presence of Electronically Activated C–H Bonds. *J. Am. Chem. Soc.* **2018**, *140* (38), 12247–12255. https://doi.org/10.1021/jacs.8b07534.

(27) Liao, K.; Yang, Y.-F.; Li, Y.; Sanders, J. N.; Houk, K. N.; Musaev, D. G.; Davies, H. M. L. Design of Catalysts for Site-Selective and Enantioselective Functionalisation of Non-Activated Primary C–H Bonds. *Nat. Chem.* **2018**, *10* (10), 1048–1055. https://doi.org/10.1038/s41557-018-0087-7.

(28) Davies, H. M. L.; Beckwith, R. E. J. Catalytic Enantioselective C–H Activation by Means of Metal–Carbenoid-Induced C–H Insertion. *Chem. Rev.* **2003**, *103* (8), 2861–2904. https://doi.org/10.1021/cr0200217.

(29) Huard, K.; Lebel, H. N-Tosyloxycarbamates as Reagents in Rhodium-Catalysed C-H Amination Reactions. *Chem. Eur. J.* **2008**, *14* (20), 6222–6230. https://doi.org/10.1002/chem.200702027.

(30) Lebel, H.; Huard, K.; Lectard, S. *N*-Tosyloxycarbamates as a Source of Metal Nitrenes: Rhodium-Catalysed C–H Insertion and Aziridination Reactions. *J. Am. Chem. Soc.* **2005**, *127* (41), 14198–14199. https://doi.org/10.1021/ja0552850.

(31) Reddy, R. P.; Lee, G. H.; Davies, H. M. L. Dirhodium Tetracarboxylate Derived from Adamantylglycine as a Chiral Catalyst for Carbenoid Reactions. *Org. Lett.* **2006**, *8* (16), 3437–3440. https://doi.org/10.1021/ol0608931.

(32) Nasrallah, A.; Boquet, V.; Hecker, A.; Retailleau, P.; Darses, B.; Dauban, P. Catalytic Enantioselective Intermolecular Benzylic C(Sp^3)–H Amination. *Angew. Chem. Int. Ed.* **2019**, *58* (24), 8192–8196. https://doi.org/10.1002/anie.201902882.

(33) Boquet, V.; Guimaraes Naves, J. A.; Brunard, E.; Nasrallah, A.; Joigneaux, M.; Sosa Carrizo, E. D.; Saget, T.; Darses, B.; Sircoglou, M.; Dauban, P. Rhodium(II)-Catalyzed Selective C(Sp^3)–H Amination of Alkanes. *Eur. J. Org. Chem.* **2023**, *26* (32), e202300352. https://doi.org/10.1002/ejoc.202300352.

(34) Wei, C.; Mo, K.-F.; Chan, T.-L. [14][14]Metaparacyclophane: First Example of an [m][n]Metaparacyclophane. *J. Org. Chem.* **2003**, *68* (7), 2948–2951. https://doi.org/10.1021/jo0267044.

(35) Ding, Q.; Wang, Q.; He, H.; Cai, Q. Asymmetric Synthesis of (–)-Pterocarine and (–)-Galeon via Chiral Phase Transfer-Catalysed Atropselective Formation of Diarylether Cyclophane Skeleton. *Org. Lett.* **2017**, *19* (7), 1804–1807. https://doi.org/10.1021/acs.orglett.7b00570.

(36) Cram, D. J.; Cram, J. M. Cyclophane Chemistry: Bent and Battered Benzene Rings. *Acc. Chem. Res.* **1971**, *4* (6), 204–213. https://doi.org/10.1021/ar50042a003.

(37) Dyson, P. J.; Humphrey, D. G.; McGrady, J. E.; Mingos, D. M. P.; Wilson, D. J. Comparison of the Reactivity of [2.2]Paracyclophane and *p*-Xylene. *J. Chem. Soc., Dalton Trans.* **1995**, No. 24, 4039–4043. https://doi.org/10.1039/DT9950004039.

(38) Singer, L. A.; Cram, D. J. Macro Rings. XXVII. Transannular Substituent Effects in π-π-Complexes of Paracyclophanes. *J. Am. Chem. Soc.* **1963**, *85* (8), 1080–1084. https://doi.org/10.1021/ja00891a011.

(39) Reich, H. J.; Cram, D. J. Macro Rings. XXXV. Transannular Directive Influences in Electrophilic Substitution of Monosubstituted[2.2]Paracyclophanes. *J. Am. Chem. Soc.* **1969**, *91* (13), 3505–3516. https://doi.org/10.1021/ja01041a015.

(40) Hassan, Z.; Spuling, E.; Knoll, D. M.; Bräse, S. Regioselective Functionalization of [2.2]Paracyclophanes: Recent Synthetic Progress and Perspectives. *Angew. Chem. Int. Ed.* **2020**, *59* (6), 2156–2170. https://doi.org/10.1002/anie.201904863.

(41) Cahn, R. S.; Ingold, C.; Prelog, V. Specification of Molecular Chirality. *Angew. Chem. Int. Ed. Engl.* **1966**, *5* (4), 385–415. https://doi.org/10.1002/anie.196603851.

(42) Pye, P. J.; Rossen, K.; Reamer, R. A.; Tsou, N. N.; Volante, R. P.; Reider, P. J. A New Planar Chiral Bisphosphine Ligand for Asymmetric Catalysis: Highly Enantioselective Hydrogenations under Mild Conditions. *J. Am. Chem. Soc.* **1997**, *119* (26), 6207–6208. https://doi.org/10.1021/ja970654g.

(43) Dahmen, S.; Bräse, S. [2,2]Paracyclophane-Based N,O-Ligands in Alkenylzinc Additions to Aldehydes. *Org. Lett.* **2001**, *3* (25), 4119–4122. https://doi.org/10.1021/ol016954r.

(44) Gibson, S. E.; Knight, J. D. [2.2]Paracyclophane Derivatives in Asymmetric Catalysis. *Org. Biomol. Chem.* **2003**, *1* (8), 1256–1269. https://doi.org/10.1039/B300717K.

(45) Yuan, S.; Liao, C.; Zheng, W.-H. [2.2]Paracyclophane-Based Isothiourea-Catalysed Highly Enantioselective α-Fluorination of Carboxylic Acids. *Org. Lett.* **2021**, *23* (11), 4142–4146. https://doi.org/10.1021/acs.orglett.1c01046.

(46) Zippel, C.; Hassan, Z.; Nieger, M.; Bräse, S. Design and Synthesis of a [2.2]Paracyclophane-Based Planar Chiral Dirhodium Catalyst and its Applications in Cyclopropanation Reaction of Vinylarenes with α-Methyl-α-Diazo Esters. *Adv. Synth. Catal.* **2020**, *362* (16), 3431–3436. https://doi.org/10.1002/adsc.202000512.

(47) Rozenberg, V.; Dubrovina, N.; Sergeeva, E.; Antonov, D.; Belokon', Y. An Improved Synthesis of (*S*)-(+)- and (*R*)-(−)-[2.2]Paracyclophane-4-Carboxylic Acid. *Tetrahedron: Asymmetry* **1998**, *9* (4), 653–656. https://doi.org/10.1016/S0957-4166(98)00015-9.

(48) Jiang, B.; Zhao, X.-L.; Xu, X.-Y. Resolution of (±)-[2.2]Paracyclophane-4,12-Dicarboxylic Acid. *Tetrahedron: Asymmetry* **2005**, *16* (5), 1071–1074. https://doi.org/10.1016/j.tetasy.2005.01.016.

(49) Dominguez, B.; Zanotti-Gerosa, A.; Hems, W. Electrophilic Substitution of Dibromoparacyclophane: A Route to Novel Paracyclophane Phosphine Ligands. *Org. Lett.* **2004**, *6* (12), 1927–1930. https://doi.org/10.1021/ol049509f.

(50) Reich, H. J.; Cram, D. J. Macro Rings. XXXVII. Multiple Electrophilic Substitution Reactions of [2.2]Paracyclophanes and Interconversions of Polysubstituted Derivatives. *J. Am. Chem. Soc.* **1969**, *91* (13), 3527–3533. https://doi.org/10.1021/ja01041a017.

(51) Braddock, D. C.; MacGilp, I. D.; Perry, B. G. Improved Synthesis of (±)-4,12-Dihydroxy[2.2]paracyclophane and its Enantiomeric Resolution by Enzymatic Methods: Planar Chiral (*R*)- and (*S*)-Phanol. *J. Org. Chem.* **2002**, *67* (24), 8679–8681. https://doi.org/10.1021/jo020451x.

(52) Vorontsova, N. V.; Rozenberg, V. I.; Sergeeva, E. V.; Vorontsov, E. V.; Starikova, Z. A.; Lyssenko, K. A.; Hopf, H. Symmetrically Tetrasubstituted [2.2]Paracyclophanes: Their Systematisation and Regioselective Synthesis of Several Types of Bis-Bifunctional Derivatives by Double Electrophilic Substitution. *Chem. Eur. J.* **2008**, *14* (15), 4600–4617. https://doi.org/10.1002/chem.200701683.

(53) Braddock, D. C.; Ahmad, S. M.; Douglas, G. T. A Preparative Microwave Method for the Isomerisation of 4,16-Dibromo[2.2]Paracyclophane into 4,12-Dibromo[2.2]paracyclophane. *Tetrahedron Lett.* **2004**, *45* (35), 6583–6585. https://doi.org/10.1016/j.tetlet.2004.07.043.

(54) Reich, H. J.; Cram, D. J. Macro Rings. XXXVI. Ring Expansion, Racemisation, and Isomer Interconversions in the [2.2]Paracyclophane System through a Diradical Intermediate. *J. Am. Chem. Soc.* **1969**, *91* (13), 3517–3526. https://doi.org/10.1021/ja01041a016.

(55) Zitt, H.; Dix, I.; Hopf, H.; Jones, P. G. 4,15-Diamino[2.2]Paracyclophane, a Reusable Template for Topochemical Reaction Control in Solution. *Eur. J. Org. Chem.* **2002**, *2002* (14), 2298–2307. https://doi.org/10.1002/1099-0690(200207)2002:14<2298::AID-EJOC2298>3.0.CO;2-E.

(56) Jayasundera, K. P.; Kusmus, D. N. M.; Deuilhé, L.; Etheridge, L.; Farrow, Z.; Lun, D. J.; Kaur, G.; Rowlands, G. J. The Synthesis of Substituted Amino[2.2]Paracyclophanes. *Org. Biomol. Chem.* **2016**, *14* (46), 10848–10860. https://doi.org/10.1039/C6OB02150F.

(57) Thennakoon, N.; Kaur, G.; Wang, J.; Plieger, P. G.; Rowlands, G. J. An Asymmetric Variant of the Bischler–Möhlau Indole Synthesis. *Aust. J. Chem.* **2015**, *68* (4), 566–575. https://doi.org/10.1071/CH14548.

(58) Clayden; Greeves; Warren. *Organic Chemistry*, 2nd edition.; Oxford University Press UK: Oxford ; New York, 2012.

(59) Fuson, R. C.; Bull, B. A. The Haloform Reaction. *Chem. Rev.* **1934**, *15* (3), 275–309. https://doi.org/10.1021/cr60052a001.

(60) Jaiswal, A. K.; Kushawaha, A. K.; Pandey, S.; Kumar, A.; Sashidhara, K. V. Halogen-Free Oxidation of Aryl Ketones and Benzyl Nitrile Derivatives to Corresponding Carboxylic Acids by using NaOH/TBHP in Aqueous Medium. *Tetrahedron.* **2023**, *136*, 133359. https://doi.org/10.1016/j.tet.2023.133359.

(61) Zippel, C.; Hassan, Z.; Parsa, A. Q.; Hohmann, J.; Bräse, S. Multigram-Scale Kinetic Resolution of 4-Acetyl[2.2]Paracyclophane via Ru-Catalyzed Enantioselective Hydrogenation: Accessing [2.2]Paracyclophanes with Planar and Central Chirality. *Adv. Synth. Catal.* **2021**, *363* (11), 2861–2865. https://doi.org/10.1002/adsc.202001536.

(62) Martínez-Castro, E.; Suárez-Pantiga, S.; Mendoza, A. Scalable Synthesis of Esp and Rhodium(II) Carboxylates from Acetylacetone and $RhCl_3 \cdot xH_2O$. *Org. Process Res. Dev.* **2020**, *24* (6), 1207–1212. https://doi.org/10.1021/acs.oprd.0c00164.

(63) Börgel, J.; Ritter, T. Late-Stage Functionalisation. *Chem* **2020**, *6* (8), 1877–1887. https://doi.org/10.1016/j.chempr.2020.07.007.

(64) Liao, K.; Negretti, S.; Musaev, D. G.; Bacsa, J.; Davies, H. M. L. Site-Selective and Stereoselective Functionalisation of Unactivated C–H Bonds. *Nature*. **2016**, *533* (7602), 230–234. https://doi.org/10.1038/nature17651.

(65) Chen, W.-B.; Xing, C.-H.; Dong, J.; Hu, Q.-S. Electron-Poor, Fluoro-Containing Arylboronic Acids as Efficient Coupling Partners for Bis(1,5-Cyclooctadiene)Nickel(0)/Tricyclohexylphosphine-Catalysed Cross-Coupling Reactions of Aryl Arenesulfonates. *Adv. Synth. Catal.* **2016**, *358* (13), 2072–2076. https://doi.org/10.1002/adsc.201600205.

(66) D'Alterio, M. C.; Casals-Cruañas, È.; Tzouras, N. V.; Talarico, G.; Nolan, S. P.; Poater, A. Mechanistic Aspects of the Palladium-Catalysed Suzuki-Miyaura Cross-Coupling Reaction. *Chem. Eur. J.* **2021**, *27* (54), 13481–13493. https://doi.org/10.1002/chem.202101880.

(67) Farhang, M.; Akbarzadeh, A. R.; Rabbani, M.; Ghadiri, A. M. A Retrospective-Prospective Review of Suzuki–Miyaura Reaction: From Cross-Coupling Reaction to Pharmaceutical Industry Applications. *Polyhedron*. **2022**, *227*, 116124. https://doi.org/10.1016/j.poly.2022.116124.

(68) Zask, A.; Helquist, P. Palladium Hydrides in Organic Synthesis. Reduction of Aryl Halides by Sodium Methoxide Catalyzed by Tetrakis(Triphenylphosphine)Palladium. *J. Org. Chem.* **1978**, *43* (8), 1619–1620. https://doi.org/10.1021/jo00402a042.

(69) Martin, R.; Buchwald, S. L. Palladium-Catalysed Suzuki–Miyaura Cross-Coupling Reactions Employing Dialkylbiaryl Phosphine Ligands. *Acc. Chem. Res.* **2008**, *41* (11), 1461–1473. https://doi.org/10.1021/ar800036s.

(70) Hong, B.; Shi, L.; Li, L.; Zhan, S.; Gu, Z. Paddlewheel Dirhodium(II) Complexes with *N*-Heterocyclic Carbene or Phosphine Ligand: New Reactivity and Selectivity. *Green Synth. Catal.* **2022**. https://doi.org/10.1016/j.gresc.2022.03.001.

(71) Ma, J.; Zhou, X.; Chen, J.; Shi, J.; Cheng, H.; Guo, P.; Ji, H. Directing Group Strategies in Rhodium-Catalysed C–H Amination. *Org. Biomol. Chem.* **2022**, *20* (38), 7554–7576. https://doi.org/10.1039/D2OB01157C.

(72) Bois, J. D. Rhodium-Catalysed C–H Amination – An Enabling Method for Chemical Synthesis. *Org. Process. Res. Dev.* **2011**, *15* (4), 758–762. https://doi.org/10.1021/op200046v.

(73) Roizen, J. L.; Harvey, M. E.; Du Bois, J. Metal-Catalysed Nitrogen-Atom Transfer Methods for the Oxidation of Aliphatic C–H Bonds. *Acc. Chem. Res.* **2012**, *45* (6), 911–922. https://doi.org/10.1021/ar200318q.

(74) Azek, E.; Khalifa, M.; Bartholoméüs, J.; Ernzerhof, M.; Lebel, H. Rhodium(II)-Catalysed C–H Aminations Using *N* -Mesyloxycarbamates: Reaction Pathway and by-Product Formation. *Chem. Sci*. **2019**, *10* (3), 718–729. https://doi.org/10.1039/C8SC03153C.

(75) Liao, K.; Pickel, T. C.; Boyarskikh, V.; Bacsa, J.; Musaev, D. G.; Davies, H. M. L. Site-Selective and Stereoselective Functionalisation of Non-Activated Tertiary C–H Bonds. *Nature*. **2017**, *551* (7682), 609–613. https://doi.org/10.1038/nature24641.

(76) Sheldrick, G. M. Crystal Structure Refinement with SHELXL. *Acta. Crystallogr*. **2015**, *71* (1), 3–8.

(77) Sheldrick, G. M. A Short History of SHELX. *Acta. Cryst. A*. **2008**, *64* (1), 112–122. https://doi.org/10.1107/S0108767307043930.

(78) Dolomanov, O. V.; Bourhis, L. J.; Gildea, R. J.; Howard, J. a. K.; Puschmann, H. OLEX2: A Complete Structure Solution, Refinement and Analysis Program. *J. Appl. Cryst*. **2009**, *42* (2), 339–341. https://doi.org/10.1107/S0021889808042726.

(79) Hibert, M.; Solladie, G. Substituent Effect during the Synthesis of Substituted [2.2] Paracyclophane by Photoextrusion of Carbon Dioxide from a Cyclic Diester. *J. Org. Chem*. **1980**, *45* (22), 4496–4498. https://doi.org/10.1021/jo01310a045.

Appendix

^{1}H NMR spectrum of **37** in $CDCl_3$

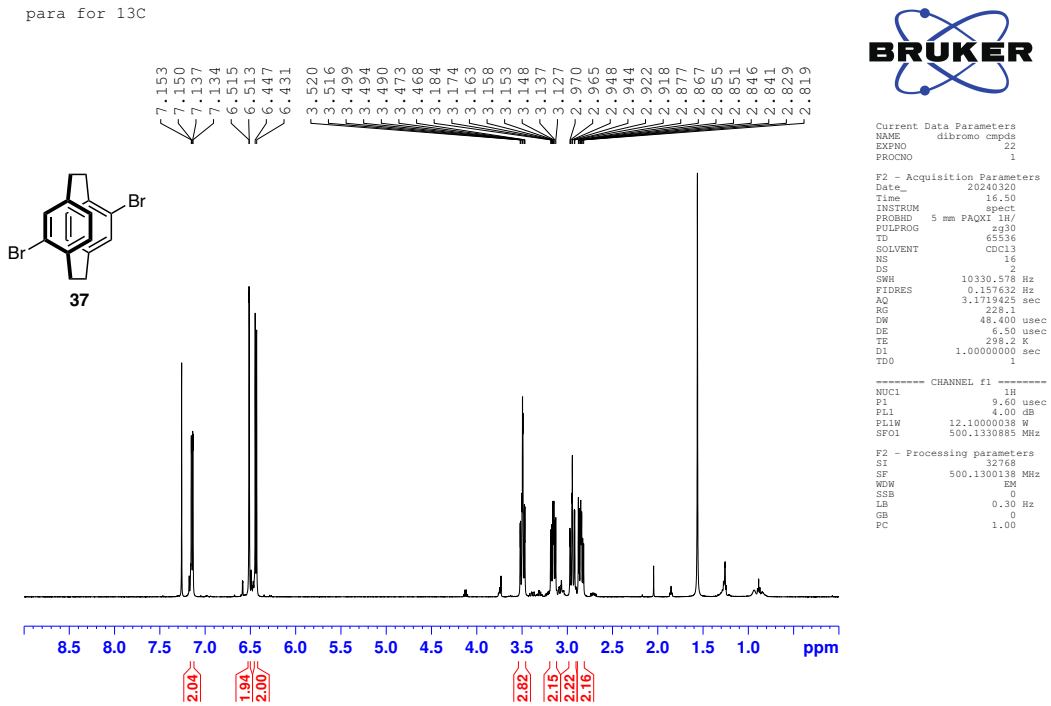


```
Current Data Parameters
NAME        dibromo cmpds
EXPNO                 22
PROCNO                 1

F2 - Acquisition Parameters
Date_           20240320
Time               16.50
INSTRUM            spect
PROBHD   5 mm PAQXI 1H/
PULPROG            zg30
TD                65536
SOLVENT           CDCl3
NS                   16
DS                    2
SWH           10330.578 Hz
FIDRES         0.157632 Hz
AQ             3.1719425 sec
RG                228.1
DW               48.400 usec
DE                6.50 usec
TE                298.2 K
D1            1.00000000 sec
TD0                    1

======== CHANNEL f1 ========
NUC1                  1H
P1                 9.60 usec
PL1                4.00 dB
PL1W        12.10000038 W
SFO1        500.1330885 MHz

F2 - Processing parameters
SI                 32768
SF          500.1300138 MHz
WDW                   EM
SSB                    0
LB                 0.30 Hz
GB                     0
PC                 1.00
```

^{13}C NMR spectrum of **37** in $CDCl_3$

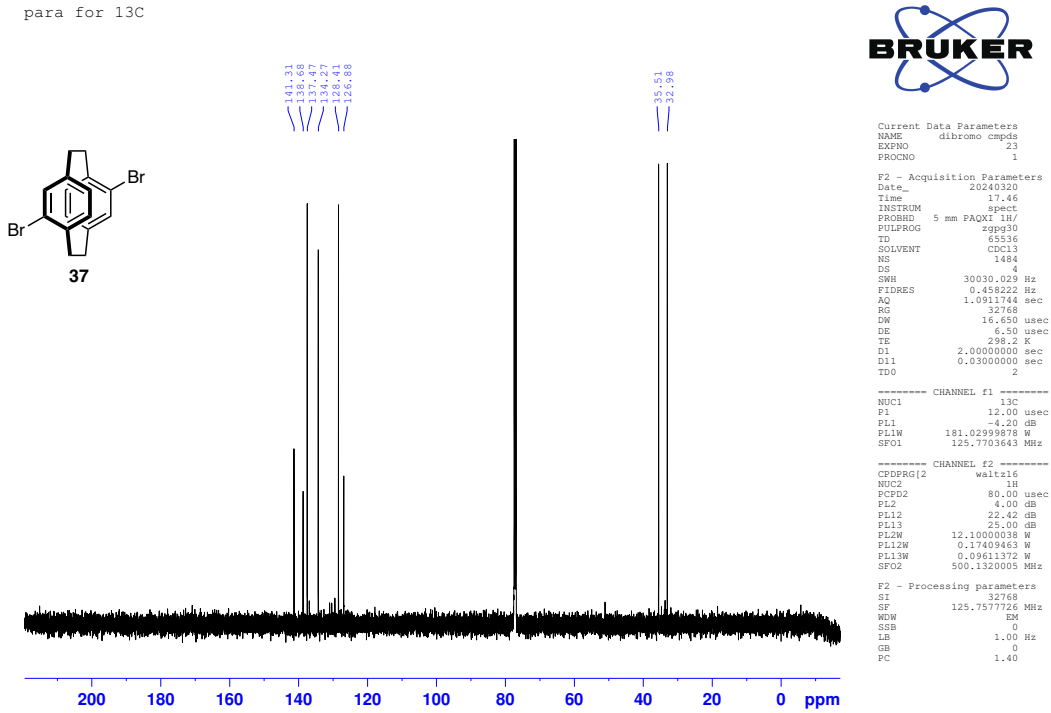


```
Current Data Parameters
NAME        dibromo cmpds
EXPNO                 23
PROCNO                 1

F2 - Acquisition Parameters
Date_           20240320
Time               17.46
INSTRUM            spect
PROBHD   5 mm PAQXI 1H/
PULPROG         zgpg30
TD                65536
SOLVENT           CDCl3
NS                 1484
DS                    4
SWH           30030.029 Hz
FIDRES         0.458222 Hz
AQ             1.0911744 sec
RG                32768
DW               16.650 usec
DE                6.50 usec
TE                298.2 K
D1            2.00000000 sec
D11           0.03000000 sec
TD0                    2

======== CHANNEL f1 ========
NUC1                 13C
P1                12.00 usec
PL1               -4.20 dB
PL1W       181.02999878 W
SFO1        125.7703643 MHz

======== CHANNEL f2 ========
CPDPRG[2         waltz16
NUC2                 1H
PCPD2             80.00 usec
PL2                4.00 dB
PL12              22.42 dB
PL13              25.00 dB
PL2W        12.10000038 W
PL12W        0.17409463 W
PL13W        0.09611372 W
SFO2        500.1320005 MHz

F2 - Processing parameters
SI                 32768
SF          125.7577726 MHz
WDW                   EM
SSB                    0
LB                 1.00 Hz
GB                     0
PC                 1.40
```

^{1}H NMR spectrum of (±)-**38** in $CDCl_3$

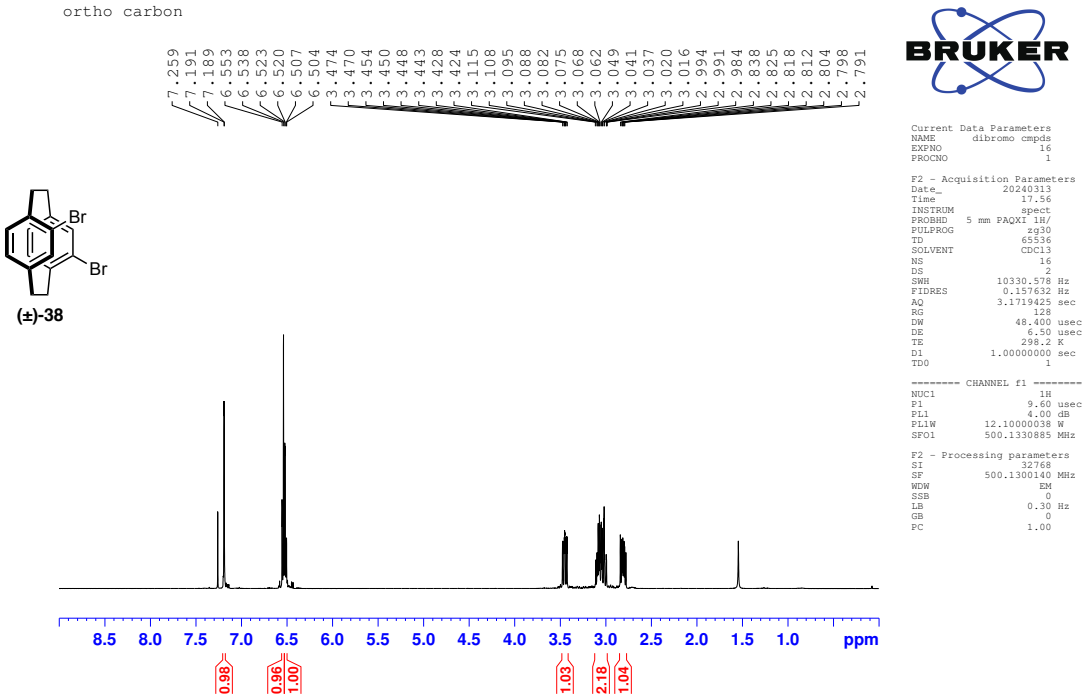

BRUKER

```
Current Data Parameters
NAME        dibromo cmpds
EXPNO                 16
PROCNO                 1

F2 - Acquisition Parameters
Date_           20240313
Time               17.56
INSTRUM            spect
PROBHD   5 mm PAQXI 1H/
PULPROG             zg30
TD                 65536
SOLVENT            CDCl3
NS                    16
DS                     2
SWH           10330.578 Hz
FIDRES         0.157632 Hz
AQ             3.1719425 sec
RG                   128
DW                48.400 usec
DE                 6.50 usec
TE                298.2 K
D1             1.00000000 sec
TD0                    1

======== CHANNEL f1 ========
NUC1                  1H
P1                 9.60 usec
PL1                4.00 dB
PL1W        12.10000038 W
SFO1        500.1330885 MHz

F2 - Processing parameters
SI                 32768
SF          500.1300140 MHz
WDW                   EM
SSB                    0
LB                  0.30 Hz
GB                     0
PC                  1.00
```

^{13}C NMR spectrum of (±)-**38** in $CDCl_3$

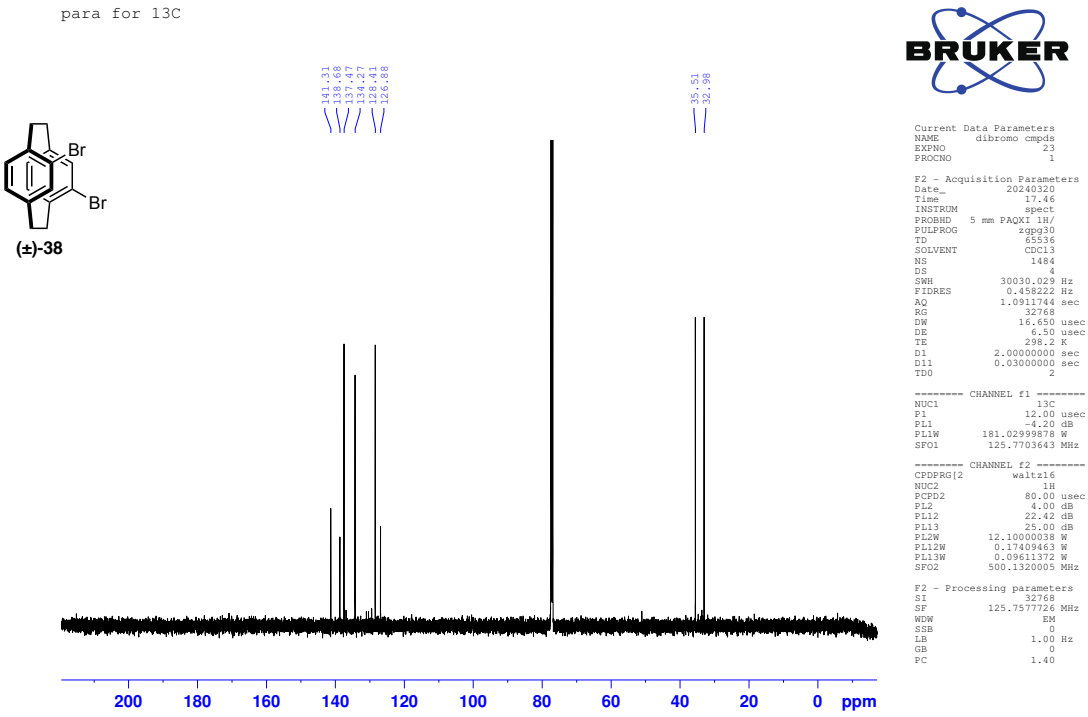

BRUKER

```
Current Data Parameters
NAME        dibromo cmpds
EXPNO                 23
PROCNO                 1

F2 - Acquisition Parameters
Date_           20240320
Time               17.46
INSTRUM            spect
PROBHD   5 mm PAQXI 1H/
PULPROG          zgpg30
TD                 65536
SOLVENT            CDCl3
NS                  1484
DS                     4
SWH           30030.029 Hz
FIDRES         0.458222 Hz
AQ             1.0911744 sec
RG                 32768
DW                16.650 usec
DE                 6.50 usec
TE                298.2 K
D1             2.00000000 sec
D11            0.03000000 sec
TD0                    2

======== CHANNEL f1 ========
NUC1                 13C
P1                12.00 usec
PL1               -4.20 dB
PL1W        181.02999878 W
SFO1        125.7703643 MHz

======== CHANNEL f2 ========
CPDPRG[2         waltz16
NUC2                  1H
PCPD2              80.00 usec
PL2                4.00 dB
PL12               22.42 dB
PL13               25.00 dB
PL2W        12.10000038 W
PL12W        0.17409463 W
PL13W        0.09611372 W
SFO2        500.1320005 MHz

F2 - Processing parameters
SI                 32768
SF          125.7577726 MHz
WDW                   EM
SSB                    0
LB                  1.00 Hz
GB                     0
PC                  1.40
```

^{1}H NMR spectrum of (±)-**39** in $CDCl_3$

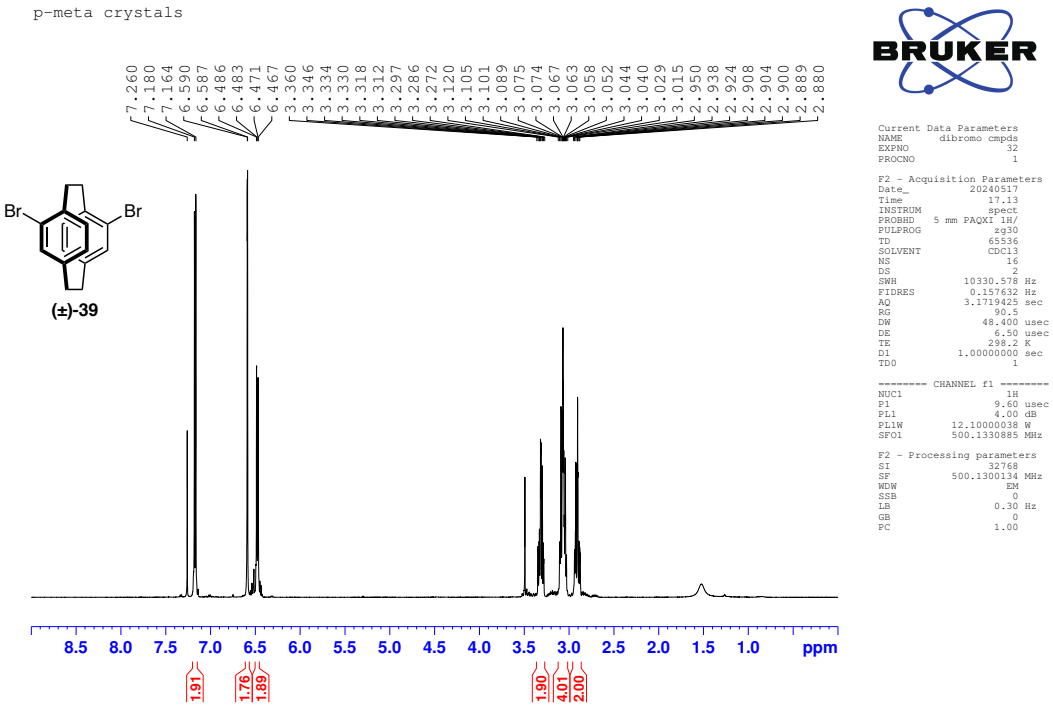

^{13}C NMR spectrum of (±)-**39** in $CDCl_3$

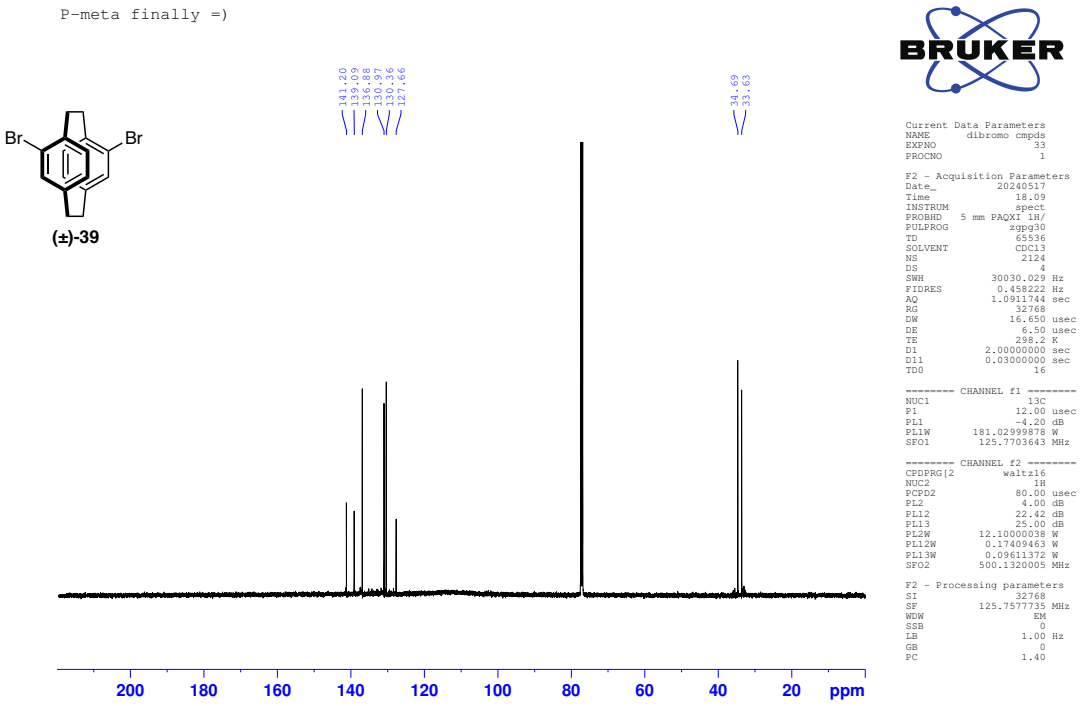

^{1}H NMR spectrum of (±)-**32** in $CDCl_3$

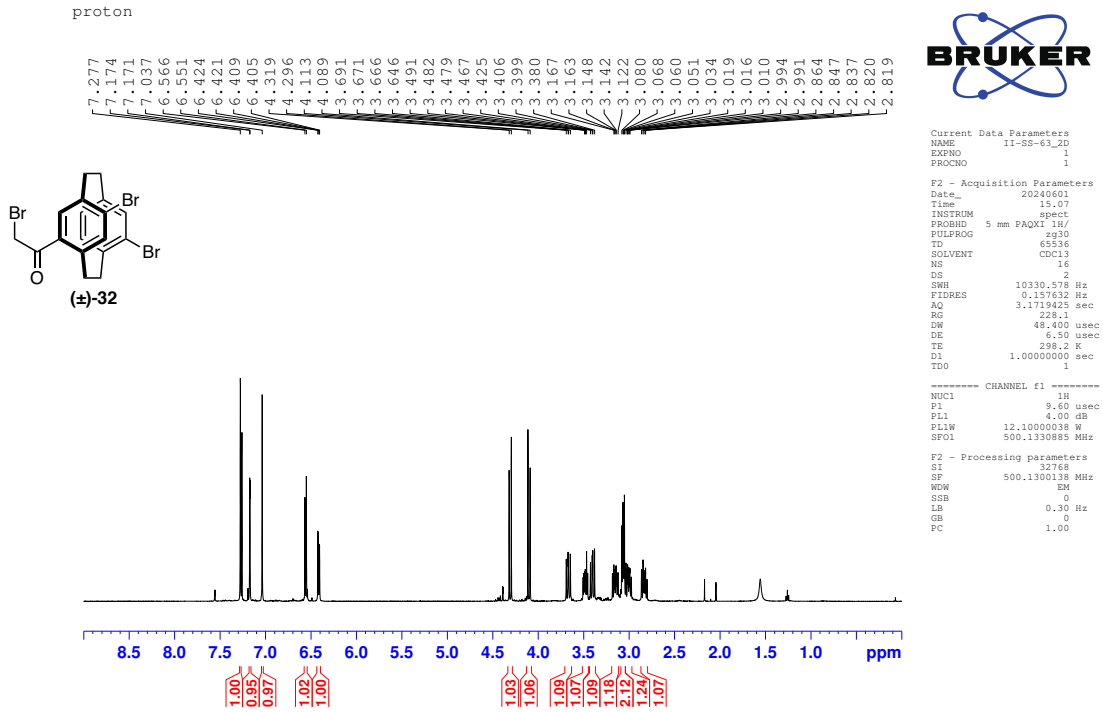

^{13}C NMR spectrum of (±)-**32** in $CDCl_3$

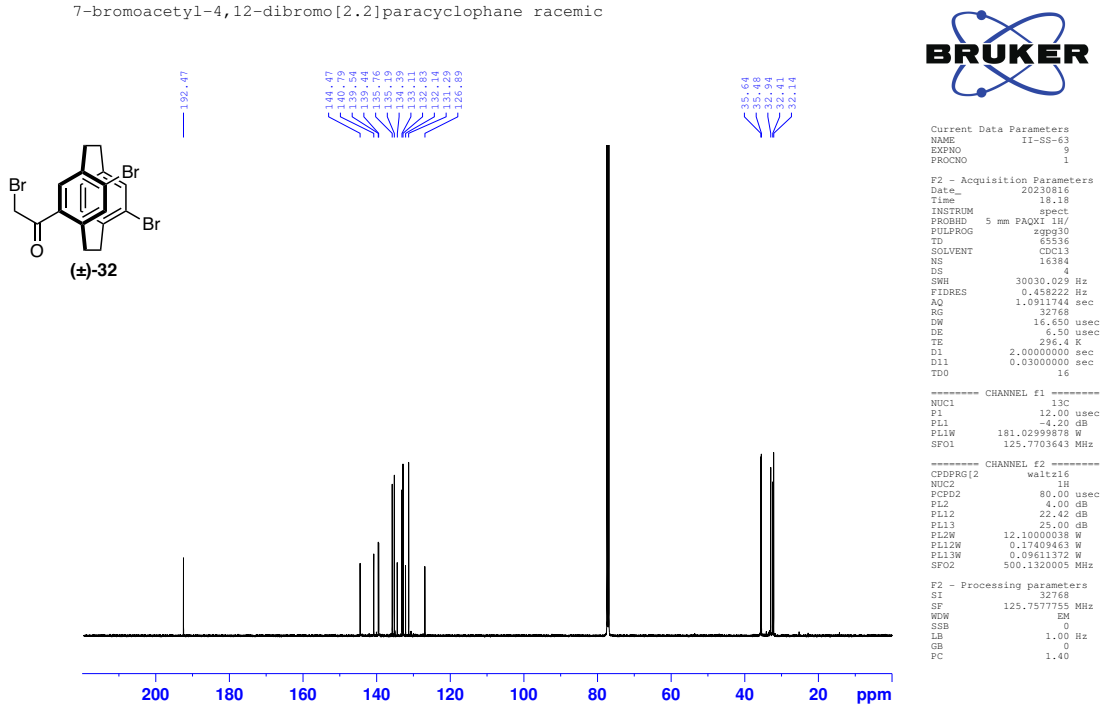

^{1}H NMR spectrum of (±)-**42** in $CDCl_3$

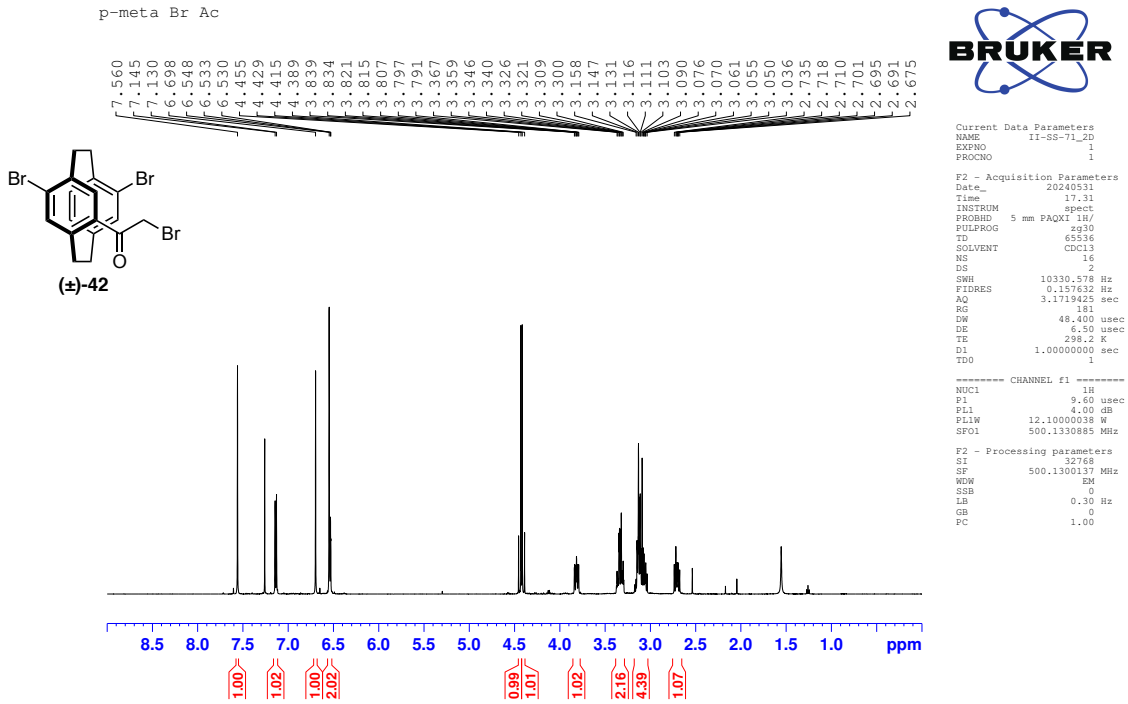

Current Data Parameters
NAME II-SS-71_2D
EXPNO 1
PROCNO 1

F2 - Acquisition Parameters
Date_ 20240531
Time 17.31
INSTRUM spect
PROBHD 5 mm PAQXI 1H/
PULPROG zg30
TD 65536
SOLVENT CDCl3
NS 16
DS 2
SWH 10330.578 Hz
FIDRES 0.157632 Hz
AQ 3.1719425 sec
RG 181
DW 48.400 usec
DE 6.50 usec
TE 298.2 K
D1 1.00000000 sec
TD0 1

======== CHANNEL f1 ========
NUC1 1H
P1 9.60 usec
PL1 4.00 dB
PL1W 12.10000038 W
SFO1 500.1330885 MHz

F2 - Processing parameters
SI 32768
SF 500.1300137 MHz
WDW EM
SSB 0
LB 0.30 Hz
GB 0
PC 1.00

^{13}C NMR spectrum of (±)-**42** in $CDCl_3$

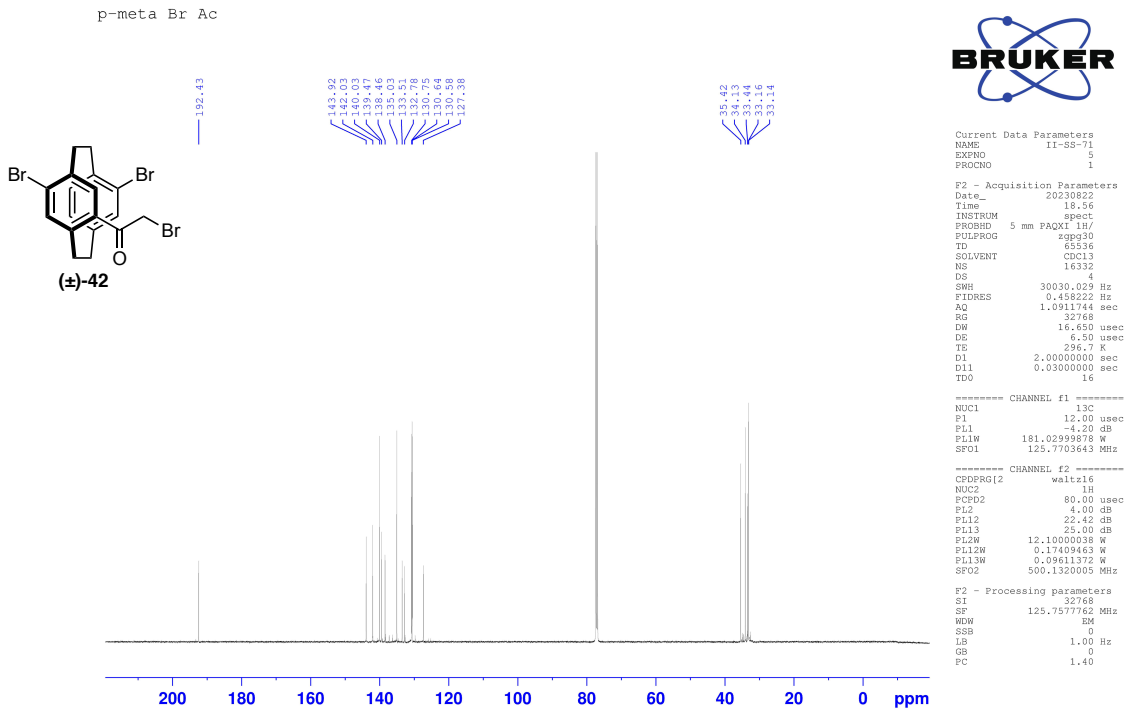

Current Data Parameters
NAME II-SS-71
EXPNO 5
PROCNO 1

F2 - Acquisition Parameters
Date_ 20230822
Time 18.56
INSTRUM spect
PROBHD 5 mm PAQXI 1H/
PULPROG zgpg30
TD 65536
SOLVENT CDCl3
NS 16332
DS 4
SWH 30030.029 Hz
FIDRES 0.458222 Hz
AQ 1.0911744 sec
RG 32768
DW 16.650 usec
DE 6.50 usec
TE 296.7 K
D1 2.00000000 sec
D11 0.03000000 sec
TD0 16

======== CHANNEL f1 ========
NUC1 13C
P1 12.00 usec
PL1 -4.20 dB
PL1W 181.02999878 W
SFO1 125.7703643 MHz

======== CHANNEL f2 ========
CPDPRG[2 waltz16
NUC2 1H
PCPD2 80.00 usec
PL2 4.00 dB
PL12 22.42 dB
PL13 25.00 dB
PL2W 12.10000038 W
PL12W 0.17409463 W
PL13W 0.09611372 W
SFO2 500.1320005 MHz

F2 - Processing parameters
SI 32768
SF 125.7577762 MHz
WDW EM
SSB 0
LB 1.00 Hz
GB 0
PC 1.40

^{1}H NMR spectrum of (±)-**43** in $CDCl_3$

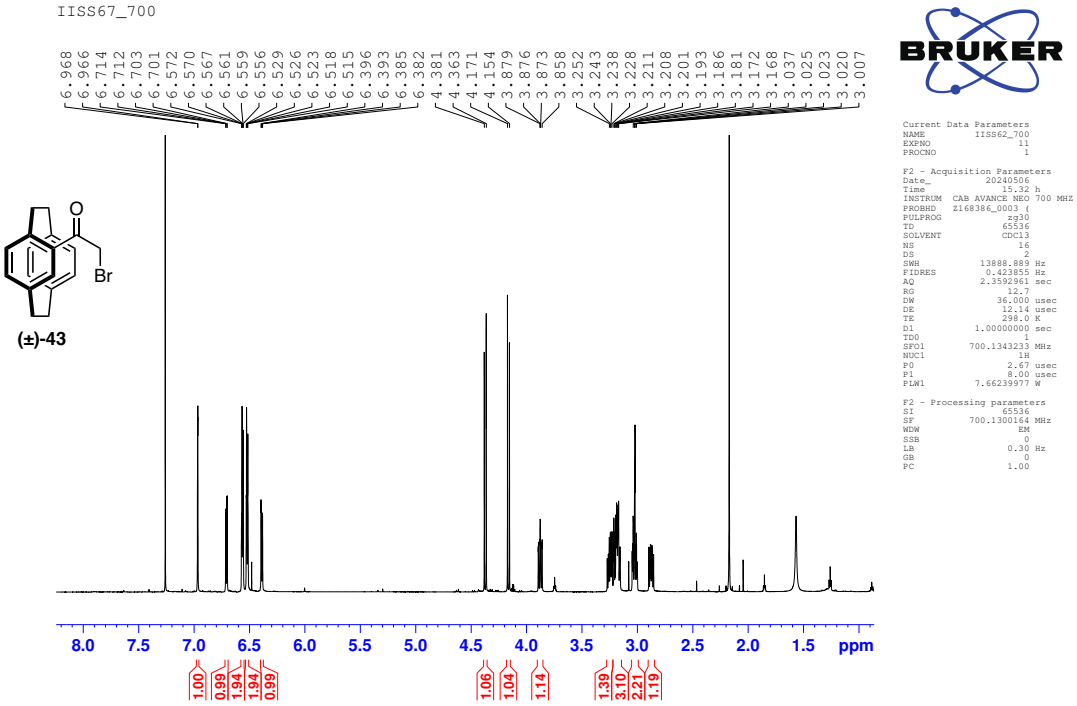

^{13}C NMR spectrum of (±)-**43** in $CDCl_3$

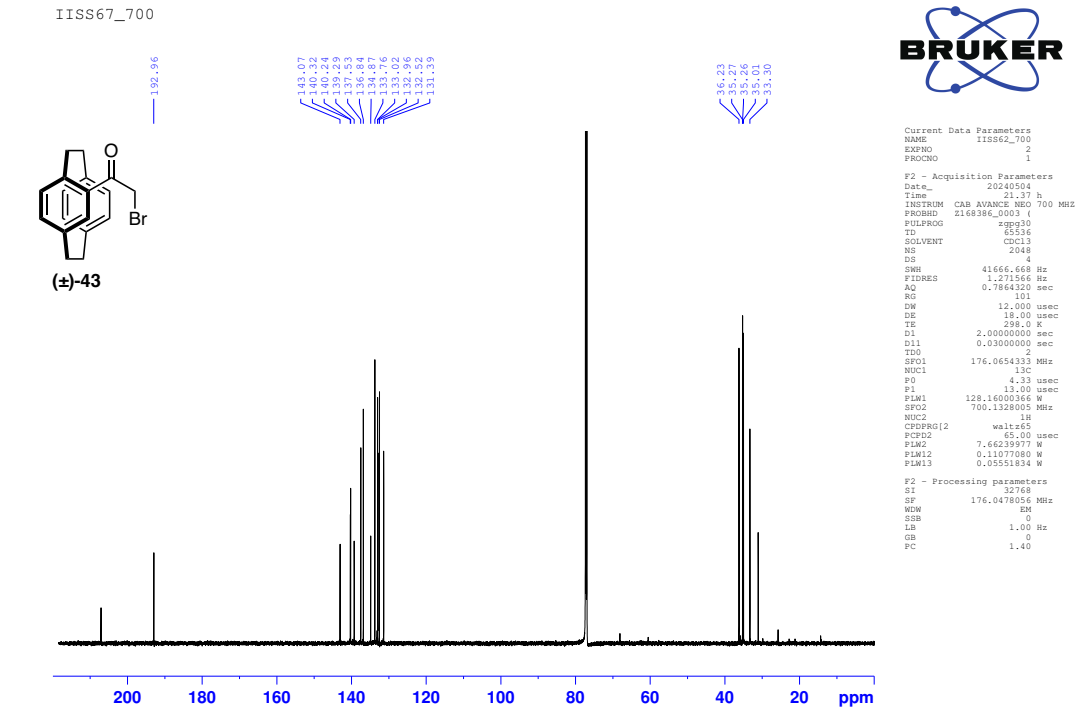

^{1}H NMR spectrum of (R_p)-**36** in $CDCl_3$

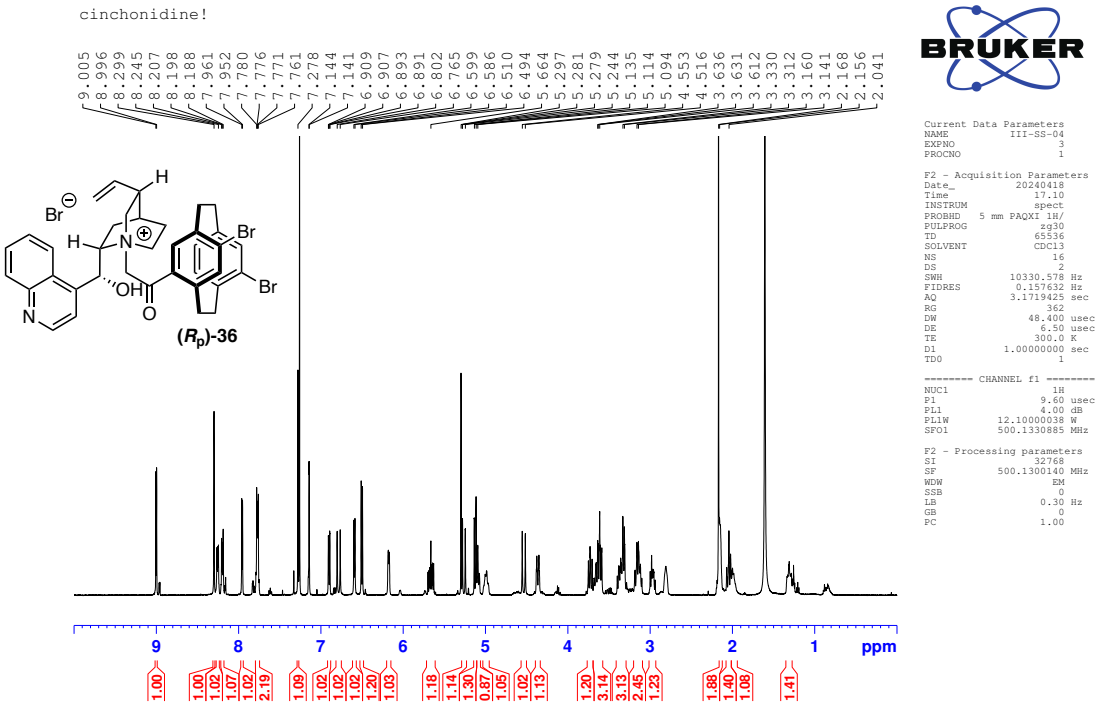

BRUKER

```
Current Data Parameters
NAME                  III-SS-04
EXPNO                         3
PROCNO                        1

F2 - Acquisition Parameters
Date_                  20240418
Time                      17.10
INSTRUM                   spect
PROBHD    5 mm PAQXI 1H/
PULPROG                   zg30
TD                       65536
SOLVENT                  CDCl3
NS                          16
DS                           2
SWH                  10330.578 Hz
FIDRES                0.157632 Hz
AQ                   3.1719425 sec
RG                         362
DW                      48.400 usec
DE                       6.50 usec
TE                      300.0 K
D1                   1.00000000 sec
TD0                          1

======== CHANNEL f1 ========
NUC1                       1H
P1                       9.60 usec
PL1                      4.00 dB
PL1W                12.10000038 W
SFO1                500.1330885 MHz

F2 - Processing parameters
SI                       32768
SF                  500.1300140 MHz
WDW                         EM
SSB                          0
LB                        0.30 Hz
GB                           0
PC                        1.00
```

^{13}C NMR spectrum of (R_p)-**36** in $CDCl_3$

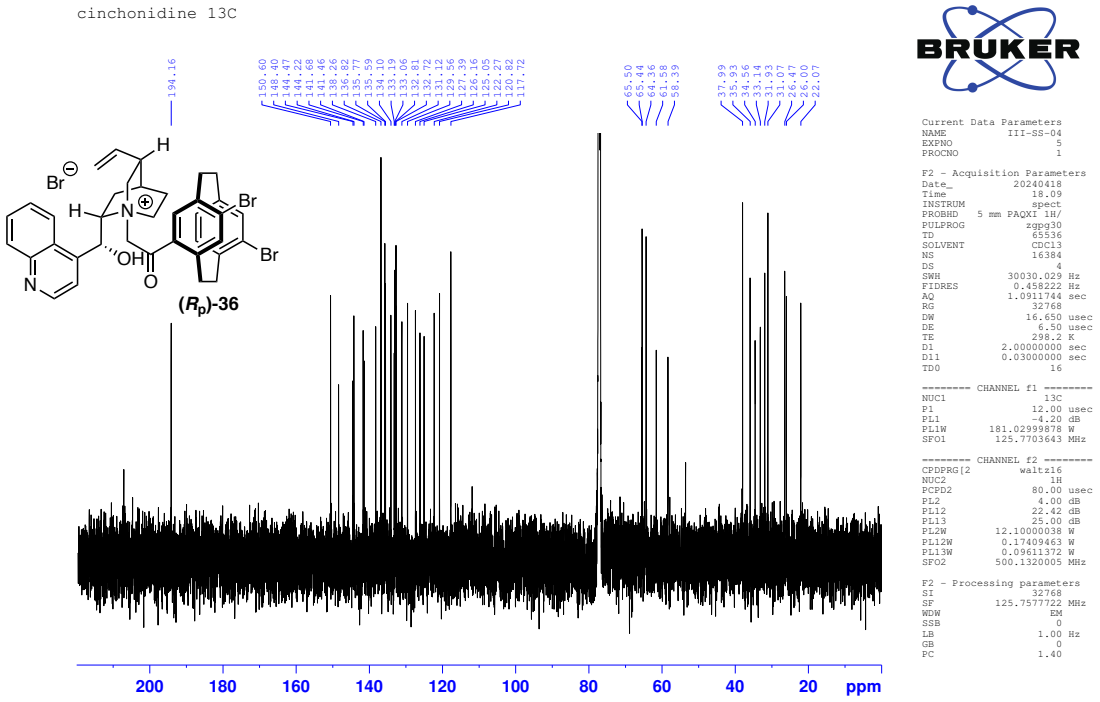

BRUKER

```
Current Data Parameters
NAME                  III-SS-04
EXPNO                         5
PROCNO                        1

F2 - Acquisition Parameters
Date_                  20240418
Time                      18.09
INSTRUM                   spect
PROBHD    5 mm PAQXI 1H/
PULPROG                 zgpg30
TD                       65536
SOLVENT                  CDCl3
NS                       16384
DS                           4
SWH                  30030.029 Hz
FIDRES                0.458222 Hz
AQ                   1.0911744 sec
RG                         362
DW                      16.650 usec
DE                       6.50 usec
TE                      298.2 K
D1                   2.00000000 sec
D11                  0.03000000 sec
TD0                         16

======== CHANNEL f1 ========
NUC1                      13C
P1                      12.00 usec
PL1                      -4.20 dB
PL1W               181.02999878 W
SFO1                125.7703643 MHz

======== CHANNEL f2 ========
CPDPRG[2             waltz16
NUC2                       1H
PCPD2                  80.00 usec
PL2                      4.00 dB
PL12                    22.42 dB
PL13                    25.00 dB
PL2W                12.10000038 W
PL12W                0.17409463 W
PL13W                0.09611372 W
SFO2                500.1320005 MHz

F2 - Processing parameters
SI                       32768
SF                  125.7577722 MHz
WDW                         EM
SSB                          0
LB                        1.00 Hz
GB                           0
PC                        1.40
```

^{1}H NMR spectrum of (S_p)-**50** in $CDCl_3$

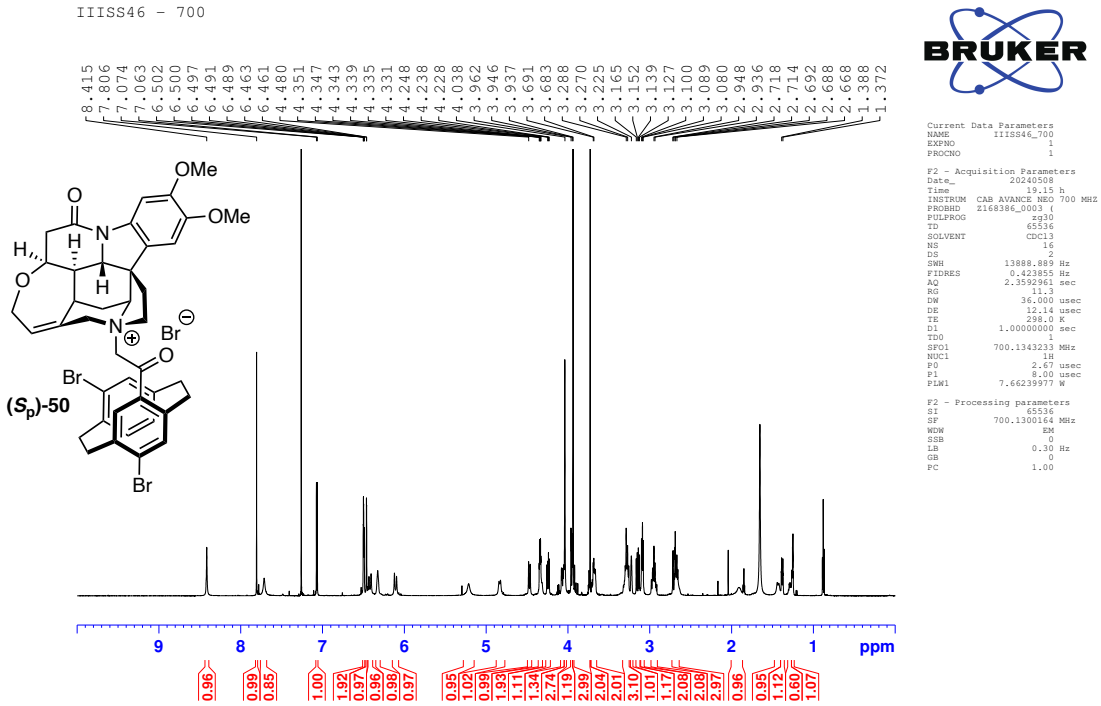

^{13}C NMR spectrum of (S_p)-**50** in $CDCl_3$

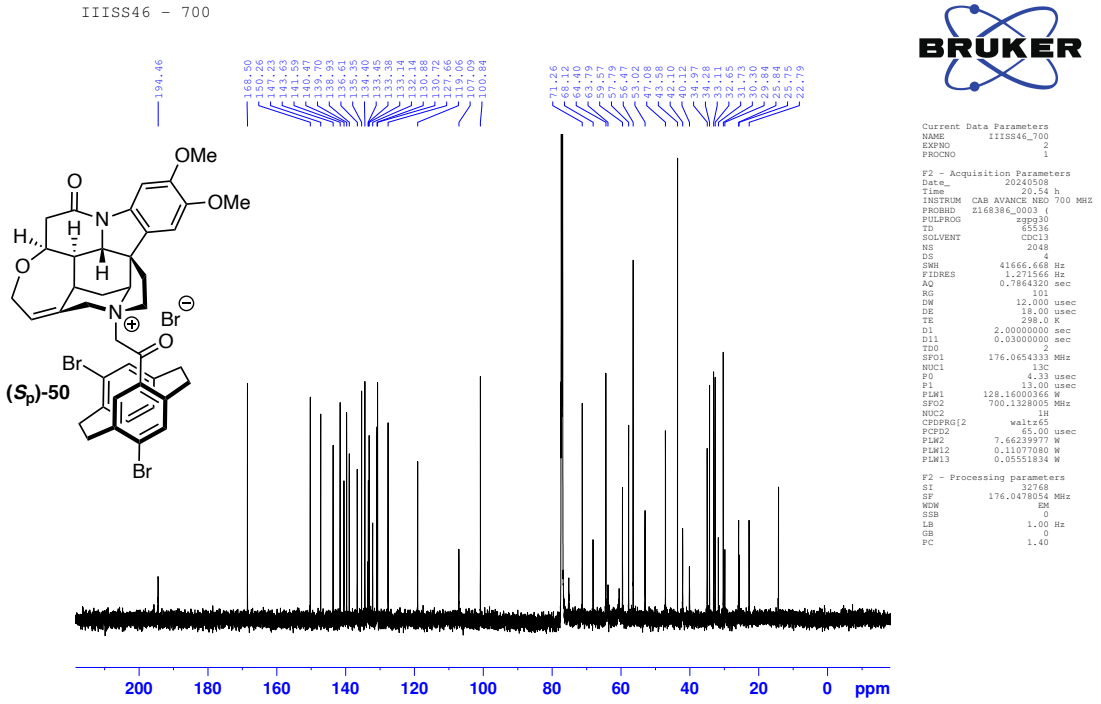

^{1}H NMR spectrum of (R_p)-**48** in $CDCl_3$

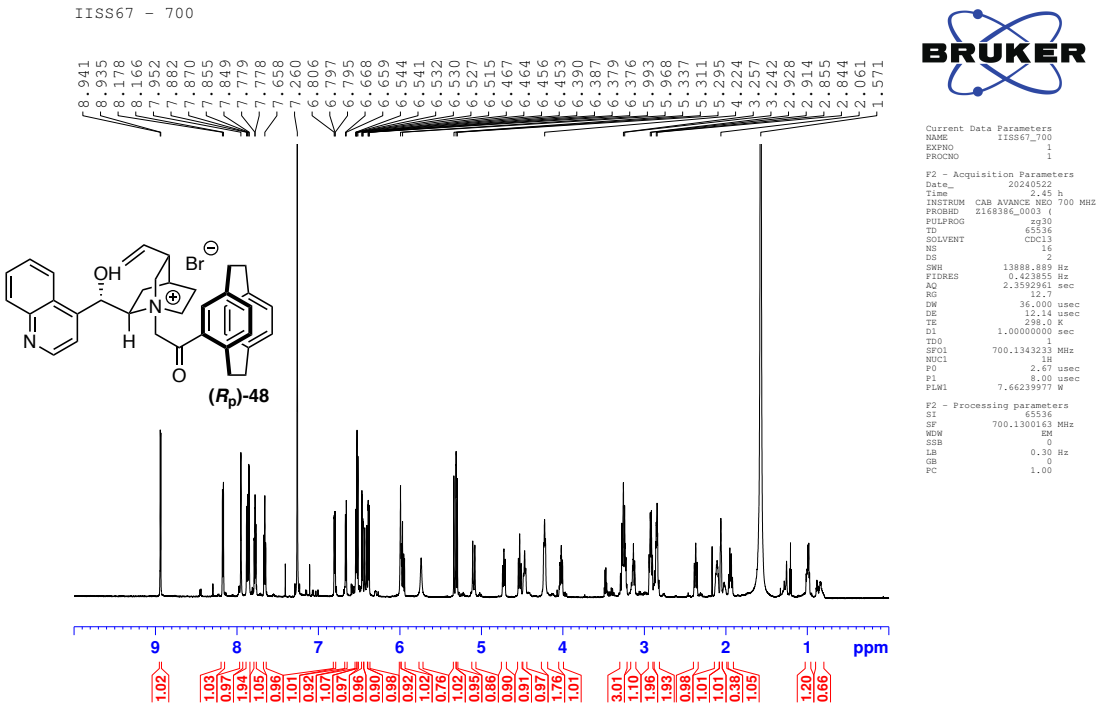

^{13}C NMR spectrum of (R_p)-**48** in $CDCl_3$

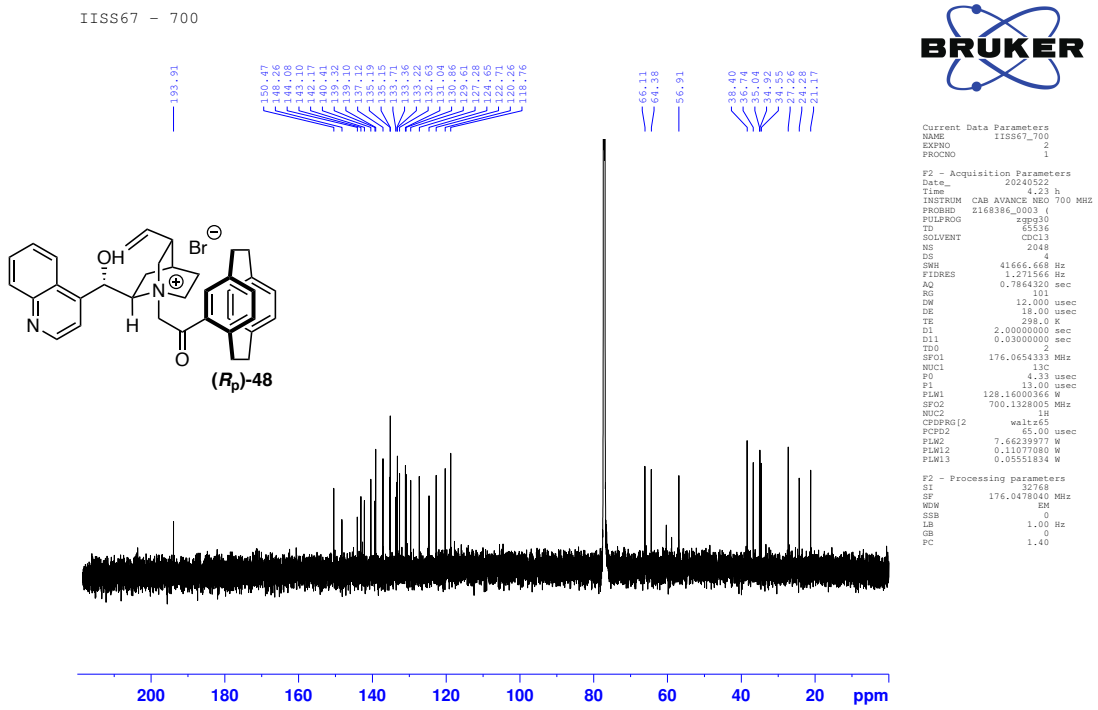

^{1}H NMR spectrum of (R_p)-**33** in $CDCl_3$

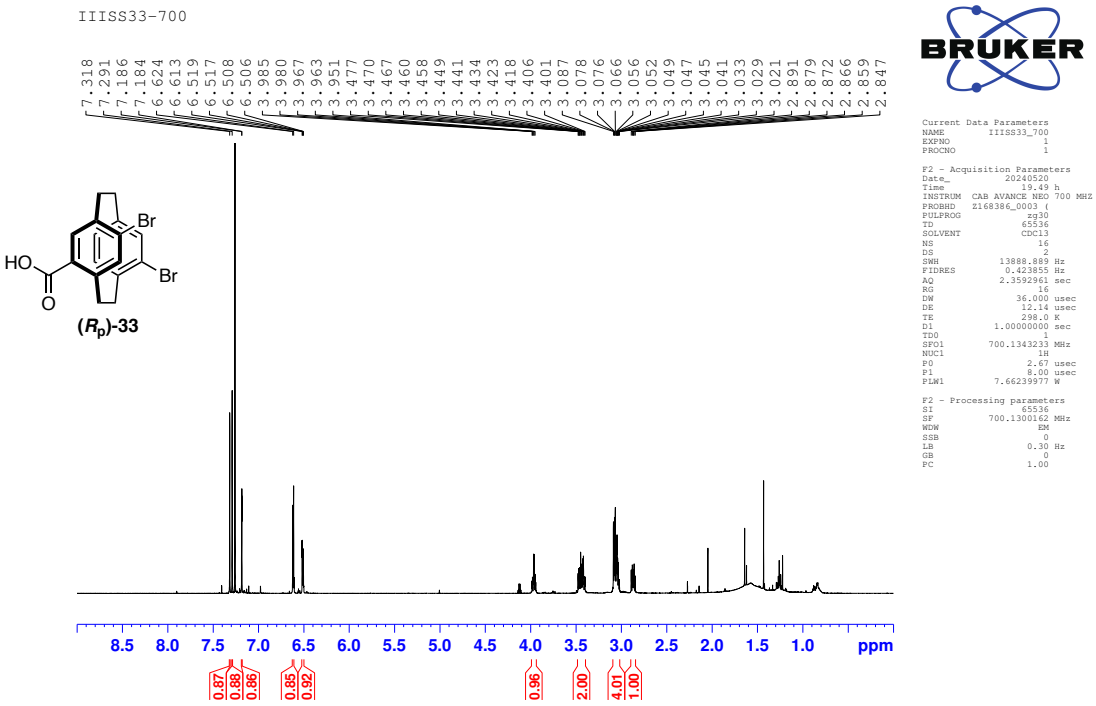

Current Data Parameters
NAME IIISS33_700
EXPNO 1
PROCNO 1

F2 - Acquisition Parameters
Date_ 20240520
Time 19.49 h
INSTRUM CAB AVANCE NEO 700 MHZ
PROBHD Z168386_0003 (
PULPROG zg30
TD 65536
SOLVENT CDCl3
NS 16
DS 2
SWH 13888.889 Hz
FIDRES 0.423855 Hz
AQ 2.3592961 sec
RG 16
DW 36.000 usec
DE 12.14 usec
TE 298.0 K
D1 1.00000000 sec
TD0 1
SFO1 700.1343233 MHz
NUC1 1H
P0 2.67 usec
P1 8.00 usec
PLW1 7.66239977 W

F2 - Processing parameters
SI 65536
SF 700.1300162 MHz
WDW EM
SSB 0
LB 0.30 Hz
GB 0
PC 1.00

^{13}C NMR spectrum of (R_p)-**33** in $CDCl_3$

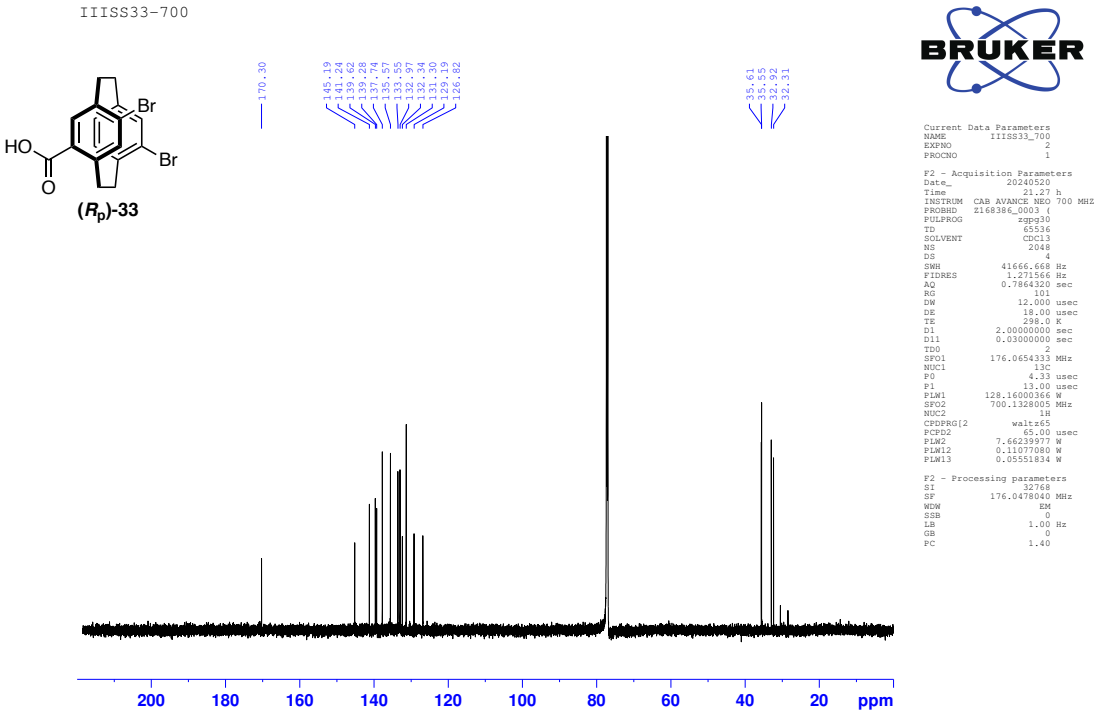

Current Data Parameters
NAME IIISS33_700
EXPNO 2
PROCNO 1

F2 - Acquisition Parameters
Date_ 20240520
Time 21.27 h
INSTRUM CAB AVANCE NEO 700 MHZ
PROBHD Z168386_0003 (
PULPROG zgpg30
TD 65536
SOLVENT CDCl3
NS 2048
DS 4
SWH 41666.668 Hz
FIDRES 1.271566 Hz
AQ 0.7864320 sec
RG 101
DW 12.000 usec
DE 18.00 usec
TE 298.0 K
D1 2.00000000 sec
D11 0.03000000 sec
TD0 2
SFO1 176.0654333 MHz
NUC1 13C
P0 4.33 usec
P1 13.00 usec
PLW1 128.16000366 W
SFO2 700.1328005 MHz
NUC2 1H
CPDPRG[2 waltz65
PCPD2 65.00 usec
PLW2 7.66239977 W
PLW12 0.11077080 W
PLW13 0.05551834 W

F2 - Processing parameters
SI 32768
SF 176.0478040 MHz
WDW EM
SSB 0
LB 1.00 Hz
GB 0
PC 1.40

^{1}H NMR spectrum of (S_p)-**34** in $CDCl_3$

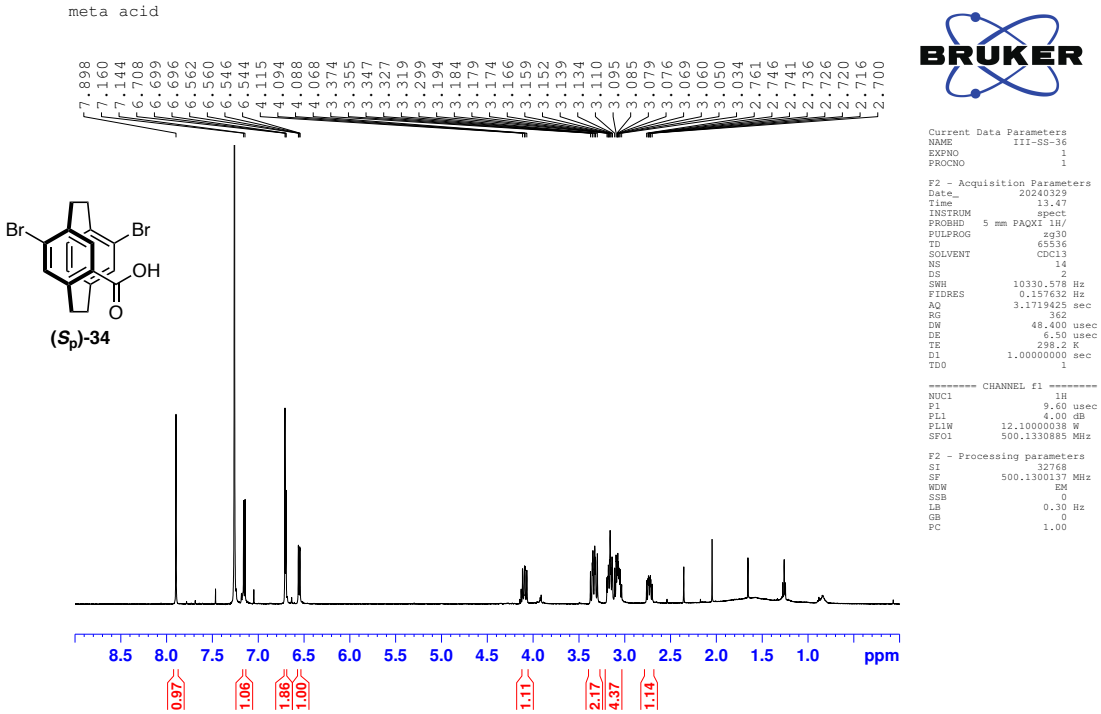

^{13}C NMR spectrum of (S_p)-**34** in $CDCl_3$

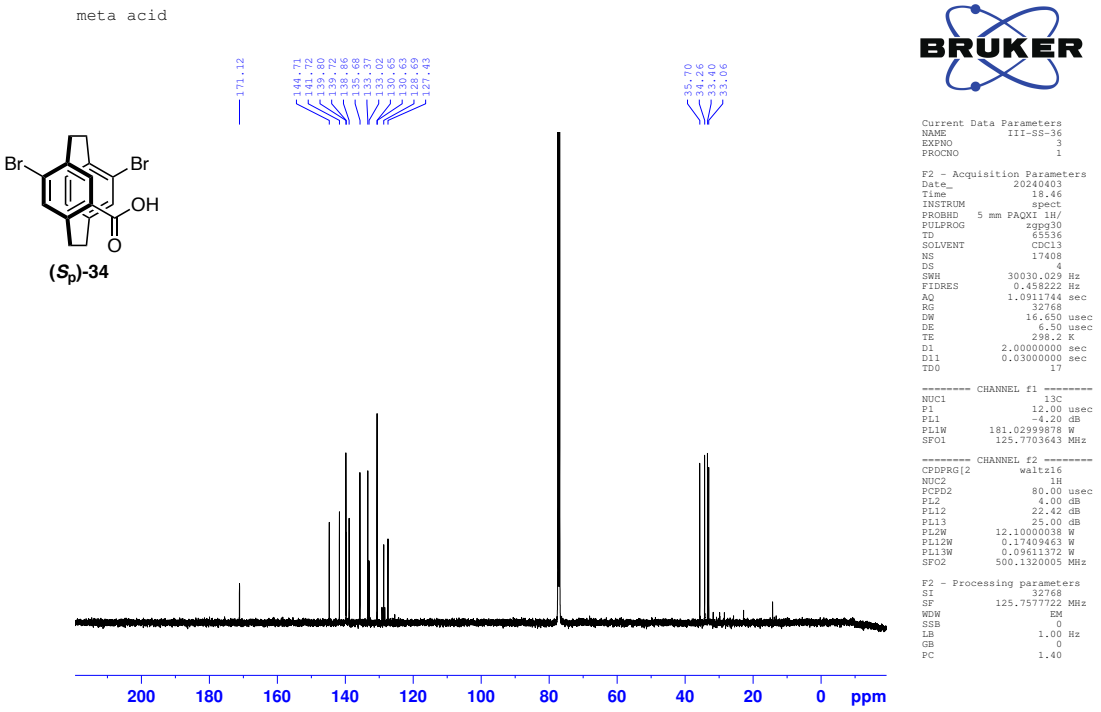

^{1}H NMR spectrum of (R_p)-**28** in $CDCl_3$

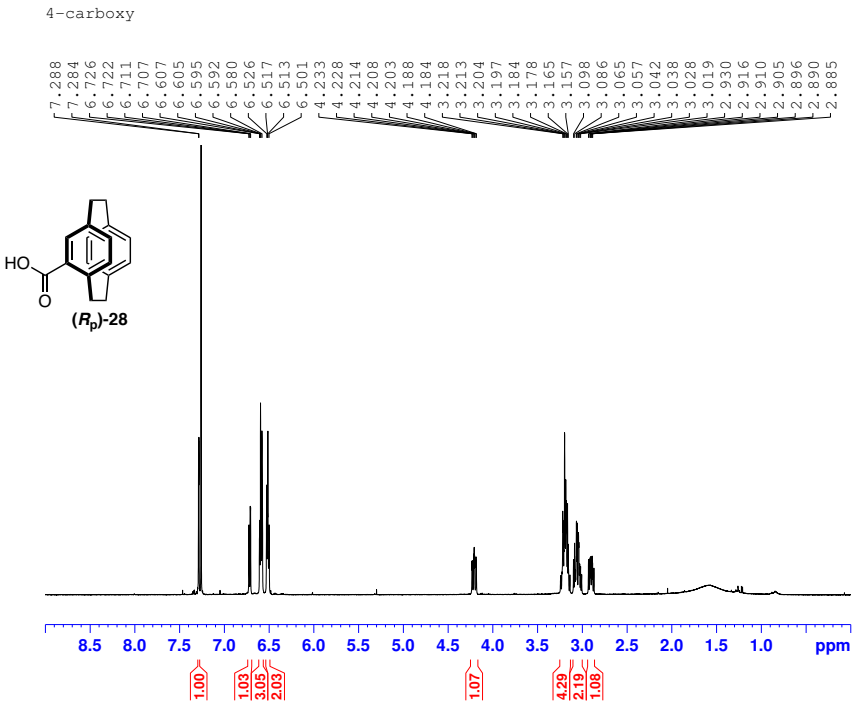

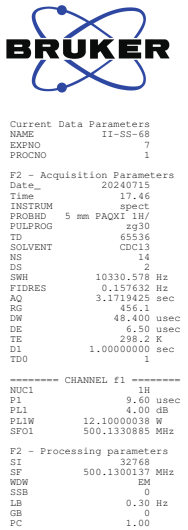

^{13}C NMR spectrum of (R_p)-**28** in $CDCl_3$

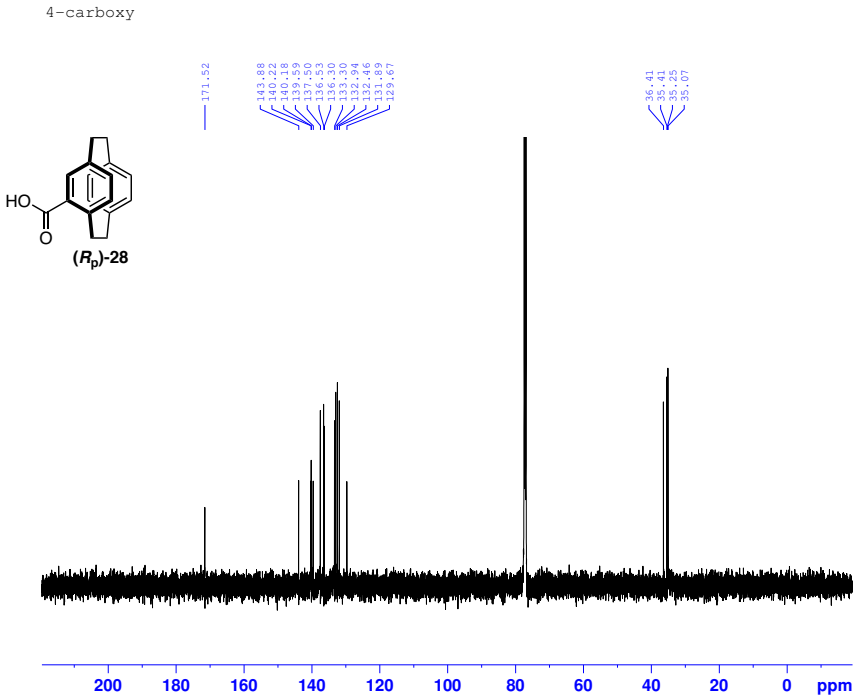

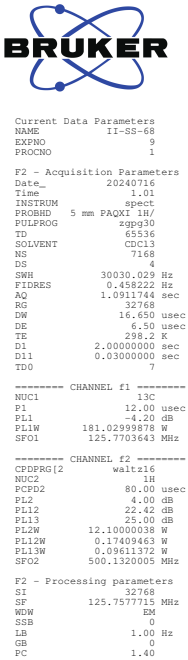

^{1}H NMR spectrum of (R_p)-**51** in $CDCl_3$

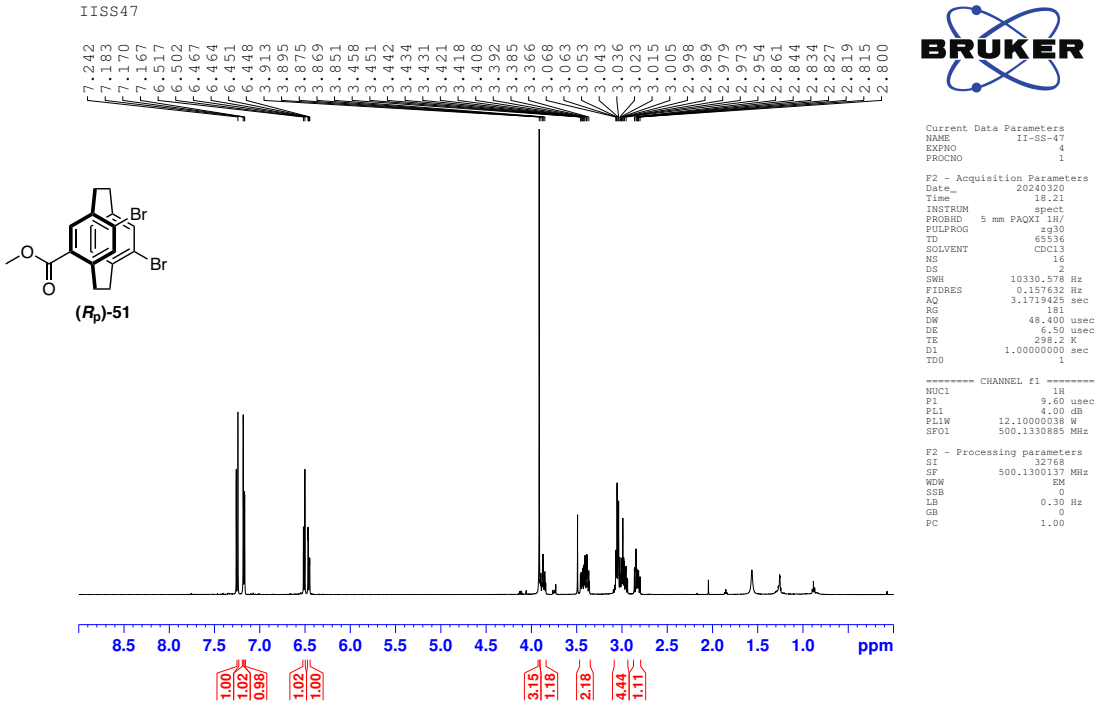

^{13}C NMR spectrum of (R_p)-**51** in $CDCl_3$

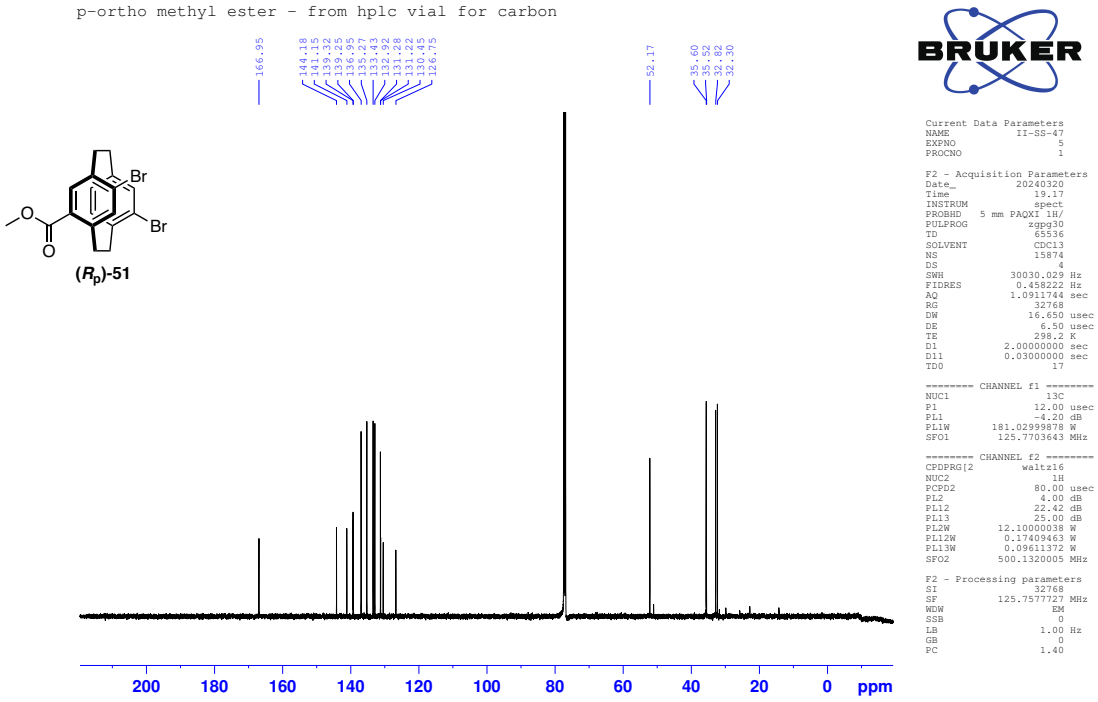

^{1}H NMR spectrum of (S_p)-**52** in $CDCl_3$

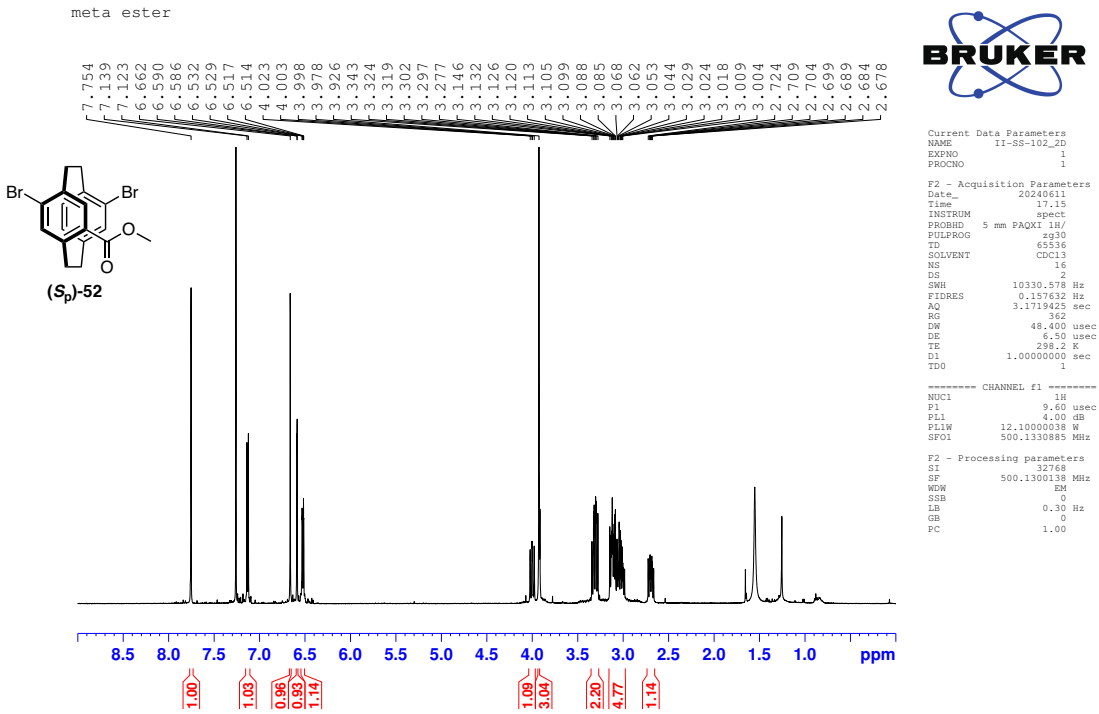

^{13}C NMR spectrum of (S_p)-**52** in $CDCl_3$

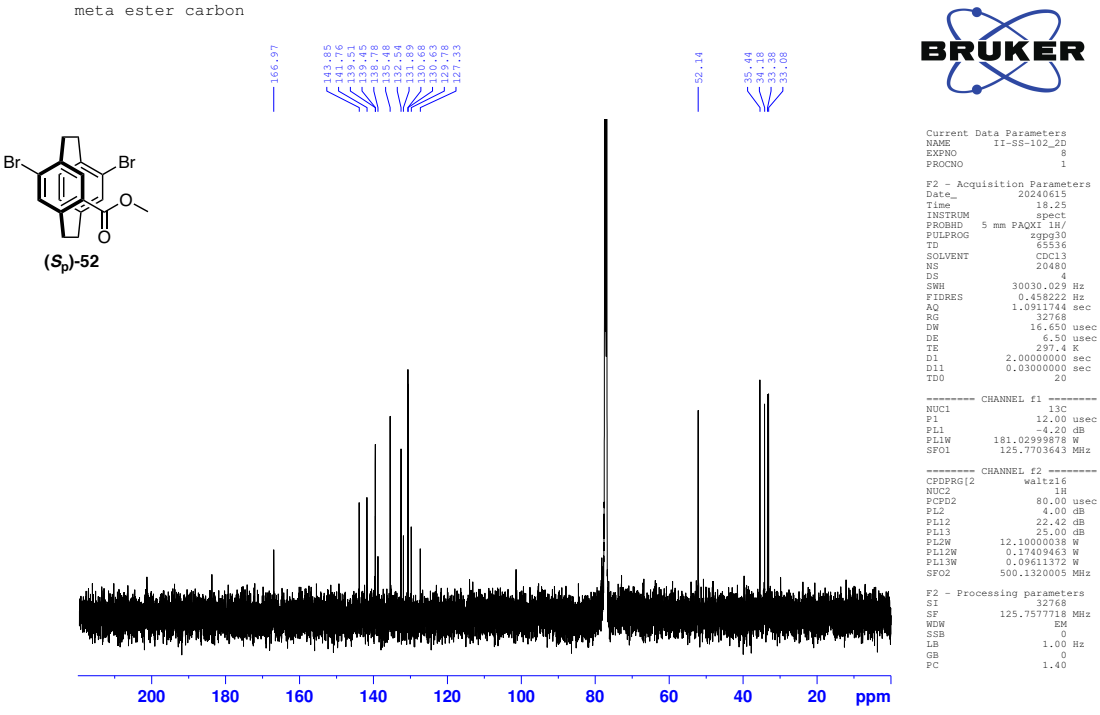

^{1}H NMR spectrum of (R_p)-**53** in $CDCl_3$

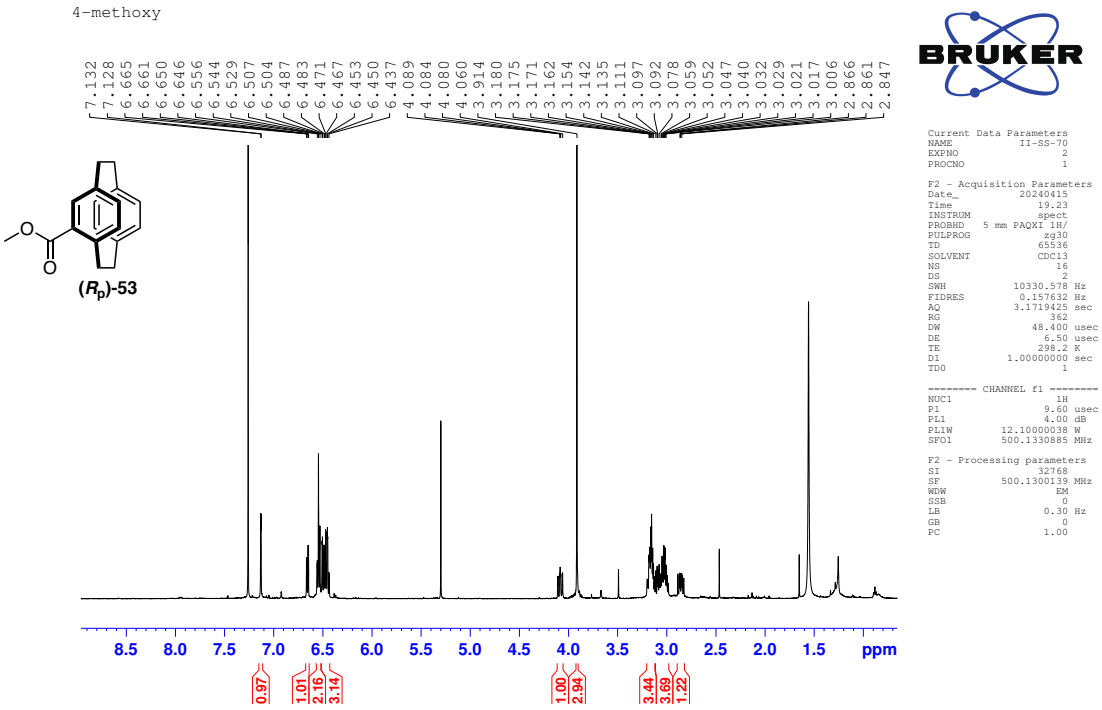

^{13}C NMR spectrum of (R_p)-**53** in $CDCl_3$

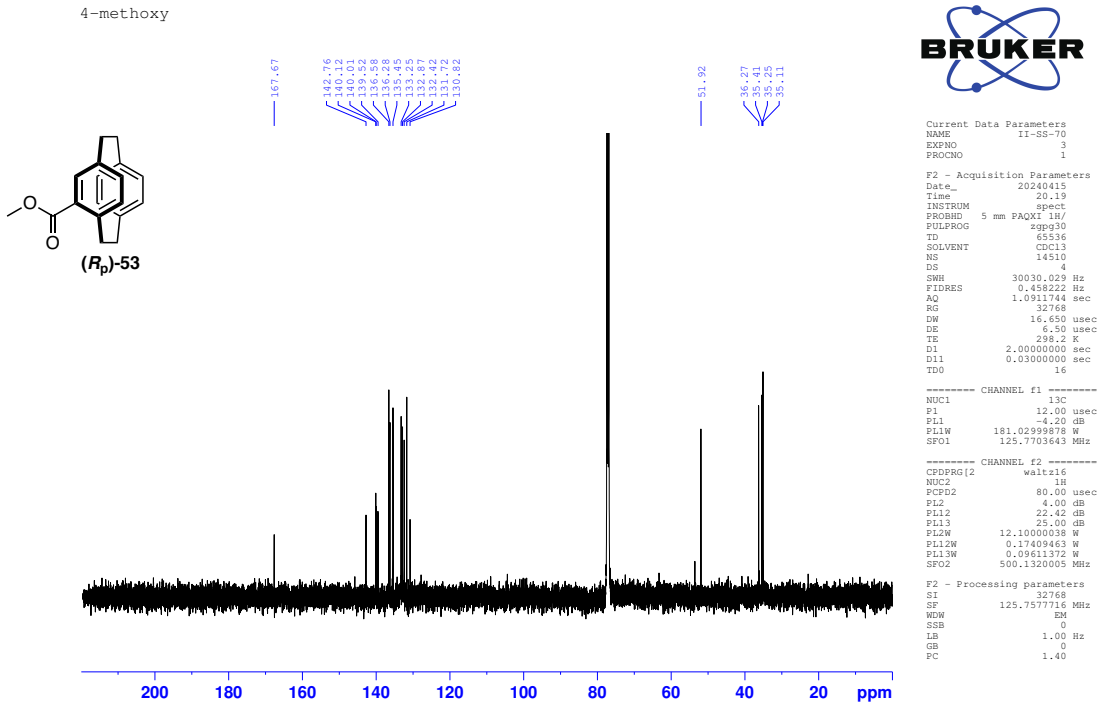

^{1}H NMR spectrum of (R_p)-**54** in $CDCl_3$

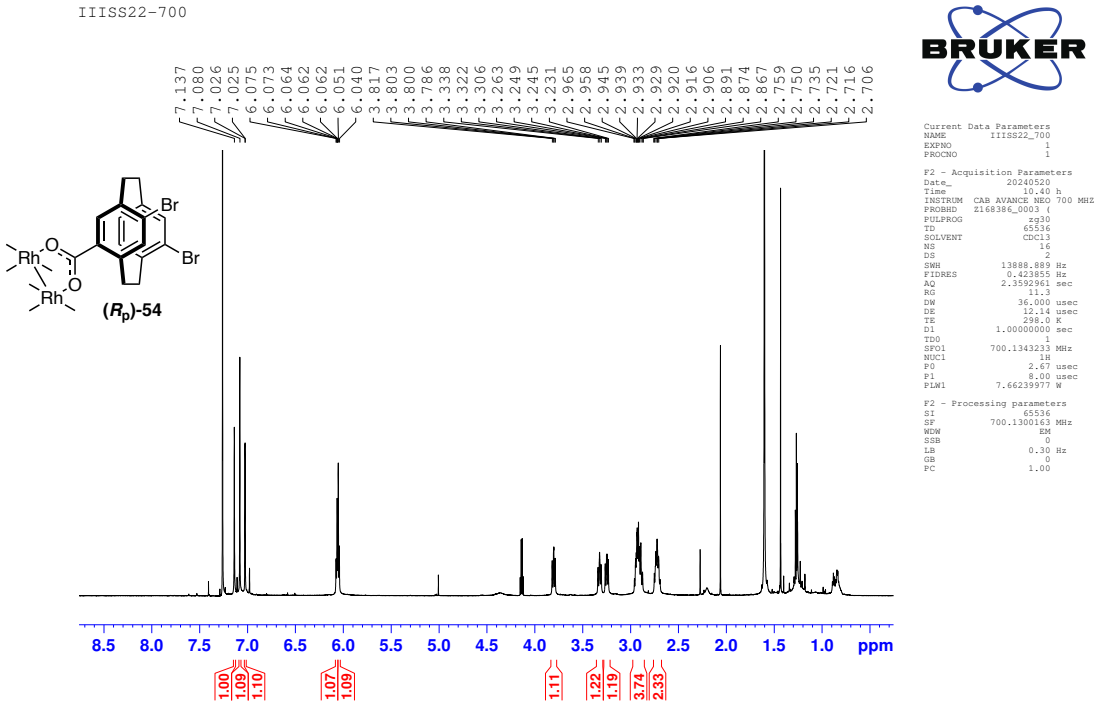

^{13}C NMR spectrum of (R_p)-**54** in $CDCl_3$

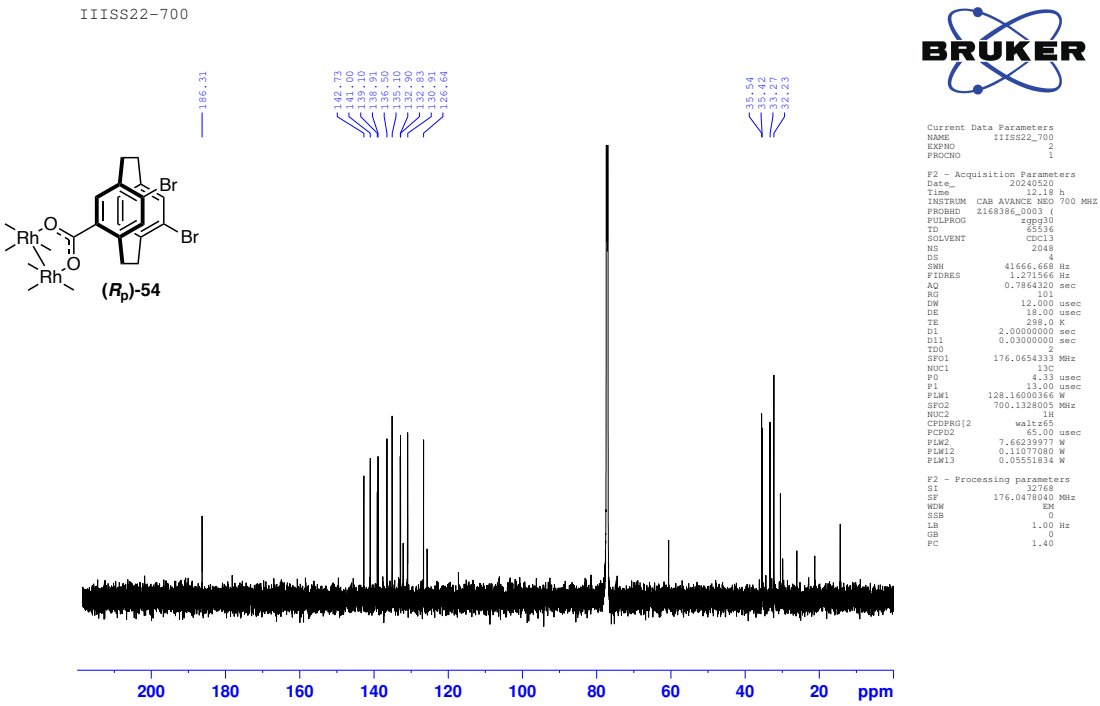

^{1}H NMR spectrum of (S_p)-**55** in $CDCl_3$

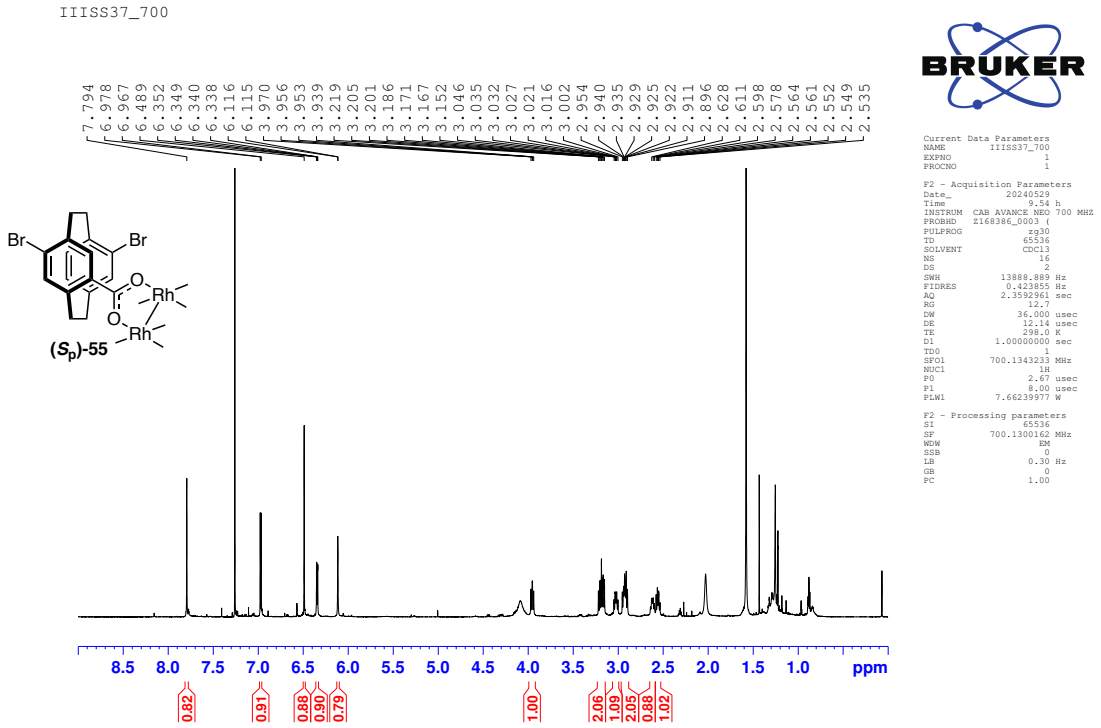

^{13}C NMR spectrum of (S_p)-**55** in $CDCl_3$

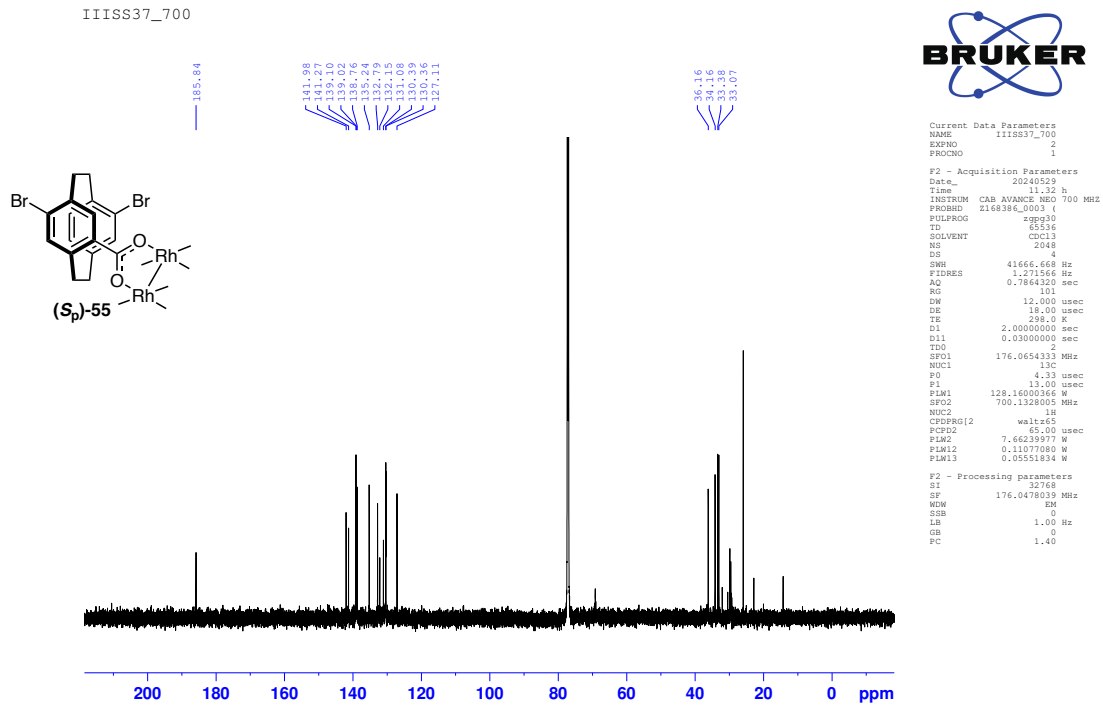

^{1}H NMR spectrum of (R_p)-**56** in $CDCl_3$

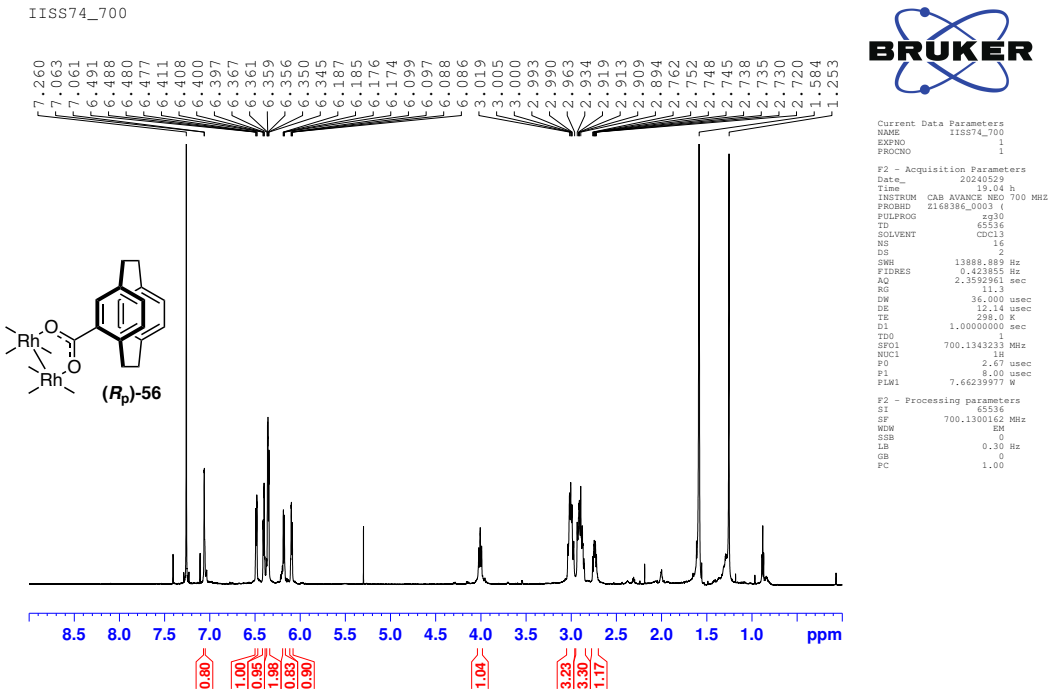

^{12}C NMR spectrum of (R_p)-**56** in $CDCl_3$

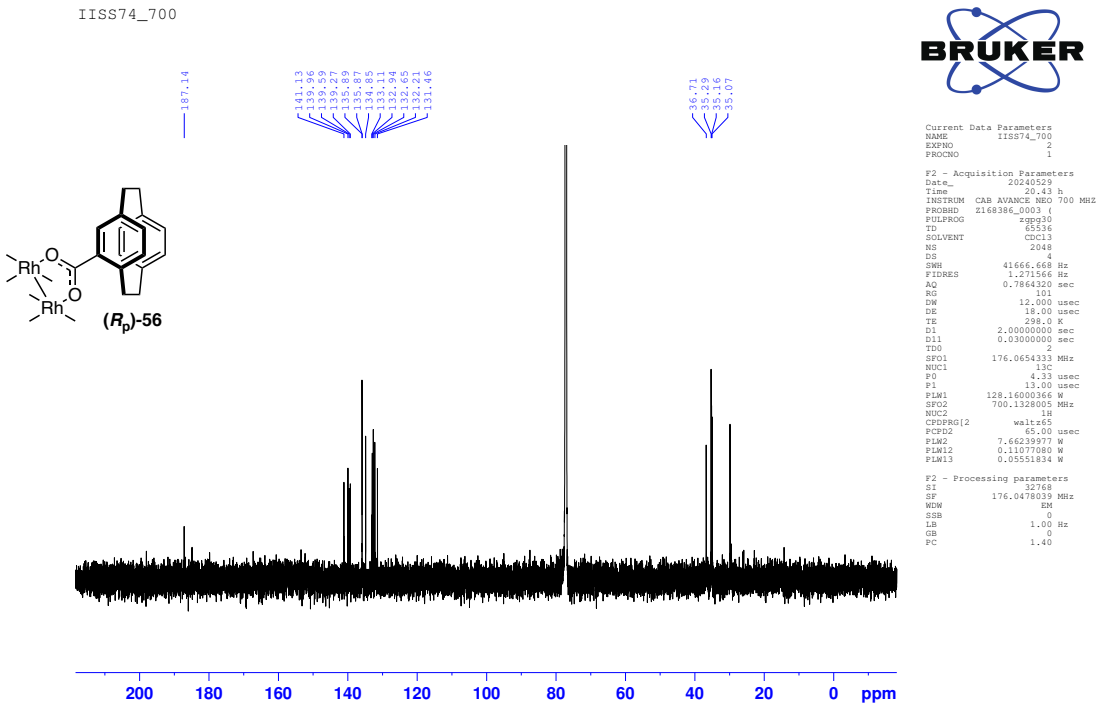

^{1}H NMR spectrum of (R_p)-**58** in $CDCl_3$

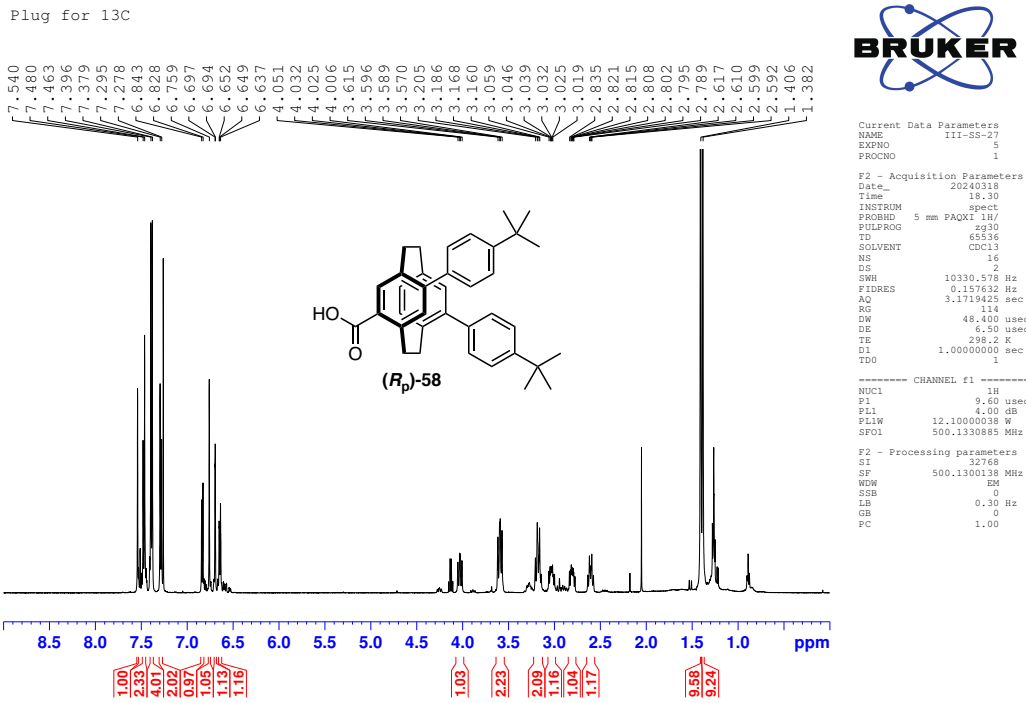

^{13}C NMR spectrum of (R_p)-**58** in $CDCl_3$

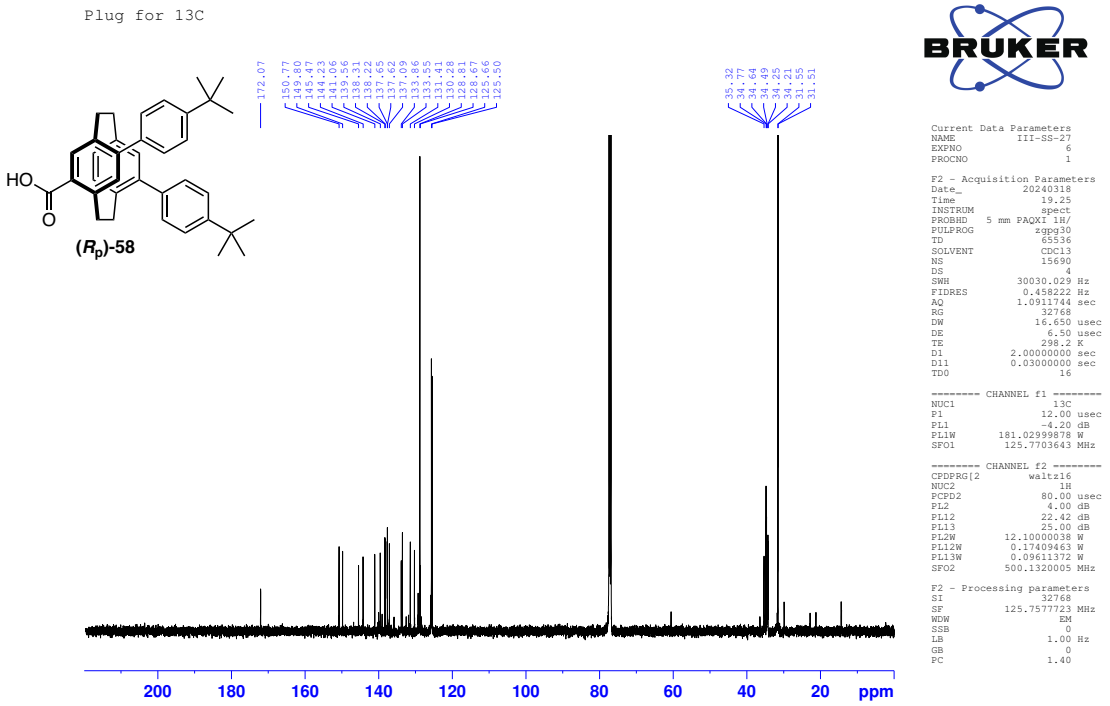

^{1}H NMR spectrum of (R_p)-**57** in $CDCl_3$

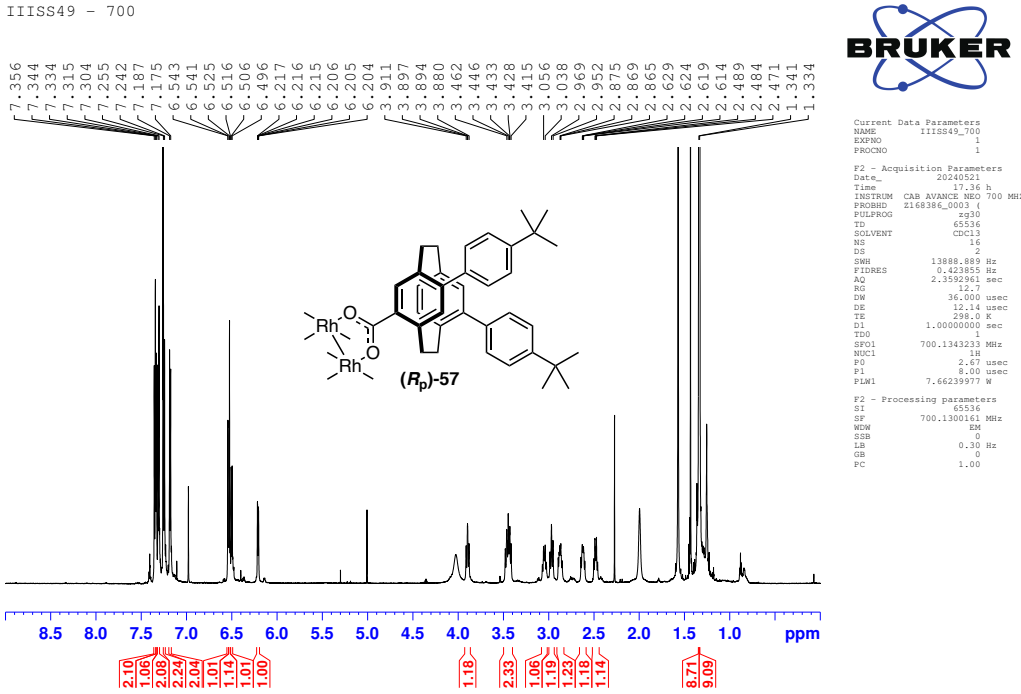

^{13}C NMR spectrum of (R_p)-**57** in $CDCl_3$

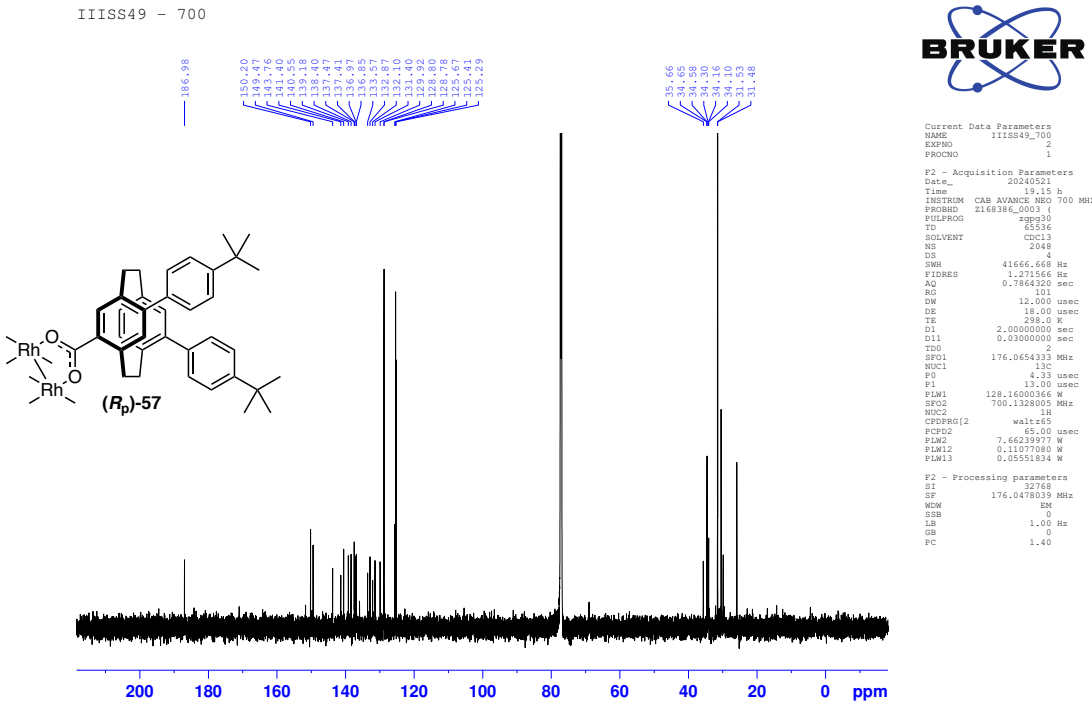

^{1}H NMR spectrum of (S_p)-**60** in $CDCl_3$

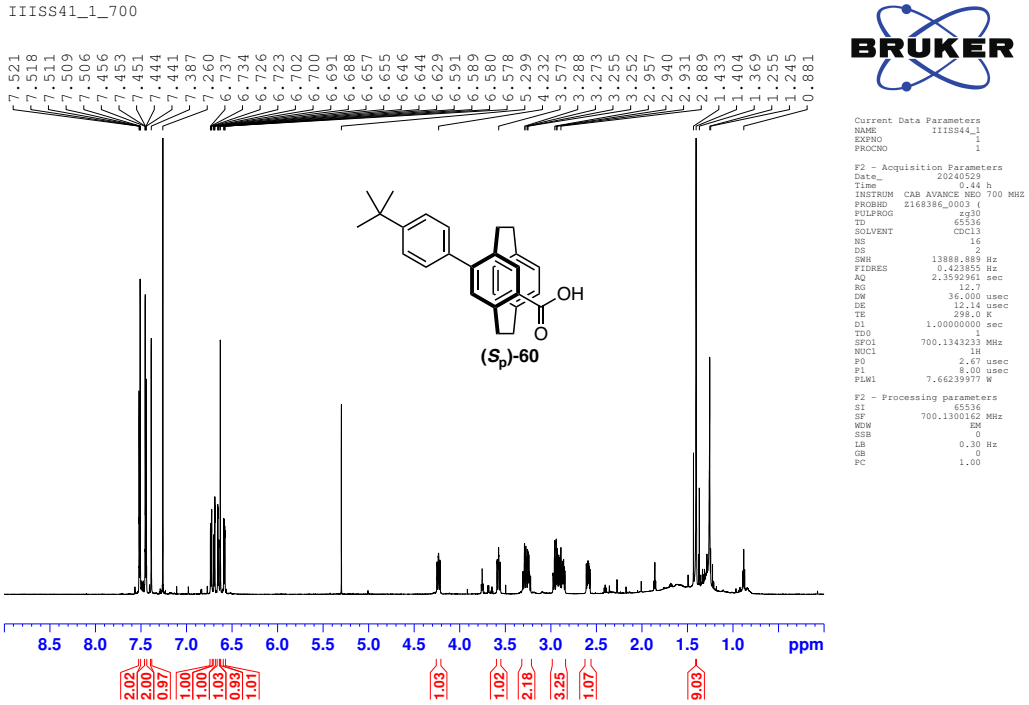

^{13}C NMR spectrum of (S_p)-**60** in $CDCl_3$

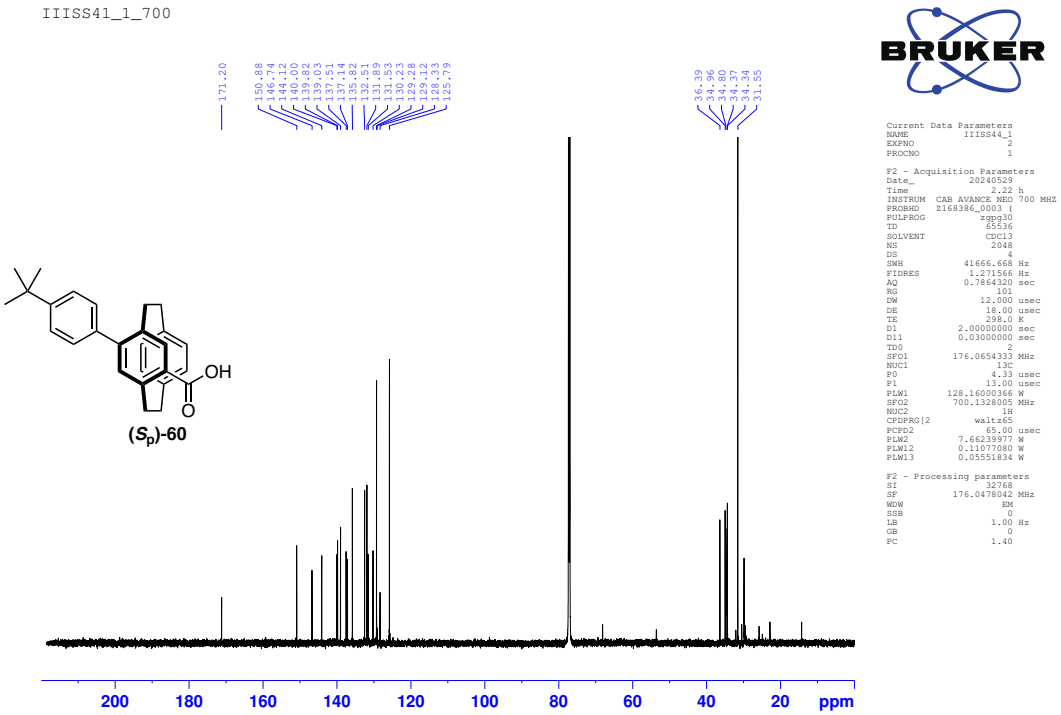

^{1}H NMR spectrum of (S_p)-**61** in $CDCl_3$

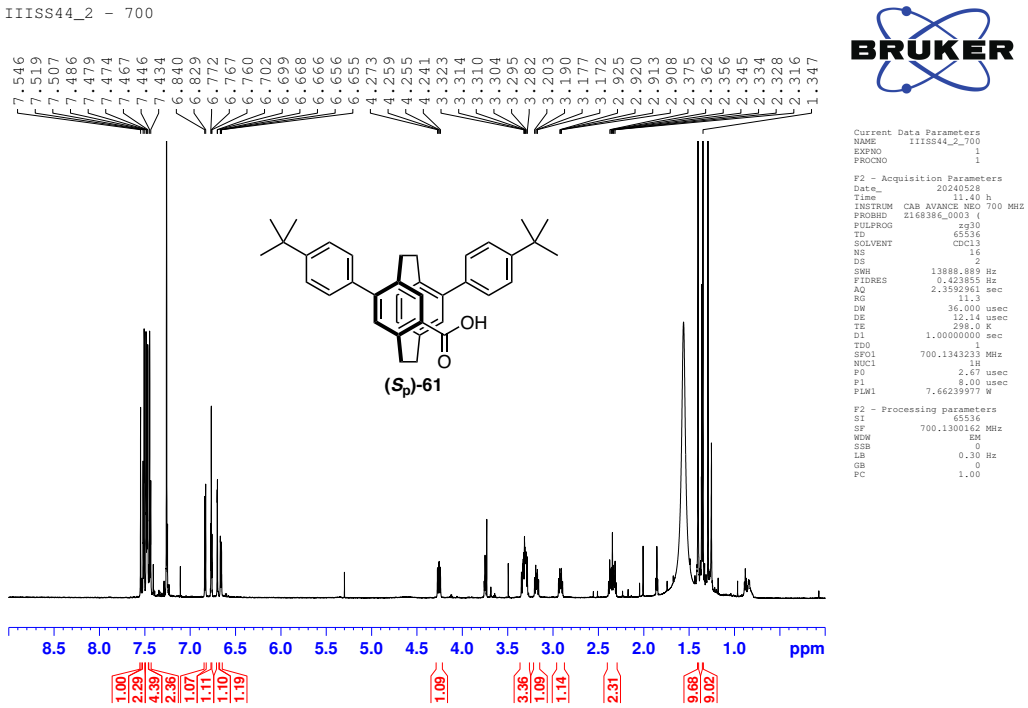

^{13}C NMR spectrum of (S_p)-**61** in $CDCl_3$

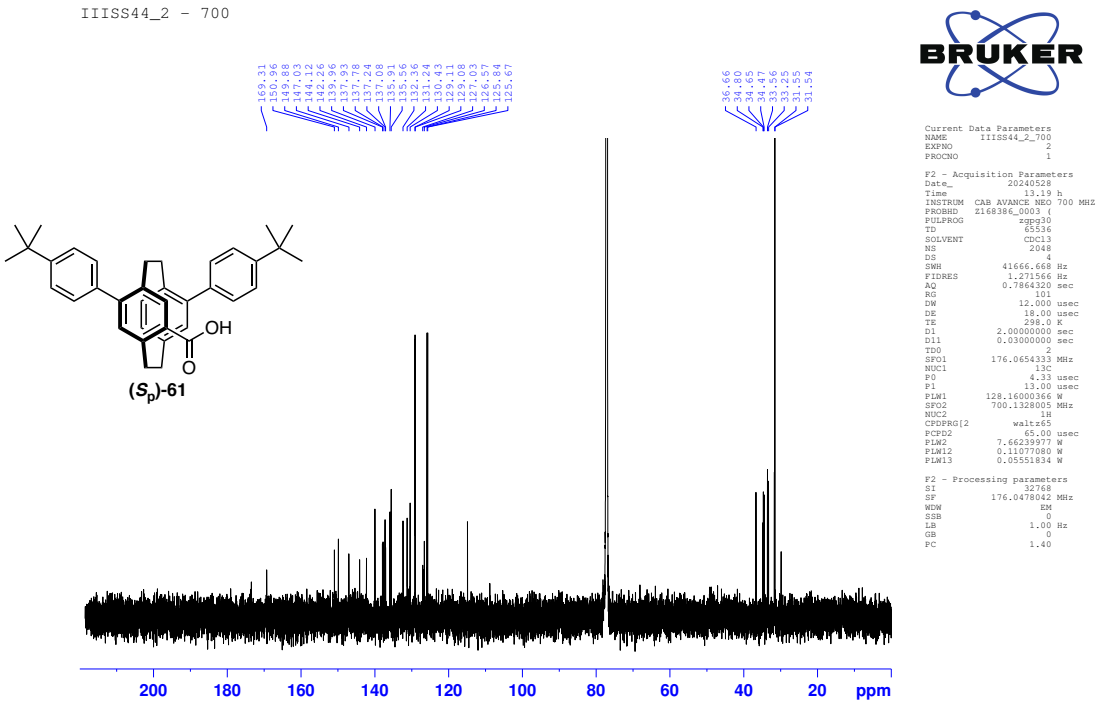

^{1}H NMR spectrum of (S_p)-**62** in $CDCl_3$

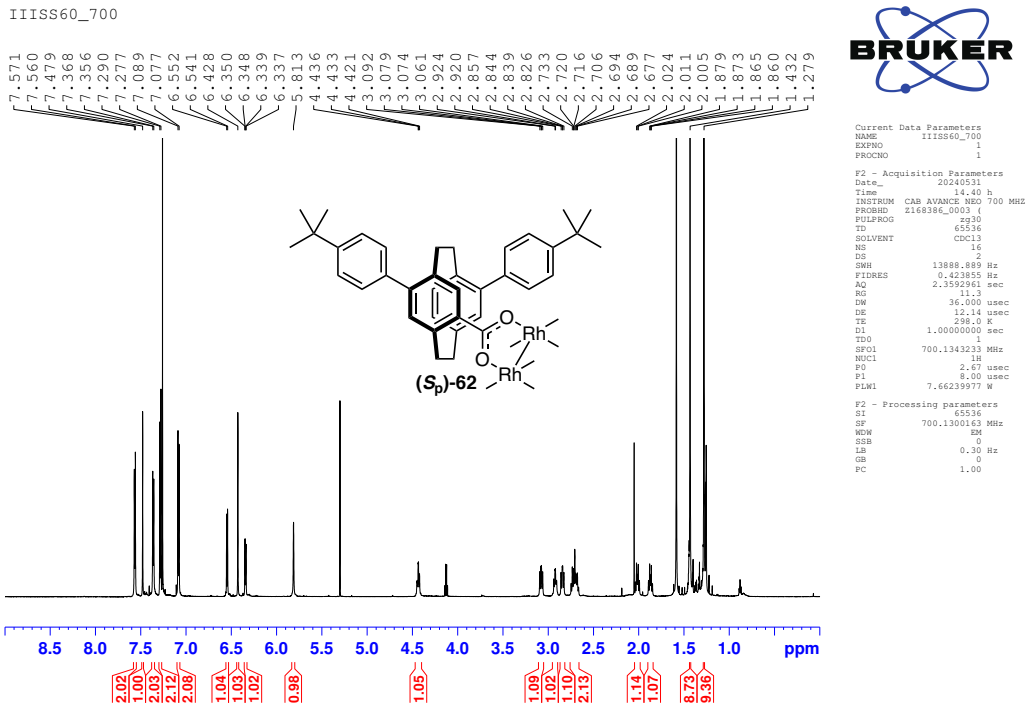

^{13}C NMR spectrum of (S_p)-**62** in $CDCl_3$

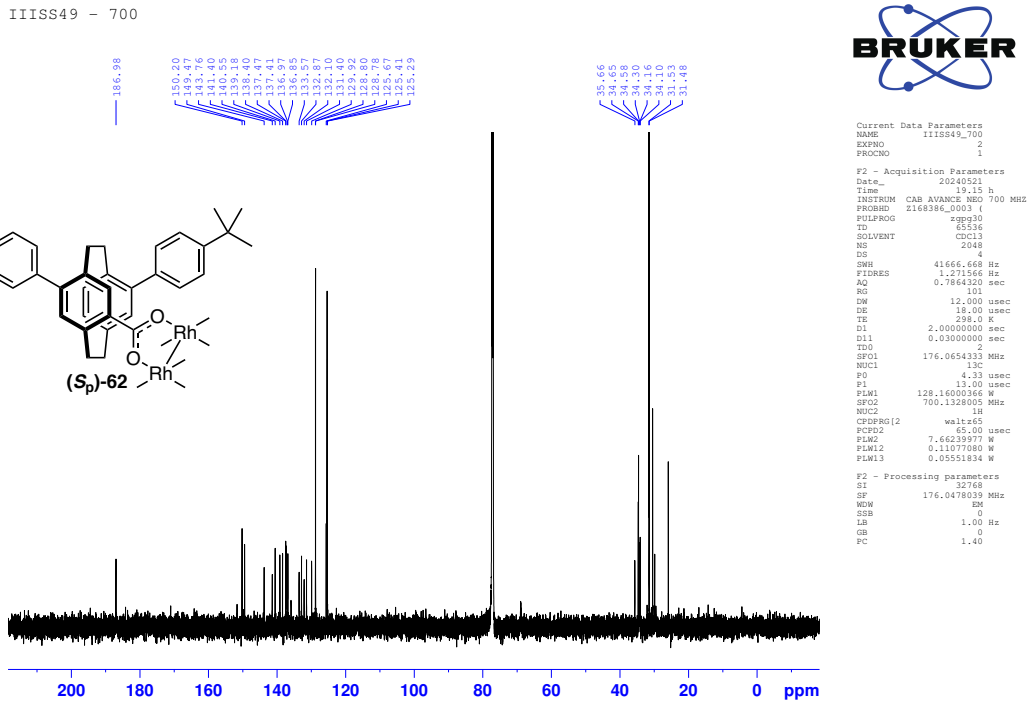

^{1}H NMR spectrum of (±)-**16a** in $CDCl_3$

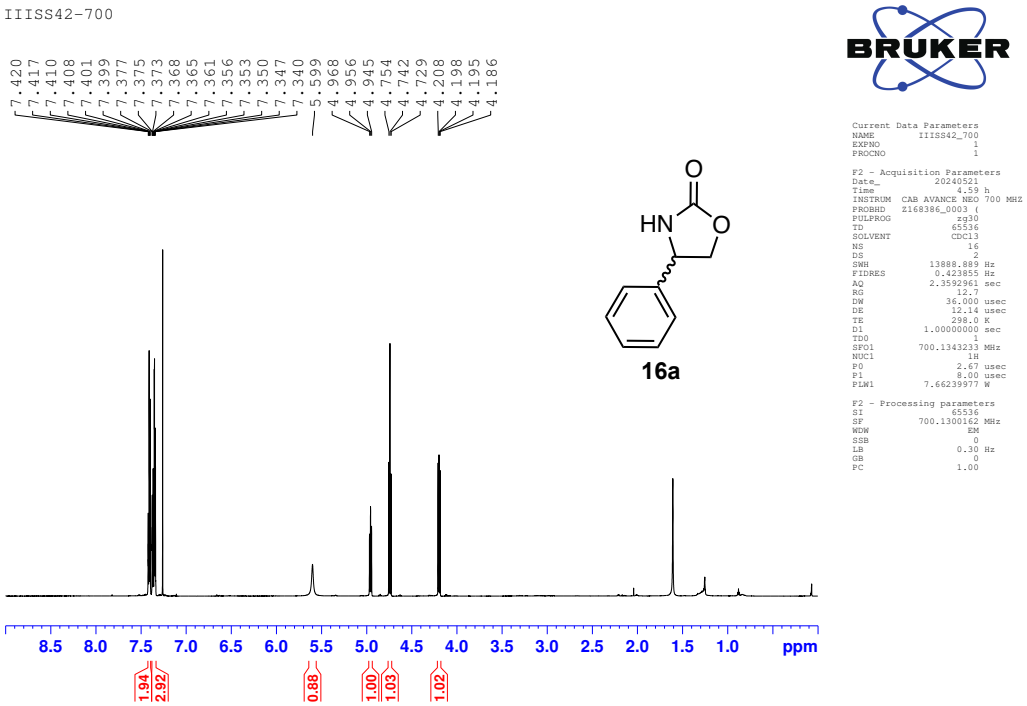

Current Data Parameters
NAME IIISS42_700
EXPNO 1
PROCNO 1

F2 - Acquisition Parameters
Date_ 20240521
Time 4.59 h
INSTRUM CAB AVANCE NEO 700 MHZ
PROBHD Z168386_0003 (
PULPROG zg30
TD 65536
SOLVENT CDCl3
NS 16
DS 2
SWH 13888.889 Hz
FIDRES 0.423855 Hz
AQ 2.3592961 sec
RG 12.7
DW 36.000 usec
DE 12.14 usec
TE 298.0 K
D1 1.00000000 sec
TD0 1
SFO1 700.1343233 MHz
NUC1 1H
P0 2.67 usec
P1 8.00 usec
PLW1 7.66239977 W

F2 - Processing parameters
SI 65536
SF 700.1300162 MHz
WDW EM
SSB 0
LB 0.30 Hz
GB 0
PC 1.00

^{13}C NMR spectrum of (±)-**16a** in $CDCl_3$

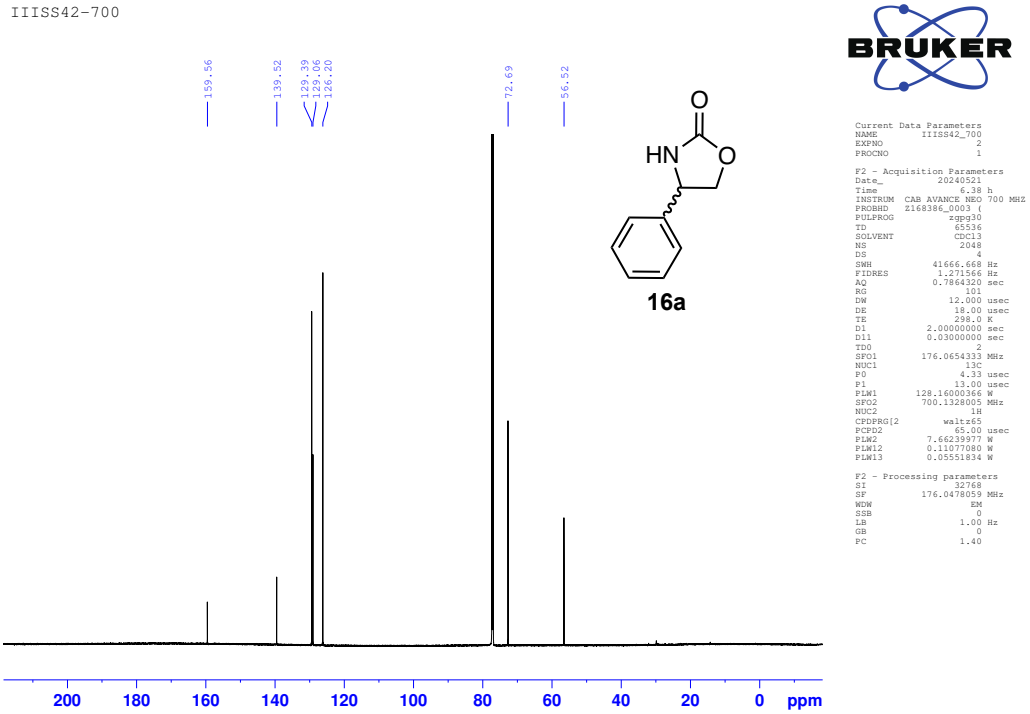

Current Data Parameters
NAME IIISS42_700
EXPNO 2
PROCNO 1

F2 - Acquisition Parameters
Date_ 20240521
Time 6.38 h
INSTRUM CAB AVANCE NEO 700 MHZ
PROBHD Z168386_0003 (
PULPROG zgpg30
TD 65536
SOLVENT CDCl3
NS 2048
DS 4
SWH 41666.668 Hz
FIDRES 1.271566 Hz
AQ 0.7864320 sec
RG 101
DW 12.000 usec
DE 18.00 usec
TE 298.0 K
D1 2.00000000 sec
D11 0.03000000 sec
TD0 2
SFO1 176.0654333 MHz
NUC1 13C
P0 4.33 usec
P1 13.00 usec
PLW1 128.16000366 W
SFO2 700.1328005 MHz
NUC2 1H
CPDPRG[2 waltz65
PCPD2 65.00 usec
PLW2 7.66239977 W
PLW12 0.11077080 W
PLW13 0.05551834 W

F2 - Processing parameters
SI 32768
SF 176.0478059 MHz
WDW EM
SSB 0
LB 1.00 Hz
GB 0
PC 1.40

^{1}H NMR spectrum of (±)-**19b** in $CDCl_3$

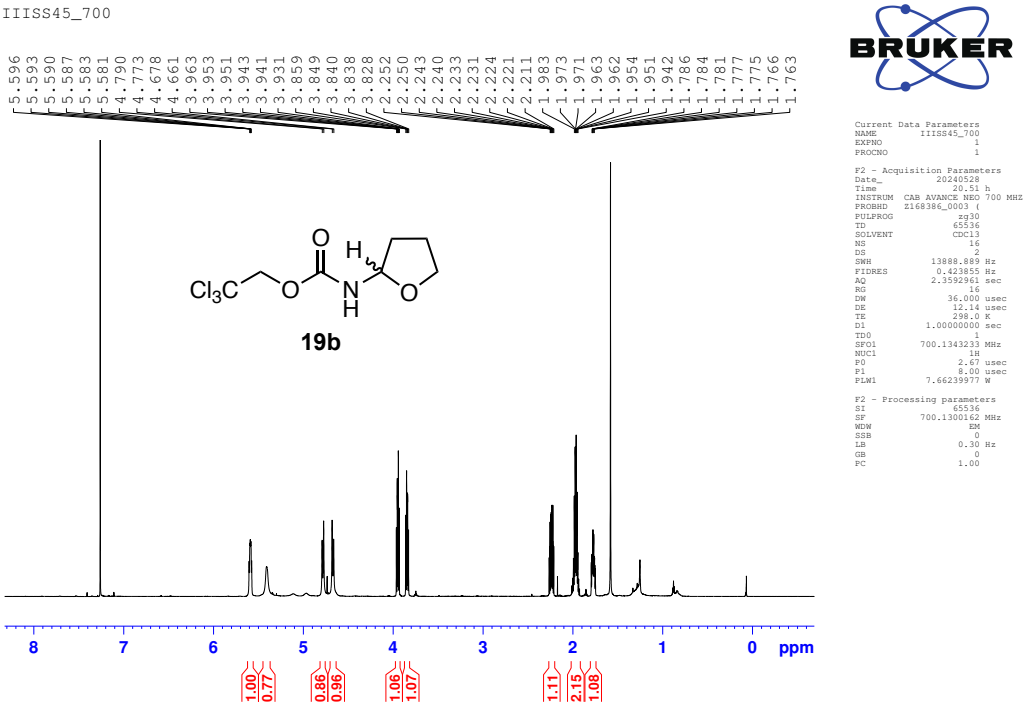

^{13}C NMR spectrum of (±)-**19b** in $CDCl_3$

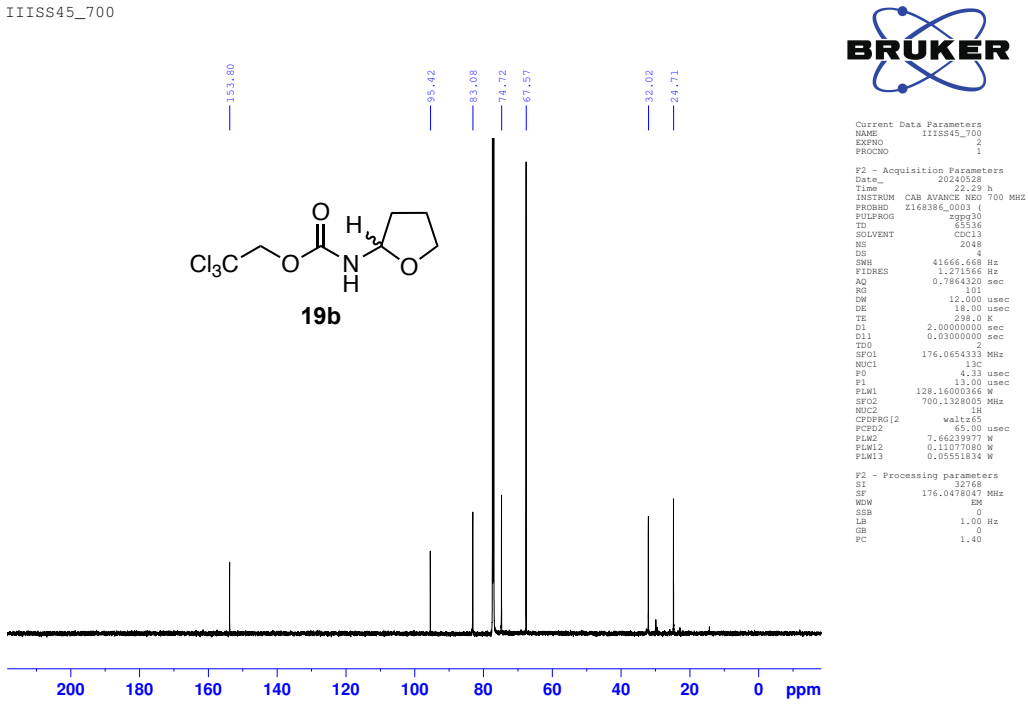

HPLC chromatogram of (±)-**51**

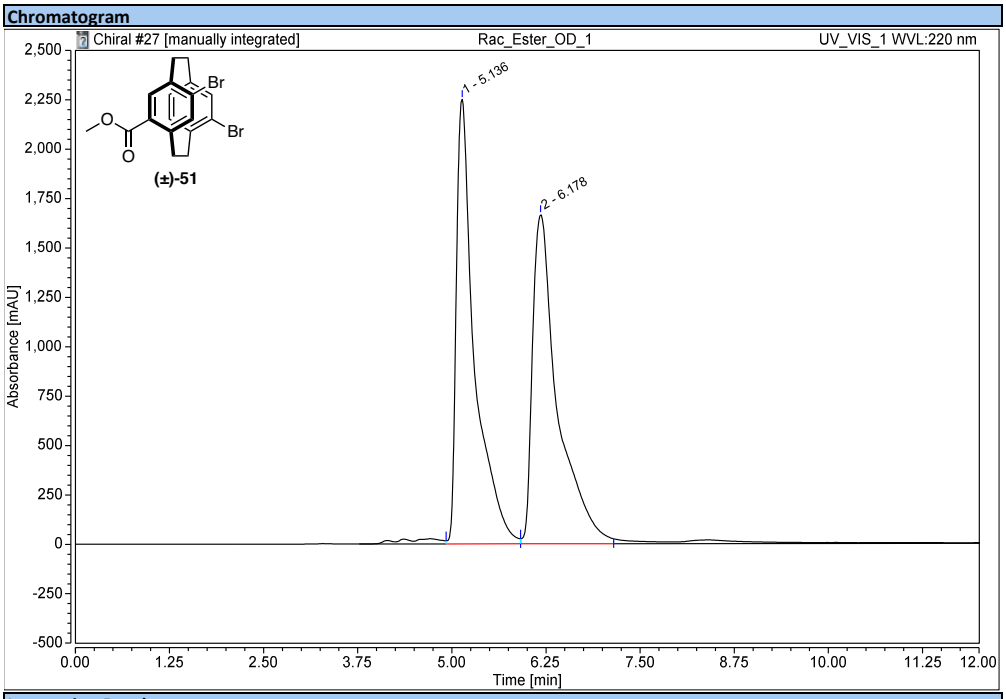

Integration Results

No.	Peak Name	Retention Time min	Area mAU*min	Height mAU	Relative Area %	Relative Height %	Amount n.a.
1		5.136	631.280	2249.923	49.64	57.45	n.a.
2		6.178	640.527	1666.596	50.36	42.55	n.a.
Total:			**1271.807**	**3916.519**	**100.00**	**100.00**	

HPLC chromatogram of (R_p)-**51**

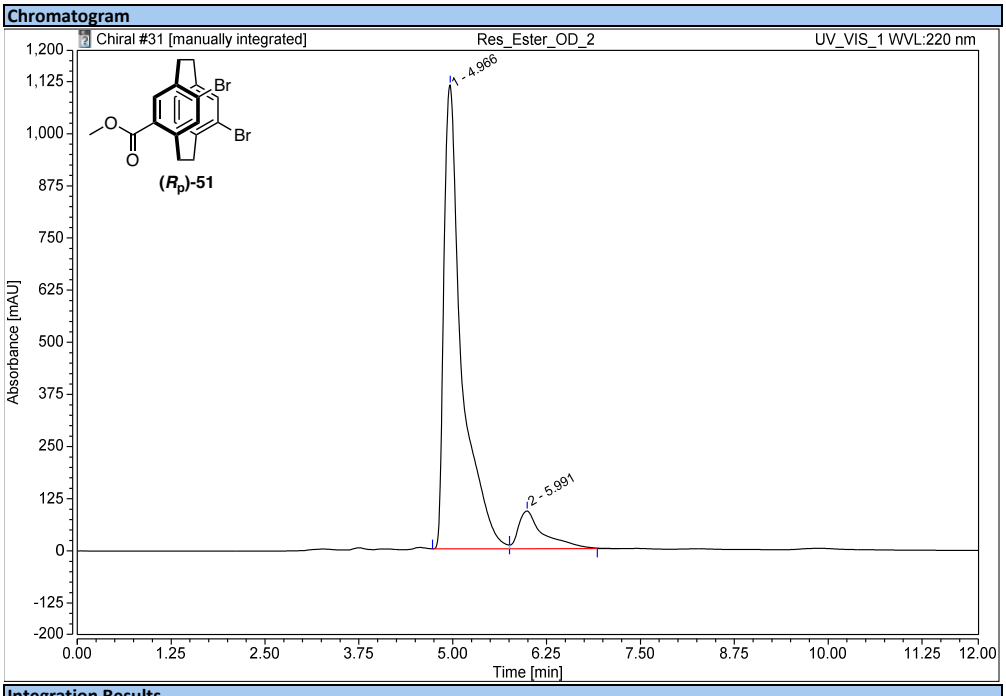

Integration Results

No.	Peak Name	Retention Time min	Area mAU*min	Height mAU	Relative Area %	Relative Height %	Amount n.a.
1		4.966	305.739	1111.713	89.73	92.47	n.a.
2		5.991	35.007	90.541	10.27	7.53	n.a.
Total:			**340.747**	**1202.254**	**100.00**	**100.00**	

HPLC chromatogram of (±)-**52**

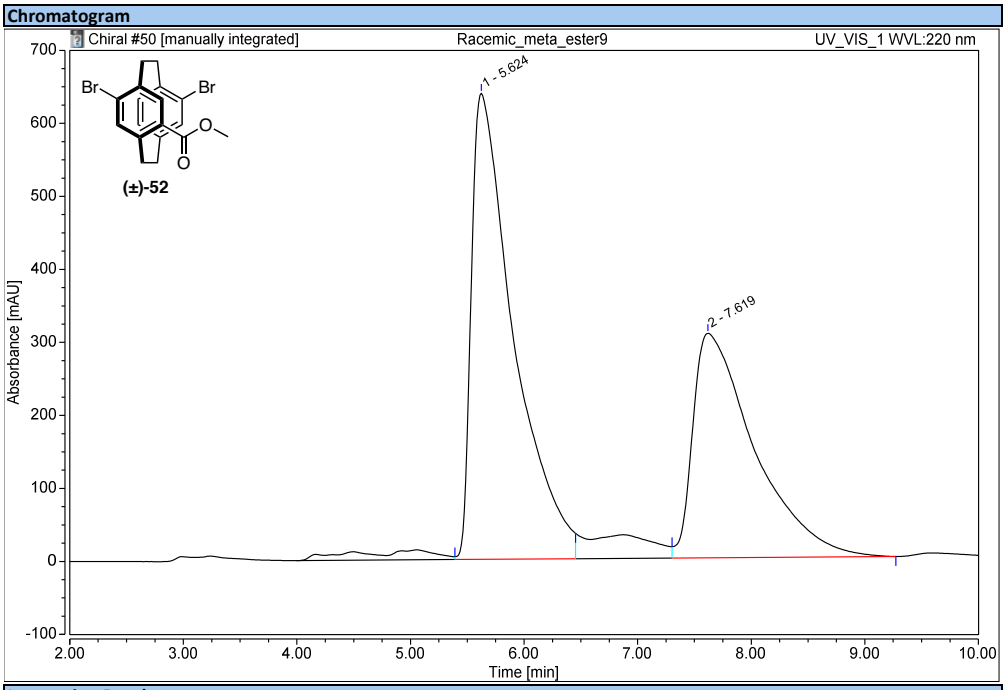

Integration Results

No.	Peak Name	Retention Time min	Area mAU*min	Height mAU	Relative Area %	Relative Height %	Amount n.a.
1		5.624	273.514	638.394	58.70	67.48	n.a.
2		7.619	192.472	307.585	41.30	32.52	n.a.
Total:			**465.985**	**945.979**	**100.00**	**100.00**	

HPLC chromatogram of (S_p)-**52**

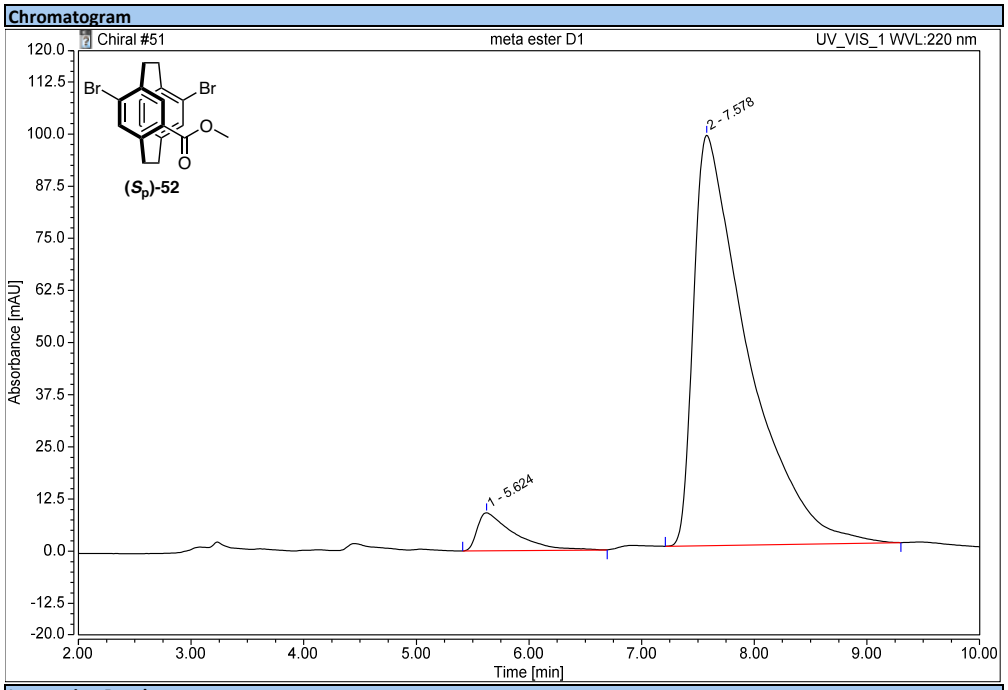

Integration Results

No.	Peak Name	Retention Time min	Area mAU*min	Height mAU	Relative Area %	Relative Height %	Amount n.a.
1		5.624	3.412	9.134	5.90	8.49	n.a.
2		7.578	54.399	98.393	94.10	91.51	n.a.
Total:			**57.811**	**107.527**	**100.00**	**100.00**	

HPLC chromatogram of (±)-**53**

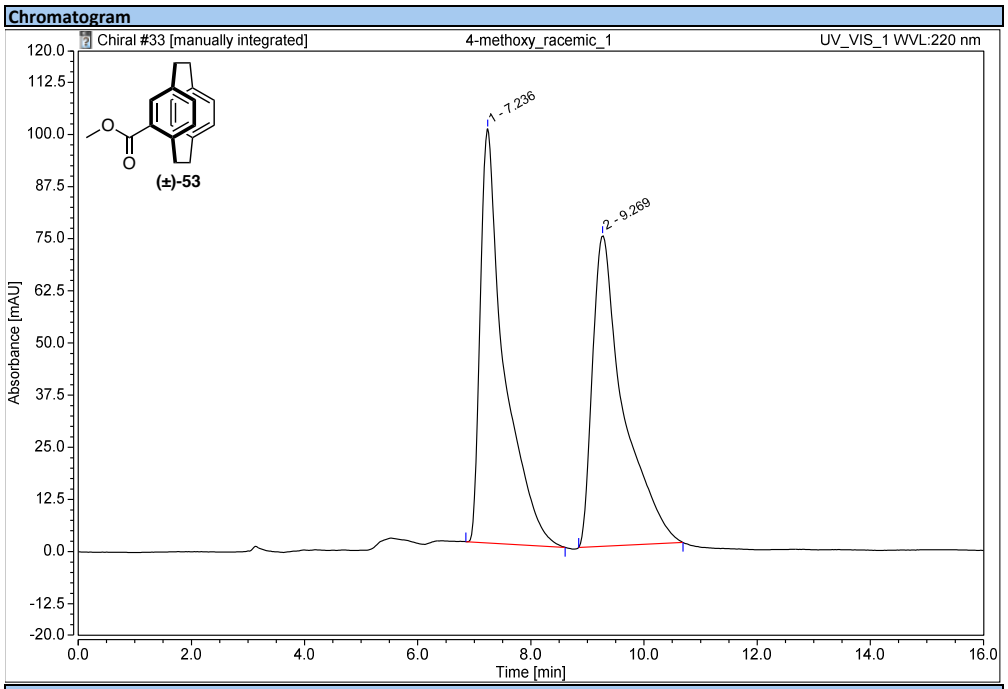

Integration Results

No.	Peak Name	Retention Time min	Area mAU*min	Height mAU	Relative Area %	Relative Height %	Amount n.a.
1		7.236	48.291	99.305	50.66	57.13	n.a.
2		9.269	47.040	74.513	49.34	42.87	n.a.
Total:			**95.331**	**173.818**	**100.00**	**100.00**	

HPLC chromatogram of (R_p)-**53**

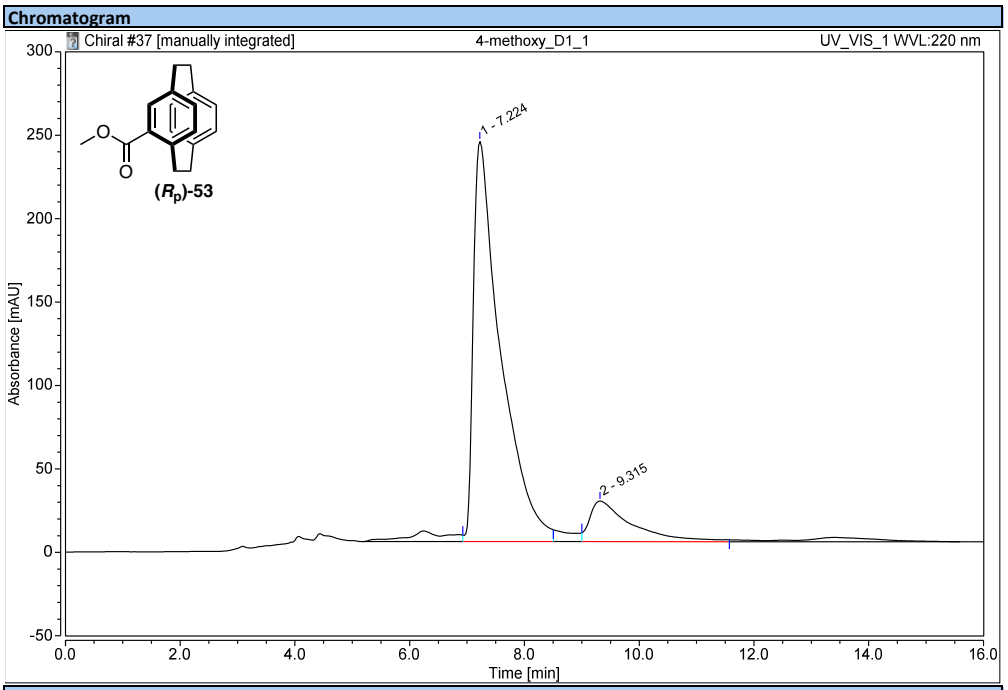

Integration Results

No.	Peak Name	Retention Time min	Area mAU*min	Height mAU	Relative Area %	Relative Height %	Amount n.a.
1		7.224	131.731	239.832	86.54	90.80	n.a.
2		9.315	20.495	24.300	13.46	9.20	n.a.
Total:			**152.226**	**264.133**	**100.00**	**100.00**	

HPLC chromatogram of **16a**, entry 1

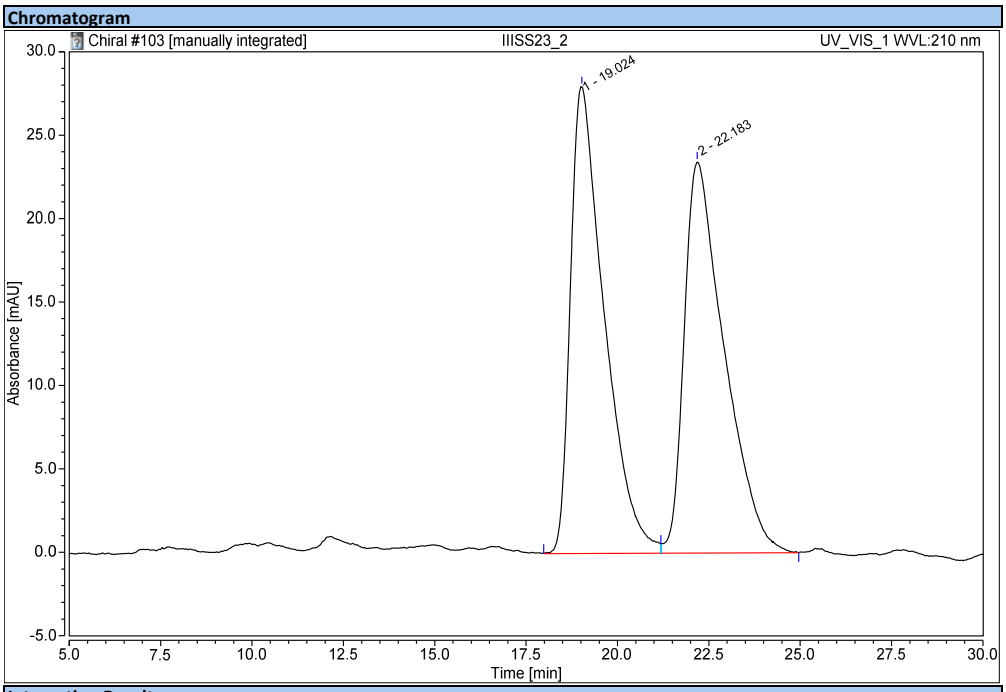

Integration Results

No.	Peak Name	Retention Time min	Area mAU*min	Height mAU	Relative Area %	Relative Height %	Amount n.a.
1		19.024	30.003	28.016	50.19	54.40	n.a.
2		22.183	29.777	23.481	49.81	45.60	n.a.
Total:			**59.780**	**51.497**	**100.00**	**100.00**	

HPLC chromatogram of **16a**, entry 2

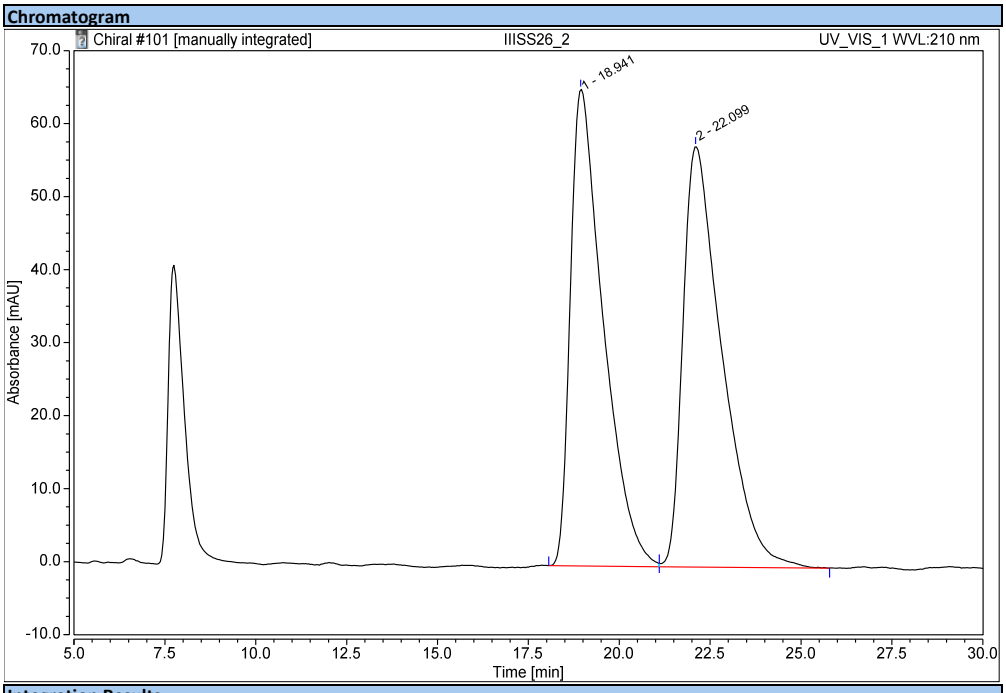

Integration Results

No.	Peak Name	Retention Time min	Area mAU*min	Height mAU	Relative Area %	Relative Height %	Amount n.a.
1		18.941	68.517	65.344	48.87	53.13	n.a.
2		22.099	71.692	57.638	51.13	46.87	n.a.
Total:			**140.210**	**122.982**	**100.00**	**100.00**	

HPLC chromatogram of **16a**, entry 3

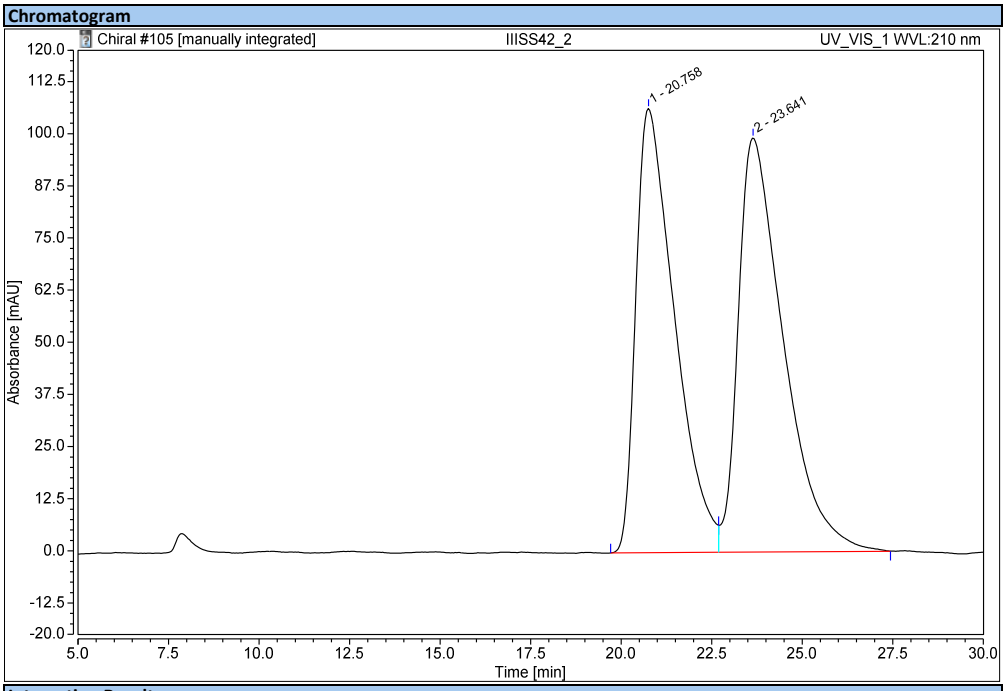

Integration Results

No.	Peak Name	Retention Time min	Area mAU*min	Height mAU	Relative Area %	Relative Height %	Amount n.a.
1		20.758	131.764	106.491	47.86	51.75	n.a.
2		23.641	143.537	99.276	52.14	48.25	n.a.
Total:			**275.301**	**205.767**	**100.00**	**100.00**	

HPLC chromatogram of **16a**, entry 4

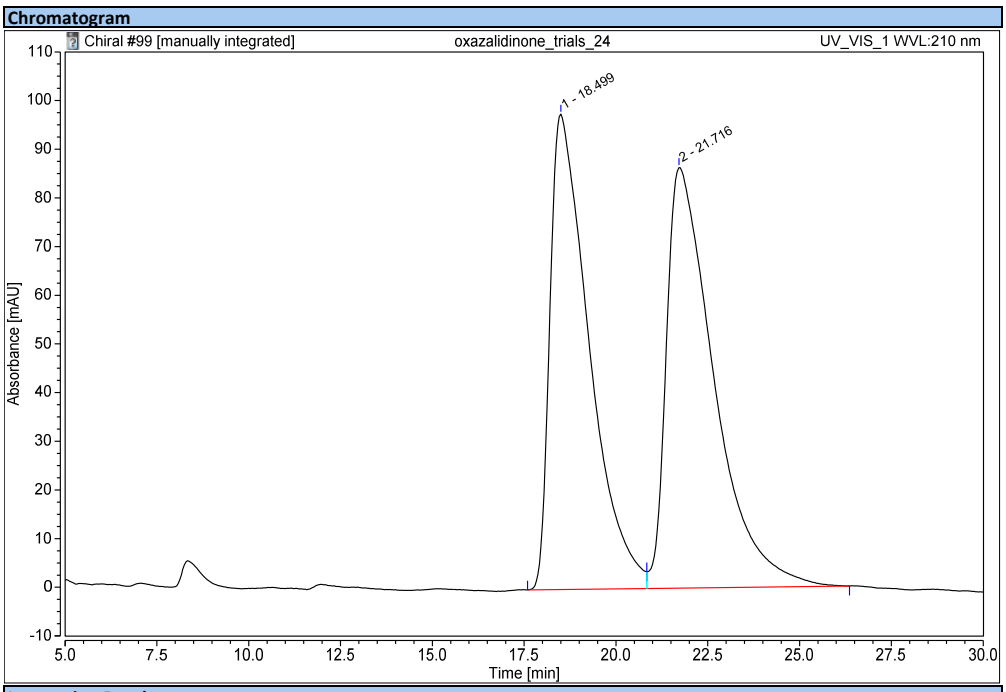

Integration Results

No.	Peak Name	Retention Time min	Area mAU*min	Height mAU	Relative Area %	Relative Height %	Amount n.a.
1		18.499	120.450	97.672	48.18	53.05	n.a.
2		21.716	129.535	86.448	51.82	46.95	n.a.
Total:			**249.985**	**184.120**	**100.00**	**100.00**	

HPLC chromatogram of **16a**, entry 5

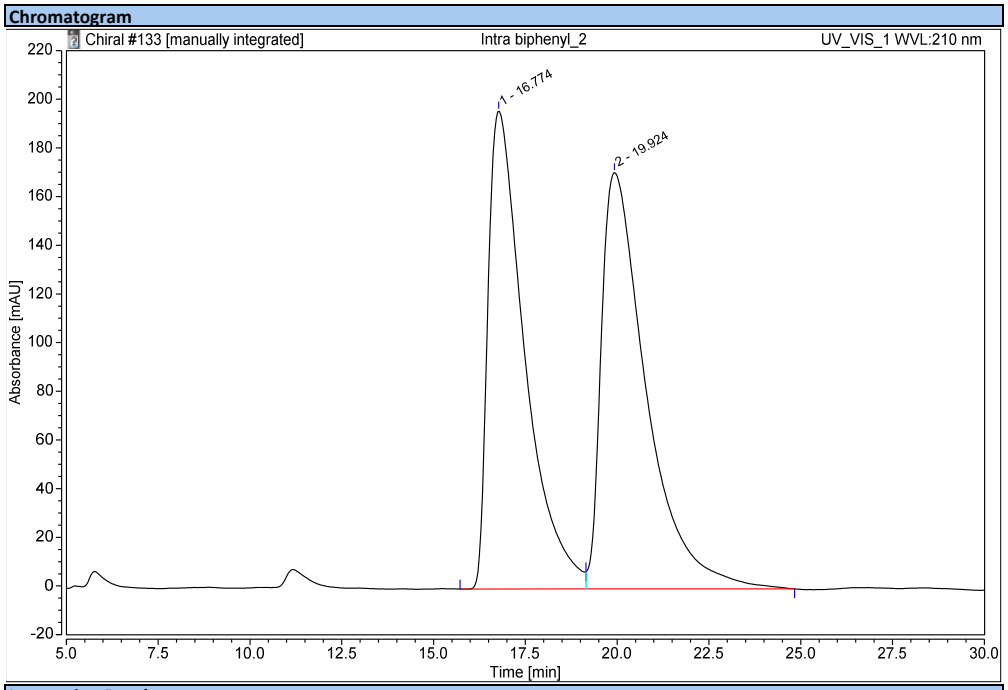

Integration Results

No.	Peak Name	Retention Time min	Area mAU*min	Height mAU	Relative Area %	Relative Height %	Amount n.a.
1		16.774	227.955	196.471	48.41	53.45	n.a.
2		19.924	242.891	171.138	51.59	46.55	n.a.
Total:			**470.846**	**367.609**	**100.00**	**100.00**	

HPLC chromatogram of (±)-**19b**, entry 6

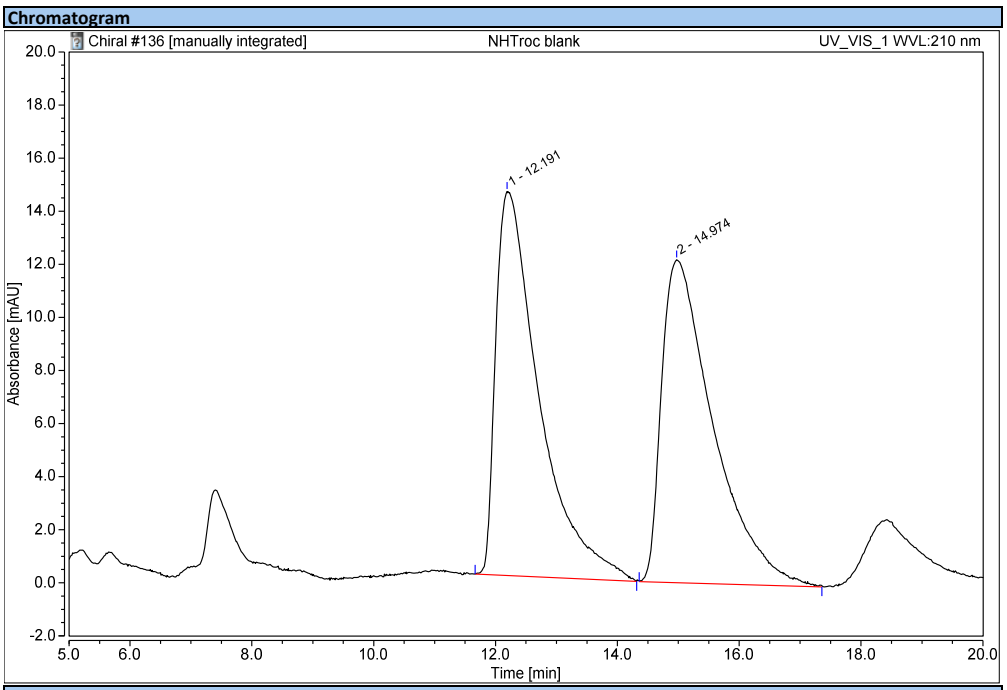

Integration Results

No.	Peak Name	Retention Time min	Area mAU*min	Height mAU	Relative Area %	Relative Height %	Amount n.a.
1		12.191	11.872	14.473	49.91	54.33	n.a.
2		14.974	11.914	12.165	50.09	45.67	n.a.
Total:			**23.786**	**26.637**	**100.00**	**100.00**	

HPLC chromatogram of **19b**, entry 7

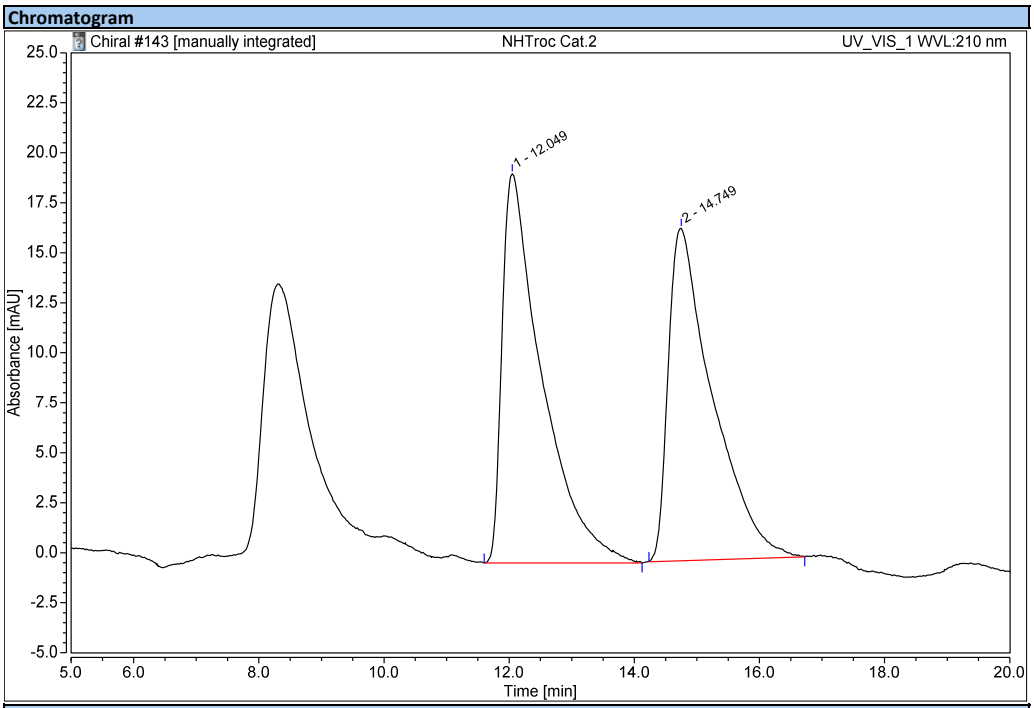

Integration Results

No.	Peak Name	Retention Time min	Area mAU*min	Height mAU	Relative Area %	Relative Height %	Amount n.a.
1		12.049	14.355	19.460	51.43	53.93	n.a.
2		14.749	13.554	16.621	48.57	46.07	n.a.
Total:			**27.909**	**36.081**	**100.00**	**100.00**	

HPLC chromatogram of **19b**, entry 8

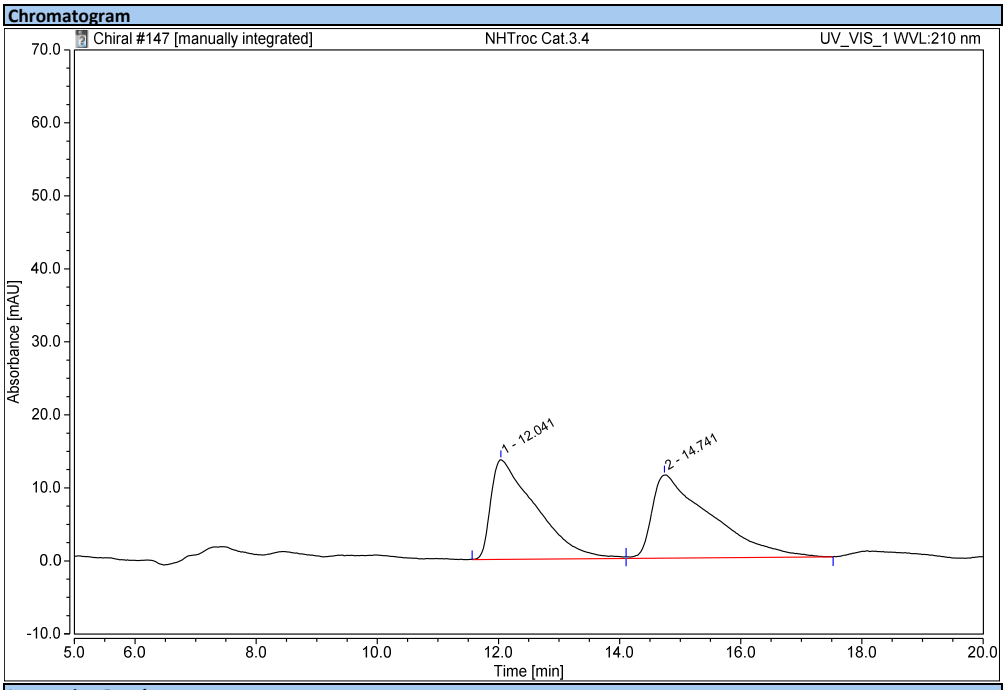

Integration Results

No.	Peak Name	Retention Time min	Area mAU*min	Height mAU	Relative Area %	Relative Height %	Amount n.a.
1		12.041	11.758	13.655	47.84	54.48	n.a.
2		14.741	12.822	11.410	52.16	45.52	n.a.
Total:			**24.580**	**25.065**	**100.00**	**100.00**	

HPLC chromatogram of **19b**, entry 9

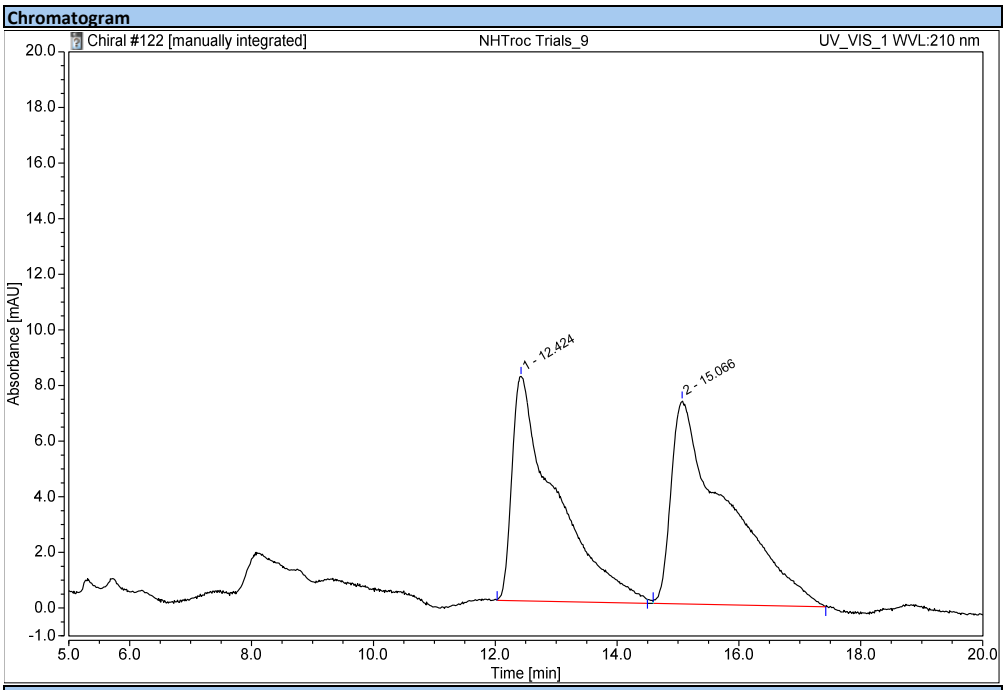

Integration Results

No.	Peak Name	Retention Time min	Area mAU*min	Height mAU	Relative Area %	Relative Height %	Amount n.a.
1		12.424	6.768	8.076	46.55	52.50	n.a.
2		15.066	7.773	7.306	53.45	47.50	n.a.
Total:			**14.542**	**15.382**	**100.00**	**100.00**	

HPLC chromatogram of **19b**, entry 10

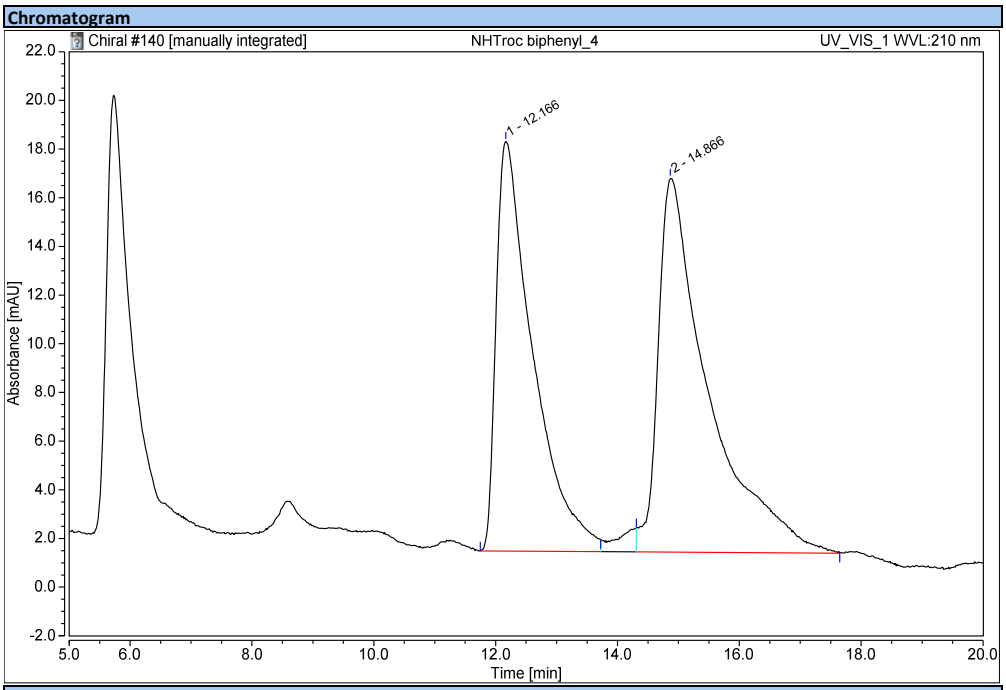

Integration Results

No.	Peak Name	Retention Time min	Area mAU*min	Height mAU	Relative Area %	Relative Height %	Amount n.a.
1		12.166	11.710	16.836	44.63	52.27	n.a.
2		14.866	14.528	15.373	55.37	47.73	n.a.
Total:			**26.238**	**32.208**	**100.00**	**100.00**	

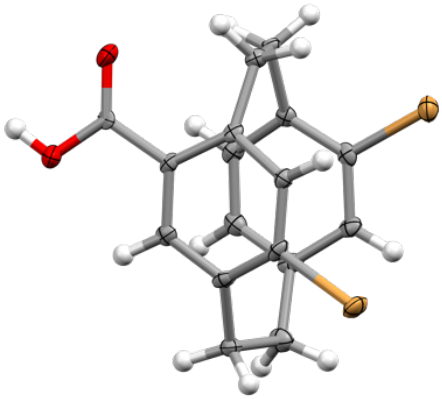

Crystal Data for $C_{17}H_{14}Br_2O_2$ (M =410.10 g/mol): monoclinic, space group $P2_1/c$ (no. 14), a = 7.4319(2) Å, b = 23.3813(8) Å, c = 8.8999(3) Å, β = 108.7890(10)°, V = 1464.10(8) Å^3, $Z(Z')$ = 4(1), T = 100.00 K, μ(CuKα) = 7.034 mm^{-1}, ϱ_{calc} = 1.860 g/cm^3, 16772 reflections measured (7.562° ≤ 2Θ ≤ 144.228°), 2854 unique (R_{int} = 0.0421, R_{sigma} = 0.0295) which were used in all calculations. The final R_1 was 0.0430 (I > 2σ(I)) and wR_2 was 0.0945 (all data).

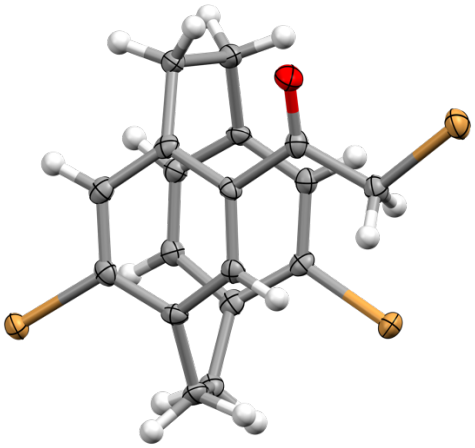

Crystal Data for $C_{18}H_{15}Br_3O$ (M =487.03 g/mol): monoclinic, space group $P2_1$ (no. 4), a = 8.8056(5) Å, b = 7.4117(4) Å, c = 12.7709(7) Å, β = 102.3170(10)°, V = 814.30(8) Å^3, $Z(Z')$ = 2(1), T = 100.00 K, μ(CuKα) = 9.169 mm^{-1}, ρ_{calc} = 1.986 g/cm^3, 17120 reflections measured (7.084° ≤ 2Θ ≤ 144.24°), 2994 unique (R_{int} = 0.0308, R_{sigma} = 0.0283) which were used in all calculations. The final R_1 was 0.0415 (I > 2σ(I)) and wR_2 was 0.1055 (all data). Flack parameter 0.41(4)

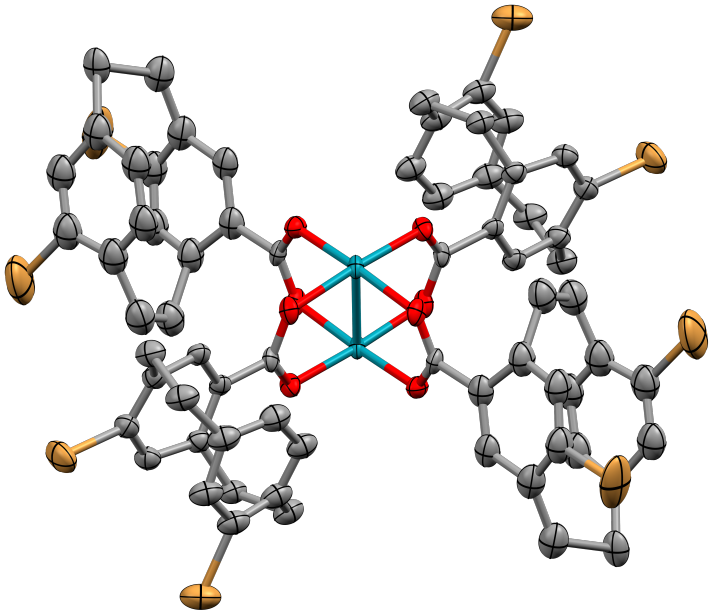

Crystal Data for $C_{80}H_{82}Br_8N_2O_8Rh_2$ (M =2044.590 g/mol): triclinic, space group P-1 (no. 2), a = 12.5569(5) Å, b = 13.5260(5) Å, c = 15.0471(6) Å, α = 66.044(2)°, β = 84.303(2)°, γ = 71.713(2)°, V = 2216.40(16) Å^3, $Z(Z')$= 1(0.5) , T = 100.00 K, μ(Cu Kα) = 7.626 mm^{-1}, ρ_{calc} = 1.532 g/cm^3, 98980 reflections measured (6.44° ≤ 2Θ ≤ 127.38°), 7259 unique (R_{int} = 0.0620, R_{sigma} = 0.0366) which were used in all calculations. The final R_1 was 0.1398 (I>=2u(I)) and wR_2 was 0.3702 (all data).

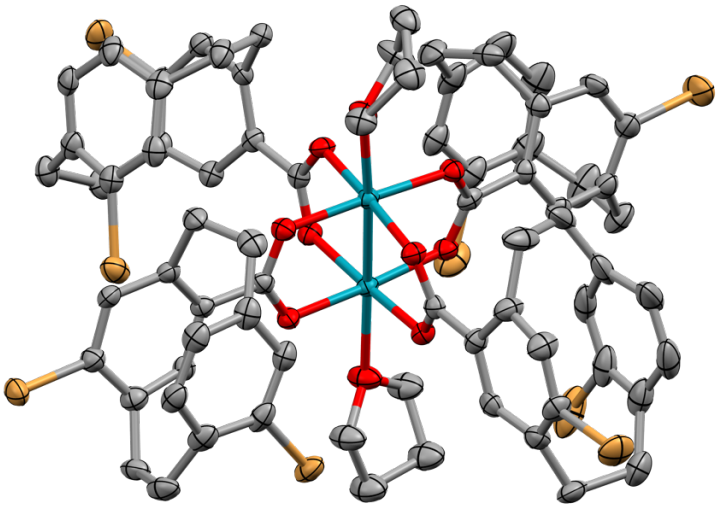

Crystal Data for $C_{76}H_{68}Br_8O_{10}Rh_2$ (M =1986.40 g/mol): monoclinic, space group $P2_1$ (no. 4), a = 13.130(2) Å, b = 20.452(3) Å, c = 14.121(2) Å, β = 111.600(4)°, V = 3525.7(9) Å^3, $Z(Z')$ = 2(1), T = 100.00 K, μ(CuKα) = 9.582 mm^{-1}, ϱ_{calc} = 1.871 g/cm^3, 69366 reflections measured (7.24° ≤ 2Θ ≤ 144.76°), 13478 unique (R_{int} = 0.0318, R_{sigma} = 0.0254) which were used in all calculations. The final R_1 was 0.0375 (I > 2σ(I)) and wR_2 was 0.0948 (all data). Flack parameter -0.005(3)

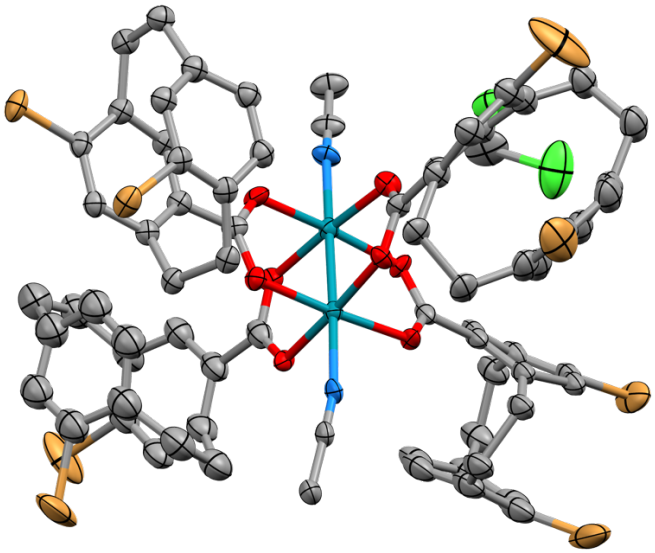

Crystal Data for $C_{75}H_{63}Br_8Cl_2N_3O_8Rh_2$ (M =2050.28 g/mol): orthorhombic, space group $P2_12_12_1$ (no. 19), a = 12.876(3) Å, b = 20.862(6) Å, c = 27.568(7) Å, V = 7405(3) Å^3, $Z(Z')$ = 4(1), T = 100.00 K, μ(CuKα) = 9.789 mm^{-1}, ϱ_{calc} = 1.839 g/cm^3, 104956 reflections measured (5.312° ≤ 2Θ ≤ 137.292°), 13260 unique (R_{int} = 0.0749, R_{sigma} = 0.0513) which were used in all calculations. The final R_1 was 0.0902 (I > 2σ(I)) and wR_2 was 0.1828 (all data). Flack parameter 0.03(2)